Sustainable Derivatization of Lignin and Subsequent Synthesis of Cross-Linked Polymers

Zur Erlangung des akademischen Grades einer

DOKTORIN DER NATURWISSENSCHAFTEN

(Dr. rer. nat.)

von der KIT-Fakultät für Chemie und Biowissenschaften

des Karlsruher Instituts für Technologie (KIT)

genehmigte

DISSERTATION

von

Lena Charlotte Over, M. Sc.

1. Referent: Prof. Dr. Michael A. R. Meier

2. Referent: Prof. Dr. Hans-Achim Wagenknecht

Tag der mündlichen Prüfung: 26.07.2017

You may never know what results come of your action,
but if you do nothing there will be no result.

Mohandas Karamchand Gandhi

Die vorliegende Arbeit wurde von Mai 2014 bis Juni 2017 unter Anleitung von Prof. Dr. Michael A. R. Meier am Institut für Organische Chemie (IOC) des Karlsruher Instituts für Technologie (KIT) angefertigt.

Erklärung

Hiermit erkläre ich wahrheitsgemäß, dass ich die vorliegende Arbeit selbständig angefertigt und keine anderen als die angegebenen Quellen und Hilfsmittel benutzt sowie die wörtlich oder inhaltlich übernommenen Stellen als solche kenntlich gemacht und die Satzung des Karlsruher Instituts für Technologie (KIT) zur Sicherung guter wissenschaftlicher Praxis beachtet habe. Des Weiteren erkläre ich, dass ich mich derzeit in keinem laufenden Promotionsverfahren befinde, und auch keine vorausgegangenen Promotionsversuche unternommen habe. Die elektronische Version der Arbeit stimmt mit der schriftlichen Version überein und die Abgabe und Archivierung der Primärdaten gemäß Abs. A (6) der Regeln zur Sicherung guter wissenschaftlicher Praxis des KIT ist beim Institut gesichert.

Karlsruhe, 26.07.2017

Danksagung

An dieser Stelle möchte ich allen danken, die an dem Gelingen dieser Arbeit beteiligt waren. Als erstes bedanke ich mich herzlich bei Prof. Michael Meier, dass er mich in seine Arbeitsgruppe aufgenommen hat und für sein Vertrauen und seine Unterstützung bei dieser Arbeit.

Der Deutschen Bundesstiftung Umwelt (DBU) danke ich nicht nur für die großzügige finanzielle Unterstützung durch das dreijährige Promotionsstipendium, sondern auch für die ideelle Förderung im Rahmen von Seminaren an interessanten Orten und mit spannendem interdisziplinärem Austausch. Besonders danke ich hier Dr. Maximillian Hempel für die Unterstützung als mein Betreuer bei der DBU und Dr. Hedda Schlegel-Starmann als Koordinatorin des Stipendienprogramms.

Des Weiteren möchte ich mich bei allen aktuellen und ehemaligen Kollegen des AK Meiers für die tolle Atmosphäre und Zusammenarbeit im Labor sowie bei gemeinsamen Aktivitäten bedanken. Besonders hervorheben möchte ich dabei Dr. Audrey Llevot, die mich immer unterstützt hat und bei den vielen Fragen weiterhelfen konnte. Merci beaucoup! Rebecca Seim und Pinar Sancar danke ich dafür, dass sie unser Labor am Laufen halten und mich bei allem Organisatorischem freundlich unterstützt haben.

Ebenso möchte ich mich bei allen Studenten, Auszubildenen und CTA bedanken, die mich während dieser Arbeit im Labor unterstützt haben: Tobias Fischer, Daniel Sack, Sven Riegsinger, Svenja Kusterer, Marcel Hergert, Carolin Albrecht, Thomas Sattelberger.

Den Mitarbeitern vom Thünen-Institut in Hamburg, besonders Isabell Kühnel und Andreas Schreiber, danke ich für die Herstellung und das zur Verfügung stellen des Organosolvlignins.

Moreover, I want to thank Prof. Henri Cramail and his group at the LCPO in Bordeaux for giving me the opportunity to work with them for three months. In particular, I also want to thank Prof. Stéphane Grélier and Etienne Grau for their scientific and Gérard Dimier for his technical support in Bordeaux.

Außerdem möchte ich mich bei Prof. Gooßen und seinen Mitarbeiterinnen Stefania Trita und Sabrina Baader für die exzellente Kooperation und die spannenden Diskussionen bedanken.

Auch für die analytische Unterstützung möchte ich mich bei verschiedenen Personen und Gruppen am KIT bedanken. Ich danke dem Analytik-Team des Organisch-Chemischen Instituts für die NMR- und IR-Messungen, sowie für die Elementaranalysen. Des Weiteren danke ich dem AK Prof. Feldmann und dem AK Prof. Roesky für das zur Verfügung stellen ihres TGA-Equipments und besonders Marieke Poss, Qian Liu, Sibylle Schneider, Pia Löser und Patrick-Kurt Dannecker für die Durch-

führung der Messungen. Dem AK Prof. Wilhelm danke ich für das zur Verfügung stellen des Zugprüfgeräts und Daniel Zimmermann für die Unterstützung bei den Messungen. Bei Ingrid Zeller in der Gruppe von Prof. Deutschmann bedanke ich mich für die SEM-Messungen. Ich bedanke mich bei der Deutschen Forschungsgemeinschaft (DfG) im Rahmen des §91b-Antrags unter der Federführung von Prof. Barner-Kowollik für die Förderung des Orbitrap-Massenspektrometers, das auch für diese Arbeit verwendet wurde. In diesem Zusammenhang bedanke ich mich auch bei dem Masse-Team des AK Prof. Barner-Kowollik für die Durchführung der Analytik. Außerdem bedanke ich mich bei dem selben Arbeitskreis dafür, dass ich die ^{31}P-NMR-Messungen an ihrem 400 MHz-Spektrometer durchführen konnte.

Abstract

Depleting fossil resources and a simultaneously increasing demand for energy and chemical products causes the demand for new, alternative products from renewable resources. Lignin is one of the most abundant biopolymers on earth, and thus a highly available natural feedstock for chemical use. Its complex macromolecular structure consists of phenylpropanoic units, making it the largest renewable resource for aromatic compounds. In addition, the high hydroxyl group content of both aliphatic and aromatic hydroxyl groups allows chemical modifications. In this work, dialkyl carbonates were used to modify the structure of lignin and to introduce new functional groups. This method is a "green" alternative to conventionally used *Williamson Ether Synthesis* with alkyl halides or alkyl sulfates.

First, the allylation with diallyl and dibenzyl carbonate was applied to various phenols, revealing an increased reactivity if aliphatic or methoxy groups are present as substituents. In a cooperation project with the group of Prof. L. J. Gooßen, renewable bisphenols derived from cashew nut shell liquid or eugenol were allylated with diallyl carbonate. The products reacted in thiol-ene polymerizations and the bisphenols were applied as polycarbonate monomers. The polymers from both pathways were compared with bisphenol A-derived polymers, indicating promising properties for its replacement.

The allylation procedure was then applied to organosolv lignin, which was extracted from beech wood chips *via* an ethanol/water pulping. Comparative studies of different solvents, bases and temperatures were performed. In the solvent-free approach, the reaction of organosolv lignin with diallyl carbonate led to a conversion of 90% of all hydroxyl groups to allyl ethers or allyl carbonates with tetrabutylammonium bromide (TBAB) as recyclable base. Also the used excess of diallyl carbonate was recovered after the reaction. Detailed structural analysis of the allylated lignin was performed *via* ^{31}P NMR, ^{1}H NMR, ^{13}C NMR, FT-IR spectroscopy and elemental analysis. SEC-MS was used to verify the functionalization and gave further insight into structural motifs in lignin. Furthermore, it was shown that allylated lignin undergoes *Claisen Rearrangements* at higher temperature (>150 °C), which led an increase of up to 28% allyl functions in the final product. In addition to allylation, also the crotylation of organosolv lignin with dicrotyl carbonate was successful, proving the transferability of the method. Moreover, self-metathesis of allylated organosolv lignin proved its reactivity towards cross-linking. In addition, plant oils – highly available renewable resources as well – were reacted with allylated lignin *via* cross-metathesis to form thermosetting films. Here, unmodified plant oil was reacted with a lignin derivative for the first time. It was found that an increasing lignin content as well as an increasing content of polyunsaturated fatty acid led to higher Young's moduli and higher cross-linking. Most films showed ductile behavior in stress/strain measurements. Only lignin contents over 70% led to brittle materials. The replacement of the conventional solvent dichloromethane by the "green" solvent dimethyl carbonate improved the sustainability of the procedure. However, the cross-linking density of the materials was decreased.

Epoxy thermosetting polymers were investigated as an additional application for the modified lignin.

Here, lignin was alkylated with epichlorohydrin in a conventional *Williamson Ether Synthesis* to obtain a lignin with an epoxy content of 3.2 mmol g^{-1}. Up to 42 wt% glycidylated lignin in a conventional epoxy thermoset with bisphenol A diglycidyl ether and isophorone diamine were cured in differential scanning calorimetry (DSC), analyzing the residual reaction heat. Furthermore, dog bone shaped specimen were analyzed for their structural properties *via* FT-IR spectroscopy, their thermal properties by DSC and thermogravimetric analysis (TGA) and mechanical properties from stress/strain measurements and dynamic mechanical analysis (DMA). A lignin content between 8 and 33% led to higher cross-linking, and thus a higher glass transition, lower swelling percentage in tetrahydrofuran, and increased stiffness (Young's modulus), compared to the lignin-free thermoset. For a more sustainable approach, the epoxidation of allylated and crotylated lignin with various epoxidation techniques was studied to demonstrate alternatives for the use of epichlorohydrin. Although the methods involving the peracids *meta*-chloroperbenzoic acid and peracetic acid or enzyme- and transition metal-catalyzed methods were successfully applied to the model compounds diallyl, dicrotyl and di-10-undecenyl carbonate as well as allylated and crotylated guaiacol, the transfer to alkylated lignin was accompanied by undefined side reactions. The detailed analysis of the modified lignin *via* ^{1}H NMR, ^{31}P NMR, FT-IR and SEC indicated partial oxidation and degradation of the organosolv lignin under the applied conditions.

Zusammenfassung

Die immer knapper werdenden Erdölressourcen und der gleichzeitig steigende Bedarf der Weltbevölkerung an Energie und chemischen Produkten führen zu der Nachfrage an neuen, alternativen Produkten aus nachwachsenden Rohstoffen. Lignin ist eines der häufigsten Biopolymere auf der Erde und dadurch ein hochverfügbares erneuerbares Ausgangsmaterial für die chemische Nutzung. Die komplexe makromolekulare Struktur ist aus phenylpropanoiden Einheiten aufgebaut, die es zu der größten nachwachsenden Quelle für aromatische Zielmoleküle machen. Außerdem besitzt Lignin einen hohen Gehalt an aliphatischen und aromatischen Hydroxylgruppen, die als Ausgangspunkt von chemischen Modifizierungen dienen können. In dieser Arbeit wurden Dialkylcarbonate verwendet, um die Struktur des Lignins zu verändern und neue funktionelle Gruppen einzuführen. Diese Methode kann als "grüne" Alternative zu der konventionellen *Williamsonschen Ethersynthese* angesehen werden, in der toxische Alkylhalogenide oder -sulfate zum Einsatz kommen.

Zuerst wurde die Reaktion mit Diallyl- und Dibenzylcarbonat an verschiedenen Phenolen getestet, wobei gezeigt werden konnte, dass aliphatische und Methoxyl-Reste die Reaktion im Vergleich zum unsubstituierten Phenol deutlich beschleunigen. In einem Kooperationsprojekt mit der Gruppe von Prof. L. J. Gooßen wurden aus Cashewnussschalenextrakt oder Eugenol gewonnene Bisphenole mit Diallylcarbonat allyliert und anschließenden zu Thiol-En-Polymeren umgesetzt, sowie in Polycarbonaten eingesetzt. Die Polymere aus beiden Studien wurden mit Bisphenol-A-basierten Polymeren verglichen und es konnte gezeigt werden, dass die Eigenschaften der Polymere aus nachwachsenden Rohstoffen vielversprechend für einen möglichen Ersatz von Bisphenol A sind.

Schließlich wurde die Allylierung von einem Organosolvlignin untersucht, welches durch einen Ethanol/Wasser-Holzaufschluss aus Buchenholz extrahiert wurde. In vergleichenden Studien mit verschiedenen Lösungsmitteln, Basen und bei unterschiedlichen Temperaturen konnten bis zu 90% der Hydroxylgruppen zu Allylethern oder Allylcarbonaten umgesetzt werden, wenn Tetrabutylammoniumbromid als recyclebare Base verwendet wurde. Der verwendete Überschuss an Diallylcarbonat konnte ebenfalls nach der Reaktion zurückgewonnen werden. Es erfolgte eine detaillierte strukturelle Charakterisierung des allylierten Lignins mittels ^{31}P-NMR, ^{1}H-NMR, ^{13}C-NMR, FT-IR-Spektroskopie und Elementaranalyse. Durch GPC-MS-Messungen wurde die erfolgte Modifizierung nachgewiesen und es wurden neue Einblicke in Strukturmotive des Lignins gewonnen. Des Weiteren konnte gezeigt werden, dass allyliertes Lignin bei erhöhten Temperaturen (>150 °C) *Claisen-Umlagerungen* eingeht und auf diese Weise der Modifizierungsgrad im Produkt um bis zu 28% erhöht werden kann. Neben der Allylierung wurde auch die Crotylierung mit Dicrotylcarbonat erfolgreich an Lignin durchgeführt und so konnte gezeigt werden, dass die Methode auf weitere Carbonate übertragbar ist. Daneben konnte die Selbstmetathese von allyliertem Lignin die hohe Reaktivität bezüglich Quervernetzung beweisen. Durch die Kreuzmetathese von Pflanzenölen – weitere hochverfügbare nachwachsende Rohstoffe – mit allyliertem Lignin konnten duroplastische Filme erhalten werden. So wurde zum ersten Mal ein Ligninderivat direkt mit unmodifizierten Pflanzenölen umgesetzt. Es stellte sich heraus,

dass ein hoher Ligninanteil sowie ein hoher Gehalt ungesättigter Fettsäuren im Pflanzenöl zu einem höheren Elastizitätsmodul und Vernetzungsgrad führte. Die meisten Filme verhielten sich während des Zugversuchs dehnbar. Nur Filme mit einem Ligningehalt über 70% führten zu spröden Materialen. Durch das Ersetzen des konventionellen Lösungsmittels Dichlormethan mit dem "grünen" Lösungsmittel Dimethylcarbonat konnte die Nachhaltigkeit der Methode erhöht werden. Allerdings wurde dadurch der Quervernetzungsgrad der Filme herabgesetzt.

Als weitere Anwendung von alkyliertem Lignin wurden duroplastische Epoxidharze untersucht. Dafür wurde Organosolvlignin mit Epichlorhydrin unter Anwendung der *Williamsonschen Ethersynthese* zu einem epoxidiertem Lignin mit einen Epoxidgehalt von 3.2 mmol g^{-1} umgesetzt. Bis zu 42 Gewichtsprozent des glycidylierted Lignins konnten in einem konventionellen Epoxidharz mit Bisphenol-A-diglycidylether und Isophorondiamin eingesetzt werden. Durch Aushärtung bei gleichzeitiger dynamischer Differenzkalorimetrie konnte die Reaktionsenthalpie bestimmt werden. Außerdem wurden knochenförmige Proben ausgehärtet, die hinsichtlich ihrer strukturellen Eigenschaften mittels FT-IR, ihrer thermischen Eigenschaften mittels dynamischer Differenzkalorimetrie und thermogravimetrischer Analyse, sowie ihrer mechanischen Eigenschaften mittels Zugversuch und dynamisch-mechanischer Analyse untersucht wurden. Dabei zeigte sich, dass ein Ligningehalt zwischen 8 und 33% zu einer höheren Quervernetzung und damit höherer Glasübergangstemperatur, niedriger Quellungsrate in Tetrahydrofuran und erhöhter Steifheit (Elastizitätsmodul) im Vergleich zu Lignin-freiem Duroplast führt. Für einen nachhaltigeren Ansatz wurden verschiedene Epoxidierungsmethoden als Alternativen zu Epichlorhydrin untersucht. Obwohl die Methoden mit den Persäuren *meta*-Chlorperbenzoesäure und Peressigsäure oder die Enzym- und Übergangsmetall-katalysierten Methoden erfolgreich für die Modellverbindungen Diallyl-, Dicrotyl- und Di-10-undecenylcarbonat angewendet werden konnten, war die Übertragung auf alkyliertes Lignin mit nicht vollständig geklärten Nebenreaktionen verbunden. Eine detaillierte Analyse mittels ^{1}H NMR, ^{31}P NMR, FT-IR und GPC wies auf Oxidation und teilweiser Zersetzung des Lignins unter den angewendeten Bedingungen hin.

Contents

1 Introduction

The demand for energy and chemical products increases with the increasing world population. At the same time, fossil resources show a decreasing trend. The lack of fossil resources is not only a problem for future energy supply, but also for the production of basic chemicals. Most chemicals of daily life, *i.e.* in food industry, for pharmaceuticals, for textiles, in paints and other segments, are still produced from petrochemical resources. In the medium term, alternative routes for their production from renewable resources need to be developed.[1]

Renewable resources that are highly discussed as alternatives to fossil oil-derived products are plant oils, starch, sugars and wood.[2] The polymer sector describes a large portion of the chemical industry. In 2015, 322 million tons of plastics were produced worldwide, with an increasing trend.[3] This volume is about 7% of the produced oil.[4] Therefore, the search for sustainable alternatives for polymeric materials is of high interest.[5,6] Besides their dependency on petrochemicals, polymers posses additional disadvantages: they are not or not fully biodegradable and thus account for environmentally pollution.[7,8] Examples are the contamination of groundwater or even direct agglomeration in human bodies with toxic agents, such as bisphenol A (BPA), a conventional monomer for epoxy resins, polycarbonates and other polymer applications.[9] Due to its estrogen mimicking behavior, BPA can lead to severe, long-term damage in human bodies.[10] In addition, the production of polymers is accompanied by environmental impacts, if the starting materials or side products are toxic. One aim of sustainable polymer chemistry is the synthesis of new, alternative products from renewable resources with enhanced properties under consideration of the "12 Principles of Green Chemistry".[11] Only the considerations of all economic, social and environmental impacts, can lead to an sustainable development, not only in chemistry. These "three pillars" are key aspects of the sustainability goals for the next century.[1,12–14]

The 12 Principles of Green Chemistry

In 1998, ANASTAS AND WARNER developed a guideline to increase the sustainability of chemical procedures that included the following points:[11]

1. **Waste prevention:** chemical procedures should be designed in a fashion that waste products are prevented.
2. **Atom economy:** synthesis should be designed in a way that most atoms involved in the reaction will be found in the desired product.
3. **Less hazardous chemical synthesis:** for the synthesis of products, procedures with low toxicity to human health or the environment should be used.
4. **Designing safer chemicals:** products should consist of lower toxicity than conventional products used for the same application.
5. **Safer solvents and auxiliaries:** solvents or additives for the reaction should be avoided or replaced by safer substitutes if used.

6. **Design for energy efficiency:** if possible, synthetic procedures should be performed at room temperature to maximize the energy efficiency.
7. **Use of renewable feedstocks:** raw materials should be from renewable resources.
8. **Reduce derivatives:** multi-step reactions and intermediates should be minimized to avoid unnecessary waste production.
9. **Catalysis:** catalytic reagents should be preferred over stoichiometric reagents.
10. **Design for degradation:** degradable products should be designed to prevent persistence in the environment.
11. **Real-time analysis for pollution prevention:** real-time, on-process monitoring controls the reaction and prevents the formation of hazardous chemicals.
12. **Inherently safer chemistry for accident prevention:** chemical substances should be chosen to minimize the potential of chemical accidents.

Due to its high availability and biological degradability, lignin is a promising renewable resource for polymer chemistry. It is one of the main components in wood and other plants. After cellulose and chitin, lignin is the third most abundant biopolymer on earth.[15] Lignin's total amount is estimated to be 300 billion tons on earth with an annual production of 20 billion tons.[16] Another advantage of lignin is that it can be isolated from lignocellulosic materials, which are not in concurrence with the food industry. This so-called second generation biomass is low priced compared to first generation biomass (*e.g.*, sugarcane, corn, wheat), which are widely used for bioethanol production.[17] For lignin, in contrast, few industrial applications are known. However, the research for new products from this renewable resource is of high interest and under continually growing investigation.[18–20] On the one hand, lignin degradation is applied to obtain aromatic monomers and on the other hand, the macromolecular structure of lignin is directly used to develop polymeric materials. However, conventional modification methods, using petrochemical, toxic reagents are still dominant in the field of lignin research. The need for more sustainable pathways in lignin chemistry was the motivation of the present thesis. In this work, new synthetic routes to polymeric materials from the renewable resource lignin, always considering the Principles of Green Chemistry, were developed and the thus obtained polymers were characterized on their structural and thermomechanical properties.

1.1 Lignin

1.1.1 Lignin as renewable resource

Lignin is a heterogeneous, complex biopolymer that can be isolated from wood and other plants. Its content in biomass varies between 15 and 28%, which makes it the third main component after hemicellulose (21–35 wt%) and cellulose (38–43 wt%).[21] The lignin content in plants is strongly dependent on the nature of the biomass. For instance, its content in hardwood is 27–28%, softwood contains 20–22% lignin, whereas annual plants have the lowest lignin content with only 15–21%.[21] In all biomass, giving mechanical stability, protecting from enzymatic and chemical degradation as well as from UV light are the main tasks of lignin.[18] Its structure contains methoxylated phenylpropanoid units, naturally built up from sinapyl alcohol (**1**), coumaryl alcohol (**2**) and coniferyl alcohol (**3**) (Figure 1.1) as main building blocks to a heterogeneous, complex, macromolecular structure.[22] These

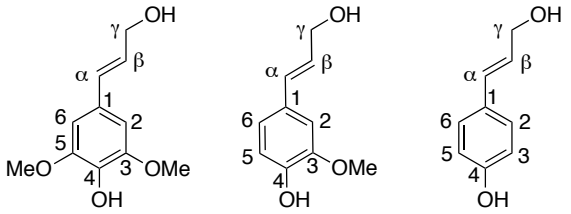

Figure 1.1: Main building blocks of lignin: sinapyl alcohol (**1**), coniferyl alcohol (**3**) and coumaryl alcohol (**2**); numbers and symbols assign the typical nomenclature for lignin motifs.

monomers lead to a highly aromatic structure, which makes lignin the largest renewable resource for aromatic compounds.[13] For the chemical use of lignin, it needs to be isolated from biomass. Pulping processes, that are mainly used in the pulp and paper sector, separate lignin from cellulose and hemicellulose. In the pulp and paper industry, 60 million tons of lignin per year are produced as side and waste product. The main part of the produced lignin is utilized for energy generation, only 5% are chemically exploited und hence, its high potential is not fully used.[23] This is the starting point of many research activities towards new materials from this renewable resource.

1.1.2 Chemical structure of lignin

Starting from the above mentioned building blocks, sinapyl alcohol (**1**) coumaryl alcohol (**2**) and coniferyl alcohol (**3**), a complex structure with a variety of binding motifs is constructed in nature. In the structural motifs of this complex structure, the phenylpropanoid units (C_9 units) of the starting materials can be recognized. However, the type of linkage between the units as well as the ratio between the three starting blocks depend on the nature of the biomass. Several motifs that describe C-C, C-*O*-C and even cyclic linkages could be identified and are represented in Figure 1.2 with the corresponding percentages in hardwood and softwood.[20,24] Numbers describe the position of the involved C atom in the aromatic ring and symbols the aliphatic position (see Figure 1.1). The most frequently found motif in lignin's structure of hardwood and softwood is the β-*O*-4 linkage of two building blocks. However, the ratio of the building blocks varies for different origins of the lignin. This also influences the methoxy group content in the lignin. Whereas hardwood lignin is mainly constructed from coniferyl alcohol (**3**), which leads to a high methoxy group content, softwood lignin contains additionally sinapyl alcohol (**1**) units. Only in lignin from annual plants, coumaryl alcohol (**2**) units are found, which leads to the lowest methoxy group content.[25] Biosynthesis of lignin starts with the synthesis of monolignols that are transported to the cell walls of the plants. In the cell walls, they are finally polymerized and bound to cellulose and hemicellulose in complex enzymatic processes.[15,26–28] Due to the high cross-linking degree of lignin itself and the linkages with other components of lignocellulosic material, no structural analysis can be performed. For structural investigations of pure lignin as well as for its chemical use, lignin needs to be isolated from the biomass. Therefore, various pulping processes are known of, which some of them alter the lignin structure chemically.

1.1.3 Isolation of lignin

The sustainable use of lignin as a renewable resource for polymer chemistry starts with its isolation. Most of the industrially produced lignin is gained from the kraft process of the pulp and paper industry, where it is mainly burned for energy recovery.[23] Using this lignin for the synthesis of valu-

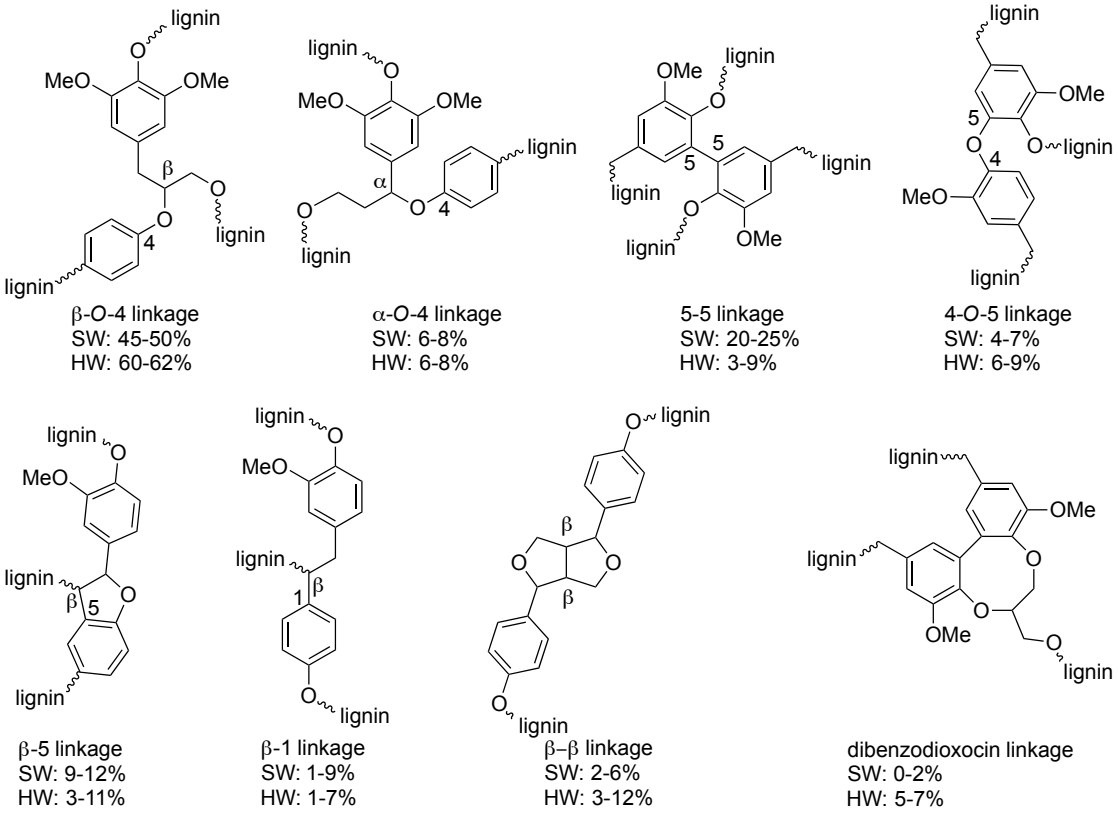

Figure 1.2: Typical linkages between two C_9 building blocks in the lignin structure and their occurrence in the macromolecular structures of hardwood (HW) and softwood (SW).[20,24] Numbers and symbols assign the corresponding carbon atoms of the building blocks.

able products presents already a more sustainable route. Nevertheless, the kraft process itself is not environmentally friendly, as stoichiometric amounts of inorganic salts are produced as byproduct. Different pulping processes and their influence on the lignin structure are discussed in the following sections.

Sulfite process. The sulfite process is the main source for commercially available lignins.[18] This pulping is performed using metal sulfites and sulfur dioxide at 140–160 °C under acidic conditions. Cellulose remains unmodified, whereas hemicellulose is depolymerized into sugar fragments and lignin is depolymerized introducing sulfonic acid groups to the lignin backbone. In addition, the lignin structure is further altered by C-C bond formation. This fragmentation and transformation to the sulfonate form leads to good solubility in water and thus difficult separation from hemicellulose fragments in the same solution. In isolated sulfonated lignins, around 30% carbohydrates, ash and other impurities can be found. In addition, this lignosulfonates have relatively high molecular weights of 20–50 kg mol^{-1}.[29] The altered structure, high molecular weights and enclosed impurities make this lignin unattractive for chemical use and valorization.

Sulfate process (kraft process). Kraft pulping produces 85% of the total lignin and thus, the highest volume of lignin worldwide.[30] The process is performed in alkaline media using sodium hydroxide and sodium sulfide as reagents. The ether bonds in lignin are cleaved and cellulose is released. Under these conditions, the structure of lignin is modified: thiol functions are introduced in the structure of lignin, increasing the sulfur content of lignin and C-C bonds are formed. The resulting Kraft lignins

have average molecular weights between 2000 and 3000 g mol^{-1} and are neither soluble in water nor in organic solvents.[29] In pulp and paper industry, the kraft lignin is burned for energy recovery. Chemical use of kraft lignin is limited due to the bad solubility, contamination with hemicellulose residues and the sulfur content.

Organosolv process. In comparison, the organosolv pulping for, which only recyclable organic solvents are necessary can be considered an eco-friendly alternative.[31] Also in this work, this more sustainable organosolv lignin, obtained from an ethanol/water pulping will be used. In this process, lignin and hemicellulose are solved in organic solvents to release cellulose as solid residue. This hydrolytic cleavage of the ether bonds, especially the above mentioned α- and β-ethers, is a key step of organosolv pulping in aqueous organic solvents. Here, lignin macromolecules of an average molecular weight of 1000 g mol^{-1} are generated and can easily be isolated in high quality.[29] Organosolv lignin is hydrophobic and soluble in organic solvents. An addition, no sulfur groups are introduced to the lignin structure. The Alcell® process, which uses ethanol or ethanol/water mixtures is the most well-known organosolv process.[32] However, since Repap Technologies Inc. stopped the production of Alcell lignin, no commercial organosolv lignin is available. Nevertheless, the process is still applied in some pilot scale lignocellulosic biorefineries and recent literature still shows high interest in the optimization of the isolation of organosolv lignin.[17,33–37] Moreover, the solvent influence on the lignin extraction efficiency and properties of the isolated lignin was reviewed.[38] For instance, it was found that aqueous acetone solution can remove >90% of lignin from wood, whereas ethanol and methanol mixtures with water lead to yields of >70%. Ethanol however, can react with α-ethers of lignin to form ethyl ethers and thus stabilize the lignin to prevent condensation reactions. Another method that is discussed, in combination with organosolv pulping or biorefinery, to prevent C-C bond formation is the addition of formaldehyde to the pulping process.[39] Thus, highly reactive intermediates react with formaldehyde and can later be hydrolyzed to yield high quality lignin.

Soda process. Extraction of lignin *via* soda pulping is performed with sodium hydroxide and was the first known chemical pulping process. Today, it is mainly used for grasses and bagasse and not applied for wood anymore.[18] The mild hydrolysis of lignin does not change its structure significantly. Just as for organosolv lignin, soda lignin contains no sulfur groups, low amounts hemicellulose residues and is thus likewise valuable.

Steam explosion. Steam explosion delignification of biomass is another sulfur-free alternative for lignin isolation that was developed to obtain a less altered lignin in a more environmentally-friendly process.[40] Compared to kraft pulping, steam explosion produces lower environmental pollution, has lower costs and uses less hazardous chemicals.[41] This process is performed in several steps. In the first period, biomass and water are rapidly heated to 130–180 °C under high pressure (13–130 bar) to hydrolyze and dissolve hemicellulose.[42,43] This step is followed by a sudden decompression that leads to an evaporation of water molecules in the cell walls and thus the aryl ethers between lignin and cellulose are cleaved *via* autohydrolysis. The isolated steam explosion lignin has similar properties as organosolv lignin. It is characterized by low molecular weight and good solubility in organic solvents.[41,43,44] The efficient aryl ether hydrolysis leads to a high content of phenolic hydroxyl groups and thus a highly reactive lignin, *e.g.*, for alkylation reactions.[45]

Biorefineries. The term biorefinery describes the conversion of renewable feedstock, such as wood, grasses, agricultural crops and wastes or municipal solid waste, into fuels, power or chem-

ical products.[46] Biorefineries can be categorized in three types: phase I, II and III.[47] A phase I biorefinery can only process grain and has fixed capabilities. Main products are ethanol and carbon dioxide. In contrast, a phase II biorefinery has more processing flexibility and produces a larger variety of products, although it also uses grain as feedsock. Products of a phase II biorefinery are starch, high-fructose corn syrup, ethanol and corn oil.[46] Phase III biorefineries can be divided in whole-crop, green and lignocellulose biorefineries. Here, a larger spectrum of feedstocks and also products is available. The only biorefinery where lignin can be isolated to obtain valuable products is the lignocellulose biorefinery. Other types treat mainly annual plants or biomass with low lignin content. The principle of most biorefineries is a treatment of biomass with sulfuric acid to hydrolyze hemicellulose und cleave lignin-cellulose bonds. However, most concepts focus on the more easily convertible fractions, hemicellulose and cellulose. After separation of lignin, cellulose is fermented to ethanol, whereas lignin is treated as waste product.[48,49] Research to evaluate methods for biorefinery lignin valorization are still going on. For instance, a recent study investigated extraction methods of lignin from lignin-rich biorefinery residues that retained most natural structures of lignin.[50] Additionally, the depolymerization by fungal oxidoreductases of biorefinery lignin residue was shown to be an efficient method for high quality lignin.[51] The original average number molecular weight (M_n) of 2100 g mol^{-1} was significantly reduced with this process. Moreover, catalytic approaches in combination with organosolv pulping in biorefinery are discussed to generate high quality products from carbohydrates as well as from lignin.[52]

1.1.4 Methods of lignin characterization

The isolated lignin can be analyzed by various analytical methods. In addition to standard methods in organic and polymer chemistry, such as NMR, IR, SEC and DSC analysis, some additional, more specific characterization methods are described for lignin. For instance, the determination of hydroxyl groups in lignin is a key analysis for further modification. A commonly used method to gain insight into the hydroxyl groups is ^{31}P NMR. Therefore, hydroxyl groups in lignin (**4**) are phosphorylated with a phosphorylation agent in a pyridine/$CDCl_3$ mixture (Scheme 1.1). Mostly 2-chloro-4,4,5,5-tetramethyl-1,2,3-dioxaphospholan (TMDP, **5**) is used, as it more stable compared to other derivatives and gives reproducible results.[53]

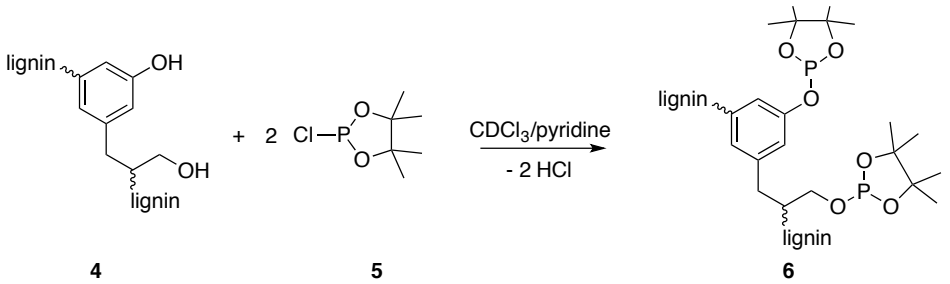

4 **5** **6**

Scheme 1.1: Phosphorylation of aliphatic and aromatic hydroxyl groups in lignin (**4**) with TMDP (**5**).

In the NMR spectrum of the phosphorylated lignin (**6**), the chemical shifts (δ) of the ^{31}P nuclei depend on their chemical environment. Hence, modified aliphatic, aromatic and carboxylic hydroxyl groups can be distinguished. The spectra are reported relatively to the signal of the product from the reaction of water with TMDP that gives the hydrolyzed form with a sharp signal at 132.2 ppm. To quantify the total amount of hydroxyl groups, an internal standard is added that does not overlap with the lignin signals. The frequently used cyclohexanol gives a TMDP product with a chemical shift at 145.6 ppm,

which appears between the aliphatic and aromatic signals of lignin.[54] Here, phosphorylated products from aliphatic hydroxyl groups can be found between 150.0 and 145.5 ppm and those from phenolic hydroxyl groups between 144.0 and 137.6 ppm. In addition, carboxylic acids in lignin result in signals at 136.0–133.6 ppm. Further analysis of the lignin can be performed in the aromatic region to gain insight into structural motifs that were discussed in Section 1.1.2, as they result in typical chemical shifts (Table 1.2). Applying ^{31}P NMR for quantitative analysis, all measurement parameters have to be taken into account for a reproducible measurement. The total hydroxyl group content, derived from the measurement depend on the chosen internal standard and the time after preparation, but also on the parameters of the NMR measurement, such as relaxation delay and number of scans.[55] It was found that cyclohexanol gives relatively constant values over a time frame of 35 hours after the preparation.[55]

Table 1.2: Chemical shifts of TMDP products with different structural motifs in lignin.[54,56]

Structural motif	δ [ppm]	Structural motif	δ [ppm]
Aliphatic OH	145.5–150.0	5-5 OH	~141.2
Phenolic OH	137.6–144.0	Guaicyl OH	139.0–140.2
Cyclohexanol	145.6	Catechol	~138.9
C-5 substituted OH	140.0–144.5	*p*-Hydroxyphenyl	137.8
β-5	~143.5	Carboxylic acid OH	133.6–136.0
Syringyl OH	~142.7	H_2O	132.2
4-*O*-5 OH	~142.3		

In addition to ^{31}P NMR, also other methods are discussed to determine the total hydroxyl group content. For instance, ARGYROPOULOS *et al.* described a quantitative ^{13}C NMR analysis to determine the total hydroxyl group content, among other functional groups.[57] In addition, aminolysis and ^{1}H NMR of acetylated lignins as well as non-aqueous potentiometry or UV spectroscopy are discussed to determine lignin's hydroxyl groups.[58] Moreover, multidimensional NMR spectrometry of ^{13}C-^{1}H correlation (HMBC, HSQC) helps to identify structural motifs in the lignin structure. For instance, it can be distinguished between aliphatic C-H correlations of β-aryl, β-5 and β-β, among others.[59] Furthermore, the methoxy group content in lignin is another functional group that can be quantified to gain insight into lignin's structure. It is determined by treatment of the lignin with sulfuric acid to achieve demethylation. Quantification of the so formed methanol can be performed *via* gas chromatography and is equal to the total methoxy group content in the original lignin.[60]

In addition to the before described analytical methods, elemental analysis is used in lignin chemistry to determine a C_9 formula. If additional functional groups were determined, *e.g.*, hydroxyl groups and methoxy groups, a structure of the form $C_9H_nO_m(OH)_o(OCH_3)_p$ can be calculated that summarizes all analytical results.[61] The origin of the C_9 formula is the structure of the three C_9 building blocks coumaryl alcohol (**2**), sinapyl alcohol (**1**) and coniferyl alcohol (**3**). Together with other analytical results, this chemical formula can help to understand structural motifs in the isolated lignin, such as linkages between the building blocks and also serves as comparable magnitude.

Molecular weight distributions of lignins can be obtained from size-exclusion-chromatography. An issue for this methods is the different solubility of different lignins. A recently reported system is based on DMSO as solvent with additional 0.5% w/v LiBr. This system can dissolve the most common lignins (kraft, organosolv, soda and lignosulfonates) and in combination with advanced polymer

chromatography (APC) was shown to measure all types of lignin with short measurement times.[62] Thus, fast screening of molecular weight distributions is possible, which is important for monitoring of reactions or biorefinery operations.

1.2 Isolation of platform chemicals from lignin

One possibility for the chemical use of lignin is the selective and unselective depolymerization of its complex structure to obtain aromatic platform chemicals. Several approaches treat the selective depolymerization of lignin. Target molecules are benzene, toluene, xylenes (BTX chemicals) and other aromatic compounds, such as phenols, which can replace substrates from petrochemical resources. In addition, more complex chemicals can be directly isolated from lignin, which would involve several synthesis steps starting from petrochemicals. Several publications deal with this valorization of lignin and isolation of various products. However, no industrial applications are known, yet, besides the isolation of vanillin.

The vanillin synthesis from lignin obtained by the sulfite process is the most well-known example for lignin as a sustainable source for a platform chemical.[63] This process was first applied in 1936 and for the first time vanillin could be isolated low priced from renewable resources. Thus, the conventional, petrochemical pathway from eugenol was replaced.[64] In the 80s, the vanillin production from lignin was at its maximum when one single paper mill produced 3.4 million kilograms of vanillin per year and could cover 60% of the world market. Today, new low priced pathways from petrochemicals dominate the vanillin production. Most lignin-based factories closed due to high expenses and risk of black liquor transport.[63] Only Borregaard Industries in Norway still operates this vanillin process. However, this example points out the huge potential of lignin as sustainable source for aromatic compounds. Borregard Industries also works on new, better technologies and routes for vanillin from lignin.[65] Still, lignin is the only relevant renewable resource for aromatic compounds.

Also scientific research shows high interest in isolation of aromatic compounds from lignin. Reviews about the catalytic conversion and degradation of lignin and biomass to lignin monomers can be found in literature.[29,48,52,66–69] In this section, only few recent approaches will be highlighted. Recently, BECKHAM *et al.* reported the fungal depolymerization of biorefinery lignin.[51] Besides lignin macromolecules with decreased molecular weights, the aromatics *p*-coumaric acid (**7**), ferulic acid (**8**), vanillin (**9**), vanillic acid (**10**), 4-hydroxy benzoic acid (**11**), 4-hydroxy benzaldehyde (**12**) and syringic acid (**13**) were found in the reaction solution after this enzymatic oxidation in variating concentration dependent on the conditions (Figure 1.3). However, it was found that some microbes are able to catabolize the resulting aromatic compounds. These and other, similar aromatic molecules, mostly containing methoxy and alkyl groups, are typical targets of lignin degradation.

Enzymatic conversion is only one of many possible approaches to depolymerize lignin to the desired aromatics. Thermomechanical conversion, such as pyrolysis, of lignin is another pathway to isolate valuable products from lignin.[70,71] For instance, pyrolytic decomposition of lignocellulosic biomass under anoxic conditions leads to the formation of various volatile and gaseous products, mono-lignols and mono-phenols as well as polysubstituted phenols. In addition, a solid product, the so called biochar is obtained. Moreover, hydrothermal conversion of biomass is another technology for the production of platform chemicals.[72–74] It is mainly studied for the generation of biofuels but also for

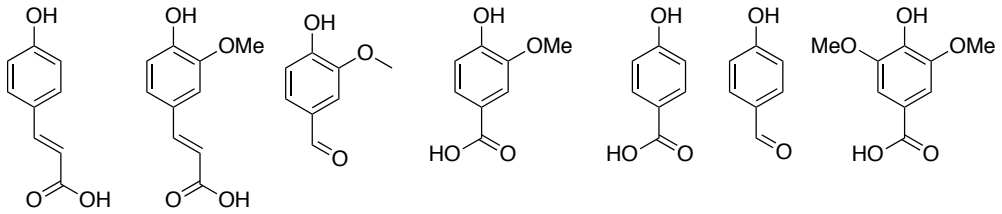

Figure 1.3: Chemical structures of platform chemicals derived from lignin.

the production of value-added products. For instance, vanillin (**9**) and other phenols or aldehydes can be a product of wet oxidation or hydrothermal liquefaction of lignin.[73] In contrast, hydrothermal gasification of lignin does not maintain the aromatic structure of lignin. Here, gases like hydrogen and methane are produced, which can be used as fuel gases.

Many reports treat the catalytic degradation of isolated lignin. SINGH *et al.* reported the hydrogenolysis of ionic liquid biorefinery lignin with Ru/C in isopropanol as hydrogen donor at 300 °C.[75] In this process, 27% of the lignin was converted to monoaromatic phenols containing alkyl and methoxy functional groups, *e.g.*, 4-ethylphenol and 2,6-dimethoxy-4-propylphenol. Moreover, the depolymerization of alkaline lignin with an original molecular weight distribution of 60 kg mol^{-1} was successfully performed using zeolites at catalyst. About 51% of the material was converted to monoaromatic compounds, such as vanillin, guaiacol and eugenol, indicating a high efficiency of the system.[76] Other oxidative degradation procedures are known that do not need any catalyst. For instance, the oxidation of lignin with hydrogen peroxide can be performed in dimethyl carbonate at 20–80 °C without any additive or catalyst.[77] Depending on the conditions and the amount of hydrogen peroxide, lignin was converted to aromatic compounds or even completely dearomatized. In another study, lignin was depolymerized in ionic liquids under oxidative conditions with hydrogen peroxide in one hour at 120 °C to a lower molecular weight lignin and aromatic compounds. Under these oxidative conditions, mainly aromatic acids were found in the product mixture, such as vanillic acid and benzoic acid.[78] CANTAT *et al.* reported the lignin degradation and simultaneous hydrosilylation.[79] This reductive degradation of lignin was performed under metal-free conditions with $B(C_6F_5)_3$ as lewis acid catalyst and triethylsilane as reagent. Up to 24 wt% of silylated monoaromatics could be isolated from formacell lignin isolated from 15 different wood plants. This procedure cleaves the ether bonds in natural lignin under mild conditions at room temperature and can also be applied to recycle synthetic polyether and polyesters.[80]

One recent development in lignin chemistry is the so called "lignin-first" approach that deals with concurrent extraction and catalytic conversion of lignin fragments in one-pot processes. This “Early-stage Catalytic Conversion of Lignins” (ECCL) is often combined with organosolv pulping.[52,81] The name originates from the fact, that lignin is valorized prior to the processing of the carbohydrates.[82] A key step of these valorization procedures is the suppression of repolymerization (C-C bond formation) of lignin during the pulping process as it occurs during other technical pulping processes (especially kraft and sulfite pulping).[81] RINALDI *et al.* reported the ECCL through nickel-catalyzed hydrogen transfer reactions yielding an efficiently depolymerized lignin oil.[83] Around 55 wt% of the oil fraction consisted of volatile components that were identified to be mostly phenols but also cyclohexanol and various aliphatic diols were found. In addition, the carbohydrate fraction possessed a

high quality as well. The obtained pulp had a low lignin residue and was susceptible for enzymatic hydrolysis. Another recently reported method to isolate lignin monomers is the reductive fractioning of biomass with Pd/C and metal triflates.[84] Also in this study, a yield of 55% monoaromatics, mainly alkylmethoxyphenols, was obtained from the lignin fraction. This percentage, obtained in both studies, is close to the theoretical maximum of monoaromatics that can be achieved, considering an ether content in lignin of 67–76%.[67]

1.3 Macromolecular use of lignin

The second category of chemical use of lignin is the use of its macromolecular structure in polymer chemistry. The present work is located in this field of chemical use to evaluate new pathways for polymer networks from macromolecular lignin. Due to the heterogeneous mixture in this biopolymer, lignin is often modified to yield desired properties, such as solubility, thermal stability or new reactivities and to homogenize the structure. The research field of macromolecular use is highly investigated in literature and is described for copolymerization as well as for blends. Furthermore, the macromolecular structure can give antimicrobial properties, UV-protection or act as antioxidant. Reviews about the use of lignin's macromolecular structure and different modification methods can be found in literature.[18,43,85–87] Here, selected examples for the state-of-the-art in this area will be given in the following sections. First, widely used modification and polymerization methods in lignin chemistry will be discussed, followed by recent approaches towards more sustainable pathways.

1.3.1 Lignin modification methods

For most copolymerizations and the use in blends, the structure of lignin is first modified. Modifications methods can be divided in methods that introduce new reactive sites and methods that functionalize hydroxyl groups of lignin. Scheme 1.2 summarizes the most important modification methods that are discussed in this section.

A straightforward method to increase reactive sites in lignin is the demethylation. Here, the numerous methoxy groups are demethylated to increase the number of phenolic hydroxyl groups. The modified product shows higher reactivity due to the higher density of reactive sides. Especially for the use in phenolic resins, this is a frequently used modification method.[88] One method to perform the demethylation is the use of molten sulfur in alkaline media. This industrial application is used for dimethyl sulfoxide (DMSO) synthesis from lignin. Sulfur is transformed to dimethyl sulfide, which can be oxidized to DMSO.[89] However, also other procedures for demethylation are know. Among different lewis and brønsted acids tested, hydrogen bromide showed the best reactivity towards demethylation.[90–92] After the treatment, the increase in hydroxyl groups is reported to be around 30%.

Another method to increase lignin's hydroxyl groups is methylolation (hydroxylmethylation) of the C-5 position of lignin. The reaction is carried out under alkaline conditions with formaldehyde as reagent in a *Lederer-Manasse Reaction*. ZHAO *et al.* showed that 90% of the C-5 position were functionalized, which corresponds to additional 0.36 hydroxyl groups per C_9 unit.[93] In a study with different types of alkaline lignin, it was found that undesired side reaction, like *Cannizarro Reaction* of formaldehyde with itself that led to further side reactions, can occur depending on the reaction conditions. Lower reaction temperature and lower pH value decreased the *Cannizarro Reaction*.

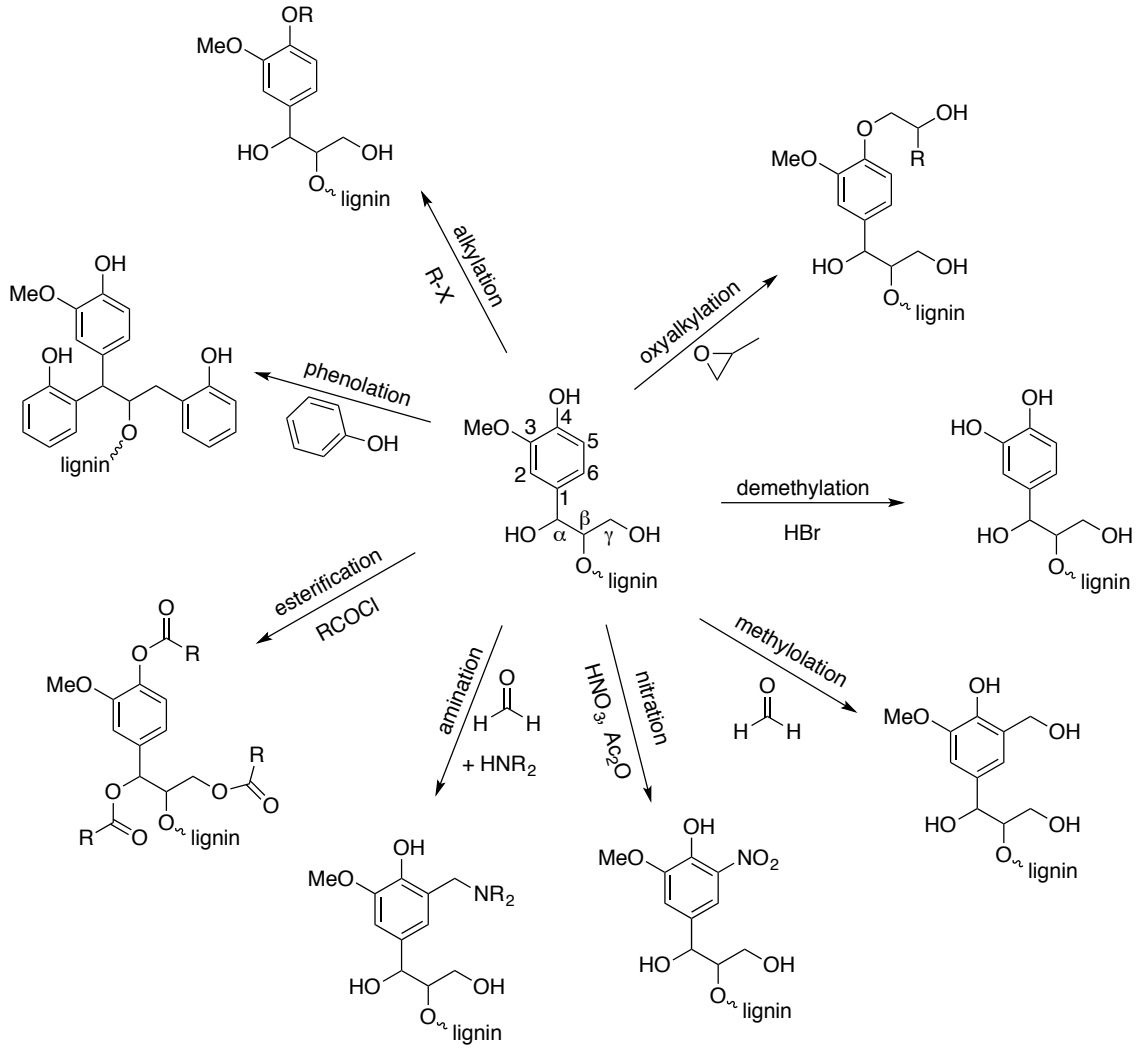

Scheme 1.2: Most-frequently discussed modification methods for lignin. Numbers and symbols label the positions of carbon atoms.

Amination and nitration are modification methods to introduce a new reactive site into the structure of lignin that does not occur in the natural form. The amination of lignin is carried out using formaldehyde and an dialkylamine in a *Mannich Reaction*.[94] The functionalization of lignin takes place at the C-5 position in the aromatic ring. The aminated lignin with dimethylamine was used as water-soluble cationic surfactant that led to a larger surface tension decrease than commercial surfactant.[94] Moreover, aminated lignin was reported to improve mechanical properties and reduce water absorption in lignin-thermoplastic composites.[95] Using diethanolamine, a reactive aminated lignin polyol for polyurethane synthesis was obtained.[96] Nitrolignin is obtained from the reaction of lignin with nitrating agents, such as nitric acid and acetic anhydride or nitric acid in concentrated acetic acid and fuming sulfuric acid. It is used for cross-linked polyurethane-nitrolignin networks.[97,98] The lignin content influences the mechanical and thermal properties of the films. Only 2.8% nitrolignin, led to an enhancement of tensile strength and elongation at break.

One of the easiest modification of hydroxyl groups is esterification with acidic compounds, acid anhydrides or acid chlorides, mostly in the presence of pyridine. Difunctional acid derivatives led to

polyester networks (see Section 1.3.3.1). However, esterification of lignin can also be used to introduce a new functional group into the structure of lignin. For instance, lignin can be modified with fatty acid chlorides to improve the thermoplastic properties.[99,100] An organosolv lignin that was esterified with dodecanoyl chloride was used as filler in a polylactic acid (PLA).[100] Although, the degradation temperature was decreased compared to neat PLA, the elongation at break increased by 25% and thus the rigidity of the material was decreased. Also the esterification of a kraft lignin with maleic anhydride, succinic anhydride or phthalic anhydride reduces the glass transition temperture of lignin, decreased its hydrophilicity and resulted in a material that is compatible with thermoplastic matrices such as polyethylene or polypropylene.[101] Butyrated or methacrylated lignin can be used as reagent in thermosetting polymers.[102]

Phenolation of lignin is performed in acidic media with phenol. In this condensation reaction, ether bonds in lignin can be cleaved, which results in a decreased molecular weight. This modification method leads to the increase of phenolic hydroxyl groups and is a commonly used method for lignosulfonate as it simplifies the structure.[103] The product can be used in phenolic resin or be further functionalized for other applications.

Etherification of lignin with alkyl oxide, especially the oxypropylation with propylene oxide, is the most well-known modification method.[104,105] This method is highly selective for phenolic hydroxyl groups. In addition, the reaction is very efficient, >99% of phenols can be converted using 2.5 equivalents propylene oxide per phenolic hydroxyl group.[106] The main effect of this methods is the homogenization of all hydroxyl groups to highly reactive aliphatic ones. These hydroxyl groups can be efficiently used to react in polyurethane synthesis.[104] Homopolymerization of propylene oxide and copolymerization with lignin are side reactions of this method. To prevent this, the reaction should be performed at low temperature and with a minimum amount of propylene oxide. A second etherification method is the alkylation, mainly performed with alkyl halides. For instance, methylation with methyl iodide or dimethyl sulfate in a conventional *Williamson ether synthesis*.[105] With dimethyl sulfate, the reaction was selective for phenolic hydroxyl groups, with methyl iodine mainly aromatic hydroxyl groups reacted. This modification method increases the thermal stability of lignin for its use in thermoplastics. For instnace, it was found that a methylated lignin was more stable than the oxypropylated derivative.[106] Both etherification methods significantly decrease the glass transition temperature of lignin. Methylated lignin was reported as filler in polypropylene blends.[107] The methylation contributed to higher thermal stability. However, methylated lignin does not show antioxidant activity, proving that the phenolic hydroxyl groups are crucial for this application.

Many more functionalization methods of lignin are discussed in the literature, *e.g.*, sulfomethylation,[108,109] sulfonation,[110] halogenation,[111,112] and silylation.[113] However, most techniques are still dominated by conventional pathways and chemicals. Only few sustainable modification methods of lignin are known, which will be discussed in Section 1.4.

1.3.2 Copolymerization of lignin in thermosets

Applications for lignin in thermoset copolymers are phenolic resins, polyurethanes (PUs) and epoxy thermosetting polymers, among others. Examples for the named applications will be discussed in this section. In general, the lignin content, molecular weight and functionality of lignin are crucial for the properties of the final product. In thermosets, lignin acts as cross-linker with or without comonomers.

In some applications, modification is necessary to increase the functional groups that are involved in the curing process.

1.3.2.1 Epoxy thermosetting polymers from lignin

Epoxy thermosetting polymers result from the reaction of an epoxy compound with a hardener (*e.g.*, amines, alcohols, thiols, carboxylic acids). A commonly used reagent is bisphenol A (BPA, **14**), which is reacted with epichlorohydrin (**15**) to form the corresponding diglycidyl ether of bisphenol A (DGEBA, **16**) (Scheme 1.3). In a nucleophilic attack, the utilized hardener, here an amine (**17**), opens the epoxide and the epoxy polymer (**18**) is formed. If polyfunctionallized epoxides or hardeners are used, cross-linked materials can be obtained. Epoxy thermosets are used in coatings, adhesives, electronic materials, composites, among others.[114]

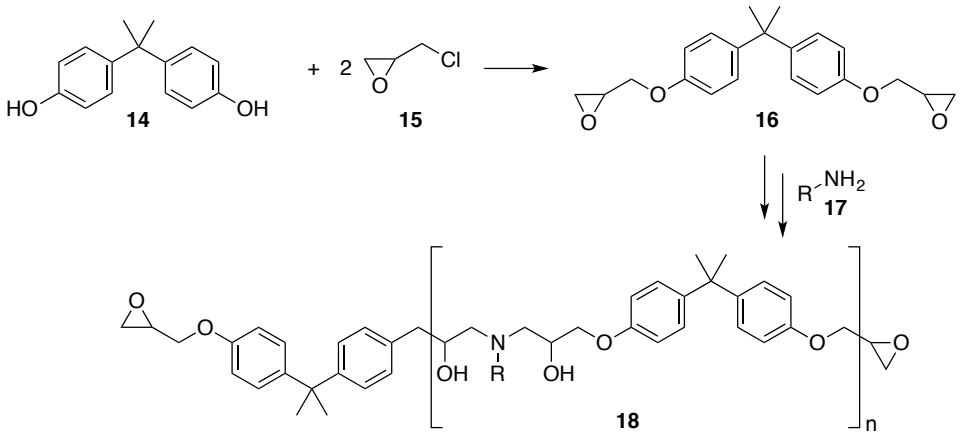

Scheme 1.3: Reaction of BPA (**14**) with epichlorohydrin (**15**) to DGEBA (**16**) and the subsequent polymerization with an amine hardener.

Hydroxyl groups in lignin can react as ring-opener for the formation of epoxy polymers. Prior to the reaction, chemical modification of lignin is necessary in some cases to increase the reactivity. One possibility is the introduction of carboxylic acid groups. HIROSE *et al.* described the synthesis of epoxy thermosets from lignin modified with ethylene glycol and succinic anhydride.[114] The introduced carboxylic acid groups were reactive enough to form the desired thermoset with ethylene glycol diglycidyl ether as epoxy component. FELDMAN *et al.* described the synthesis of epoxy polymers without previous modification.[115–118] After copolymerization with up to 40 wt% lignin, the adhesive strength of the material was clearly improved. In this application, unmodified lignin was polyblended with different epoxy-hardener systems. Moreover, DELMAS *et al.* used Biolignin^{TM}, a mixture of short chain, linear lignin oligomers, and polyethylene glycol diglycidyl ether to form a BPA-free epoxy thermoset.[119] The obtained bio-based product revealed similar thermal and mechanical properties as BPA-based thermosets indicating a high potential of lignin in epoxy polymer synthesis.

Besides the use as hardener, lignin can also be used as epoxy compound in epoxy polymers. Therefore, epoxy functions need to be introduced. In literature, this is performed using the conventional epoxidation reagent epichlorohydrin. Detailed literature discussion about this glycidylated lignin in epoxy thermosets can be found in Chapter 6. Here, only one recent example in combination with lignin modification will be highlighted. ABU-OMAR AND ZHAO described the the synthesis of an epoxy thermoset with highly functionalized organosolv lignin.[92] First, lignin (**19**) was demethylated using

hydrogen bromide to increase the phenolic hydroxyl groups forming compound **20**. In an additional step, lignin was modified with dihydroeugenol (**21**), a lignin-based monomer, in a phenolation (to form **22**). Then, phenol-formaldehyde reactions were performed to yield a novolac-type lignin monomer (**23**) with a highly increased aromatic hydroxyl group content (Scheme 1.4). After glycidylation of the phenolic hydroxyl groups with epichlorohydrin, the modified lignin was cured with diethylenetriamine to yield epoxy thermosets. The thermal properties of the product were similar with and without incorporation of lignin.

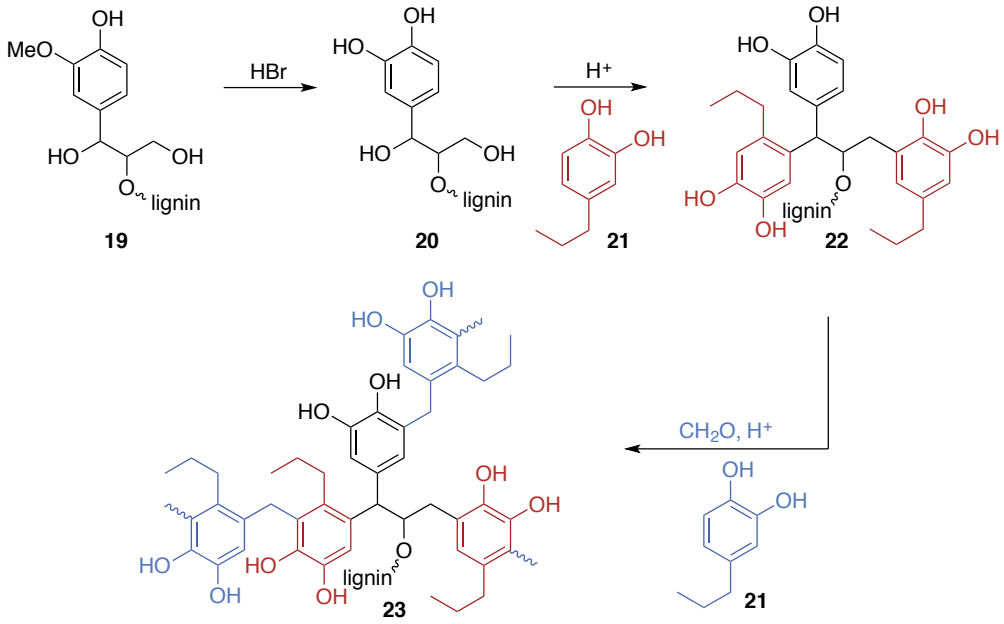

Scheme 1.4: Successive lignin demethylation and phenolation with dihydroeugenol to yield a highly phenolic macromolecule.[92]

1.3.2.2 Polyurethanes from lignin

Polyurethanes (PUs) are materials with a wide range of applications (*e.g.*, coatings, foams, adhesives, sealings, fibers and films).[43] In the general reaction for the synthesis of PUs, an alcohol reacts with an isocyanate to form a urethane bond. Thus, the reaction of 1,6-diisocyanatohexane (**24**) with butane-1,4-diol (**25**) leads to the formation of polyurethane **26** (Scheme 1.5).

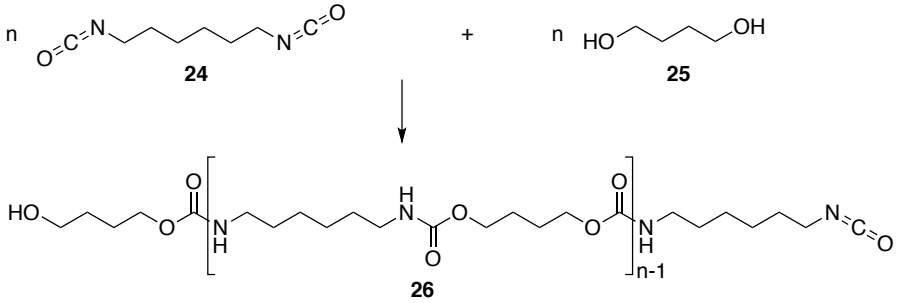

Scheme 1.5: Synthesis of an conventional polyurethane from 1,6-diisocyanatohexane (**24**) with butane-1,4-diol (**25**).

In this type of reaction, lignin can be used as polyol. However, in lignin-based polyurethanes, comonomers are often needed for an efficient reaction. CHUNG *et al.* described the synthesis of a

polyurethane with a demethylated lignin and toluene-2,4-diisocyanate.[91] Polyethylene glycol (PEG) was used as comonomer to obtain a product with a lignin content of 17 wt% with increased strength compared to the lignin-free PU. CHERADAME *et al.* described the polymerization of up to 30 wt% kraft lignin with hexamethylene diisocyanate with and without PEG as comonomer.[120] Stability, thermal and mechanical properties of the PUs were comparable to those of industrial materials. The copolymerization with PEG increases the chain mobility and decreases thus the glass transition temperature of the polymer.[121]

Besides PEG, other comonomers are discussed. POHJANLEHTO *et al.* synthesized a lignin-based PU with up to 15 wt% lignin and a renewable content of 35 wt%.[122] Here, besides lignin, a trihydroxyl glutaric acid derivative was polymerized with methylene diphenyl diisocyanate. Other bio-based polyols were obtained from castor oil and polymerized with kraft lignin and diphenylmethane diisocyanate.[123] A lignin content of up to 30 wt% was applied and mechanical properties were tuned depending on the structure of the castor oil derived comonomer. Oxypropylated lignin was used in rigid PU foams with 10 wt% glycerol as comonomer and yielded good thermal properties.[124]

Furthermore, the PU synthesis without comonomer was described for kraft lignin that was extracted with methyltetrahydrofuran. Thus, a lignin content of up to 90 wt% in a PU with an aromatic polyisocyanate was evaluated.[125] A higher lignin content led to increased thermal stability and good adhesive properties. The lignin extraction with a high boiling solvent yielded a lignin that was used in a PU with an additional hydroxyl source, which led to a lignin content of up to 60 wt% in the final product and tensile strengths of up to 41.6 MPa.[126]

In general, a higher molecular weight of lignin, both kraft lignin and organosolv lignin, leads to higher material strength.[127,128] Likewise, the mass percentage of lignin is crucial for material properties. For kraft lignin, a mass percentage higher than 30%, and for organosolv lignin, a lignin ratio of only 18% leads already to a brittle material. Not only the difference in pulping leads to differences in properties, also within organosolv pulping, the kind of procedure need to be distinguished. Depending on the utilized solvent in the pulping process, properties of the PU products can vary.[129] In a comparative study, the lignin extraction with acetone, ethanol or acetic acid led to different hydroxyl group contents; thus, different reactivities and also variating glass transitions temperatures in the prepared PUs were observed. Possible applications, described for lignin-based polyurethanes are water absorption, fire-resistant PU foams and PU foams for automotive parts.[130–133]

1.3.2.3 Lignin in phenolic resins

Phenol formaldehyde or phenolic resins are applied in adhesives, coatings and composites, among others.[43] They have outstanding heat and organic solvent resistance as well as excellent mechanical properties. Their synthesis starts from the acid- or base-catalyzed reaction of phenol (**27**) and formaldehyde (**28**) to diol **29** or **30** that react further to a cross-linked resin **31** (Scheme 1.6). Phenol formaldehyde resins are the most important products from phenol.[134] Both starting materials, phenol (**27**) and formaldehyde (**28**), are toxic and mainly gained from petrochemical resources. The synthesis of phenolic resins from the renewable feedstock lignin represents an environmentally friendly alternative. Due to its phenolic hydroxyl groups, lignin can replace phenol in this synthesis. However, the hydroxyl groups in lignin are sterically hindered and lower concentrated than in pure phenol. Thus, the reactivity is decreased and mostly, only parts of phenol are replaced. MULLER *et al.* de-

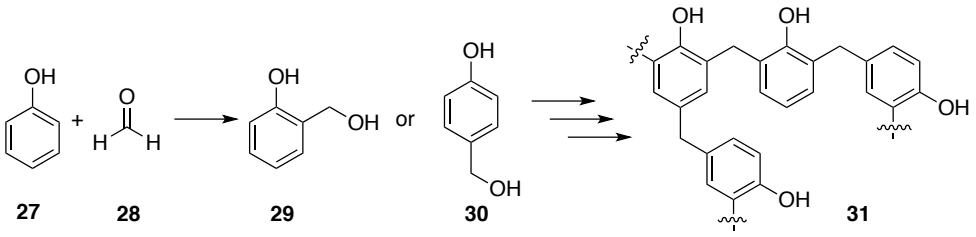

Scheme 1.6: Synthesis of an conventional phenolic resin from phenol (**27**) and formaldehyde (**28**).

scribed the use of kraft lignin, steam explosion lignin and acid pulping lignin in a phenoplast.[135,136] Cured products with up to 60 wt% substituted phenol, revealed similar properties in shear test and thermal analysis as commercial phenolic resins. KOUISNI *et al.* showed the use of kraft lignin in phenolic resins in plywood.[137] They replaced 30 wt% of commercial phenol without observing any property change. However, higher lignin contents led to deviation in shear strength. BENAR *et al.* described the replacement of 50 wt% phenol by acetosolv and formacell lignin.[138] In another report, novolac-type phenolic resins from three types of lignin (kraft, soda, sulfonate) were synthesized.[139] Both studies reported a higher viscosity of lignin-based materials but also a higher reactivity and thus, shorter curing time. A possible reported application for lignin-based phenolic resins are brake friction materials or adhesives for oriented structural boards.[140,141]

1.3.3 Use of lignin in thermoplastics

In addition to copolymerization of lignin in thermosetting materials, unmodified or modified lignin finds also application in thermoplastic materials. Here, lignin can be used as comonomer as well, but in most thermoplastics, lignin is blended to the material to obtain a certain property. For instance, lignin can give UV protection or increase the thermal stability.[18] In the following section some examples for lignin in polyester, polyolefins and other thermoplastics are discussed.

1.3.3.1 Lignin-based polyester

Examples for industrial polyesters are polyethylene terephthalate (PET) and polylactic acid (PLA). For instance, terephthalic acid (**32**) and ethylene glycol (**33**) react to PET (**34**) in a typical polycondensation reaction (Scheme 1.7).

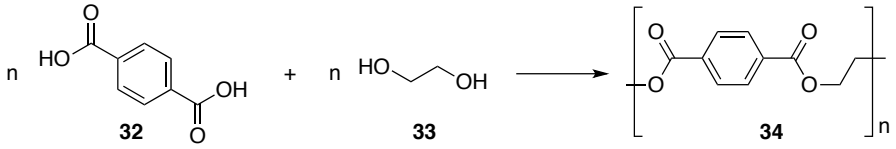

Scheme 1.7: Synthesis of PET (**34**) from terephthalic acid (**32**) and ethylene glycol (**33**).

Due to its high hydroxyl group content, lignin can react as polyol in such a condensation reaction. For instance, it was shown that polyesters can be synthesized starting from steam explosion lignin and dodecanedioyl dichloride to yield an average number molecular weight of 6400 g mol^{-1}.[42] Moreover lignin was reacted with adipic acid and/or phthalic acid anhydride. The formed polyesters were analyzed with FT-IR, SEC and viscosity tests revealing similar properties to conventional polesters.[142] SIVASANKARAPILLAI *et al.* succeeded to copolymerize lignin with triethanolamine and adipic acid.[143] Moreover, the use of lignin in polyester blends is described.[144–147] In general, lignin contributes to

material strength, reduces the cost of the material and can increase the biological degradation of the polyesters.

1.3.3.2 Lignin-polyolefin blends

Polyolefins, such as polyethylene (PE), polypropylene (PP) und polyisobutylene are industrial thermoplastics with applications in films, packaging and others. They are synthesized from the corresponding alkene, *e.g.*, ethylene (**35**) for PE (**36**) or propene (**37**) for PP (**38**) (Scheme 1.8). Although polyolefins are unpolar and do not seem structurally compatible with lignin, lignin can be incorporated into polyolefin blends. For instance, a lignin modified with maleic anhydride or dichloroethan was soluble in polypropylene and acted as stabilizer.[148] Moreover, it was reported that lignin-polyolefin blends showed higher biological degradability than pure polyethylene.[18,149] Lignin as filler with up to 30 wt% in PE or PP led to small decreases of mechanical properties and changes in the melt flow index.[150] However, heat and light resistance were improved.

35 **36** **37** **38**

Scheme 1.8: Formation of PE (**36**) and PP (**38**) from the corresponding alkenes.

Widely used halogenated polyolefins are polytetrafluoroethylene (PTFE) and polyvinyl chloride (PVC), which are synthesized from the alkenes tetrafluoroethylene and vinyl chloride, respectively. The use of lignin blends with PVC is described in literature. Here, it was found that the phenolic hydroxyl groups in lignin interact with the hydrogen atoms in PVC.[151] The strength of interaction was dependent on the origin of the lignin, thus the wood and the pulping process. In general, all different lignins diminished the impact strength of the PVC and led to lower weathering stability. However, softwood lignin gave better results than hardwood lignin.

1.3.3.3 Interaction of lignin with polyethylene glycol (PEG)

Polyethylene glycol (PEG, **40**) is an oligomer or polymer of ethylene oxide (**39**) (Scheme 1.9). It is characterized by ether functions and terminal hydroxyl groups, which form strong hydrogen bridges. Lignin can be used in PEG-lignin blends, where the aromatic hydroxyl groups form hydrogen bridges with the ether functions in PEG, which leads to excellent miscibilities.[152,153] Compared to kraft lignin, organosolv lignin led to better thermoforming properties in blends with a lignin weight fraction from 0–100%.[152] In addition, thermal properties were increased with lignin addition.

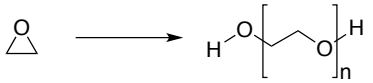

39 **40**

Scheme 1.9: Formation of polyethylene glycole (PEG, **40**) from ethylene oxide (**39**).

1.3.3.4 ARBOFORM®: an industrial application

The only technical application for the chemical use of macromolecular lignin is performed by the company TECNARO in Ilsfeld, Germany.[23] So-called ARBOFORM® is a mixture of lignin with natural fibers from flax, hemp and other fiber plants to form fiber-reinforced composites. The product can

be applied as conventional thermoplastic in spray castings, *e.g.*, for loudspeaker housing, musical instruments and automotive interior.

1.4 Sustainable synthetic pathways to polymers from lignin

The different possibilities to use lignin as resource for platform chemicals or as starting point for polymer synthesis were discussed in the previous sections. It was shown that conventional modification and polymerization methods for lignin still dominate in the field of lignin chemistry. Replacing these methods by sustainable pathways is one of the main challenges for the use of lignin. In this part, recent advances of sustainable synthetic pathways towards lignin-based polymers are described.

1.4.1 Modification methods for lignin

The heterogeneous structure of lignin is the main issue for the use of lignin. Depending on the origin and the pulping method every lignin has a different structure, which challenges its chemical use. Nevertheless, lignin is highly functionalized with aromatic and aliphatic hydroxyl groups. These hydroxyl groups are the starting point of numerous modifications aiming new reactive sites or enhanced properties for lignin, *e.g.* better solubility or reactivity. Classical modification methods were discussed in Section 1.3.1. In this section, the progress in sustainability of these modification methods is discussed. A first step to increase the sustainability of a process is the reduction of solvent or the change of a catalyst to a more sustainable one. Changing a substrate is often more challenging. The esterification of the hydroxyl groups in lignin with anhydrides or acid chloride is an easy and efficient modification methodology. For this modification method, pyridine is often used as solvent and activation agent. Recently also solvent-free, catalyst-free esterification methods were used, *e.g.*, for acylation[154] or maleation.[148]

A new approach was presented by AVÉROUS *et al.* describing the esterification of lignin with oleic acid.[155] Although, oleic acid needs to be chlorinated with acid oxalyl chloride to effectively esterify lignin, a second bio-based building block is utilized. To introduce a new functionality, the double bonds of the product were epoxidized with peracetic acid, the introduced oxirane rings opened and subsequently, the substrate with increased hydroxyl group content was used for PU synthesis. The sustainability of this work is the use of a second renewable resource, a new green epoxidation method for lignin and simultaneously, a new method to homogenize the nature of the hydroxyl groups prior to the use in PUs, which is conventionally performed *via* oxypropylation with propylene oxide. However, the subsequent use in PUs can be improved as diisocyanates are used, which are toxic reagents.

Another modification method is the alkylation of hydroxyl groups, which is conventionally performed with alkyl halides or alkyl sulfates. For this procedure, a stoichiometric amount of bases is necessary and inorganic salts are produced as byproducts. A more sustainable approach is the catalytic alkylation with organic carbonates. ARGYROPOULOS *et al.* described the effective methylation of

acetone-soluble softwood kraft lignin with dimethyl carbonate.[156] Up to 82% of the aliphatic and 100% of the aromatic hydroxyl groups were thus methylated. The methylation led to an increase of the thermal stability of lignin, which is necessary for the use in thermoplastics, *e.g.*, in blends with polyethylene.[107] A catalytic approach for the selective allylation of aromatic hydroxyl groups in lignin was recently developed in our group applying *Tsuji-Trost Allylation* with allyl methyl carbonate.[157] In this work, dialkyl carbonates will be used as alkylation agent for both, aliphatic and aromatic hydroxyl groups to introduce new functional groups into the structure of lignin to improve its reactivity.

The oxypropylation of lignin with propylene oxide is one of the most extensively studied modification reactions of lignin (see section 1.3.1).[86] Recently, cyclic organic carbonates were shown to be an effective alternative oxyalkylation of organosolv lignin (**41**) (Scheme 1.10).[158] Propylene carbonate (**42**) is less toxic compared to propylene oxide and the procedure uses potassium carbonate as catalyst. The resulted polyol (**43**) can be used in PU synthesis.

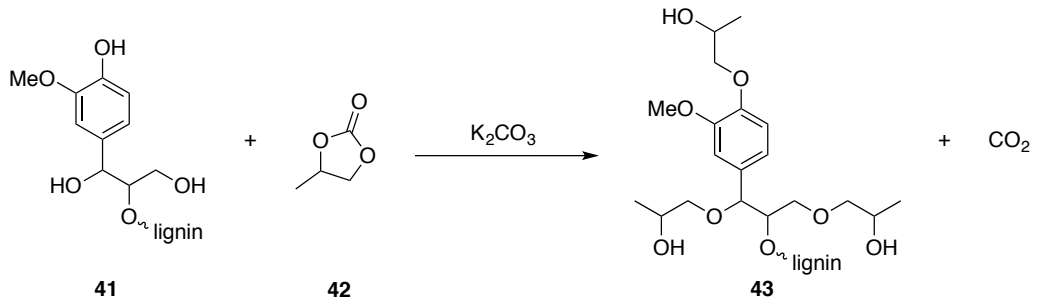

41 **42** **43**

Scheme 1.10: Oxypropylation of organosolv lignin (**41**) with propylene carbonate (**42**) as sustainable oxyalkylation agent.[158]

1.4.2 Lignin in copolymers and blends

Biodegradability is another aspect of green chemistry, so is the use of lignin in biodegradable polymers. The simplest example is unmodified lignin blended with polylactic acid (PLA), a prime example for biodegradable polymers.[159–163] More challenging is the modification of lignin prior to the use in blends. Lignin can be copolymerized with L-lactic acid *via* ring opening polymerization (ROP) with 1,5,7-triazabicyclo[4.4.0]dec-5-ene (TBD)[164] or stannous octoate[165] as catalyst. The resulting polymer was blended with PLA. In the same way, lignin can be copolymerized with ε-caprolactone *via* ROP.[166–169] The ROP is an easy polymerization method, no solvent is necessary and low catalyst amounts (~1 wt%) are sufficient.

Not only for the earlier mentioned modification methods, also in copolymerization methods, conventional, petroleum-based substrates still dominate the field of the chemical use of lignin. To the best of my knowledge, only one example for a lignin-based non-isocyanate polyurethane (NIPU) is known.[170] The presented polymer with a biomass content of 85% uses carbonated soybean oil and 3-aminopropyltriethoxysilane to form the urethane bond. Lignin is then reacted with the silane function. An issue of the work is the used silane, which may be replaced by another, bio-based compound, which could react with lignin.

In phenolic resins, lignin can be used as phenol replacement. Usually only parts of phenol are replaced by lignin and formaldehyde is still used as reagent (see section 1.3.2.3). Recently, a

phenolic-type resin was presented where organosolv lignin and glutaraldehyde fully replaced phenol and formaldehyde, respectively.[171] This resin, that can be completely obtained by natural resources, is a good example for the potential of the sustainable use of lignin.

1.4.3 Polymers from lignin derivatives

Vanillin, ferulic acid, guaiacol, syringaldehyde, hydroxybenzoic acid and similar aromatic monomers can be potentially isolated by lignin degradation (see section 1.2). Various polymers from these lignin derivatives are described in literature, mainly as replacement for conventional, toxic compounds such as BPA.[172]

Lignin derivatives like vanillin are not symmetrically concerning their bifunctionality. A new method for their dimerization was recently published.[173] The presented dimerization is laccase-catalyzed, uses oxygen as oxidant and no purification step is necessary. Thus, the process is an efficient and sustainable way to obtain symmetrical bifunctional monomers for new polymer syntheses.

Another interesting approach is the direct use of the product mixture obtained from the industrial lignin-to-vanillin process. CAILLOL *et al.* investigated the synthesis of epoxy thermosets therefrom.[174] The idea of the use of the mixture is positive as it prevents an additional separation step. Unfortunately, only commercial products were used and mixed in the representative ratio in the presented work and no "real" mixture from a vanillin isolation process was employed.

One recent example for the sustainable copolymerization of lignin derivatives are polyesters from vanillin.[175,176] Vanillin (**9**) was converted to acetylferulic acid, hydrogenated and polyesterified to compound **44** (Scheme 1.11). The resulting polymer showed similar thermal properties as polyethylene terephthalate (PET, **34**, see Scheme 1.7) and may be a suitable bio-based replacement. This example reinforces the potential of lignin derivatives for sustainable polymers.

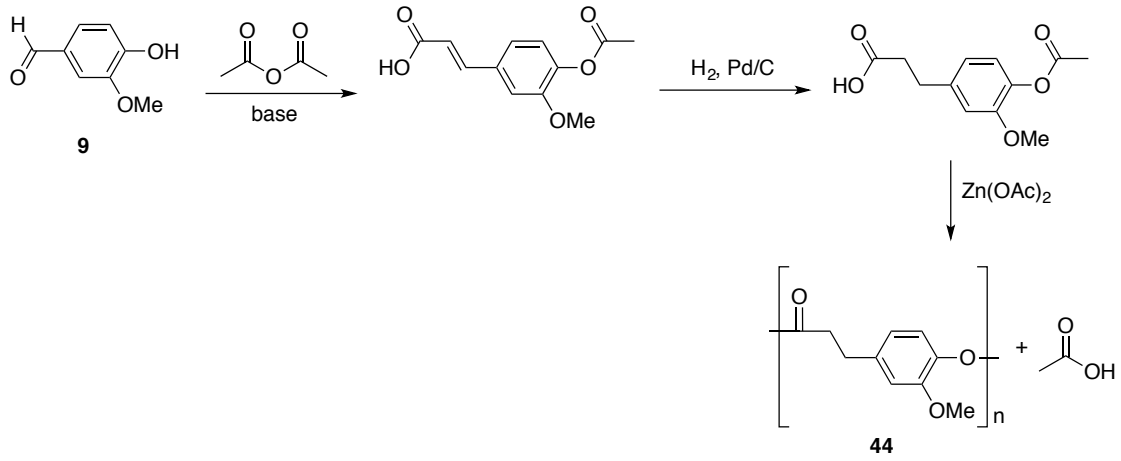

Scheme 1.11: Synthesis of a vanilin-based polyester with PET-like properties.[175]

2 Aim of this work

In the introduction, several approaches for the chemical use of lignin were discussed. It was shown that its modification and use in polymer chemistry is dominated by conventional methods based on petrochemical resources, toxic agents and non-environmentally friendly pathways. However, research for more sustainable pathways is going on. The aim of this work is to present a new sustainable modification method for lignin that allows the introduction of new reactive sites into its structure. Furthermore, it is shown that the modified lignin can be utilized for cross-linked networks to replace conventional thermosetting polymers from petrochemical resources. In all steps, the "12 Principles of Green Chemistry" are considered as guideline. For this study, an organosolv lignin from an ethanol/water pulping was chosen as starting material. This material is an more sustainable alternative to kraft lignin, which is mainly produced in pulp and paper industry. Starting from this lignin, the alkylation of the aromatic and aliphatic hydroxyl groups with dialkyl carbonates is evaluated. Organic carbonates are environmentally friendly alkylation agents that replace alkyl sulfates and halides, which are conventionally used for alkylation of phenols and also of lignin. The reaction is catalytic and produces only carbon dioxide and the alkyl alcohol as side product, which are in turn possible starting materials of dialkyl carbonate synthesis.

For the purpose of lignin modification, model studies with phenolic compounds are performed to gain insight into the influence of the different side chains of the phenols on the alkylation procedure. In preliminary work of Oliver Kreye, unsubstituted phenol and ferulic acid, a lignin derivative, were successfully ethylated, allylated and benzylated with the corresponding dialkyl carbonates. Starting from these results, diallyl and dibenzyl carbonate are used as reagents for the alkylation of different phenols in this work. Substrates with methoxy and alkyl side chains were chosen as these functions represent typical functional groups of lignin.

For lignin, the allylation with diallyl carbonate is studied in detail in this thesis. Different bases, reaction temperatures and reaction time are employed to find optimal reaction conditions. Structural analysis of the modified lignin *via* ^{31}P NMR, ^{1}H NMR, ^{13}C NMR, FT-IR spectroscopy and elemental analysis are discussed in detail. In addition, the use of SEC-MS gives evidence for structural motifs in the unmodified and modified biopolymer and for the first time, mass analysis of lignin fragments are performed.

The reactivity of this allylated lignin is confirmed by performing self-metathesis and cross-metathesis in combination with plant oils as second renewable resource. Moreover, modification of the alkylated lignin towards application in epoxy thermosetting polymers is evaluated.

3 Sustainable alkylation of phenols

Parts of the results in this chapter and associated parts in the Experimental Part were previously published in: O. Kreye, L. C. Over, T. Nitsche, R. Z. Lange, M. A. R. Meier, *Tetrahedron* **2015**, *71*, 293–300.

http://www.sciencedirect.com/science/article/pii/S0040402014016378

3.1 Introduction

Dialkyl carbonates can be used as alternative alkylation agents to replace conventionally used alkyl halides and sulfates. The most studied organic carbonate for this purpose is dimethyl carbonate (DMC, **45**). It is considered as "green" chemical, as it can be obtained *via* sustainable routes and be used as replacement for conventional, toxic reagents and solvents in organic synthesis. Conventionally, it is produced from phosgene. However, industrial relevant sustainable alternatives are known.[177–179] For instance, DMC (**45**) can be obtained directly from methanol (**46**) and carbon dioxide (**47**) or from urea (**48**) and methanol (**46**) (Scheme 3.1a and b). A third method starts from ethylene oxide (**39**) and carbon dioxide (**47**) with the formation of ethylene carbonate (**49**) as intermediate (Scheme 3.1c).

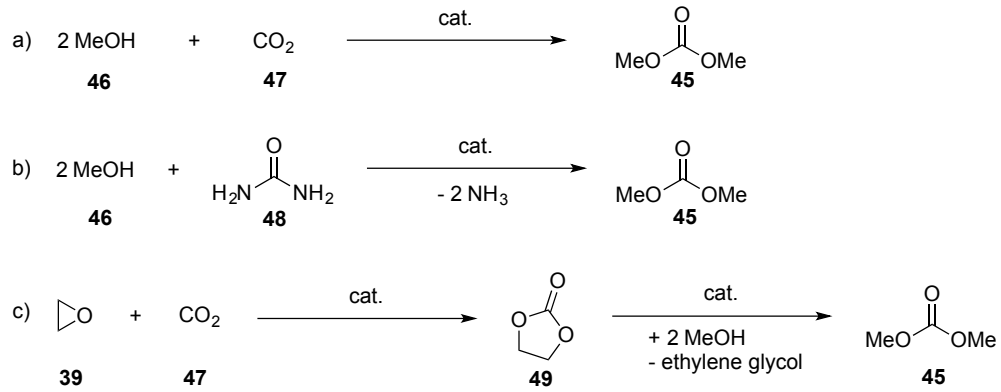

Scheme 3.1: Phosgene-free synthesis alternatives for dimethyl carbonate (DMC, **45**).

DMC (**45**) and its derivatives, *e.g.*, diethyl carbonate (DEC), ethylene and propylene carbonate, are used as "green" solvents in organic chemistry.[177,180] For instance, DMC can substitute chlorinated or aromatic solvents, such as dichloromethane and toluene. FISCHMEISTER *et al.* showed that ruthenium-catalyzed olefin metathesis is was as efficient in DMC as in the conventional solvents.[181] Furthermore, its application as reagent in organic synthesis is versatile. In our group, the activation of hydroxamic acids with DMC to initiate Lossen rearrangements was recently investigated to give sustainable access to methyl carbamates and amines.[182,183] The dimethyl carbamates were further used to synthesize non-isocyanate polyurethanes (NIPUs), a more sustainable approach to

conventional polyurethanes. DMC can further be utilized as methoxycarbonylation or methylation agent. As such, it can be used in chlorine-free synthesis by replacing $SOCl_2$ in the synthesis of methoxycarbonyl derivates or phosgene ($COCl_2$) in the synthesis of organic carbonates.[184] It was demonstrated that dialkyl carbonates are efficiently obtained *via* transesterification of DMC with the corresponding alkyl alcohol and 1,5,7-triazabicyclo[4.4.0]dec-5-ene (TBD) as organocatalyst.[185] In addition, DMC is an already well established methylation agent and thus, represents an eco-friendly alternative to alkyl halides or sulfates, which are conventionally used in *Williamson Ether Synthesis*.[186–190] Compared to these conventional alkylation agents, DMC shows a lower reactivity at low temperatures, one reason for its low toxicity. In addition to the advantages of DMC itself, the procedure can be performed with substoichiometric amounts of a base and the only side products are methanol and CO_2, which are in turn possible starting materials for DMC synthesis. However, for the desired methylation reaction in organic synthesis, increased temperatures are necessary.[184] In Scheme 3.2 a postulated mechanism of *O*-methylation of phenol (**27**) with tetrabutylammonium bromide (TBAB, **50**) as base catalyst is decribed.[189] TBAB deprotonates the phenol to form the phenolate (**51**), which attacks the methyl group of DMC (**45**). Anisol (**52**) is formed, followed by a decarboxylation and the production of CO_2 and methanol as side products.

Besides TBAB, a large variation of bases are discussed as reactive catalysts for the methylation reaction. Depending on the reaction conditions and the catalyst, different products can be formed. Besides *O*-methylation, *C*-methylation or methoxycarbonylation can occur. Most studies concentrate on substrates with few functional groups next to the phenolic hydroxyl group. OUK *et al.* describe the *O*-methylation of phenol, *p*-cresol, 4-chlorophenol, 2-naphthol, the higher substituted eugenol and 2,6-di-*tert*-butyl-4-methylphenol with different bases as catalysts. Among various bases tested, TBAB led to the highest yields at 130 °C and potassium carbonate at 160 °C.[188,189] However, it was observed that multiple functional groups in the molecule and steric hindrance of the phenols led to lower yields. Another active catalyst for *O*-methylation of phenols with DMC is 1,8-diazabicyclo[5.4.0]undec-7-ene (DBU). SHIEH *et al.* reported the *O*-methylation of 1-naphthol, 2,4,6-trichlorophenol, *p*-chlorophenol und 2,6-dimethoxyphenol unter mild conditions with high yields in presence the of DBU. Moreover, they found that microwave irradiation decreased the reaction time significantly.[191] 1,2-Dimethylimidazol (DMI) was shown to be another suitable base for the selective

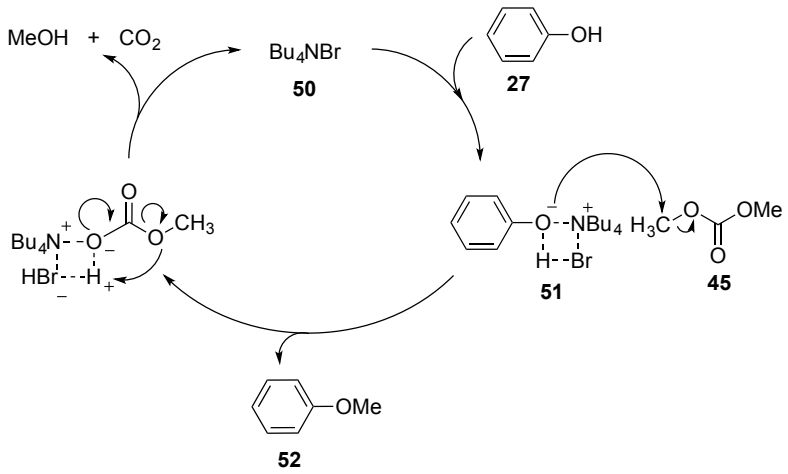

Scheme 3.2: Methylation mechanism of phenol (**27**) with dimethyl carbonate (DMC, **45**).

O-methylation of 4- und 2-hydroxybenzoic acid, 4-hydroxy-3-methoxybenzoic acid and 3-ethoxy-4-hydroxybenzoic acid.[192] SHEN *et al.* reported the selective *O*-methylation of phenols like *o*-cresol, *o*-methoxyphenol, 2,3-dimethylphenol, *p*-chlorophenol, 3-*tert*-butyl-4-hydroxyanisol und 2-naphthol in various ionic liquids as base catalysts.[193] Among the tested ionic liquids at a reaction temperature of 120 °C, 1-*N*-butyl-3-methylimidazolium chloride ([BMIm]Cl) led to the best results, with quantitative yields for the different phenols. In contrast to other bases, even higher substituted phenols were efficiently methylated and selectivities of 100% were achieved, *i.e. C*-methylation could be prevented.

Not only phenolic hydroxyl groups can be methylated with DMC. Alkali metal-exchanged faujasites catalyze the *N*-methylation and *S*-methylation of amines and thiols as well as the *O*-methylation of carboxylic acids with DMC.[194–196] Carboxylic acids react with DMC under the influence of an amine bases, such as DBU or L-methionine, as catalyst to form methyl esters in very good to quantitative yields.[197,198] Aliphatic hydroxyl groups react with DMC under the formation of methyl carbonates instead of methyl ethers. Aliphatic alkoxides are stronger bases than resonance-stabilized phenolic or carboxylic alkoxides and attack the carbonyl-*C* atom instead of the methyl-*C* atom of dimethyl carbonate. Studies with substrates that contain both aliphatic and aromatic hydroxyl groups showed that the reactivity is both temperature and base dependent.[190] Using potassium carbonate, aliphatic hydroxyl groups reacted with DMC at 90 °C to the corresponding methyl carbonate, whereas for the aromatic hydroxyl groups significantly higher temperatures were necessary (165 °C) to react to the methyl ether. With faujasites as catalyst, aliphatic hydroxyl groups tended to form methyl ether.

In the beginning of this work, only few literature was known for other organic carbonates as alkylation agent. Some publications discussed ethylation with diethyl carbonate (DEC),[188,192,199] benzylation with dibenzyl carbonate (DBC),[200] and *tert*-butylation with di-*tert*-butyl carbonate.[201] Our group started to investigate the use of diallyl carbonate as allylation agent. In preliminary work, Oliver Kreye successfully alkylated phenol (**27**) and ferulic acid (**8**) with diethyl (DEC), dibenzyl (DBC) and diallyl carbonate (DAC) using DBU (**53**) as catalyst. The corresponding reactions for the allylation with DAC (**54**) to products **27a** and **8a** are shown in Scheme 3.3. Side products of the reactions are CO_2 (**47**) and allyl alcohol (**55**). As described in Section 1.2, ferulic acid (**8**) can be obtained from lignin degradation and thus can be considered bio-based.[175] In this allylation procedure, both hydroxyl groups, phenolic and carboxylic, are converted to the corresponding allyl ether and allyl ester, respectively. Thus, a difunctional monomer is obtained that can be applied in polymer synthesis, such as acyclic diene metathesis (ADMET, see Section 5.1) or thiol-ene polymerization.[202]

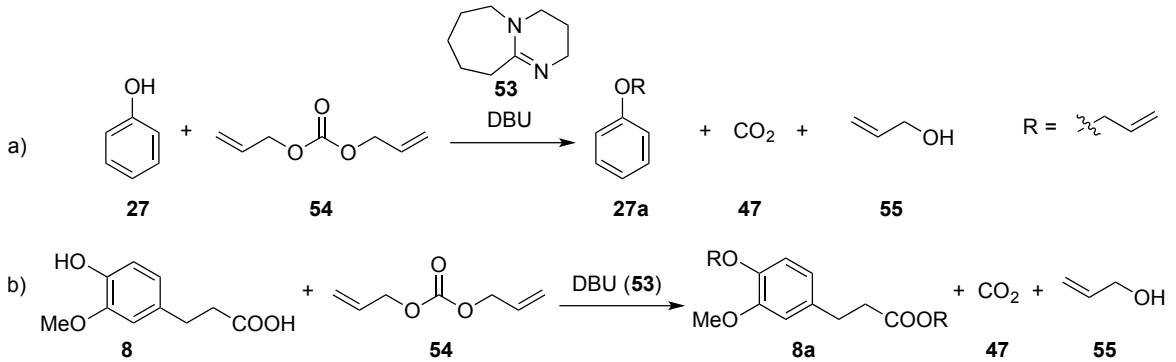

Scheme 3.3: Allylation of a) phenol (**27**) and b) ferulic acid (**8**) with diallyl carbonate (DAC, **54**).

Thiol-ene reaction

Thiol-ene polymerization is an efficient and mild polymerization technique that was used in this work to polymerize allylated diphenols. This reaction is the radical addition of an aliphatic thiol (**56**) to a (mostly terminal) double bond of an alkene (**57**), leading to *anti*-Markownikow products and is known for more than 100 years.[203,204] It can be used to introduce new functional groups, *e.g.*, alcohol functionalities *via* addition of mercaptoethanol or for polymerization of dienes with dithiols. The mechanism consists of two steps (Scheme 3.4).[205] First, a thiyl radical (**58**) is formed *in situ*, which can be initiated by radical starters that are either thermally initiated or photo-initiated. A common thermal initiator is azobis(isobutyronitrile) (AIBN), on the other hand, UV initiation can be performed using dimethoxy-2-phenylacetophenon (DMPA).[206] For highly reactive compounds, no initiator is necessary as it was shown that thiyl radicals are still formed.[207] In the described mechanism, the thiyl radical adds to the alkene (**57**) to form a carbon radical (**59**). This step can be reversible reaction, and thus, allows *cis*/*trans*-isomerization. This newly formed radical subsequently reacts with another thiol in an irreversible reaction to give the thiol-ene addition product (**60**) and forms a new thiyl radical allowing radical chain propagation.

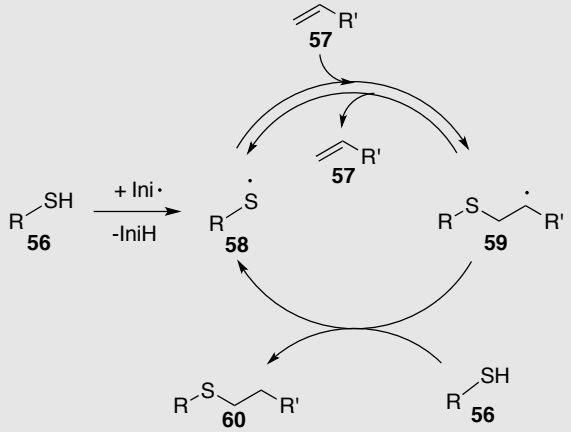

Scheme 3.4: Mechanism of thiol-ene addition.

The widespread use of the reaction can be attributed to its high tolerance towards other functional groups. It can be performed under mild and solvent-free conditions and has a high atom-economy. Modification of monomers as well as synthesis of linear polymers and polymer networks are described *via* thiol-ene chemistry. For instance, thiol-ene addition was discussed as an efficient derivatization and polymerization method for fatty acid derivatives.[206,208–214] Herein,terminal double bonds are more reactive towards thiol-ene addition than internal double bonds. However, also the internal double, for instance of methyl oleate, can undergo thiol-ene reaction.[206] However, in case of methyl oleate regioisomers are formed and therefore terminal alkenes are preferentially used due to the selective formation of *anti*-Markovnikow products.

Thiol-ene chemistry can also be used for dendrimer synthesis.[215–217] For instance, a fourth generation dendrimer starting from a tris-alkene triazine core was synthesized *via* iterative photo-induced thiol-ene addition of 1-thioglycerol and esterification with 4-pentenoic anhydride with high efficiency.[215] Another application of thiol-ene chemistry was evaluated in our group: the synthesis of an AB-type monomer from 10-undecenal and 3-mercaptopropionic acid.[218] The monomer was

further polymerized using Passerini addition polymerization. The sulfurs in the backbone of the polymer could be oxidized afterwards to sulfones to increase the glass transitions temperatures of the polymers. Besides, an iteration of thiol-ene and Passerini addition was evaluated in our group leading to sequence-controlled polymers.[219] This iterative procedure allowed the introduction of different side chains at a desired position of the polymer. HAWKER *et al.* showed the efficient end group and backbone modification with thiol-ene addition of various polymers.[220] Applying a library of different thiols and polymers, the desired thiol-ene products could be obtained in quantitative yield. Furthermore, they observed that thermal initiation with AIBN as radical starter led to lower yields and longer reaction times compared to photoinitiation with DMPA.

Only few examples of thiol-ene chemistry with lignin derivatives/allylated phenols are discussed in literature. GABBASOVA *et al.* converted various allyl phenyl ether *via* thiol-ene addition with hexanethiol and AIBN as initiator in very good to excellent yields.[221] Only sterically hindered *ortho-tert*-butyl phenol led to a lower yield of only 65%. Furthermore, in the group of RITTER, the use of thiol-functionalized 4-alkylphenols synthesized from thiol-ene chemistry of allylated 4-alkylphenols was successfully applied to obtain molecules that were used as chain transfer agents in free-radical polymerization.[222] Recently, a gold-catalyzed hydrothiolation of different alkenes was decribed.[223] This alternative non-radical procedure led to high yields for aliphatic alkenes, however the allyloxy phenol was isolated in only 55% yield.

Salicylic acid and 4-hydroxybenzoic acid are candidates that can be potentially obtained from lignin (compare Section 1.2). ROBERTSON *et al.* describe their allylation with allyl bromide and subsequent photo-induced thiol-ene curing with a tetrathiol cross-linker yielding networks of high thermal stability (>340 °C) and low glass transition temperatures.[224] Besides the above mentioned thiol-ene polymerization of allylated ferulic acid in combination with an oleic acid derived diene and 1,4-butanedithiol,[202] undecenylated vanillin was likewise polymerized *via* thiol-ene chemistry in our group.[225] Using ADMET polymerization, slightly lower molecular weights were obtained from allylated ferulic acid but higher molecular weights from undecenylated vanillin. JOHANSSON *et al.* evaluated the polymerization with allylated coniferyl alcohol, a lignin model substrate, to form cross-linked materials with tris(3-mercaptopropionate) as trifunctional cross-linker.[226] Thermosets with fully converted double bonds were obtained that were stable up 160 °C. More recently, thiol-ene cross-linking of a modified soda lignin was reported.[227] Modification of lignin was performed using an acyl chloride derivative to introduce a maleimide function in the structure of lignin. Thus, an ene component was obtained that was then cross-linked with different di-, tri- and tetrathiols to achieve networks of high cross-linking density and low glass transition temperatures (<20 °C).

Starting from the preliminary alkylation results of Oliver Kreye, a substrate scope of phenols and carboxylic acids was investigated in terms of reactivity towards their alkylation with DAC and DBC. In this chapter, the allylation and benzylation of different phenol derivatives is discussed in detail. For selected phenols, crotylation and undecenylation was likewise investigated. For allylation of phenolic compounds that can serve as models for the renewable material lignin, still only Williamson ether synthesis with allyl halides is discussed in literature.[226,228,229] The allyl function is an interesting group for lignin as it can be the starting point for cross-linking or further modification, such as epoxidation. However, renewability of lignin is not enough, also more sustainable modification pathways should

be considered. The aim of this work was to evaluate the influence of different functional groups in phenols on the alkylation reactivity with dialkyl carbonates to gain insight into the reaction for later application on the biopolymer lignin.

3.2 Results and Discussion

3.2.1 Synthesis of dialkyl carbonates

Synthesis of diallyl (**54**, DAC), dibenzyl (**61**, DBC), dicrotyl (**62**, DCC) and di-10-undecenyl carbonate (**63**, DUC) from DMC (**45**) and the corresponding alcohols allyl alcohol (**55**), benzyl alcohol (**64**), crotyl alcohol (**65**) and 10-undecenol (**66**) was performed using a known procedure (Scheme 3.5).[185] The reaction is catalyzed by 1–5 mol% 1,5,7-triazabicyclo[4.4.0]dec-5-ene (TBD, **67**) at 80–120 °C. Slowly increasing the temperature to 120 °C permits the distillation of evolved methanol (**46**) as side product. However, parts of the starting material DMC may also evaporate, which leads to decreased yields of 52–80%. The hereby synthesized dialkyl carbonates were used as alkylation agents in this work.

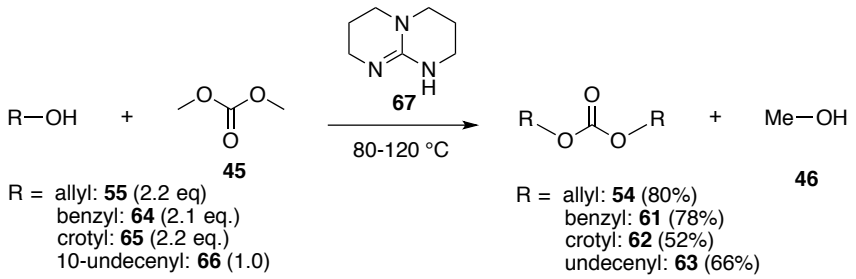

Scheme 3.5: Synthesis of dialkyl carbonates from dimethyl carbonate (DMC, **45**) und the corresponding alkyl alcohols.

3.2.2 Alkylation of phenols as lignin model substrates

Alkylation of phenols with organic carbonates is an effective alternative to Williamson ether synthesis. Based in the preliminary studies of the ethylation, benzylation and allylation of phenol and ferulic acid with the corresponding dialkyl carbonates performed by Oliver Kreye (see introduction of this Chapter), the aim of this work was to analyze the influence of different side groups of phenols and to gain insight into their reactivity and possible side reactions for later lignin application. In the preliminary work, it was already found that DBC (**61**) is more reactive than DAC (**54**) under the same conditions and that the allylated product may undergo *Claisen Rearrangement*. This possibility of rearrangement as side reaction during the allylation caused significantly lower yields for allylation compared to benzylation. An allyloxy benzene (**27a**) can undergo a classical *Claisen Rearrangement*,[230] first forming a cyclohexadienone (**68**), followed by keto-enol tautomerization to form *ortho*-allylated phenol (**69**) (Scheme 3.6). In an additional [3,3]-sigmatropic rearrangement (*Cope Rearrangement*), a *para*-allylated phenol (**70**) can be formed. Proof of the formation of these possible side products during the performed allylation reactions was obtained *via* GC-MS analysis. Additional peaks appeared with identical *m/z* values as the product but deviating retention time. In addition, di- or tri-allylated products were observed. The regenerated phenol function can react a second or third time to form a higher number of side products. The formation of these side products decreases the yields of the allylated phenols. Yet, these results are not hindering the later application to lignin. In contrast, an

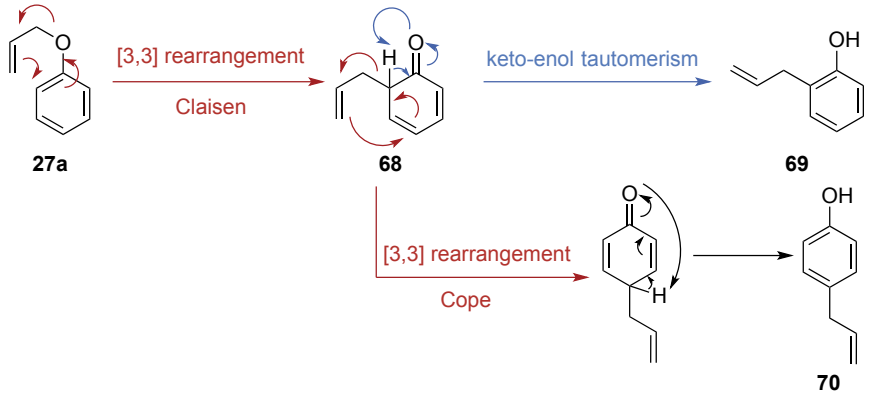

Scheme 3.6: Rearrangement mechanism of allyloxy benzene (**27a**).

even higher alkylation ratio per aromatic unit may be achieved. Here, phenols with different functional groups were chosen to investigate their influence on the reactivity (Figure 3.1). Methoxy, aliphatic and aromatic groups as well as the combination of them are typical functional groups in lignin's structure as well. Thus, the choice of substances promised to be representative models for lignin. The reactivity of DAC (**54**) and DBC (**61**) towards the allylation and benzylation of phenols containing different functional groups was evaluated in detail and will be discussed in the three groups: a) methoxy, b) aliphatic and aromatic group containing and c) multiple group containing phenols (Figure 3.1). For DCC (**62**) and DUC (**63**), only selected reactions were performed. Some of the reactions were performed by Tobias Fischer under my co-supervision in the scope of a six-week internship in our group. The corresponding reactions are marked in the Experimental Part in Section 9.2.2.

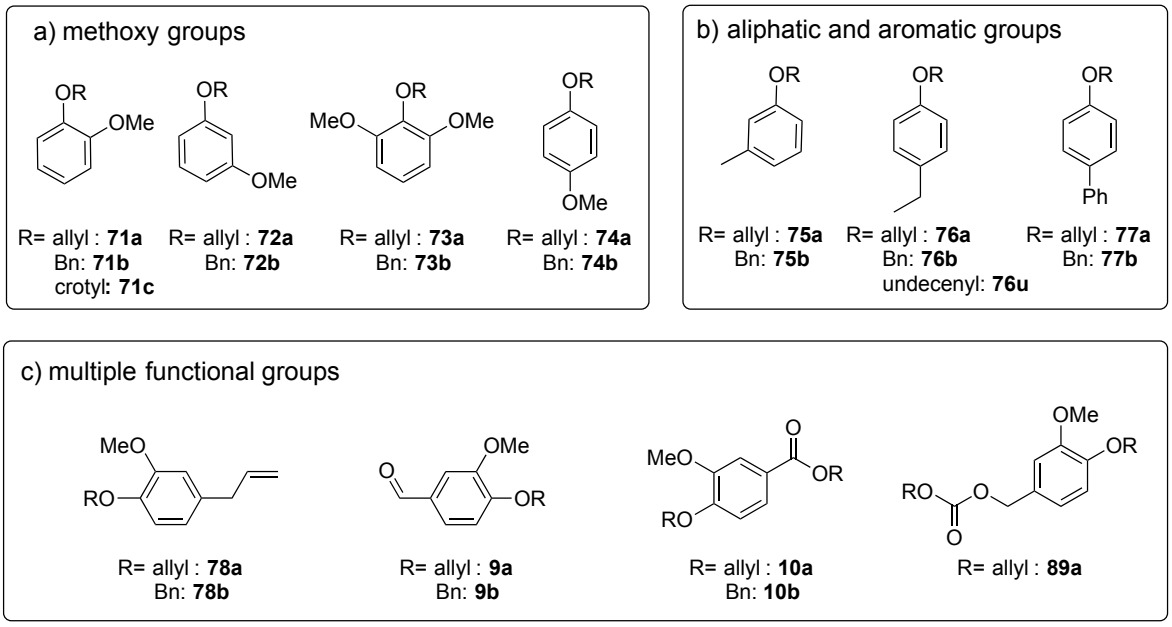

Figure 3.1: Structures of alkylated phenols in this work sorted by the choice of functional groups: a) methoxy, b) aliphatic and aromatic group containing and c) multiple functional group containing alkylated phenols.

Following the concept of sustainable alkylation, two synthetic procedures were evaluated for the allylation and benzylation with DAC (**54**) and DBC (**61**), respectively. Either conventional heating under reflux was performed at 150 °C for 17 hours or the reaction mixture was exposed to microwave irradiation, decreasing the reaction time to 2.5 hours at the same temperature. Alkylated products were obtained in yields of up to 97%, *e.g.*, for allyloxy-4-methoxybenzene (**74a**) (Table 3.1, entry 7). All reactions were followed by GC-MS analysis.

Methoxy group containing phenols. In general, it was found that the alkylation of substituted phenols is accelerated compared to unsubstituted phenol (**27**). As a result, lower temperatures (150 °C instead of 180–220 °C) could be used. Methoxy groups have a +M effect, which leads to a higher electron density in the aromatic ring. This in turn generates a stronger nucleophile in the deprotonated form compared to unsubstituted phenol (**27**). However, for *ortho*-substituted phenolic hydroxyl groups, also the *Claisen Rearrangement* increased. For guaiacol (**71**), which contains a methoxy group in ortho position, a reaction temperature of 130 °C for 5 hours led to a yield of 80% (Table 3.1, entry 1). At 140 °C, the side reaction was significantly faster, leading to an isolated yield of only 62% after 5 hours reaction time. It is known that higher temperatures accelerate *Claisen Rearrangement*.[231] Further decrease of the reaction temperature to 110 °C prohibited *Claisen Rearrangement*. However, only 70% isolated yield was achieved as the conversion of the starting material was still incomplete after 10 hours. For 2,6-dimethoxyphenol (**73**), a yield of only 30% was obtained after 2.5 hours at 150 °C (Table 3.1, entry 5). Compared to the mono-functionalized phenol (**71**), *Claisen Rearrangement* was even more accelerated. Also a decrease in temperature to 140 or 130 °C did not lead to a better result. In GC-MS, the rearranged product was detected. Under the same conditions, the benzylated product 2-benzyloxy-1,3-dimethoxybenzene (**73b**) was isolated in a yield of 90% (Table 3.1, entry 6). In contrast, *para*-methoxyphenol (**74**) was converted to allyloxy-4-methoxybenzene in an isolated yield of 97% (Table 3.1, entry 7). These results indicate that the acceleration of *Claisen Rearrangement* is a results of sterical hindrance from the already present methoxy group in *ortho* position.

Table 3.1: Isolated yields for the allylation and benzylation of different methoxy group-containing phenols with DAC and DBC respectively.

entry	substrate	product	*t* [h]	*T* [°C]	yield [%]
1	guaiacol (**71**)	allyloxy-2-methoxybenzene (**71a**)	5	140	62
			5	130	80
			10	110	70[b)]
2	guaiacol (**71**)	benzyloxy-2-methoxybenzene (**71b**)	17[a)]	150	89
3	3-methoxyphenol (**72**)	1-allyloxy-3-methoxybenzene (**72a**)	2.5	150	65
4	3-methoxyphenol (**72**)	1-benzyloxy-3-methoxybenzene (**72b**)	2.5	150	84
5	2,6-dimethoxyphenol (**73**)	2-allyloxy-1,3-dimethoxybenzene (**73a**)	2.5	150	30
			2.5	140	32
			2.5	130	26[b)]
6	2,6-dimethoxyphenol (**73**)	2-benzyloxy-1,3-dimethoxybenzene (**73b**)	2.5	150	90
7	4-methoxyphenol (**74**)	allyloxy-4-methoxybenzene (**74a**)	2.5	150	97
8	4-methoxyphenol (**74**)	benzyloxy-4-methoxybenzene (**74b**)	2.5	150	90

Condition: Method B (microwave), 150 °C, 2.5 h, 0.2 eq. DBU; [a)] Method A (reflux); [b)] incomplete conversion.

Aliphatic or aromatic group containing phenols. Aliphatic functional groups in *meta* or *para* position led to increased allylation and also *Claisen Rearrangement* activity. For the standard procedure, only 66% of allylated *m*-cresol (**75a**) could be isolated (Table 3.2, entry 1). A decrease of the reaction time to 1.5 hours, increased the yield to 80%. For *p*-ethylphenol (**76**), a reaction temperature of 140 °C and reaction time of 30 minutes led to a yield of 90%. An excellent yield was achieved for the phenol containing a phenyl group, *p*-phenylphenol (Table 3.2, entry 3). 97% of the desired product were isolated after 1.5 hours at 150 °C. The +I effect of aliphatic chains seems to accelerate the *Claisen Rearrangement* more significantly than the +M effect of the phenyl function.

Phenols with multiple functional groups. The combination of different functional groups, such as in eugenol (**78**), vanillin (**9**), vanillic acid (**10**) or vanillic alcohol (**79**), led to significantly lower yields and further optimization was necessary. For instance, eugenol showed very low conversion with DBU or potassium carbonate and led to poor allylation yields (Table 3.2, entry 7). However, benzylation with DBU and potassium carbonate was likewise decreased (Table 3.2, entry 8). Therefore, rearrangement could not have caused the low yield of allylated product. It was found that dimethylimidazole (DMI) was an effective base for benzylation. The product could be isolated in a yield of 87% after 2 hours at 150 °C. However, DMI was not suitable for the allylation. The reaction temperature had to be decreased to 130 °C to avoid *Claisen* and *Cope Rearrangement* of the allylic product and the initial allyl function, respectively. Under these conditions, tetrabutylammonium bromide (TBAB) led to the best result with an isolated yield of 75% after 3 hours and full conversion (Table 3.2, entry 7).

Table 3.2: Isolated yields for the allylation and benzylation with DAC and DBC, respectively, of different phenols containing aliphatic or aromatic functional groups.

entry	substrate	product	base	*t* [h]	*T* [°C]	yield [%]
1	*m*-cresol (**75**)	**75a**	DBU	2.5	150	66
			DBU	1.5	150	80
2	*m*-cresol (**75**)	**75b**	DBU	2.5	150	93
3	4-ethylphenol (**76**)	**76a**	DBU	0.5	140	90
4	4-ethylphenol (**76**)	**76b**	DBU	2.5	150	97
5	4-phenylphenol (**77**)	**77a**	DBU	1.5	150	97
6	4-phenylphenol (**77**)	**77b**	DBU	17[a)]	150	95
7	eugenol (**78**)	**78a**	DBU	2	130	10
			K_2CO_3	5	130	26
			K_2CO_3	3	130	62[c)d)]
			DMI	2	150	low[b)]
			TBAB	3	130	75
8	eugenol (**78**)	**78b**	DBU	2.5	160	low[b)]
			K_2CO_3	2.5	160	66
			DMI	2	150	87
			TBAB	2.5	160	low[b)]
9	vanillin (**9**)	**9a**	TBAB	5	110	49
10	vanillin (**9**)	**9b**	DBU	17[a)]	150	47
11	vanillic acid (**10**)	**10a**	TBAB[c)]	1	130	62
12	vanillic acid (**10**)	**10b**	TBAB[c)]	1	130	44
13	vanillin alcohol (**79**)	**79a**	TBAB	27[e)]	90	33

Condition: Method B (microwave), 150 °C, 2.5 h, 1.5 eq. dialkyl carbonate per OH, 0.2 eq. DBU; [a)] Method A (reflux); [b)] low conversion, not isolated; [c)] with addition of DMSO as solvent; [d)] 17% starting material isolated; [e)] 10 eq. DAC, Method C (pressure tube).

Still, rearranged derivatives were observed as side products in GC-MS. Vanillic acid and vanillic alcohol, both compounds with two possible reactive sides, were successfully converted to the desired products but in poor yields. An issue could be the reactivity of the formed ester and carbonate. For instance, 10 equivalents of DAC were used for the allylation of vanillic alcohol as with lower amounts, a mixture of undefined products was found and no desired product formation was observed.

In summery, the allylation and benzylation studies showed that the use of organic carbonates is an effective and sustainable alternative to Williamson ether synthesis. The procedure can be applied to phenols with variable functional groups. However optimization studies are necessary for substrates with different functional groups.

Use of other dialkyl carbonates. Furthermore, the application of two additional alkylation agents, namely DCC (**62**) and DUC (**63**) was studied. Here, DCC showed a similar reactivity compared to DAC for the alkylation of guaiacol. The desired product crotyloxy-2-methoxybenzene (**71c**) was isolated in a yield of 85% after 20 hours at 120 °C under reflux condition. The formed crotyloxy product can undergo a *Claisen Rearrangement* as well (Scheme 3.7). The rearranged product (**80**) was detected in GC-MS with the same *m/z* value as the desired product. In addition, signals of the allylic protons H^f and H^g of the rearranged product (**80**) appeared in ^{1}H NMR at 5.00 and 6.04 ppm (Figure 3.2). By integration of the allylic double bonds and comparison with the integral of the desired internal double bond signals of H^b and H^c, the percentage of rearranged product can be calculated. In a temperature study, NMR analysis showed that at 120 °C almost no rearrangement product (**80**) was present after 18 hours (Table 3.3, entry 1). Increasing the temperature to 130, 140 and 150 °C, increased the side product ratio to 6, 11 and 18%, respectively, calculated by NMR integration (Table 3.3, entries 2–4).

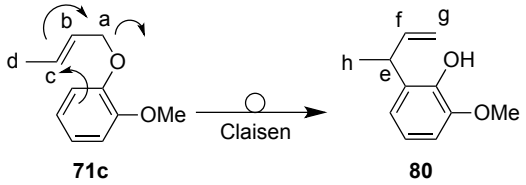

71c **80**

Scheme 3.7: Rearrangement mechanism of crotyloxy-2-methoxybenzene (**71c**).

Table 3.3: Side reaction study for the crotylation of guaiacol (**71**).

entry	*T* [°C]	time [h]	side product (NMR) [%]
1	120	18	~0
2	130	21	6
3	140	21	11
4	150	21	18

Condition: guaiacol (1.00 mmol) was reacted with DCC (2.44 mmol, 1.2 equ.) and TBAB (0.406 mmol, 0.2 equ.) in a pressure tube. ^{1}H NMR measurement was performed after washing procedure (see work-up section 9.2.2).

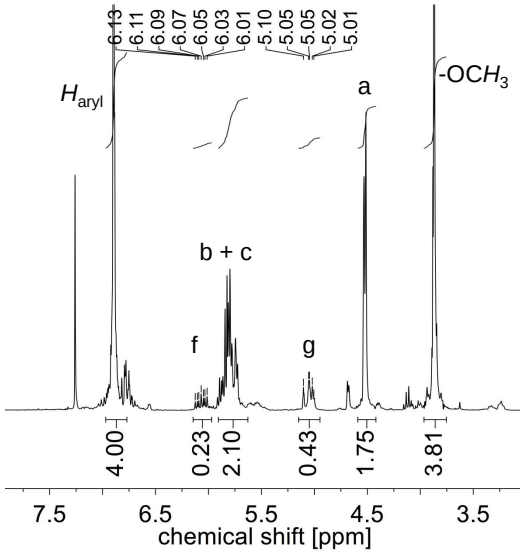

Figure 3.2: ^{1}H NMR of product mixture from the crotylation of guaiacol after washing.

Di-10-undecenyl carbonate (DUC) is another interesting alkylation agent as its starting material 10-undecenol is a commercially available castor oil derived molecule and thus renewable.[232] However, it was found that the reactivity of DUC was significantly lower than the one of the previously tested carbonates DAC, DBC and DCC. Reaction temperatures of 120–150 °C led to no conversion for the tested phenols, vanillin (**9**) and 4-ethylphenol (**76**) (Table 3.4, entry 1 and 2). However, a higher reaction temperature of 220 °C led to a successful conversion of 4-ethylphenol (**76**). Herein, 59% of the desired product were isolated after 4 hours at 220 °C (Table 3.4, entry 3). In contrast, guaiacol showed still very low conversion after 8 hours at 220 °C (Table 3.4, entry 4). Exposing vanillin and vanillic alcohol to the conditions, insoluble, black materials were obtained (Table 3.4, entries 5 and 6). Most probable the conditions were to harsh for the aldehyde in vanillin and the formed carbonate in vanillin alcohol may also led to further reaction.

Table 3.4: Reaction optimization of the undecenylation of phenols with DUC.

entry	substrate	product	pase	*t* [h]	*T* [°C]	yield/result [%]
1	vanillin (**9**)	**9u**	TBAB	7	120–150	no conversion
2	4-ethylphenol (**76**)	**76u**	DBU	3	130	no conversion
3	4-ethylphenol (**76**)	**76u**	DBU	4	220	59
4	guaiacol (**71**)	**71u**	DBU	8[a)]	220	low conversion
5	vanillin (**9**)	**9u**	DBU	4	220	polymer
6	vanillic alcohol (**79**)	**79u**	DBU	4	220	polymer

[a)] Method C (pressure tube).

3.2.3 Polymers from stilbene derivatives

Parts of this section and associated parts in the Experimental Part were previously published in:
A. S. Trita, L. C. Over, J. Pollini, S. Baader, S. Riegsinger, M. A. R. Meier, L. J. Goossen,
Green Chem. **2017**, *19*, 3051–3060.

http://pubs.rsc.org/en/content/articlelanding/2017/gc/c7gc00553a

3.2.3.1 Allylation of stilbene derivatives

The established allylation procedure, discussed in detail in Section 3.2.2, was then applied to diphenols. This work was developed in cooperation with Stefania Trita and coworkers in the group of Prof. Dr. L. J. Gooßen (Ruhr-Universität Bochum). The cooperation partners found a new method to prepare stilbene derivatives from bio-based eugenol (**78**) and 3-(non-8-enyl)phenol (**81**) from cashew nut shell liquid (CNSL) (Scheme 3.8).[233] The first step consists of an isomerizing metathesis at the alkene chain of the phenols. Here, an isomerizing catalyst $[Pd(\mu\text{-Br})(^{t}Bu_3P)]_2$ (**Pd-1**) was used in combination with a metathesis catalyst, Umicore M51 (**M51**) or Umicore M73 SIPr (**M73 SIPr**), to give the methoxy (**82**) and hydroxy stilbene (**83**). In isomerizing metathesis, a stepwise shortening of olefinic side chains takes place.This concept was previously applied for the synthesis of tsetse fly attractant from CNSL.[234] In a second step, the stilbenes were hydrogenated with palladium on carbon or activated charcoal to give the methoxy (**84**) and hydroxy diphenol (**85**). These four monomers were starting point of further modification in our group. The aim of this work was to synthesize polymers

with similar characteristics to polymers from the conventionally used bisphenol A (BPA). As polycarbonates are a typical application for BPA, the herein described diphenols should be investigated as alternative precursors. Thiol-ene polymerization was chosen as second type of polymerization. Therefore, allylation of the diphenols was necessary. In first studies, the synthesized monomers were tested in polymerization and the molecular weight distributions and thermal properties of the corresponding polymers were characterized.

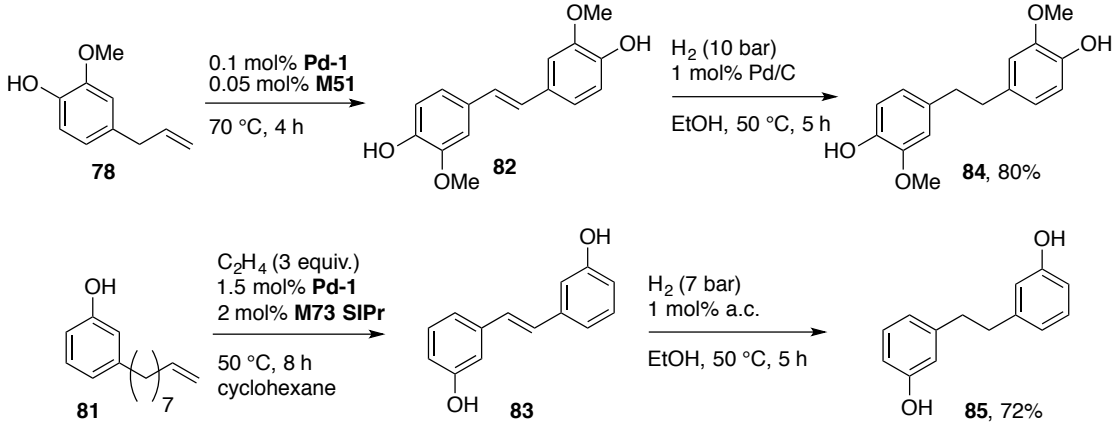

Scheme 3.8: Isomerizing metathesis of eugenol (**78**) and 3-(non-8-enyl)phenol (**81**) to stilbene derivatives **82** and **83** followed by hydrogenation to **84** and **85** performed in the group of Prof. Dr. L. J. Gooßen. Pd-1: $[Pd(\mu\text{-}Br)(^tBu_3P)]_2$; a.c.: activated charcoal.

Within the scope of his bachelor thesis under my co-supervision, Sven Riegsinger allylated the four compounds with diallyl carbonate (Scheme 3.9).[235] The reactions were performed with four equivalents of DAC and one equivalent TBAB for a successful diallylation at 120 °C for 20 hours under reflux conditions. The excess of DAC and TBAB could be recovered during work-up. As discussed for the phenols in Section 3.2.2, also the evaluated diphenols show a trend to lower yield if a methoxy group is located in *ortho* position to the phenolic hydroxyl group. The sterically hindered eugenol-based methoxy compounds **82a** and **84a** were isolated in very good yields of 84 and 89%, respectively. Excellent yields over 90% were achieved for the CNSL-based monomers **83a** and **85a**. In addition, Sven Riegsinger did preliminary studies for the following polycarbonates and thiol-ene polymers. Further optimization of the procedure led to the here discussed results that were obtained in the scope of the present work and published in a joint article with the cooperation partners from Ruhr-Universität Bochum.[236]

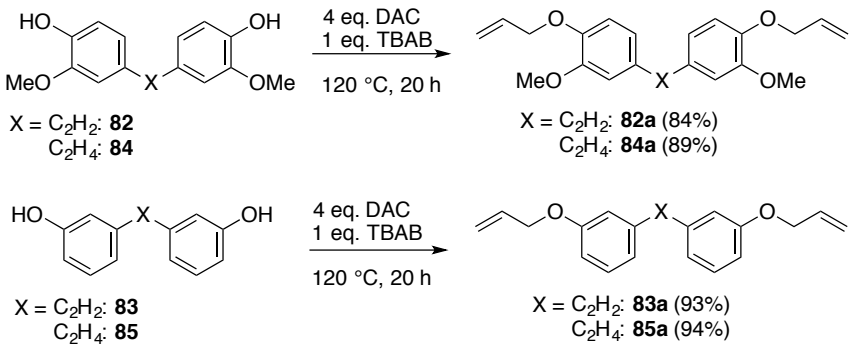

Scheme 3.9: Allylation of stilbene derivatives with DAC.

3.2.3.2 Polycarbonates

Due to their similar structure, the synthesized stilbene derivatives were investigated as alternative for BPA in polycarbonate synthesis. Polycarbonates were chosen as possible polymer application as they are a typical example for the use of BPA. A mild method with diphenyl carbonate (**86**) instead of conventionally used phosgene was applied to increase the sustainability of the procedure. The polymerization was carried out in substance at 180 °C with lithium hydroxide as catalyst (Scheme 3.10 for the representative reaction of **82** with **86** to form polycarbonate **PC82**). The formed phenol (**27**) evaporated at this temperature and was thus removed from the reaction mixture.

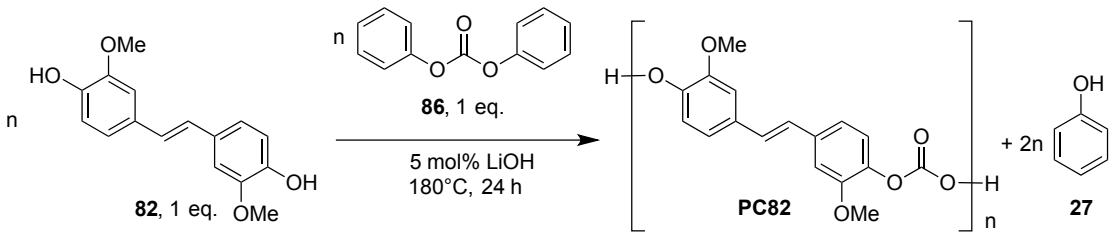

Scheme 3.10: Polycarbonate formation of methoxy compound **82** with diphenyl carbonate.

Table 3.5 summarizes the properties of the synthesized polycarbonates from the stilbene derivatives (**82**, **84**, **83**, **85**) and BPA (**14**) as reference substrate. Average number molecular weight distributions (M_n) and their dispersities ($Đ$) were obtained from size-exclusion chromatography (SEC) in tetrahydrofuran (THF). The two methoxy monomers (**82** and **84**) and the hydrogenated hydroxyl monomer (**85**) showed similar reactivity, which is shown by the similar M_n after the full reaction time of 24 hours (Table 3.5, entry 1, 3 and 4). The obtained M_n values ranged from 2200 to 3500 g/mol. Dispersities ($Đ$) vary between 1.5 and 2.0, as can be expected for a step-growth polymerization. Although the reactivity of the monomers towards polycarbonate formation is significantly lower than the one for BPA (**14**), the M_n and dispersities show that the monomers can be used for polycarbonate formation. Under the same conditions, BPA led to a polymer **PC14** that was insoluble in THF. In order to allow a comparison with the bio-based polycarbonates, the reaction time for BPA was reduced to 3 hours, affording **PC14**-2 with a M_n in the desired range (Table 3.5, entry 6). The CNSL-derived monomer **83** led to THF-insoluble polymer already after 40 min, which could not be analyzed by SEC. Cross-linking of the stilbene double bond could be excluded due to the different behavior of the methoxy stilbene (**82**). In addition, no radical sources or very high temperatures (> 320 °C) were present implicating the cross-linking of unsaturated polymers.[237,238] This means that the hydroxyl group in *meta*-position to the stilbene double bond is more activated compared to the hydroxyl group in *meta*-position to the hydrogenated, aliphatic side chain as well the hydroxyl group in BPA, which is in *para*-position to the aliphatic group. A reason for the lower reactivity of the methoxy compounds may be the sterical hindrance of the hydroxyl group.

Thermal properties, such as melting points and glass transition temperature, depend on the chemical structure of the polymer as well as on the molecular weight. Thus, only polymers with similar M_n can be compared, especially for rather low-molecular weight materials as obtained here. The melting points of polycarbonates **PC82**, **PC84** and **PC85** were below 150 °C, whereas the BPA-based polymer **PC14**-2 with similar M_n melted at 224–228 °C, a difference attributable to structural factors. The glass transition temperature (T_g) ranged from 25 °C for **PC85** to 127 °C for **PC82** for the polymers with M_n of 2000–3500 g mol^{-1}. Eugenol-based polymer **PC84** showed a T_g of 81 °C,

in agreement with literature reports.[239] This temperature is comparable to that of **PC14**-2 at similar molecular weight, indicating a similar rigidity of the two polymers. Rigid polymer backbones and bulky side chains lead to high T_g values.[240,241] Hydrogenation of the stilbene increased the flexibility of the chain reflected by a decrease in T_g and melting point of polymer **PC84** compared to its unsaturated equivalents **PC82**. Steric hindrance in the proximity of the hydroxyl group could be a reason why eugenol-derived polymer **PC84** presents higher T_g than its CNSL equivalent **PC85**. For **PC83** and **PC85**, melting points and T_g are hard to compare due to differences in the M_n. All polymers showed semicrystalline behavior, which is typical for PCs precipitated from methanol.[242] All polymers posses of excellent degradation temperatures ($T_{d\,5\%}$). For materials with a similar molecular weight range, the $T_{d\,5\%}$ of **PC84** (319 °C) is closest to that of the BPA-based polymer **PC14**-2 (314 °C). **PC82** and **PC85** have slightly lower degradation temperatures, but the values for all polycarbonates are within a narrow range between 292 and 332 °C. Raised degradation temperatures increasing the molecular weight are expected.[243]

Overall, polymers with a wide range of thermal properties were obtained. The reactivity of the monomers and characteristics of the polymers are promising in terms of a possible substitution of bisphenol A, but intensive future research will be required to ultimately prove this.

Table 3.5: Summary of the analytical results of polycarbonates precipitated in methanol.

entry	polymer	M_n [°C]	$Đ$ [°C]	T_m [g/mol]	T_g	$T_{d\,5\%}$ [°C]
1	**PC82**	2800	2.0	146 – 148	127	305
2	**PC83**	-[a)]	-[a)]	258 – 262	160	313
3	**PC84**	3500	1.5	106 – 108	81	319
4	**PC85**	2200	1.6	143 – 146	25	292
5	**PC14**	- [a)]	-[a)]	280 – 290	115	332
6[b)]	**PC14**-2	2700	1.3	224 – 228	79	314

[a)] insoluble in THF; [b)] 3 h reaction time; properties of materials precipitated from methanol, see Experimental Part for details.

3.2.3.3 Thiol-ene polymerization

To complete the study, a second polymer category was investigated. Thiol-ene polymerization is an efficient, sustainable polymerization methodology due to mild conditions and high conversion.[244,245] The allylation of the diphenols with diallyl carbonate was descibed in the beginning of this section. The thiol-ene polymerization was carried out stirring the allylated monomer with an equimolar amount of decane-1,10-dithiol (**87**) and 2.5 mol% of the radical initiator azobis(isobutyronitrile) (AIBN) under argon atmosphere at 75 °C for 5 hours (Scheme 3.11, for the example of the hydrogenated methoxy derivative **84a**).

The properties of the thiol-ene polymers and the analogous BPA-based reference polymer **PTE14** are summarised in Table 3.6. It was observed that the hydrogenated hydroxyl monomer (**85a**) had the highest reactivity. The liquid mixture became viscous already after 30 min reaction time and yielded to the highest molecular weight of 16000 g/mol (Table 3.6, entry 4). The corresponding non-hydrogenated monomer (**83a**) led to a significantly lower molecular weight of 3100 g/mol (Table 3.6,

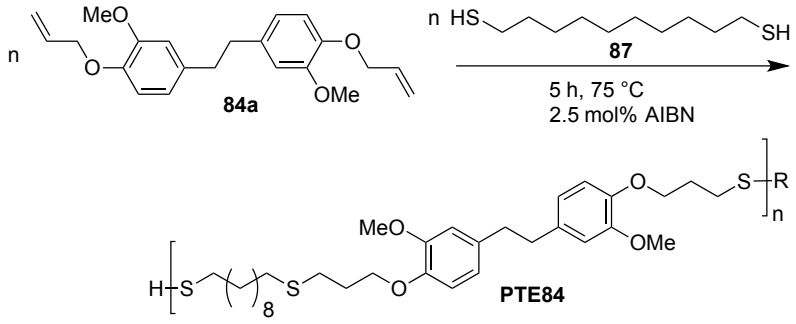

Scheme 3.11: Thiol-ene polymerization of hydrogenated methoxy compound **84a** and decene-1,10-dithiol (**87**) to the corresponding polymer **PTE84**.

Table 3.6: Summary of the analytical results of thiol-ene polymers precipitated in methanol.

entry	polymer [℃]	T_m [℃]	M_n [g/mol]	$Đ$	$T_{d\,5\%}$ [℃]
1	**PTE82**	25 – 50	2700	1.7	301
2	**PTE83**	25 – 50	3100	7.1	316
3	**PTE84**	25 – 50	4300	3.0	336
4	**PTE85**	25 – 50	16600	5.3	311
5	**PTE14**	rt	5200	3.6	270

entry 2). The broad dispersity ($Đ$ = 5.3) of polymer **PTE83**, as well as a broadening of the ^{1}H NMR peaks (see Experimental Part), indicated that cross-linking took place. This assumption is supported by the same observation for the non-hydrogenated methoxy thiol-ene polymer (**PTE82**), but with a lower reactivity (shown by lower M_n), which may be explained by the increased steric hindrance of the *ortho*-methoxy group in **82a**. The allylated CNSE derivative **83a** is liquid at room temperature, whereas the eugenol counterpart **82a** has a melting point of 141 ℃, making the reaction in bulk impossible. For the polymerization of **82a**, additional solvent was required and consequently, the lower concentration could also decrease the obtained molecular weight obtained. For the polymerization of compound **84a** no additional solvent was necessary due to its lower melting point at 91 ℃. However, the molecular weight was relatively low with 4300 g/mol (Table 3.6, entry 3) but similar to the one obtained from allylated BPA (**14a**, Table 3.6, entry 5) which indicated a similar reactivity.

All thiol-ene polymers showed similar thermal properties, with degradation temperatures ranging from 270 ℃ in the case of **PTE14** to 336 ℃ for **PTE84**. The stilbene derivatives (**PTE82**, **PTE84**, **PTE83**, **PTE85**) possess melting points between 25 and 50 ℃. The BPA-based polymer was liquid at room temperature. In addition, no recrystallization of the samples could be observed in the DSC traces cooling down to -50 ℃ as the samples needed two days at room temperature to recrystallize.

The results obtained in the thiol-ene polymerization point to another potential application of these monomers derived from renewable resources. The saturated monomers are suitable for linear polymers, whereas cross-linking in the stilbene-based monomers may allow their use in resins. Comparing these results to those for PCs described above, a wide range of properties may be achieved. Unsurprisingly, the thiol-ene polymers were obtained in higher molecular weights due to better solubility during polymerization as well as less steric hindrance of the monomers employed. These preliminary investigations suggest that the prepared polymers from renewable resources have promising prop-

erties, but further investigations are clearly required to assess the mechanical properties of the bulk materials.

In addition to the evaluation of potential use for polymer applications, the estrogenicity of the monomers was tested by the group of Prof. Dr. L. J. Gooßen. The yeast estrogen screen (YES) test revealed that the methoxy group containing monomers **82** and **84** are significantly less estrogenic than BPA (**14**), whereas the CNSL derivatives **83** and **85** posses similar estrogen activity as **14**.[236] These results are important, as they show that the eugenol-derived monomers did not only lead to similar polymerization behavior as BPA, but are in addition more harmless considering the estrogenicity.

3.3 Conclusion and Outlook

In this chapter, the alkylation with organic carbonates was discussed as effective alternative to Williamson ether synthesis. The conditions of the procedure were optimized using GC-MS and GC analysis. Alkylated phenols could be isolated in excellent yields up to 98%. Compared to unsubstituted phenol, it was shown that alkylation with organic carbonates is accelerated by alkyl, aryl or methoxy substituents. The allylation and crotylation with DAC (**54**) and DCC (**62**), respectively, showed Claisen rearrangement as side reaction. It was found that due to sterical effects, *ortho*-substituted phenols showed higher tendency to rearrangement. In this case, lower temperatures could decrease the side reaction and thus increase the yield. Whereas diallyl carbonate (DAC, **54**), dibenzyl carbonate (DBC, **61**) and dicrotyl carbonate (DCC, **62**) showed high reactivity, di-10-undecenyl carbonate (DUC, **63**) was shown to be inefficient und not suitable as alkylation agent for all phenols. For highly reactive 4-ethylphenol (**76**), the desired undecenylated product **76u** could be obtained in a yield of only 59%. There is still a potential for optimization. However the results from allylation and crotylation promise excellent adaptability for more complicated structures such as lignin.

In a second part, four different diphenolic stilbene derivatives (**82**, **83**, **84** and **85**), that were isolated from renewable resources by a cooperation partner, were investigated for polymer application. The established allylation procedure with DAC (**54**) could be successfully transferred to the difunctional monomers. The diphenolic and the diallyl monomers were applied in polycarbonates and thiol-ene polymers, respectively. It could be shown that thermal properties of the synthesized polymers are promising bio-based, easy-accessible alternatives for bisphenol A. However, future investigation of mechanical properties are necessary to complete the study.

4 Alkylation of organosolv lignin

Parts of this chapter and associated parts in the Experimental Part were previously published in:
L. C. Over and M. A. R. Meier, *Green Chem.* **2016**, *18*, 197–207.

http://pubs.rsc.org/en/Content/ArticleLanding/2016/GC/c5gc01882j

4.1 Introduction

Besides cellulose and chitin, lignin is one of the most abundant biopolymers on earth.[15] With a content of 15–30 wt%, lignin is a main component of biomass such as wood and annual plants. The total lignin resources on earth are estimated to be 300 billion tons, with a natural production of 20 billion tons per year.[16] Thus, it is a very attractive renewable resource and – especially with regard to the production of aromatic compounds – probably the most promising alternative to petroleum-based materials.[246] Most of the available lignin is isolated through chemical pulping of wood during the production of fibrous chemical pulps, *e.g.*, for paper production. However, there are only few commercial applications of lignin-derived products. Most of the isolated lignin, mainly kraft lignin, is burned for energy recovery. Thus, the energy demand of the pulp mill can be covered, but lignin is not used as a valuable raw material. Organosolv pulping represents an eco-friendly alternative to the kraft process[31] and is mainly used in lignocellulose biorefineries (see Section 1.1.3 for more pulping processes).

Lignin has a complex cross-linked structure with variably linked phenylpropanoid units, wherein the three main building blocks are: sinapyl alcohol (**1**), coumaryl alcohol (**2**) and coniferyl alcohol (**3**) (see Section 1.1.2 for more details). The unique chemical structure qualifies lignin for many possible applications. On the one hand, the complex structure of lignin could be fragmented to prepare diverse aromatic platform chemicals such as benzene, toluene, xylene (BTX chemicals) or vanillin derivatives, which could replace identical products from petrochemistry.[29,63,246] On the other hand, the macromolecular structure of lignin can be used for the preparation of polymeric materials. Herein, many possible applications are proposed in the literature; for instance, the use of lignin as polyol for polyurethanes[247–249] or as phenol substitute in phenolic resins.[135,250] Furthermore, lignin can be used in blends to increase mechanical stability or biodegradability.[145] The use of lignin in polymer chemistry is discussed in detail in Section 1.3.

Although the potential of lignin as renewable raw material is often discussed, economically competitive processes are required for industrial substitution of petroleum oil. As unmodified lignin forms instable, unreactive and insoluble materials at high temperatures and extremely acidic or basic conditions,[251] lignin is often modified prior to polymerization. One well-known modification is the oxyalkylation of lignin with propylene oxide to reduce the brittleness and to improve the viscoelastic proper-

ties.[104] A more sustainable oxyalkylation was recently presented by LEHNEN *et al.*[158] using propylene carbonate. Conventional alkylations of phenols are performed using methyl halides and dimethyl sulfates (Williamson ether synthesis).[252] The Williamson ether synthesis is also described for the *O*-methylation of the phenolic hydroxyl groups in lignin to increase its thermal stability.[105] Using allyl bromide, ZOIA *et al.* obtained an allylated lignin that could undergo Claisen rearrangements.[228] However, the used reagents are toxic and not environmentally benign. Moreover, stoichiometric amounts of a base are required. In contrast, the use of dialkyl carbonates would allow a sustainable, non-toxic and environmentally friendly modification of the phenolic building blocks of lignin – an already well-established method for low molecular weight phenolic substances (*e.g.*, phenol, naphtol, *o*-/*p*-cresol, eugenol).[188,189,253–255]

Recently, ARGYROPOULOS *et al.*[156] applied this methylation method to acetone-soluble softwood kraft lignin thereby increasing the thermal stability of lignin. For lignin[156] as well as for diverse model compounds,[190] it is described that aliphatic hydroxyl groups are converted to carboxymethylated structures at lower temperatures (~90 °C) by a nucleophilic attack at the carbonyl C atom of the carbonate, whereas aromatic hydroxyl groups are etherified to yield methoxy groups above reaction temperatures of 120 °C due to a nucleophilic attack at the methyl group. Moreover, the ethylation,[188,199] and benzylation[200] of phenols with diethyl carbonate (DEC) and dibenzyl carbonate (DBC) is described. In Chapter 3 the highly efficient etherification of different phenols using DBC and diallyl carbonate (DAC) in the presence of substoichiometric amounts of 1,8-diazabicyclo[5.4.0]undec-7-ene (DBU) was discussed.

In this chapter, the sustainable, solvent-free and non-toxic allylation of beech wood organosolv lignin (OL, **88**) with diallyl carbonate to obtain an allylated lignin is described. The product was thoroughly characterized *via* ^{1}H, ^{13}C, ^{31}P NMR and IR spectroscopy, as well as detailed mass analysis, and can serve as monomer for further polymerization.

4.2 Results and discussion

The utilized OL (**88**) was isolated *via* an ethanol–water pulping at the Thünen Institute of Wood Research and used without any further fractionation (for details, see Experimental part, Section 9.3.1). The SEC analysis of OL in THF revealed a number average molecular weight M_n of 1200 g mol^{-1} with a dispersity $Đ$ of 3.1 (Table 4.1). ^{31}P NMR studies were performed according to a procedure described by ARGYROPOULOS *et al.* with 2-chloro-4,4,5,5-tetramethyl-1,2,3-dioxaphospholan (TMDP) as phosphorylating agent and cyclohexanol as internal standard to obtain the absolute amount of hydroxyl groups (Figure 4.1).[256] Aliphatic hydroxyl groups can be found between 150.0 and 145.5 ppm, whereas the signals of aromatic hydroxyl groups are located between 144.6 and 137.0 ppm. The quantitative analysis revealed an amount of 3.83 mmol aliphatic and 2.23 mmol aromatic hydroxyl groups per gramm of the isolated OL (**88**). The ratio of the syringyl to guaiacyl units is 1.65 (determined by ^{13}P NMR studies), implying that in average every C_9 unit should contain 1.33 methoxy groups. From these results and the elemental analysis, a C_9 formula can be proposed, $C_9H_{7.1}O_{1.2}(OH)_{1.2}(OMe)_{1.3}$, which is comparable to similarly isolated lignin.[158]

Table 4.1: Analytic data of the isolated OL (**88**) from SEC, ^{31}P NMR and elemental analysis.

M_n	$Đ$	$X_{OH}^{aliph.}$	$X_{OH}^{arom.}$	Syringyl units	Guaiacyl units	X_{OH}^{total}	C	H	N	O[a)]
[g mol^{-1}]		[mmol g^{-1}]	[mmol g^{-1}]	[mmol g^{-1}]	[mmol g^{-1}]	[mmol g^{-1}]	[%]	[%]	[%]	[%]
1200	3.1	3.83	2.23	1.39	0.84	6.06	61.53	6.15	0.26	32

[a)] calculated by difference to 100

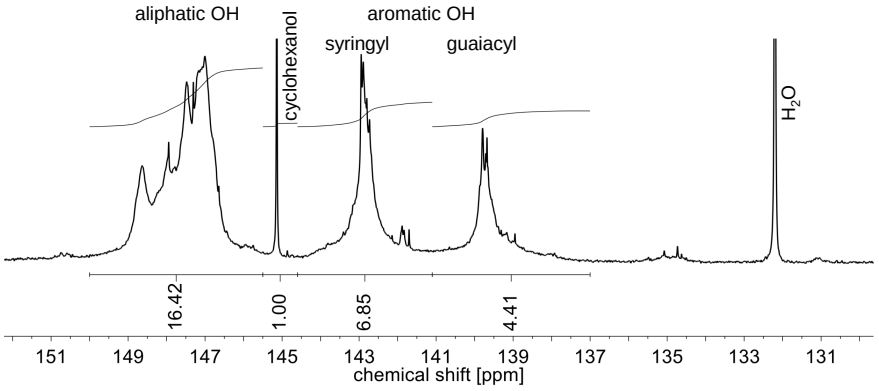

Figure 4.1: ^{31}P NMR spectrum of unmodifed OL with 2-chloro-4,4,5,5-tetramethyl-1,2,3-dioxaphospholan as phosphorylating agent and cyclohexanol as internal standard.

4.2.1 Solvent influence on the allylation of organosolv lignin using different bases

The optimization of the allylation reaction of OL (**88**) was performed using DAC (**54**) as reagent and solvent, elevated temperatures and different bases in varying amounts. In this section the influence of an additional co-solvent is discussed. The resulting product (**89**) of this allylation reaction contains etherified aromatic hydroxyl groups and carboxyallylated aliphatic hydroxyl groups (Scheme 4.1).

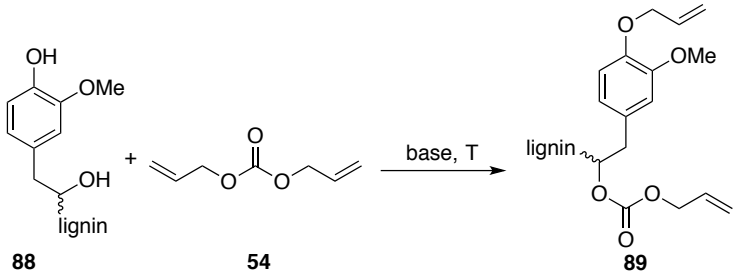

Scheme 4.1: Allylation of OL with DAC resulting in the etherification of aromatic hydroxyl groups and the carboxyallylation of the aliphatic hydroxyl groups.

In first studies, the solvents dimethyl formamide (DMF), dimethyl sulfoxide (DMSO) and dimethyl acetamide (DMAc) were tested for the allylation procedure. Potassium carbonate (K_2CO_3) and DBU were used as bases, since they have been shown to promote the efficient allylation of diverse phenols with diallyl carbonate (see Chapter 3). Products from allylation attempts of OL (**88**) were analyzed by ^{1}H NMR and in case of successful allylation, the conversion of the hydroxyl groups (X_{OH}) was determined by ^{31}P NMR studies. Additionally, the allylated products were analyzed by SEC measurements to determine the number average molecular weight M_n and the dispersity $Đ$ in order to investigate degradation or cross-linking of the substrate. The results for the solvent screening are shown in Table 4.2. All reactions were performed at 120 °C with ten equivalents of DAC. It was found that most of the products were insoluble in THF after isolation, independent of the used solvent (Table 4.2, entries 1, 2, 4, 11, 13, 15 and 17). For the use of K_2CO_3 as base, products were soluble if no solvent was added but no allylation was observed (Table 4.2, entries 3 and 5). Using DBU as base, a succesful allylation was observed in DMSO (Table 4.2, entries 6 and 12). Already after five hours, a conversion of 85% of all hydroxyl groups was achieved according to ^{31}P NMR analysis. After 24 hours, the conversion was 95%. In DMAc, an proceeded allylation of OL could be observed but the product was not completely soluble anymore (Table 4.2, entry 18). Without a solvent, no desired product was obtained with DBU, but only THF-insoluble solids. A reason may be the poor miscibility of DBU in DAC. During the reactions without solvent, agglomeration was observed, which may have led to intramolecular reaction of lignin and thus badly soluble products.

Although, no allylation was observed in absence of a base or DAC, an increase in molecular weight was found for all isolated products compared to unmodified OL (1200 g mol^{-1}). In literature, a side reaction of lignin with DMSO is postulated (Scheme 4.2).[156] DMSO forms an activated species in the presence of a base (**90**). Aliphatic hydroxyl groups in lignin (**88**) can attack the sulfur atom of the activated species. The intermediate **91** reacts in an intramolecular second nucleophilic attack to form the product **92**. This reaction does not explain an increase in molecular weight, yet. However, due to the ring strain, the formed product **92** is unstable and could be attacked by another nucleophil such as a second lignin molecule to form a dimer, ultimately leading to cross-linking.

Table 4.2: SEC (THF) results and conversion from ^{31}P NMR for the solvent influence on the allylation of OL (**88**).

Entry	Time [h]	Base (eq.)	Solvent	M_n [g mol^{-1}]	$Đ$	$X_{OH}^{aliph.}$ [%]	$X_{OH}^{arom.}$ [%]	X_{OH}^{total} [%]
DMF								
1	5	K_2CO_3 (0.5)		1700[b)]	3.6	[b)]		
DMSO								
2	5	K_2CO_3 (0.5)		2200[b)]	2.9	[b)]		
3	5	K_2CO_3 (0.5)	– [a)]	2000	3.3	x	x	x
4	5	K_2CO_3 (2)		2000[b)]	4.5	[b)]		
5	5	K_2CO_3 (2)	– [a)]	1500	2.6	x	x	x
6	5	DBU (2)		1300	2.2	85	84	85
7	5	DBU (2)	– [a)]	1100	2.6	[c)]		
8	5	K_2CO_3 (2)	no DAC	2000	2.5	x	x	x
9	5	–	no DAC	1900	2.8	x	x	x
10	5	–		1600	2.8	x	x	x
11	24	K_2CO_3 (2)		1800[b)]	3.8	[b)]		
12	24	DBU (2)		900	1.9	92	100	95
DMAc								
13	5	K_2CO_3 (0.5)		1700[b]	2.7	[b)]		
14	5	–	– [a)]	2400	3.2	x	x	x
15	20	K_2CO_3 (0.5)		1700[b)]	3.1	[b)]		
16	20	K_2CO_3 (0.5)	no DAC	2000	2.3	x	x	x
17	20	K_2CO_3 (0.5)	– [a)]	2000[b)]	2.5	[b)]		
18	20	DBU (0.5)		2000	2.4	85[c)]	57	75
19	20	–	no DAC	1900	2.6	x	x	x

Conditions: OL (**88**) (0.915 mmol OH) was dissolved in 900 µL of the solvent and mixed with DAC (**54**) (9.15 mmol). The specified amount of the base was added at the reaction temperature. The solution was stirred for 5 – 24 h at 120 °C in a 15 mL pressure tube. [a)] without solvent; [b)] product was not completely soluble in THF, no NMR analysis was performed; [c)] product was neither completely soluble in DMSO-d_6 nor in pyridine/$CDCl_3$(1.6:1); x: no allylation observed in ^{1}H-NMR.

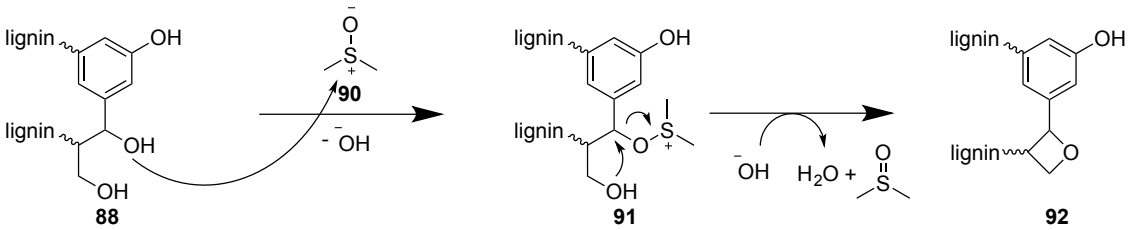

Scheme 4.2: Postulated side reaction of lignin with DMSO according to ARGYROPOULOS *et al.*[156]

4.2.2 Optimization of the allylation of organosolv lignin using different bases

Due to the solubility issues and possibility of a side reaction, a solvent-free reaction was evaluated. For the allylation of OL under neat conditions in a pressure tube with an excess of DAC, the range of bases was expanded (Table 4.3). Besides K_2CO_3[186,190,253,257] and DBU,[191] also cesium carbonate (Cs_2CO_3)[255] and TBAB[189] are discussed in literature for efficient alkylation of diverse phenols with dialkyl carbonates. Sodium hydroxide was already described for the *O*-methylation of acetone soluble kraft lignin.[156] In the solvent-free allylation of OL using potassium carbonate, cesium carbonate and sodium hydroxide, no functionalization was observed (Table 4.3, entries 1–12). For these three bases, regardless of the amount used, no new signals appeared in the allyl region of the respective ^{1}H NMR spectra. The obtained M_n values of these products varied between 1500 and 2000 g mol^{-1} and were thus slightly higher than for the unmodified OL (M_n = 1200 g mol^{-1}). However, the SEC curves hardly differed from the curve of the unmodified lignin (Figure 4.2). Only with NaOH as the base, a shift towards lower molecular weights was observed, a possible sign of degradation.

Allylations using DBU as a base usually resulted in insoluble products (Table 4.3, entries 13–16). A key problem is that OL (**88**) itself is not soluble in DAC but in DBU, thus, agglomeration takes place during the reaction, which hinders a good stirring of the reaction mixture. However, using two equivalents of DBU, the product was soluble in THF and could be analyzed via SEC. Results (Figure 4.2) were similar to that of the starting material, but the ^{1}H NMR showed new signals in the allyl region between 4.0 and 6.0 ppm. However, the allylation could not be quantified using ^{31}P NMR, since the product was not completely soluble in $CDCl_3$/pyridine or in DMSO-d_6. Anyway, due to the similar SEC curve, the amount of allylation must have been rather low. Thus, DBU was shown to be a suitable base only for the reaction in a solvent – such as DMSO – but not under the desired solvent-free conditions.

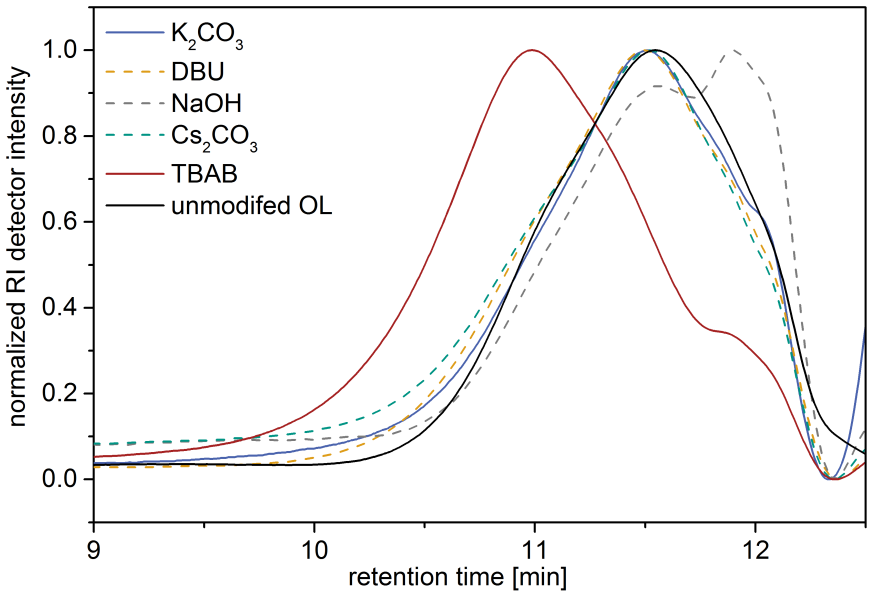

Figure 4.2: SEC traces for organosolv lignin and the reaction products of the allylation with different bases. Reaction conditions: 10 eq. DAC, 2 eq. base, 5 h, 120 °C.

With TBAB as a base, an efficient allylation under solvent-free conditions could be obtained (Table 4.3, entries 17–20). The M_n values ranged between 1,900 and 2,700 g mol^1. Thus, a significant shift towards higher molecular weights was observed (Figure 4.2). The ^{31}P NMR studies revealed the quantitative conversion of phenolic hydroxyl groups after five hours using only 0.5 equivalents of the base, though the conversion of the aliphatic hydroxyl groups was significantly lower (Table 4.3, entry 19). With 0.2 equivalents of TBAB, a very low conversion was observed (Table 4.3, entry 20). However, increasing the amount of TBAB (1–2 equivalents) enabled high conversion of both aliphatic and aromatic hydroxyl groups of OL (Table 4.3, entries 17 and 18). The efficient functionalization of OL using TBAB could be attributed to the high phase transfer activity of this ammonium salt. In contrast to the other bases, OL was instantly dissolved after the addition of TBAB, which resulted in a homogenous reaction mixture and enabled an efficient allylation reaction. Besides its phase transfer activity in this reaction, TBAB shows catalytic activity towards the alkylation of phenols with dialkyl carbonates. THIÉBAUD *et al.* published a plausible mechanism for the methylation with dimethyl carbonate, where TBAB deprotonates the phenol forming a complexed phenolate that attacks the methyl group of DMC.[189] A similar reactivity is conceivable for the reaction with DAC.

4.2.3 Optimization of the allylation of organosolv lignin with TBAB

TBAB was shown to be the most efficient base among the tested bases for the allylation of OL. Thus, additional studies were carried out to optimized the reaction conditions. Herein, the conversion of the hydroxyl groups was monitored for different reaction times and different reaction temperatures (Table 4.4). An extension of the reaction time at 120 °C from 3 to 5 or 15 hours did not lead to any further increase of the conversion (Table 4.4, entries 2, 6 and 10). Already after three hours, 88% of all hydroxyl groups of OL were converted, regardless whether one or two equivalents of TBAB per hydroxyl group were used. With 0.5 equivalents of TBAB, the reaction was significantly slower and a reaction time of 15 hours was required to obtain a conversion of 86% (Table 4.4, entry 4). Contrary to the results obtained with DBU, the addition of DMSO as solvent did not lead to any further increase of the conversion. After 24 hours, the conversion of the aliphatic hydroxyl groups was even 10% lower compared to the reaction without a solvent after 15 hours (Table 4.4, entries 1 and 2). The same observation was made for the reactions performed with and without solvent in a time frame of five hours, which indicated that the use of a solvent is disadvantageous (Table 4.4, entries 5 and 6). A reduction of the reaction temperature from 120 °C to 100 °C or 90 °C led to lower conversions for both aliphatic and aromatic hydroxyl groups, and longer reaction times (Table 4.4, entries 13–18). It is well established for DMC that the aliphatic hydroxyl groups react preferentially at 90 °C compared to phenolic hydroxyl groups.[190] This selectivity between the different kinds of hydroxyl groups was not observed using DAC and lignin. The aromatic hydroxyl groups still reacted preferentially at a reaction temperature of 90 °C. Shorter reaction times did not lead to progressive allylation; after one hour at 120 °C with 0.5 equivalents TBAB only 23% of all hydroxyl groups were converted.

Table 4.3: SEC and ^{31}P NMR studies of the allylation of OL using different bases.

Entry	Eq. of base	M_n [g mol^{-1}]	$Đ$	$X_{OH}^{aliph.}$ [%]	$X_{OH}^{arom.}$ [%]	X_{OH}^{total} [%]
K_2CO_3						
1	2	1500	2.6	x	x	x
2	1	1700	3.0	x	x	x
3	0.5	2000	3.3	x	x	x
4	0.2	1900	2.9	x	x	x
Cs_2CO_3						
5	2	1600	3.0	x	x	x
6	1	1500	2.6	x	x	x
7	0.5	1700	3.1	x	x	x
8	0.2	1500[a)]	3.1	[a)]		
NaOH						
9	2	1600	2.9	x	x	x
10	1	1700	2.9	x	x	x
11	0.5	1700	2.9	x	x	x
12	0.2	1600	3.1	x	x	x
DBU						
13	2	1100	2.70	[b)]		
14	1	1200[a)]	2.5	[a)]		
15	0.5	900[a)]	2.2	[a)]		
16	0.2	900[a)]	2.1	[a)]		
TBAB						
17	2	2700	3.5	84	100	90
18	1	2400	3.7	79	100	87
19	0.5	2100	3.8	55	99	71
20	0.2	1900	3.8	18	29	23

Conditions: OL (**88**) (0.915 mmol OH) was suspended in DAC **54** (9.15 mmol) and the specified amount of the base was added at the reaction temperature. The solution was stirred for 5 h at 120 °C in a 15 mL pressure tube. [a)]Product not completely soluble in THF. [b)] Product not completely soluble in $CDCl_3$/pyridine for NMR analysis; x: no allylation observed in ^{1}H NMR.

Table 4.4: SEC and ^{31}P NMR studies of the allylation of OL with TBAB at different temperatures.

Entry	Time [h]	TBAB [eq.]	M_n [g mol^{-1}]	$Đ$ [g mol^{-1}]	$X_{OH}^{aliph.}$ [%]	$X_{OH}^{arom.}$ [%]	X_{OH}^{total} [%]
120 °C							
1	24[a)]	2	2100	3.4	72	99	82
2	15	2	2100	3.1	81	100	88
3	15	1	2100	3.4	79	99	87
4	15	0.5	2300	4.2	78	99	86
5	5[a)]	2	2300	3.5	76	99	85
6	5	2	2700	3.7	84	100	90
7	5	1	2400	3.8	79	100	87
8	5	0.5	2100	3.8	55[b)]	99	71
9	5	0.2	1900	3.8	18	29	22
10	3	2	1700	3.4	82	100	88
11	3	1	1800	3.6	79	100	87
12	3	0.5	1800	4.7	68	100	80
100 °C							
13	15	2	1600	3.6	76	99	84
14	15	1	2100	4.1	67	100	79
15	5	2	1900	3.8	65	100	78
16	5	1	1700	3.4	13	66	33
17	5	0.5	1700	2.7	11	31	19
18	3	2	2400	2.9	25	88	49
19	3	1	1700	2.9	14	35	22
20	3	0.5	1700	2.8	16	22	19
90 °C							
21	15	2	1800	4.1	65	100	78
22	15	1	2000	3.5	50	99	68
23	5	2	2500	2.7	14	65	33
24	5	1	2100	2.8	17	39	25
25	5	0.5	1800	2.3	23	24	24

Conditions: In a 15 mL-pressure tube OL (0.915 mmol OH) was suspended in DAC (9.15 mmol) and the specified amount of TBAB was added at the reaction temperature. [a)] DMSO was added as solvent; [b)] product not completely soluble in THF.

4.2.4 Sustainability of the allylation procedure for lignin

To increase the sustainability of the reaction, it was tried to lower the amounts of the reagents. Using only 0.2 equivalents of TBAB, the reaction was poorly catalyzed and the solubility of OL in DAC was decreased, which further indicates the phase transfer catalyst activity of TBAB. Nevertheless, the relatively high amount of at least 0.5 equivalents of TBAB per hydroxyl group was almost completely recovered (97%) from the aqueous phase after precipitation of the product and separation by filtration. The recovered TBAB was used for other allylation reactions of OL without any further purification. After five hours at 120 °C, a conversion of all hydroxyl groups in OL of 85% was obtained (with 0.5 equivalents of the recycled TBAB), which is comparable to the reaction using commercial TBAB (Table 4.4, entry 8). Furthermore, the amount of DAC could be decreased. In a reaction with five or three equivalents of DAC per hydroxyl group (instead of ten), similar conversions were obtained. DAC itself can be considered as green reagent, since it is non-toxic and can be synthesized from DMC in a sustainable pathway (see Section 3.1). The recovery of DAC from the reaction mixture was possible *via* extraction or distillation. Although only 60% of the DAC could be recovered in this way, this increases the overall sustainability of the procedure.

4.2.5 Analysis of the allylated organosolv lignin

^{1}H NMR spectroscopy. The allylation of lignin was followed by ^{1}H NMR spectroscopy in DMSO-d_6 (Figure 4.3). The newly emerging proton signal between δ = 6.3 and 5.8 ppm can be assigned to the proton H^b of the allyl function and the proton signal of the terminal CH_2 is located between δ = 5.7 and 4.8 ppm, whereas the newly emerging proton signal between δ = 4.7 and 4.2 ppm can be assigned to the internal CH_2 group. Assuming that the amount of the aromatic protons does not change during the reaction, the integrals perfectly fit to the assigned functional group. It has to be noted that the integral of the methoxy groups between δ = 3.0 and 3.5 ppm decreased after the allylation due to an overlap with the signal of the aliphatic hydroxyl groups before the reaction. Whether the hydroxyl groups were etherified or carboxyallylated cannot be distinguished by ^{31}P or ^{1}H NMR studies. Therefore, further analytical experiments were carried out.

FT-IR spectroscopy. In order to study the allylation process in more detail, IR analysis was performed before and after the reaction of OL with DAC and TBAB (Figure 4.4). The distinctive broad band of the O–H bond stretching vibration at $\tilde{\nu}$ = 3100 to 3700 cm^{-1} almost completely disappeared after the reaction. Interestingly, a new signal appears at $\tilde{\nu}$ = 1745 cm^{-1}, which is typical for a C=O bond stretching vibration contained in carbonates. This carbonate must have been formed *via* carboxyallylation of the aliphatic hydroxyl groups. The bands of the internal aromatic C=C double bond stretching vibrations are observed in both spectra at $\tilde{\nu}$ = 1592 and 1510 cm^{-1} as well as the deformation vibration of the methoxy groups at $\tilde{\nu}$ = 1460 and 1410 cm^{-1}. The out of plane deformation vibration of the newly formed $CH{=}CH_2$ is observed at $\tilde{\nu}$ = 990 and 910 cm^{-1}.

^{13}C NMR spectroscopy. ARGYROPOULOS *et al.* showed that, using 1,3,5-trioxane as internal standard, it is possible to perform a quantitative ^{13}C NMR analysis of lignin.[57] This method was applied to allylated OL without determining T1 of the system and adapting the parameters for exact quantitative results. Thus, it was possible to compare the unmodified and allylated OLs relative to each other in a straightforward fashion. In the product sample, new signals of the allyl function appear at δ = 137.5–130.5 ppm for C^B (4.6 mmol g^{-1} by difference to the starting material), at δ = 116.0–118.0 ppm (raised

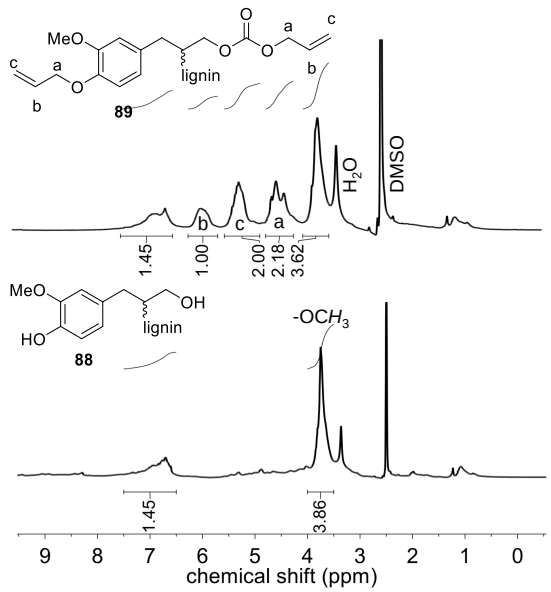

Figure 4.3: ^{1}H NMR spectra of unmodified OL (**88**, bottom) and allylated OL (**89**, top) in DMSO-d_6 (δ = 2.50 ppm). The signal at δ = 3.33 ppm results from the water present in the deuterated solvent.

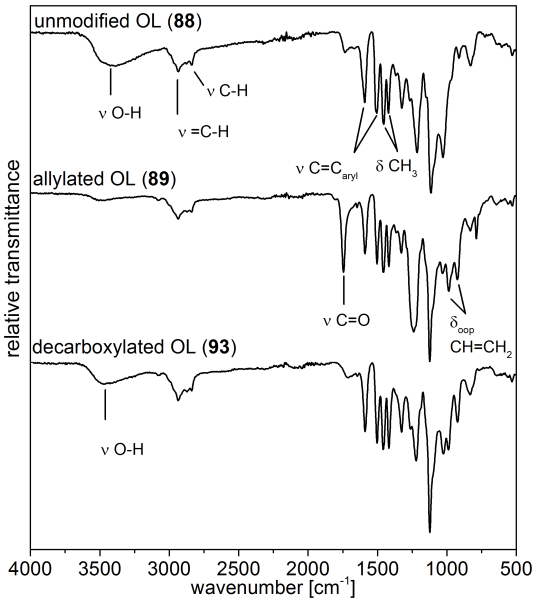

Figure 4.4: FT-IR spectra (ATR) before (top) and after (middle) the allylation of lignin with DAC as well as after decarboxylation (bottom).

about 4.2 mmol g^{-1}) for C^{C} and at δ = 67.0–74.0 ppm for C^{A} (raised about 4.3 mmol g^{-1}) (Figure 4.5). If compared to the initial OL, the relative increase of the integrals with a ratio of approximately 1:1:1 perfectly fit to the introduced allyl function in the product. The ^{13}C NMR spectrum of the unmodified lignin shows a signal at δ = 60.0 ppm, which is typical for aliphatic alcohols (1.5 mmol g^{-1}). This signal almost completely disappeared in the spectrum of the allylated lignin (0.1 mmol g^{-1}). Furthermore, the integrals of the signals related to the carbon content of the *O*-bonded aromatic ^{13}C atoms C^3 and C^4 between 140.0 and 155.0 ppm stayed constant during the reaction (6.0–6.2 mmol g^{-1}). For the non-substituted C^2 and C^3, with a signal between 108.2 and 102.2 ppm, a decrease from 3.9 to 2.6 mmol g^{-1} was observed. This decreased amount of aromatic carbons per gram may be explained by the increase of the total amount of carbons after modification. The same observation is found for the methoxy groups, which show a signal between 57.3 and 54.2 ppm (decrease from 7.0 to 5.7 mmol g^{-1}). Relatively to the methoxy carbons, it is observed that the integral between 140.0 and 155.0 ppm increased (Figure 4.5). Figure 4.5 also shows that besides the *O*-bonded aromatic ^{13}C atoms C^3 and C^4, additional carbon signals appear. An explanation could be the formation of carboxyallylated products, which include carbonyl C atoms that could be referred to the signal around 155.0 ppm.

4.2.6 Decarboxylation reaction as a proof of carbonate formation

For methylations using DMC, it is well established that aliphatic hydroxyl groups are converted to methyl carbonates whereas aromatic hydroxyl groups are etherified.[156,190] In Chapter 3, it was shown that phenol model substances can selectively be converted to allyl ethers using DAC. To verify whether the aliphatic hydroxyl groups in lignin were converted into ether groups or if they were carboxyallylated with DAC, product **89** was treated with LiOH to cleave the potentially formed carbonates (Scheme 4.3). The obtained defunctionalized lignin (**93**) was analyzed by ^{31}P NMR, ^{1}H NMR

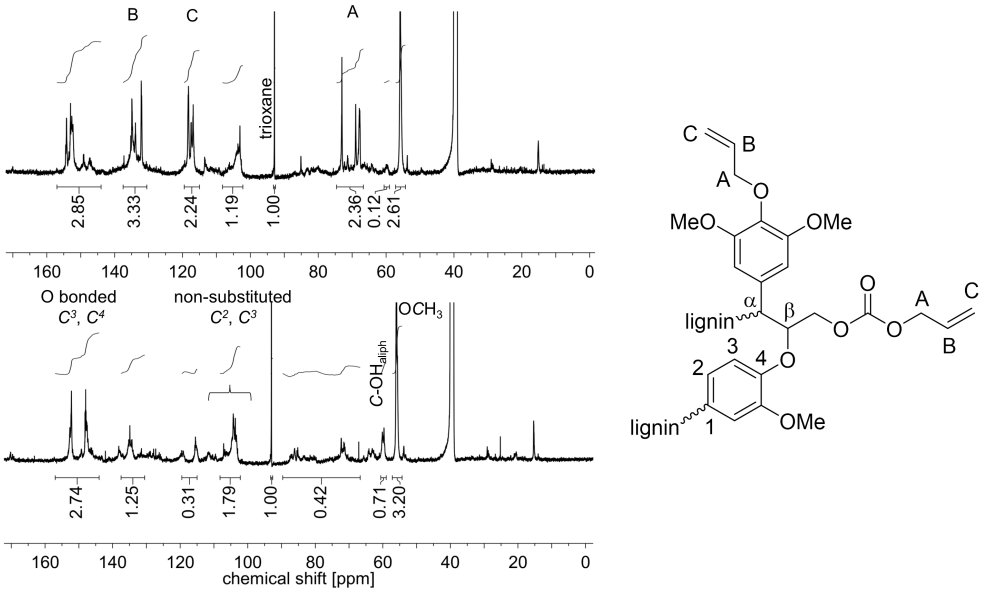

Figure 4.5: ^{13}C NMR spectra of unmodified OL (**88**, bottom) and allylated OL (**89**, top) with 1,3,5-trioxane as internal standard (92.9 ppm) in DMSO-d_6 and the structure of allylated OL of two β-*O*-4 linked C_9 fragments. The spectrum of unmodified OL **88** was integrated relatively to the internal standard 1,3,5-trioxane at 93.0 ppm.

and IR spectroscopy. ^{31}P NMR analysis revealed that after the treatment with LiOH only 24% of the aliphatic hydroxyl groups in the decarboxylated product (**94**) were still allylated, whereas 71% were allylated before. The content of aromatic hydroxyl groups remained unchanged; thus, the conversion of the aromatic hydroxyl groups before and after the treatment with LiOH was determined equally to 99% (Table 4.5). Moreover, the ^{1}H NMR revealed that the integral of the allyl protons decreased after the treatment with LiOH relatively to the unchanged aromatic protons. Thus, this data show that the aliphatic hydroxyl groups at least partially underwent a carboxyallylation, whereas the aromatic hydroxyl groups were completely etherified. For further verification, the modified lignin was studied by IR analysis before and after treatment with LiOH (Figure 4.4, bottom). Here, the signal of the O–H bond stretching vibration between $\tilde{\nu}$ = 3100 and 3700 cm^{-1} increased after the treatment with LiOH (Figure 4.4) if compared to the allylated OL. Furthermore, the signal related to the C=O bond stretching vibration of the carbonate at $\tilde{\nu}$ = 1740 cm^{-1} almost completely disappeared after the treatment with LiOH, indicating that this signal was induced by the formed carbonates. All in all, conclusive NMR and IR analysis clearly revealed that besides the etherification of the aromatic hydroxyl groups, the aliphatic hydroxyl groups of lignin were mainly converted into allyl carbonates.

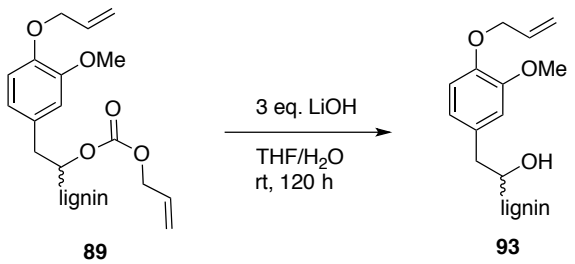

Scheme 4.3: Decarboxylation of allylated lignin (**89**) using LiOH.

Table 4.5: Percentage of converted (allylated) hydroxyl groups due to ^{31}P NMR analysis after the allylation and after the performed decarboxylation.

	$X_{OH}^{aliph.}$ [%]	$X_{OH}^{arom.}$ [%]	X_{OH}^{total} [%]
After allylation of OL	71	99	82
After treatment with LiOH	24	99	54

Conditions for the decarboxylation: allylated OL and LiOH (2 eq. per original OH) were stirred in THF/H_2O, at room temperature for 120 h.

4.2.7 Thermal properties of allylated organosolv lignin

DSC and TGA studies were carried out to investigate the thermal properties of the allylated OL compared to the unmodified OL. It was shown that the glass transition temperature is decreased with an increased allylation grade (Figure 4.6a). The unmodified OL shows a glass transition temperature at 120 °C. After allylation of around 90% of the hydroxyl groups, the glass transition decreased to 70 °C, whereas with a conversion of 33% the glass transition temperature decreased to 95 °C. DSC analysis showed a novel exothermic transition in the sample of the allylated product, which occurs between 180 and 250 °C, depending on the allylation grade, that is not present in the unmodified OL (Figure 4.6b).

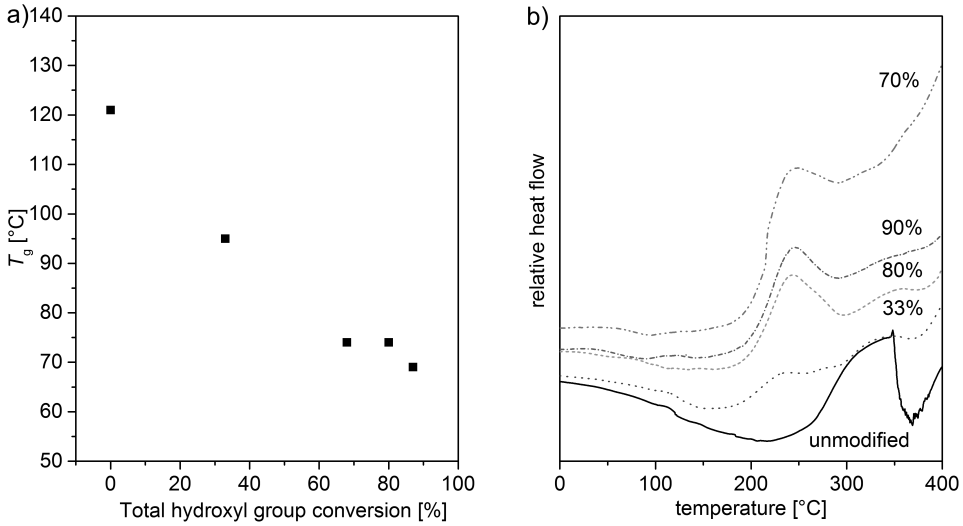

Figure 4.6: a) Glass transition temperature in dependence as a function of conversion of all hydroxyl groups obtained from DSC studies (oven temperature program: 25 °C to 170 °C (5 K min^{-1}) – 170 °C (1 min) – 170 °C to -50 °C (5 K min^{-1}) – -50 °C (1 min) – -50 °C to 170 °C (5 K min^{-1}) – 170 °C (1 min) – 170 °C to 25 °C (5 K min^{-1})); **b)** DSC curve of unmodified OL (**88**) and allylated OL (**89**) with different percentage of hydroxyl group conversion heating from -50 to 400 °C with a heating rate of 5 K min^{-1}.

Applying several heating cycles to 170 °C to the allylated and unmodified OL, it turned out, that the molecular weight distribution of the allylated sample increased its molecular weight upon this heat treatment. In contrast, the unmodified OL remained almost unchanged under these conditions (Figure 4.7a). Thus, the allylated OL (**89**) shows less thermal stability than the lignin (**88**) prior to modification. This decreased stability may be due to the high reactivity of the allyl function that can be used for further modification or polymerization. This exothermic peak could result from a cross-

linking induced by the new allyl functional groups as no degradation is observed in the TGA at this temperature (Figure 4.7b). An insoluble product was formed after one heating cycle to 260 °C and SEC analysis was not possible anymore. For both samples, the allylated and the unmodified OL, an exothermic transition was observed in the DSC studies starting above 220 °C. Due to TGA analysis, it corresponds to the degradation of lignin (Figure 4.7b), with the degradation temperatures of $T_{d\ 5\%}$ = 218 °C and 235 °C (of 5% mass loss) for allylated and unmodified OL, respectively.

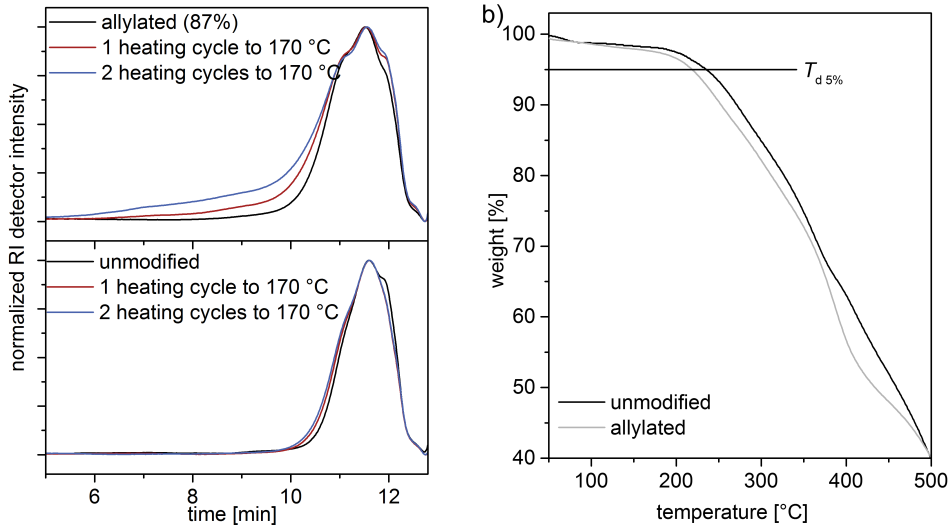

Figure 4.7: a) SEC traces for the allylated (top) and unmodified (bottom) OL after different heating circles to 170 °C (One cycle: 25 to 170 °C (5 K min^{-1}); constant at 170 °C for 1 min; 170 to –50 °C (–5 K min^{-1}); constant at -50 °C for 1 min; –50 °C to 25 °C (5 K min^{-1})); **b)** TGA traces of unmodifed and allylated OL with a heating rate of 5 K min^{-1}.

4.2.8 Structural information before and after allylation

Elemental analysis. Elemental analysis was carried out prior and after functionalization of OL (Table 5). It was shown that the carbon as well as the hydrogen content increased. Prior to allylation, the C_9 empirical formula of OL was proposed to be $C_9H_{7.1}O_{1.2}(OH)_{1.2}(OMe)_{1.3}$. Assuming that all aromatic hydroxyl groups were converted into allyl ethers and aliphatic hydroxyl groups were carboxyallylated, the resulting empirical formula should be $C_9H_{7.1}O_{1.2}(OH)_{0.08}(OMe)_{1.3}(O_{allyl})_{0.44}(OCOO_{allyl})_{0.68}$, which is equal to $C_{14.3}H_{16.7}O_{5.1}$ and in agreement with the results of the elemental analysis. If during the allylation only ethers would be formed, the empirical formula can be estimated to $C_{13.7}H_{16.7}O_{3.7}$, which would lead to the following composition of C: 68%; H: 6.9% and O: 25%. Therefore, the results of the elemental analysis are in agreement with the NMR and IR study of the allylated OL treated with LiOH and give further evidence that the aliphatic hydroxyl groups were carboxyallylated, whereas the aromatic hydroxyl groups were etherified.

Table 4.6: Elemental analysis of OL prior to and after functionalization with DAC.

	C [%] [%]	H [%] [%]	N [%] [%]	O[a)] [%]
OL (**88**)	61.53	6.15	0.25	32.1
Allylated OL (**89**)	64.32	6.16	0.00	29.5

[a)] Calculated by difference to 100.

SEC–ESI–MS studies. The unmodified and allylated lignin was analyzed with a SEC–ESI–MS system having a refractive index (RI) and a mass detector connected in parallel in order to enable the determination of absolute molecular weights of the oligomers.[258] For the allylated OL, the molecular weight distribution is shifted towards lower retention times (see inserted graph in 4.8). However, for low retention times (<16.5 min) no mass fragments were detected. At 16.5 minutes, small signals appear in the region of *m/z* = 1600 for the allylated OL and around *m/z* = 1400 for the unmodified OL. Going to higher retention times and simultaneously lower *m/z* values, the intensity of the novel signals increased. Below *m/z* = 1000, the lignin fragments seem to be better ionizable and monoisotopic masses could be observed. Nevertheless, not until a retention time of 17.5 min, the intensity of the mass signals was high enough for an appropriate analysis. Here, the unmodified lignin shows a maximum *m/z* peak at 691.3080 (resolution *r* = 85 000), whereas the allylated OL has a maximum peak at *m/z* = 811.4011 (*r* = 81 000). The difference in the exact mass of these two peaks is Δm = 120.0931. Considering the resolution ($r = m/z/\Delta m/z$), the maximal deviation of the exact masses between 691 and 811 can be $\Delta m/z$ = 0.008 and 0.010, respectively. Thus, the mass difference is in the correct range to assign it to the addition of exactly three allyl groups (+ 3 × C_3H_4, Δm_{calc} = 120.0939 u). In addition, the mass difference of Δm = 120.0931 between OL and the allylated OL is found for several mass fragments at a retention time of 17.5 min, which could also be assigned to three added allyl functions.

At a retention time of 18.0 minutes, an exact mass difference of Δm = 80.0626 ± 0.0001 ($\Delta m/z$ = 0.006) is found for at least two different mass fragments of OL and modified OL, which is in agreement with the addition of two allyl groups (Δm_{calc} = 80.0626) (Figure 4.8). Mass differences for the addition of four allyl groups are observed at higher retention times. Most likely, the mass fragments that showed the formation of three or two allyl ethers only contained three or two phenol groups, respectively, and no further hydroxyl groups as the ^{31}P NMR studies showed a conversion of 90%.

Although the detected strong peaks can only be correlated to ether formation, some mass differences that could be correlated to carboxyallylation of aliphatic hydroxyl groups were also detected. At a retention time of 17.0 minutes, some mass fragments could be correlated to the carboxyallylation of the aliphatic hydroxyl groups of OL due to the observed mass differences of Δm = 124.0680 (1 × ether + 1 × carbonate), 164.0850 (2 × ether + 1 × carbonate), 248.1060 (2 × ether + 2 × carbonate) and 252.0642 (3 × carbonate), which are in good agreement with the calculated mass differences. However, the peaks of those mass differences are rather weak, which could originate from worse ionization of these products. At a retention time of 18.0 minutes, two new weak peaks appear in the mass spectrum of the allylated OL that can be likewise assigned to two peaks in the spectrum of OL with a corresponding mass difference of 164.0838 (2 × ether + 1 × carbonate).

Besides the observed mass differences in the unmodified and the allylated OL, a Δm of 28.0313 and 30.0104 is repeatedly observed for the different mass fragments within the same sample at all retention times. The exact mass difference of the mass fragments could be assigned to additional C_2H_4 and CH_2O groups, respectively.

The additional C_2H_4 unit most probably is a result of the pulping process, since the presence of ethanol and water can lead to the formation of an ethyl ether or an alcohol, respectively.[32] Interestingly, the *m/z* values at a retention time of 18.0 minutes for the unmodified OL of 499.2290 and

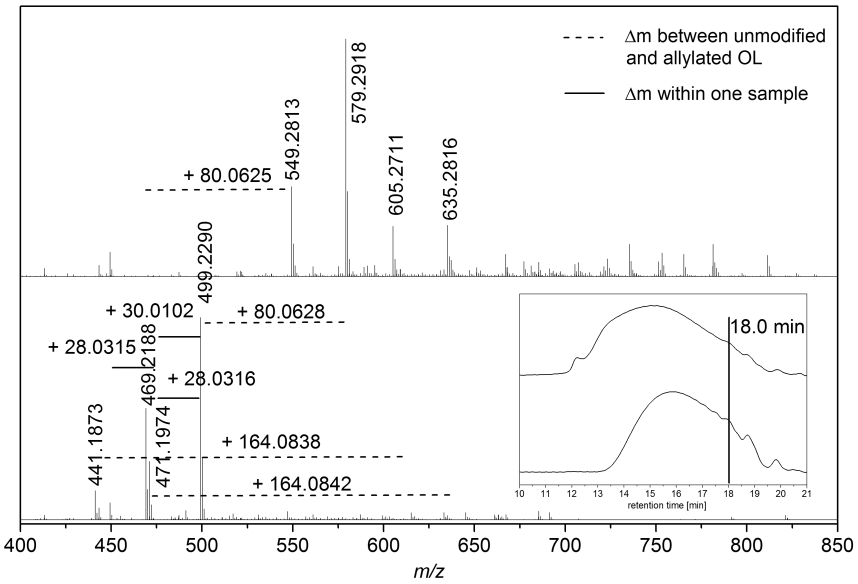

Figure 4.8: Mass spectra of unmodified (bottom) and allylated lignin (top) at a retention time of 18.0 minutes. Inserted graph shows corresponding SEC traces for unmodified (bottom) and allylated lignin (top).

471.1974 show this difference of 28.0351 (Figure 4.8). The mass analysis of the allylated OL revealed that in the first case the corresponding twofold allyl etherified product (Δm = 80.0629) and for the second case a twofold allyl etherified and one time carboxyallylated product (Δm = 164.0842) is found. The observation is in good agreement with the hypothesis of the introduced ethyl group that would prevent the carboxyallylation.

Proposed structures for the *m/z* values 499.2290 and 471.1974 that only differ in one ethyl function can be found in Figure 4.9. However, the intensity of the proposed ethyl ether product is higher. For all other discussed retention times, either no carboxyallylation was observed or the intensity of the carboxyallylated products was low, which also indicates that fewer aliphatic hydroxyl groups were present. Apparently either the amount of the ethyl functionalized products or non-aliphatic hydroxyl group-carrying molecules are higher or their ionization efficiency is increased compared to those containing aliphatic hydroxyl groups.

The frequently observed difference in CH_2O (Δm = 30.0104) for different peaks at all retention times could result from a methoxy group. This indicates that the molecules inducing the *m/z* values of 499.2290 and 469.2188 at a retention time of 18 minutes would only differ in an additional methoxy group at the aromatic ring (Figure 4.8 for mass spectrum, Figure 4.9 for proposed structures).

The exact masses obtained from the SEC–ESI–MS measurement allow the calculation of molecular formulas for the structure of the lignin fragments. Due to the fragmentation pattern and the mass defect, the range of C and H content is limited. Assuming that only oxygen is included as third element, that every formed allyl ether implies a phenolic unit (4 ring double bond (RDB) equivalents) and that the molecule is ionized with Na^+, only one reasonable elemental formula is possible for each mass peak (see examples in Figure 4.9). The obtained formulas reveal that cyclic structures, *i.e.* cyclic ethers, are necessary to propose defined structures. These structures may be rare in the overall lignin structure. Nevertheless, the cleavage of the α- and β-ether – that are the most

frequently repeated linkages in the non-isolated lignin – is a key step in organosolv pulping.[32] Thus, these ethers may be cleaved first, leaving the cyclic ethers in the molecules with low amount of C_9 repeating units unmodified.

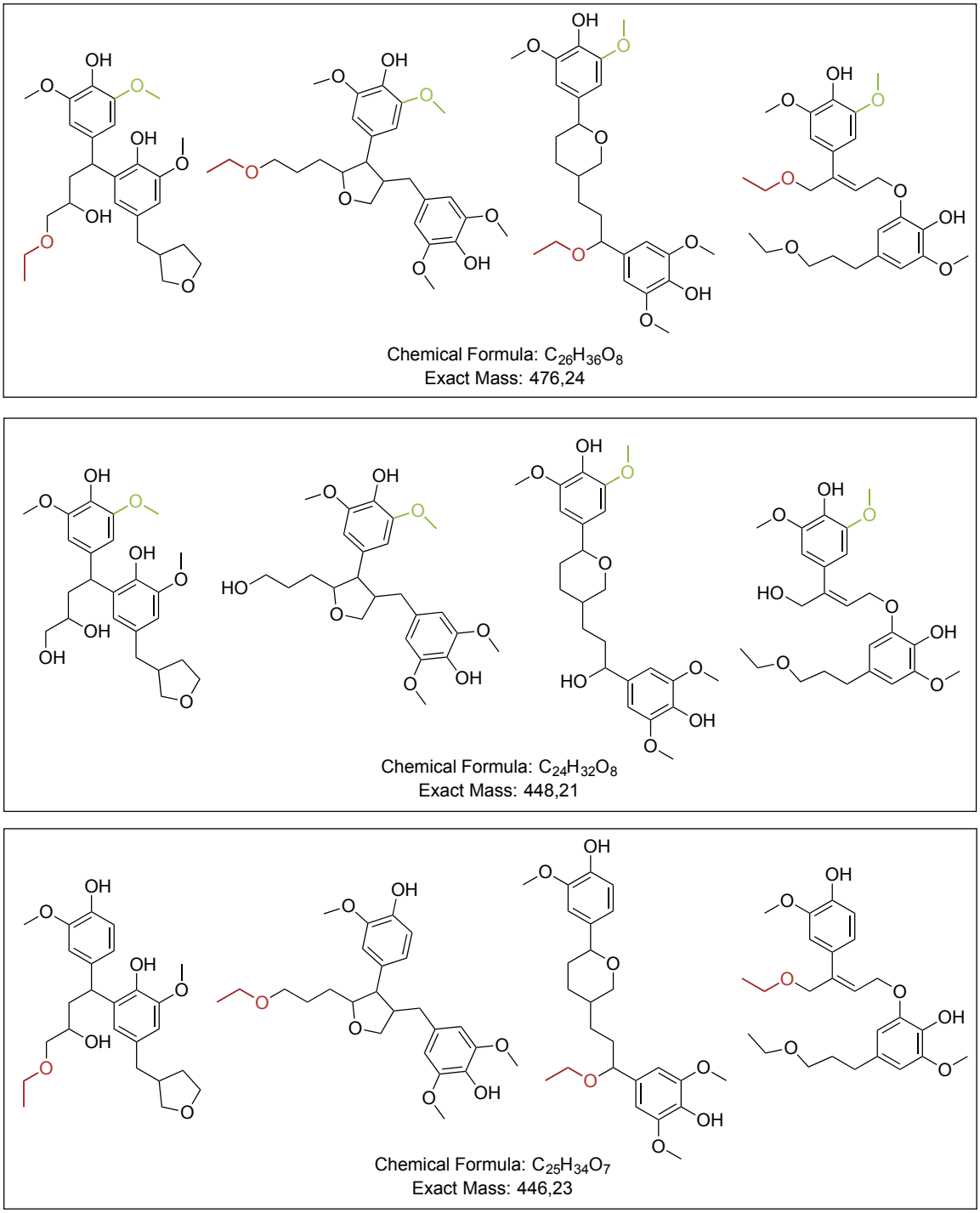

Figure 4.9: Proposed chemical structures for m/z = 499.2302 $[M+Na]^+$ (top), m/z = 471.1989 $[M+Na]^+$ (middle) and m/z = 269.2188 $[M+Na]^+$ (bottom).

4.2.9 Self-metathesis of allylated organosolv lignin

To demonstrate the accessibility of the allyl functions for further polymerizations, a self-metathesis of allylated OL (**89**) to compound **95** was performed in DCM with Hoveyda-Grubbs catalyst 1st and 2nd Generation (HG1 and HG2) (Scheme 4.4). Details about the principle of olefin metathesis and the structures of the catalysts can be found in Chapter 5. In this study, SEC analysis showed that products of increased molecular weights were formed after stirring at room temperature for 15 hours with a concentration of 0.1 mg mL^{-1} (Figure 4.10). HG2 showed a higher efficiency than HG1 under the same conditions. During the reaction with 2 mol% HG2, higher molecular weight products formed and the dispersity increased. If higher concentrations (0.2 mg mL^{-1}) were used, the solution gelled after stirring at room temperature for 60 or 30 minutes with HG1 or HG2, respectively. This indicates that the material started to crosslink. The final product was insoluble and could not be further analyzed. These first experiments prove that the allyl functional groups in modified lignin remain accessible and reactive and may, for instance, be converted using olefin metathesis.

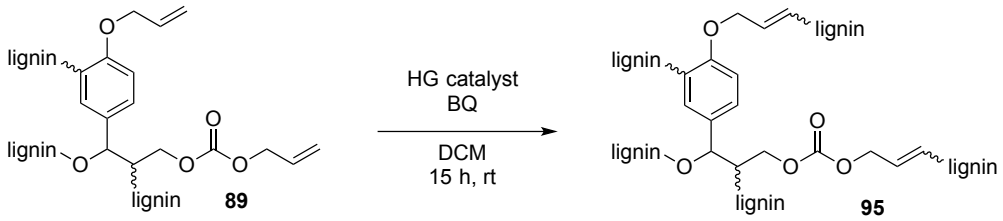

Scheme 4.4: Self-metathesis of allylated lignin (**89**).

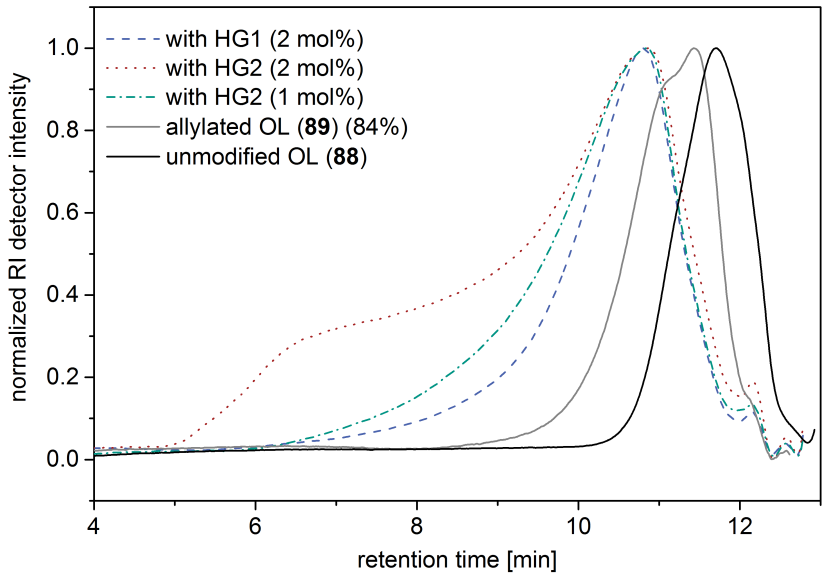

Figure 4.10: SEC traces of the unmodified and allylated OL compared to the traces of the metathesis of the allylated OL under different conditions: allylated OL was stirred in DCM (0.1 mg mL^{-1}) with HG1 or HG2 (1 or 2 mol%) and benzoquinone (3 or 6 mol%).

4.2.10 Evaluation of Claisen rearrangements

The Claisen rearrangement of lignin modified with allyl bromide is described in the literature.[228] In this work, the influence on the increase in allyl functions was evaluated performing the allylation with diallyl carbonate, followed by Claisen rearrangement and a subsequent second allylation. Additionally, this reaction was compared to a one-pot Claisen rearrangement-allylation reaction. This study was performed by Marcel Hergert in a six-week internship under my co-supervision.

For the first allylation step, allylation conditions as described in Section 4.2.3 were chosen by the scale was increased to 1.00 g of OL (**88**). The reaction was performed with DAC (**54**) at 120 °C for 15 hours using TBAB (**50**) as base to the allylated lignin **96** (Scheme 4.5). After isolation and characterization (^{1}H NMR, ^{31}P NMR, IR), the product was converted to the Claisen-rearranged product **97** at 150 °C in DMSO. The last step describes a second allylation of the previously reformed phenolic hydroxyl groups and was performed at 120 °C for 15 hours to yield the allylated compound **98-1**. In all products, the allyl function was observed in ^{1}H NMR, but no visible change of integrals could be determined due to the resolution of the measurement. Nevertheless, ^{31}P NMR studies were performed to analyze the changes in hydroxyl groups. The results, presented in Table 4.7, show a conversion of 73% of aliphatic and 100% of aromatic hydroxyl groups after the first allylation step to compound **96** (Table 4.7, entry 1). During the Claisen rearrangement, all syringyl hydroxyl groups and 29% of guaiacyl units are reformed (Table 4.7, entry 2).

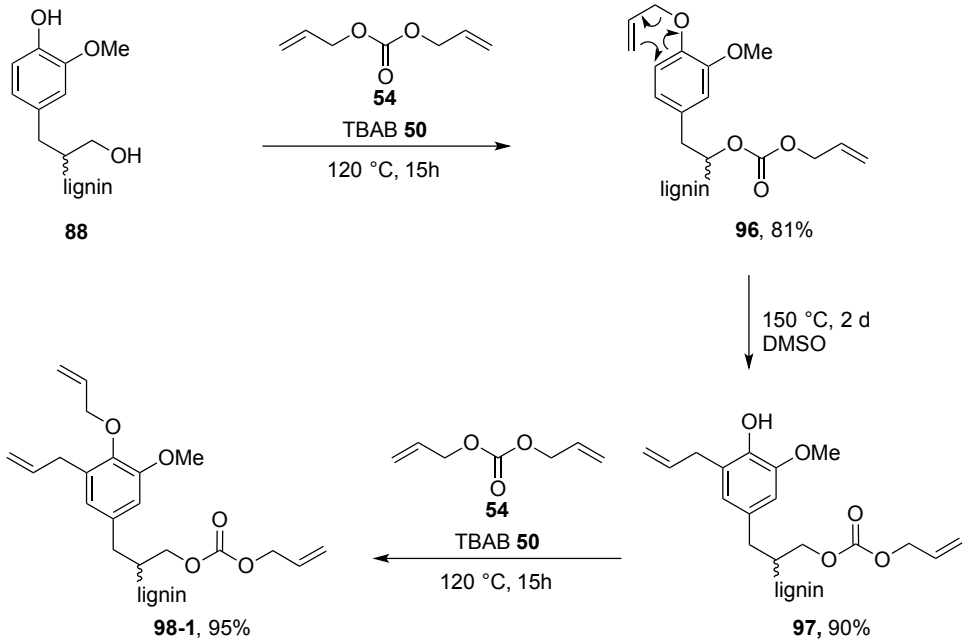

Scheme 4.5: Claisen rearrangement study: In a first allylation step OL (**88**) is converted to the allylated derivative **96**. The second step describes the Claisen rearrangement at 150 °C to yield the rearranged product **97**. In a third step the lignin is allylated a second time to obtain the multiple allylated lignin **98-1**.

As described in Section 1.1.2, beech wood lignin only contains guaiacyl or syringyl/condensed phenolic units. Here, condensed units like 4-*O*-5' or 5-5' linkages are summerized under syringyl units. The newly formed guaiacyl units during Claisen rearrangement can only be explained by a bond cleavage of lignin or the allyloxy bond. Scheme 4.6 shows the possible reaction pathways under lignin cleavage. In Scheme 4.6a, a guaiacyl unit (**88G**) is allylated to **88Ga**. The subsequent Claisen

rearrangement leads to a condensed ("syringyl") unit (**88Gb**). This phenolic hydroxyl group appears in the ^{31}P NMR between 144.6 and 141.0 ppm. Additionally, a lignin cleavage could be possible if the structure contains 4-*O*-5' or 5-5' linkages (here a 4-*O*-5' linkage is exemplary chosen). This cleavage would lead to a "guaiacyl" unit (**88Gc**) to give a signal between 141.0 and 138.0 ppm.

If a syringyl unit (**88S**) is allylated, no subsequent Claisen rearrangement of the product **88Sa** is possible (Scheme 4.6b). Nevertheless, a cleavage can take place to yield a guaiacylic unit **88Sb** that is able to undergo Claisen rearragement. The resulting product **88Sc** would again give a signal in the syringyl region.

A third pathway decribes the cleavage of the newly formed allyloxy bond (Scheme 4.6c). If a guaiacyl unit in **88** is allylated to **88Ga**, a cleavage of the ether can occur to reform the original guaiacyl unit **88Gd** that is identical to **88G**. Thus, the two different possible pathways to **88Gc** and **88Gd** (Scheme 4.6, framed structures) may explain the appearance of guaiacyl units after Claisen rearrangement. The possibility of cleavage under these conditions is supported by the decrease of the number avarage molecular weight (M_n) from 2200 after the first allylation (Table 4.7, entry 1) to 1400 for the Claisen rearranged product (Table 4.7, entry 2) and by the fact that original organosolv pulping was performed at similar temperature.

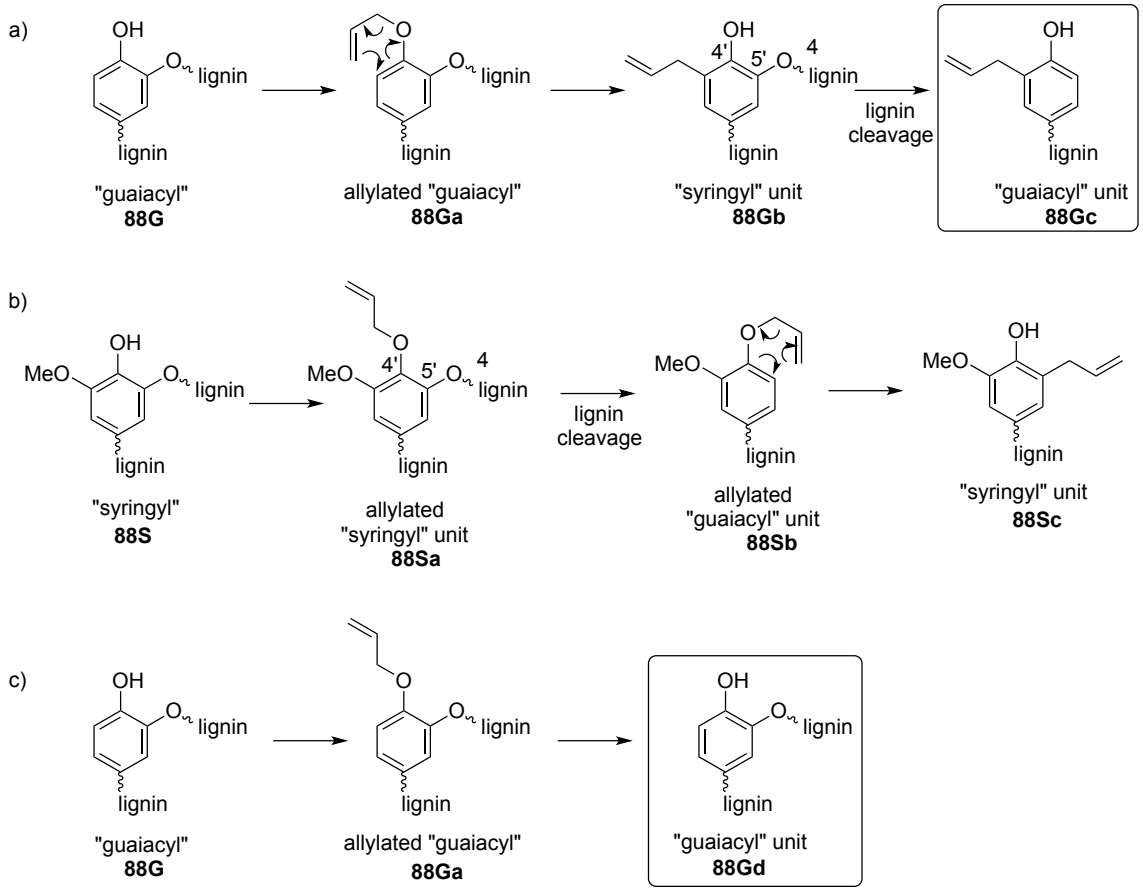

Scheme 4.6: a) Claisen rearrangement of a guaiacyl unit (**88G**) with subsequent lignin cleavage; **b)** Claisen rearrangement of a syringyl unit (**88S**) with previous lignin cleavage; **c)** Claisen rearrangement of a guaiacyl unit (**88G**) with subsequent ether cleavage.

The second allylation that followed the Claisen rearrangement led to a conversion of 98% of all hydroxyl groups in the product **98-1** (Table 4.7, entry 3). Compared to the reaction with simultaneous allylation and Claisen rearrangement at 150 °C to give product **98-2**, the step-wise reaction was more efficient. In the combined reaction, only 79% of all hydroxyl groups were converted (Table 4.7, entry 4). However, this study can give a hint about how the Claisen rearrangement can increase the functional groups. The Claisen rearrangement was observed for about 28% of all hydroxyl groups (compare Table 4.7, entry 1 and 2). This means that the functionalization of **98-1** is at least 126% and for **98-2** the functionalization may correspond to 107%, as all aromatic hydroxyl groups are converted. The low functionalization of the aliphatic hydroxyl groups is due to their lower reactivity. Under the applied conditions, TBAB may have been decomposed partly, which may have prevented an efficient allylation of the aliphatic hydroxyl groups. However, 92% of the used TBAB was recovered. Another reason may be a lower reactivity of the aliphatic hydroxyl groups at higher temperature. A better yield may be obtained, performing the reaction 120 °C for 24 hours, before increasing the temperature to 150 °C.

Table 4.7: Percentage of converted (allylated) hydroxyl groups due to ^{31}P NMR analysis and SEC results for the products of the Claisen rearrangement study compared to unmodified OL (**88**).

Entry	Compound	$X_{OH}^{aliph.}$ [%]	$X_{OH}^{arom.}$ [%]	$X_{OH}^{syringyl}$ [%]	$X_{OH}^{guaiacyl}$ [%]	X_{OH}^{total} [%]	M_n (THF) g mol^{-1}	$Đ$
1	**96**[a)]	73	100	100	100	84	2200	3.7
2	**97**[b)]	85	12	0	71	56	1400	2.6
3	**98-2**[a)]	96	100	100	100	98	2300	2.7
4	**98-2**[c)]	65	100	100	100	79	2400	5.7

Conditions for the allylation: [a)] 120 °C, 15 h, 260 wt% DAC, 200 wt% TBAB; [b)] 150 °C, 48 h, DMSO; [c)] 150 °C, 72 h, 240 wt% DAC, 40 wt% TBAB.

In addition, IR spectroscopy was performed (Figure 4.11). The observation are in agreement with the results from ^{1}H and ^{31}P NMR. In contrast to unmodified lignin (**88**), the band of carbonyl bond stretching vibration (ν) at 1745 cm^{-1} and the out-of-plane deformation vibration (δ_{oop}) of the allylic CH=CH$_2$ group at 990 and 910 cm^{-1} are present in all products (**96**, **97**, **98-1** and **98-2**). Main difference of the product spectra is observed in the region of O-H stretching vibration between 3100 and 3700 cm^{-1}. In this area, a decrease of the absorption is observed after the first allylation (**96**). Claisen rearrangement (**97**) led to reappearance of the signal and after the second allylation (**98-1**) no hydroxyl groups were present anymore. As already discussed for the ^{31}P NMR, the direct procedure to **98-2** led to a less efficient allylation and thus, few hydroxyl groups are still present in the product.

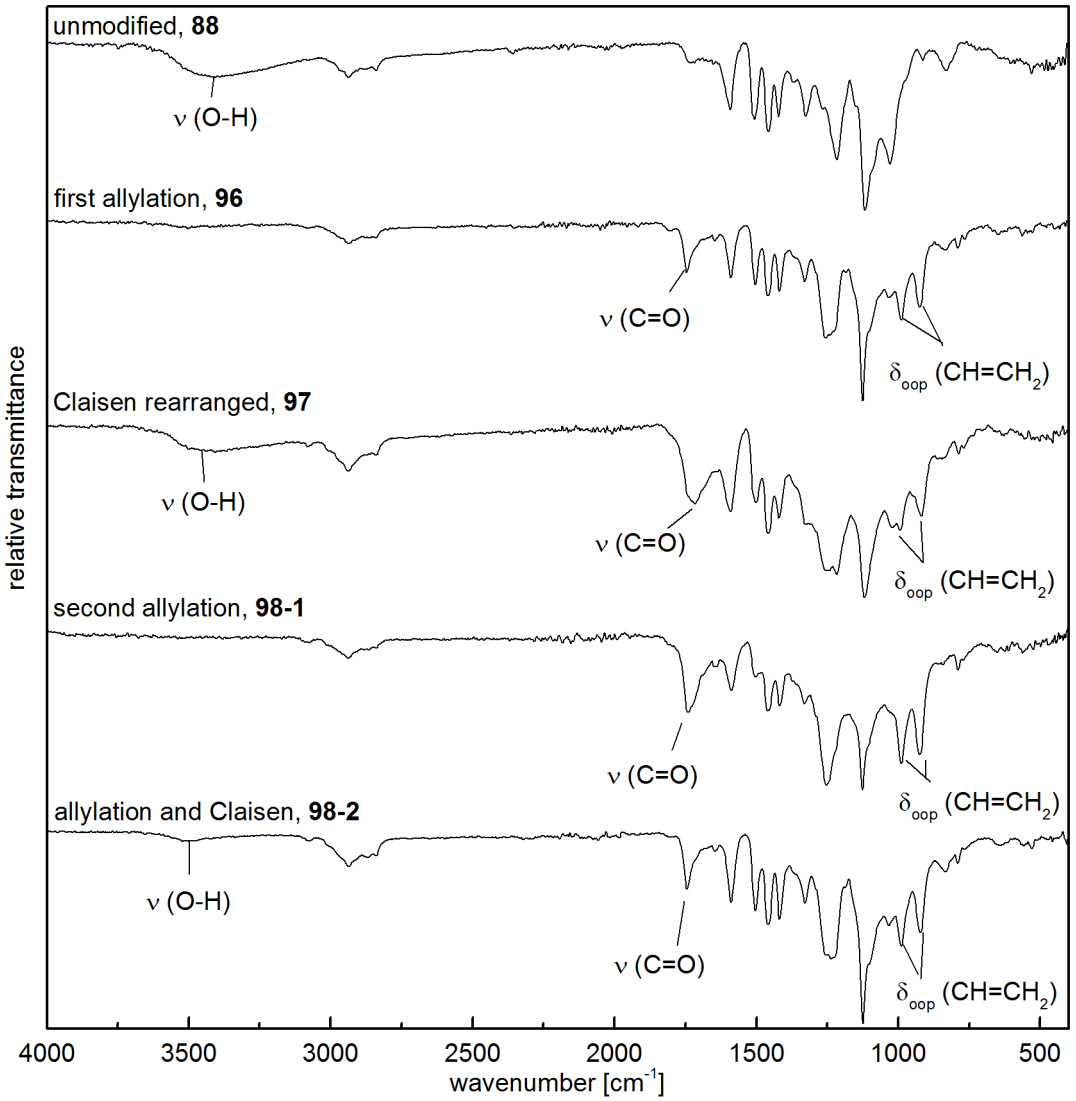

Figure 4.11: IR analysis of Claisen rearrangement study of allylated lignins **96**, **97**, **98-1** and **98-2**.

4.2.11 Crotylation of organsosolv lignin

By analogy with the allylation, organosolv lignin (**88**) was crotylated with dicrotyl carbonate (DCC, **62**) and TBAB as a base to crotylated lignin (**99**) (Scheme 4.7).

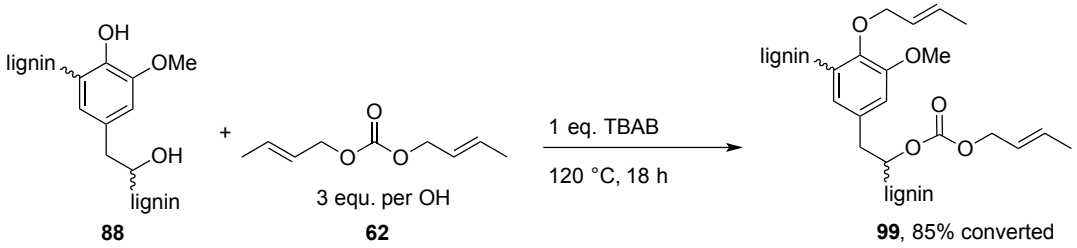

Scheme 4.7: Crotylation of OL with DCC resulting in the etherification of aromatic hydroxyl groups and the carboxycrotylation of the aliphatic hydroxyl groups.

The successful crotylation was confirmed by ^{1}H NMR (Figure 4.12). Three new signals of the crotyl function appeared in the spectrum at 5.59–5.75, 4.39–4.50 and 1.69 ppm, which can be assigned to the unsaturated protons (H^{b} and H^{c}), the CH_2 group and the terminal CH_3 group, respectively.

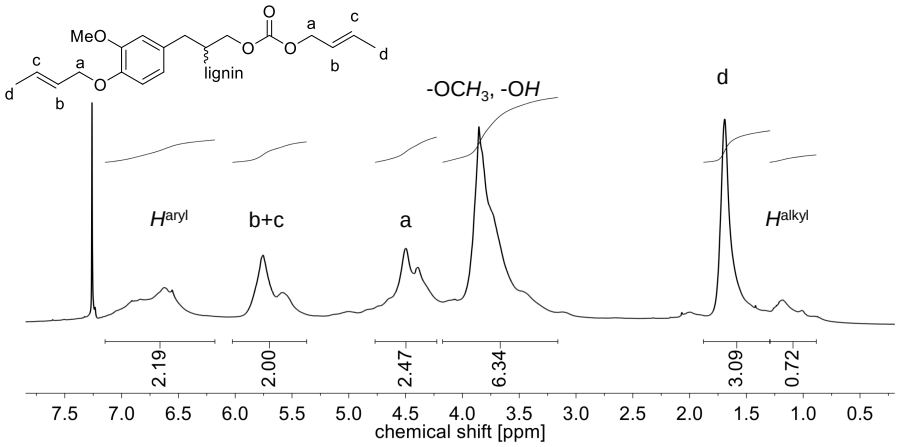

Figure 4.12: ^{1}H NMR of crotylated organosolv lignin (**99**) in $CDCl_3$.

The conversion of the hydroxyl groups was dependent on the reaction temperature, reaction time as well as the amount of starting material (Table 4.8). Reaction temperature and time were varied to optimize the reaction. ^{31}P NMR revealed that only 85% of all hydroxyl groups were converted after 18 hours at 120 °C (Table 4.8, entry 1). With increasing reaction temperature, the achieved conversion increased. A reaction temperature of 140 or 150 °C led to almost full conversion (Table 4.8, entries 3 and 4). A longer reaction time of 120 hours at 120 °C could likewise increase the conversion to 96% (Table 4.8, entry 6). Molecular weights of the products was between 2600 g mol^{-1} for poorly converted **99** and 4500 g mol^{-1} for highly converted **99** and thus, both significantly increased compared to unmodified OL (1200 g mol^{-1}).

^{1}H NMR of the products from different reaction temperatures revealed that Claisen rearrangement increases with increasing temperature (Figure 4.13). Relatively to the aromatic signals, the protons of the newly formed terminal double bond (H^{f} and H^{g}) show an increasing signal at around 5.00 ppm with increasing temperature. The signals of protons H^{b} and H^{c} also show an increasing trend. On

the one hand, aromatic protons decrease due to Claisen rearrangement, which can be explained by the proceeding conversion at higher temperature. The trend towards Claisen rearrangement with increasing temperature is in agreement with the earlier discussed observation during the crotylation of guaiacol (see Section 3.2.2).

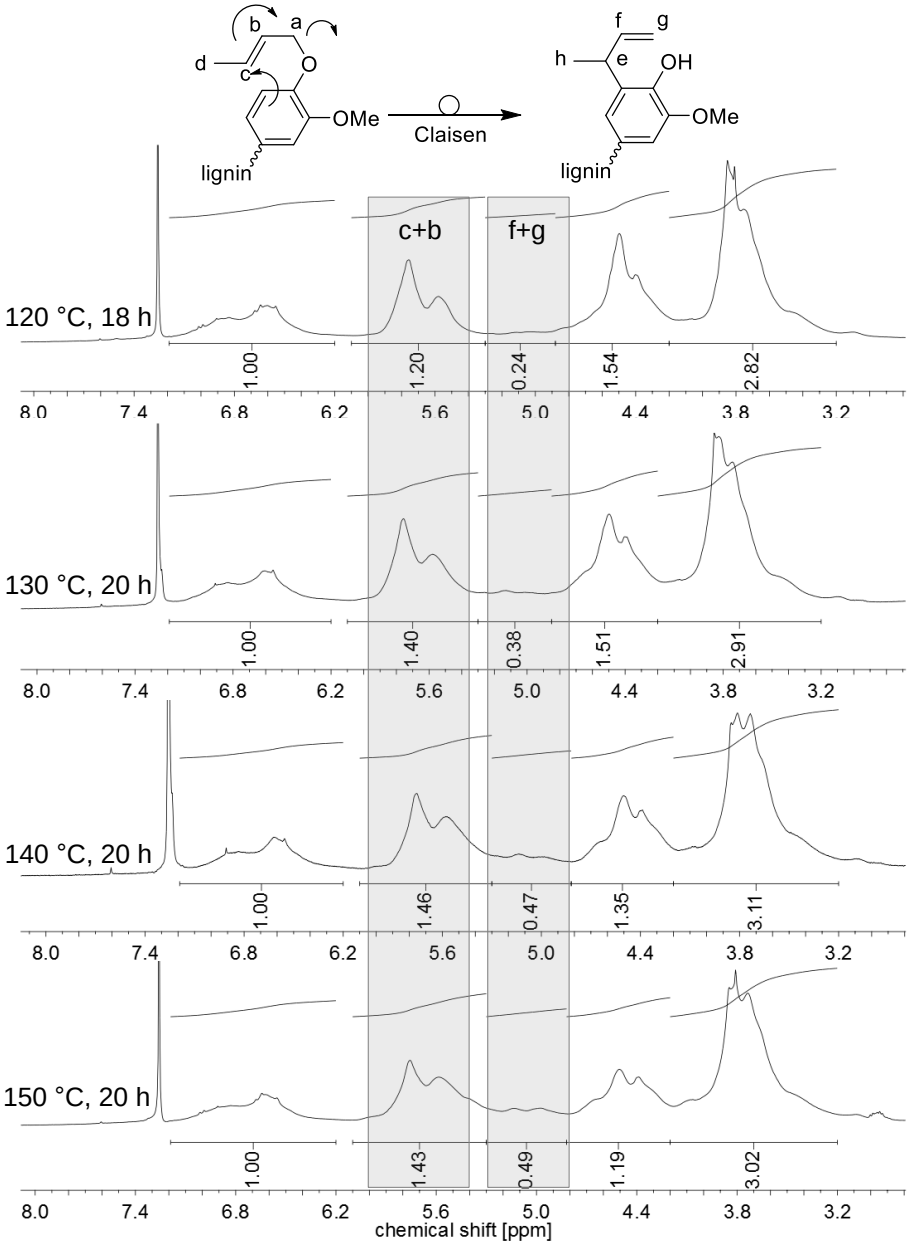

Figure 4.13: ^{1}H NMR study (in $CDCl_3$) of Claisen rearrangement (inserted scheme) during crotylation of organosolv lignin (**88**) for different reaction temperatures.

Scale-up of the reaction was performed at 100 °C to prevent Claisen rearrangement. It was found that higher amounts of starting material significantly decreased the conversion. For a 10 g-scale, 61% of all hydroxyl groups were converted after two days, whereas only 44% conversion was achieved for a 30 g-scale under the same conditions (Table 4.8, entries 7 and 8).

Glass transition temperatures (T_g) of the products show a clear decreasing trend with increasing

modification efficiency. Unmodified lignin (**88**) shows a glass transitions at 120 °C, whereas the glass transition temperature of a highly converted **99** was decreased to 56 °C (Table 4.8, entry 3). If only 61 or 44% were converted, the T_g was found to be 84 and 98 °C, respectively (Table 4.8, entries 7 and 8).

Table 4.8: SEC (THF) results and conversion from ^{31}P NMR for the temperature and time influence on the crotylation of OL.

entry	T [°C]	time [h]	TBAB [eq.]	M_n [g mol^{-1}]	$Đ$	T_g [°C]	$X_{OH}^{aliph.}$ [%]	$X_{OH}^{arom.}$ [%]	X_{OH}^{total} [%]
1	120	18	1	3400	2.5	71	75	100	85
2	130	21	1	3300	2.4	58	90	100	94
3	140	21	1	3900	2.1	56	97	100	98
4	150	21	1	4500	2.0	55	93	100	96
5	120	48	1	4200	2.1	71	70	100	82
6	120	120	1	4300	2.2	62	92	100	96
7	100	48	0.2	2600	3.6	84	33	100	61[a]
8	100	48	0.2	2600	3.1	98	4	100	44[b]

Conditions: in a 25 mL pressure tube, OL (150 mg, 0.915 mmol) was suspended in DCC (1.56 g, 9.15 mmol, 10 eq.) and heated to the desired temperature. TBAB (295 mg, 0.915 mmol, 1 eq.) was added. [a] 10 g scale, 6 eq. DCC; [b] 30 g scale, 6 eq. DCC.

4.3 Conclusion and Outlook

The efficient and sustainable allylation of beech wood OL including a detailed characterization was shown. Up to 90% of all hydroxyl groups were allylated using diallyl carbonate as reagent at relatively low temperatures between 90 and 120 °C. In a comparative screening, TBAB showed the highest reactivity towards the reaction compared to other bases. One of the advantages of TBAB is that it acts as phase transfer catalyst and no further solvent is necessary during the allylation reaction. An amount of 0.2 equivalents of TBAB per hydroxyl group is necessary for an efficient allylation reaction. However, this amount can be recovered quantitatively from the aqueous phase and recycled for further allylation reactions, which increases the sustainability of the reaction. Higher reaction temperatures led to Claisen rearrangements of the allylated lignin and could thus increase the functionality by up to 28%.

With the aid of NMR and IR spectroscopy, the formation of the allyl function was confirmed. Furthermore, the SEC coupled mass spectra revealed new insights into the structure of lignin. The obtained exact mass differences showed mainly allyl ether formation and almost no carboxyallylation was observed for the detected masses, which might be due to a poor ionization efficiency for these structures. However, the carboxyallylation of aliphatic hydroxyl groups was proved by decarboxylation with LiOH. Thus, a higher content of aromatic hydroxyl groups compared to the amount of aliphatic hydroxyl groups is present in the low molecular weight lignin fragments. Although higher masses (>1000 g mol^{-1}) were not detected, this method gives new information about structural motifs, such as the high probability of cyclic ethers in the structure.

Performing the allylation of OL, a new functional group was introduced into the structure of lignin.

As a short demonstration, the self-metathesis of the allylated OL showed how easily accessible the allyl functions are for further chemical transformations. Thus, the allylated product is a promising, sustainable starting material for further functionalization or direct polymerization. In addition, crotylation with dicrotyl carbonate showed that the reaction conditions can easily be applied for other carbonates, opening an easy access to new functionalities in lignin.

5 Cross-metathesis of allylated organosolv lignin with plant oils

Parts of this chapter and associated parts in the Experimental Part were reproduced with permission from: L. C. Over, M. Hergert, M. A. R. Meier, *Macromol. Chem. Phys.* **2017**, *accepted manuscript*, DOI: 10.1002/macp.201700177.

http://onlinelibrary.wiley.com/doi/10.1002/macp.201700177/abstract

5.1 Introduction

Decreasing fossil feedstocks and simultaneously growing global population, accompanied by an increasing demand for energy and resources, stimulate the development of materials from renewable resources. As the polymer sector accounts for a large portion of the chemical industry, the search for sustainable alternatives for polymeric materials is of high interest.[5,6] Lignin is one of the most abundant biopolymers on earth and the largest natural resource for aromatic compounds (see Section 1.1). Plant oils constitute another interesting renewable resource with high availability. Unsaturated fatty acids and their derivatives are versatile substrates for various modifications, leading to the synthesis of platform chemicals, monomers and polymers.[2,259–261] Olefin metathesis is a transition metal-catalyzed C-C bond formation and is as such a highly discussed modification and transformation methodology for plant oil derivatives.[262]

Olefin metathesis
This equilibrium reaction can be described as metal-catalyzed exchange of alkylidene moieties between alkenes.[263] Cleavage as well as formation of C=C bonds can be induced by this modification technique. Various transformations can be found. Olefinic double bonds can be coupled or cleaved applying self- or cross-metathesis, ring-closing and ring-opening at the double bonds can be achieved and polymerization be performed by ring-opening metathesis polymerization (ROMP) or acyclic diene metathesis (ADMET) (Scheme 5.1).

The reaction principle of olefin metathesis has been known since 1955, when a catalytic polymerization procedure of norbornene with Ti^{II} was reported.[264] In 1964, BANKS AND BAILEY described the "disproportionation" of propylene to ethylene and butene in a process with a molybdenum hexacarbonyl-alumina catalyst.[265] During this time, NATTA *et al.* reported their studies about ring opening polymerization of cyclic olefins.[266–269] It was in 1972, when the term "olefin metathesis" was first introduced by CALDERON. Several mechanism were suggested, including a "quasi-cyclobutane",[263] or the coordination of both alkenes to form a metallocyclopentane as

intermediate.[270,271] HÉRISSON AND CHAUVIN postulated an olefin metathesis mechanism in 1970, which is still generally accepted today (Scheme 5.2).[272] It consists of a [2+2] cycloaddition of a C=C double bond with a metal-carbene to form an instable metallocyclobutane intermediate. In this equilibrium reaction, it can either react back to the starting materials or towards the product, both by cycloreversion. Due to this reversibility, product mixtures are obtained. In addition, the reaction generally does not show stereocontrol and thus, *E* and *Z* products are both obtained. However, mostly the thermodynamically more stable *Z* product is formed. To shift the equilibrium towards the desired products, driving forces such as formation of a stable product (*e.g.* ring formation), release of ring strain or the formation of an volatile byproduct (*e.g.* ethylene) are necessary.[263]

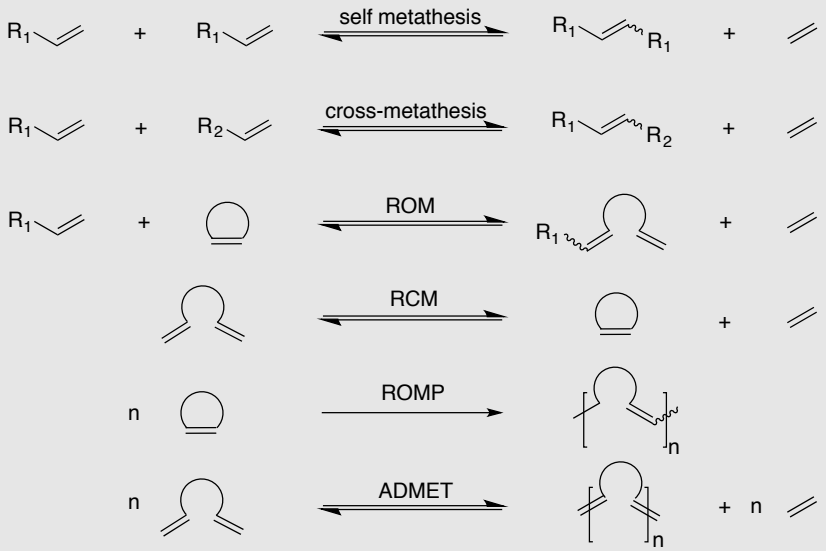

Scheme 5.1: Types of transition metal catalyzed olefin metathesis reactions: self-metathesis, cross-metathesis, ring opening metathesis (ROM), ring closing metathesis (RCM), ring opening metathesis polymerization (ROMP) and acyclic diene metathesis (ADMET) polymerization.

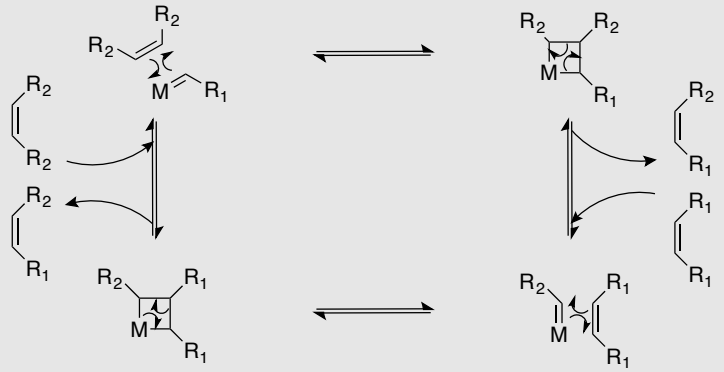

Scheme 5.2: Mechanism of olefin metathesis postulated by HÉRISSON AND CHAUVIN.[272]

In the following years after CHAUVIN's publication, several groups reported evidences for the proposed mechanism.[273–276] Till the early 1980s, the utilized catalysts were poorly defined homogeneous and heterogeneous systems (*e.g.*, WCl_6/Bu_4Sn, MoO_3/SiO_2 and Re_2O_7/Al_2O_3).[277] The proposition and understanding of the mechanism led to the development of catalysts involving various transition metals and alkylidene units. The first well-characterized and highly reactive alkylidene catalysts were molybdenum- or tungsten-based and of the general formula $(NAr)(OR')_2M{=}CHR$. Two

examples of the first homogeneous single-component metathesis catalysts are complex **C1** and **C2** (Figure 5.1) that were synthesized in the group of SCHROCK.[278–281] However, complexes of early transition metals exhibit high oxophilicity of the metal centers and are thus oxygen and moisture sensitive. Furthermore, it was shown that these catalysts were incompatible with aldehydes and alcohols.[277] Later transition metals are more tolerant towards other functional groups, which led to the development of ruthenium-based alkylidene catalysts. Complex **G1** was one of the first ruthenium catalysts for olefin metathesis (Grubbs 1st generation catalyst). Ruthenium catalyst synthesis starts from $RuCl_2(PPh_3)_3$ and reaction with alkyl or aryl diazoalkanes. The phosphine ligand can be varied *via* phosphine exchange. Different phosphine ligands were used and it was found that the metathesis activity of the catalyst increases the more bulky and the more basic the phosphine is: PPh_3, P^iPr_3 < PCy_3.[282] Mechanistic studies helped to understand the ligand influence on the catalysts activity and induced the design of new complexes. Further improvement of the catalysts activity was obtained with the introduction of *N*-heterocyclic carbene ligands that led to the development of **G2** (Grubbs 2nd generation catalyst).[283] HOVEYDA and coworkers introduced a chelating isopropoxybenzylidene ligand, which led to the catalysts **HG1** and **HG2** (Hoveyda-Grubbs 1st and 2nd generation catalysts). The chelating moiety led to increased stability of the complex and recyclability of the complex was reported.[284] However, the so-called postulated "boomerang" mechanism (release-return mechanism) of the isopropoxybenzylidene chelating ligand was later investigated by PLENIO *et al.* with no evidence found.[285] The studies suggest that the recovered complex is more likely a non-initiated complex rather than the reformed complex from the proposed release-return mechanism.

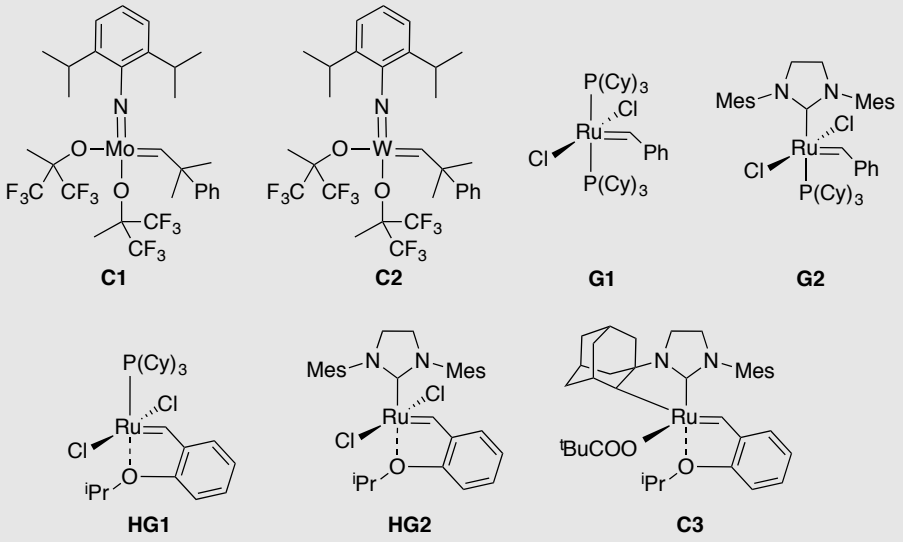

Figure 5.1: Chemical structure of different transition metal catalysts active for olefin metathesis.

An issue that was observed, especially if second generation catalysts were used, is a temperature depending double bond isomerization. Mechanistic studies revealed that the formation of ruthenium-hydride species are the reason for this isomerizations. Phenylphosphoric acid, benzoquinones and other additives were shown to supress the isomerization.[286,287] The research for new catalysts with selective properties, for instance stereoselectivity and enantioselectivity, or increased reactivities is still going on. The first enantioselective olefin metathesis catalysts were described by GUBBS *et al.*, an important step for natural substance synthesis.[288,289] Moreover, a new ruthenium-based catalyst

(**C3**) was reported from the same group that is highly *Z*-selective.[290] Besides the research towards new catalysts, also other aspects of the procedure are object of research. For instance, *Fischmeister et al.* reported the use of DMC as "green" alternative for conventionally used DCM or toluene.[181] Second-generation Grubbs (**G2**) and Hoveyda catalysts (**HG2**) showed similar activity in DCM and DMC in RCM of various substrates. For cross-metathesis, yields were slightly lower with DMC instead of DCM, but still in a very good region.

The importance of olefin metathesis in organic synthesis was recognized with the joint Nobel prize award for Yves Chauvin, Robert H. Grubbs and Richard R. Schrock in 2005.

From plant oils, a large variety of target products can be prepared *via* metathesis, for instance, α-olefins, α,ω-dienes, α,ω-diols, α,ω-diesters, ω-functional aldehydes and many more.[291–293] For macromolecular chemistry, acyclic diene metathesis (ADMET) is a well-established methodology for the synthesis of high molecular weight polymers from plant oil renewable resources.[294–296] The synthesis of monomers and linear polymers *via* cross-metathesis or ADMET of 10-undecenol derivatives was described by RONDA *et al.*.[297,298] They introduced thermally curable functional groups to yield phosphorous-containing thermosets with flame retardant activity. CRAMAIL *et al.* showed routes from fatty acid-based α,ω-dienes to polyurethanes and polyesters *via* ADMET polymerization.[299,300] In our group, star- and block-copolymers from 10-undecenyl acrylate *via* ADMET polymerization were intensively studied.[214,301,302] In addition, various linear polymers starting from 10-undecenoic acid, 10-undecenal, methyl oleate or methyl erucate were prepared using ADMET.[202,211,303–305]

Likewise, the application of plant oils in renewable thermosets is described *via* various methods. Besides copolymerization to produce epoxy thermosets[306,307] or polyurethanes,[308] and radical homopolymerization,[309] metathesis is an equally powerful but up to date less investigated tool for the synthesis of renewable thermosets from plant oils. LAROCK *et al.* intensively investigated the preparation of cross-linked materials *via* ring-opening metathesis polymerization (ROMP) starting from castor oil modified with norbornenyl function.[310–313] The development of sustainable pathways to lignin-based polymers is one of the main challenges in lignin chemistry, as conventional methods are still dominating this field (see Section 1.4). Besides the utilization in blends, lignin was shown to be a suitable reagent for copolymers such as polyurethanes, epoxy resins and phenolic resins.[43,314] Although combining the rigidity of the aromatic structure of lignin and the flexibility of vegetable oil's long aliphatic chains is an interesting approach, only few thermosets that incorporate both lignin- and plant oil-based monomers are reported. In triglyceride-based thermosetting polymers employing acrylated fatty acid methyl esters as diluent, butyrated lignin was added to increase the glass transition temperature.[309] However, a lignin content as low as 5 wt% increased the viscosity of the mixture and thus hindered the processability of the resin. DENG *et al.* described the synthesis of non-isocyanate polyurethanes from epoxidized soybean oil and kraft lignin.[170] A total biomass content of 85 wt% in the product was obtained. Increasing the lignin content from 20 to 50 wt% led to an increase of tensile strength from 0.3 to 1.3 MPa. AVÉROUS *et al.* esterified lignin with plant oil-based oleic acid to prepare a bio-based polyol for polyurethane synthesis.[155] Thus, materials with up to 89% bio-based content and improved properties for durable applications were obtained.

To the best of my knowledge, no use of unmodified or unfractioned plant oil in combination with

lignin was described yet. Additionally, the application of olefin metathesis in lignin chemistry is a new methodology to form thermosets. In Chapter 4, the sustainable allylation of organosolv lignin with diallyl carbonate as “green” alkylation agent was discussed in detail. Likewise, the reactivity of the allylated lignin towards self-metathesis was already described as proof of concept. In this chapter, the use of the previously described allylated lignin with different plant oils in cross-metathesis to yield thermosetting polymers is described. The thermomechanical properties of the final material depending on the lignin content and plant oil source are discussed.

5.2 Results and Discussion

The synthesis of the herein used allylated lignin (**98-2**) was described in Chapter 4. **98-2** was isolated in a 30 g batch after a reaction time of 3 days at 150 °C, using 3 eq. of DAC as reagent and 0.2 eq. TBAB as catalyst. The conversion of hydroxyl groups was determined *via* ^{31}P NMR spectroscopy. 79% of all hydroxyl groups were converted after the allylation procedure compared to the unmodified lignin. From the Claisen rearrangement study, it was estimated that additional 28% of the hydroxyl groups in lignin performed Claisen rearrangement and thus increased the functionality of the product to about 6.5 mmol g^{-1}. Details of the Claisen rearrangement study are described in Section 4.2.10.

5.2.1 Metathesis film curing of allylated lignin with different plant oils

The film formation of allylated lignin (**98-2**) and different plant oils *via* cross-metathesis curing was investigated (see Scheme 5.3 for a representative trigyceride (**100**) of olive oil). The network (**101**) formation is expected to be accompanied by the production of octadec-9-ene (**102**) and dodec-6-ene (**103**) as well as ethylene (**35**), amongst other olefins, as by-products of the self-metathesis of the fatty acid side chains as well as of allylated lignin. The use of a solvent is necessary for the film

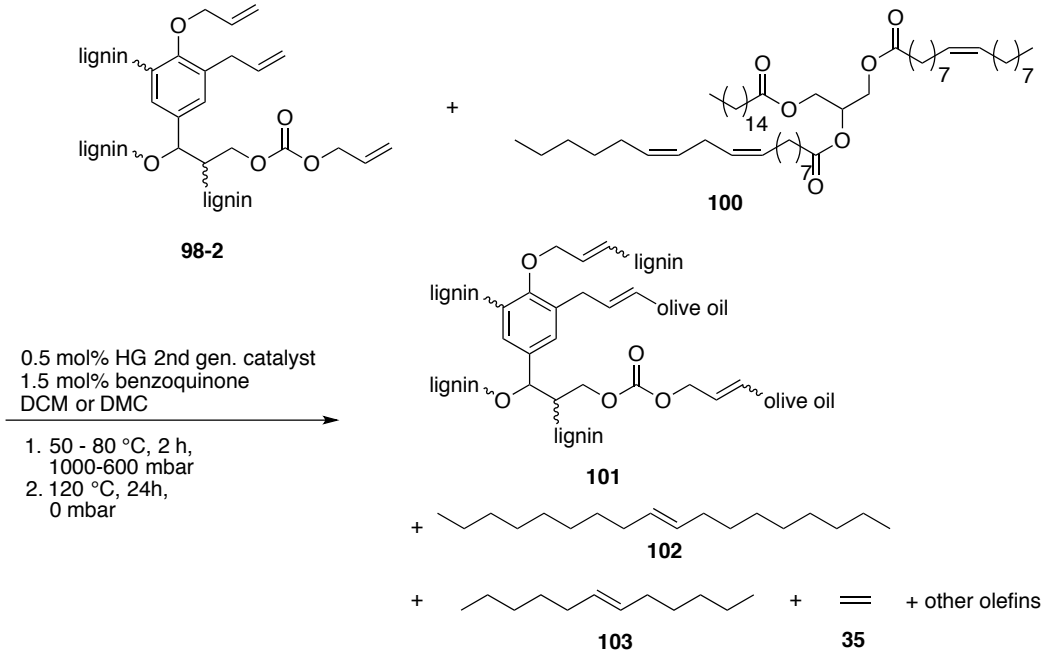

Scheme 5.3: Cross-metathesis of allylated lignin (**98-2**) with plant oil (representative triglyceride from oleic acid, palmitic acid and linoleic acid) (**100**) to form a cross-linked network (**101**); possible side products are, amongst others, octadec-9-ene (**102**), dodec-6-ene (**103**) and ethylene (**35**).

preparation, as the starting materials are not miscible prior to the reaction. Film formation was carried out with dichloromethane or dimethyl carbonate at 50–80 °C in a vacuum oven, slowly reducing the pressure to 600 mbar over two hours. Thus, homogenous films with comparable thicknesses between 0.13 and 0.20 mm were formed and cured at different temperatures under vacuum. The influence of the ratio of lignin to plant oil, the nature of the oil, the curing temperature as well as the solvent on the mechanical and thermal properties of the films (**101**) is discussed in the following.

5.2.2 FT-IR spectroscopy of lignin-plant oil thermosets

FT-IR spectra of the starting materials as well as the thermoset products were recorded to verify the successful metathesis reaction. Films with 50 wt% lignin content were exemplarily chosen for a first discussion. In the FT-IR spectrum of the cured film from 50 wt% olive oil and 50 wt% allylated lignin, characteristic bands of both starting materials can be observed (Figure 5.2a). Remaining unmodified hydroxyl groups in lignin show an absorption band of the O-H stretching vibration (ν) at 3500 cm^{-1}. C-H stretching vibration absorption bands of CH and CH_2 groups can be found in all three spectra at 2850 and 2920 cm^{-1}, respectively. Carbonyl functions of the ester groups in olive oil as well as the carbonates in allylated lignin result in a strong band at 1744 cm^{-1}. Aromatic C=C stretching vibration absorption bands characteristic for lignin can be found at 1584 and 1502 cm^{-1} in the starting material as well as in the product. Likewise, the absorption of the methoxy group's deformation vibration is observed at 1413 and 1450 cm^{-1}. As the products are cured *via* metathesis, the change of the unsaturated groups is the most interesting modification. Olive oil shows a distinct band at 722 cm^{-1}, which is a typical region for H-C=C-H out-of-loop deformation vibrations (δ_{oop}) in cis-oriented double bonds, whereas the terminal double bonds in allylated lignin result in two deformation vibration bands at 921 and 988 cm^{-1}. Low intensities of those peaks in the final product indicate the presence of remaining unreacted terminal double bonds. HG2 has a cis/trans selectivity of around 20:80.[315] Thus, the intensity of cis-oriented double bonds in the final product is expected to be low. A new strong band appears at 964 cm^{-1} in the final thermoset that can be assigned to the

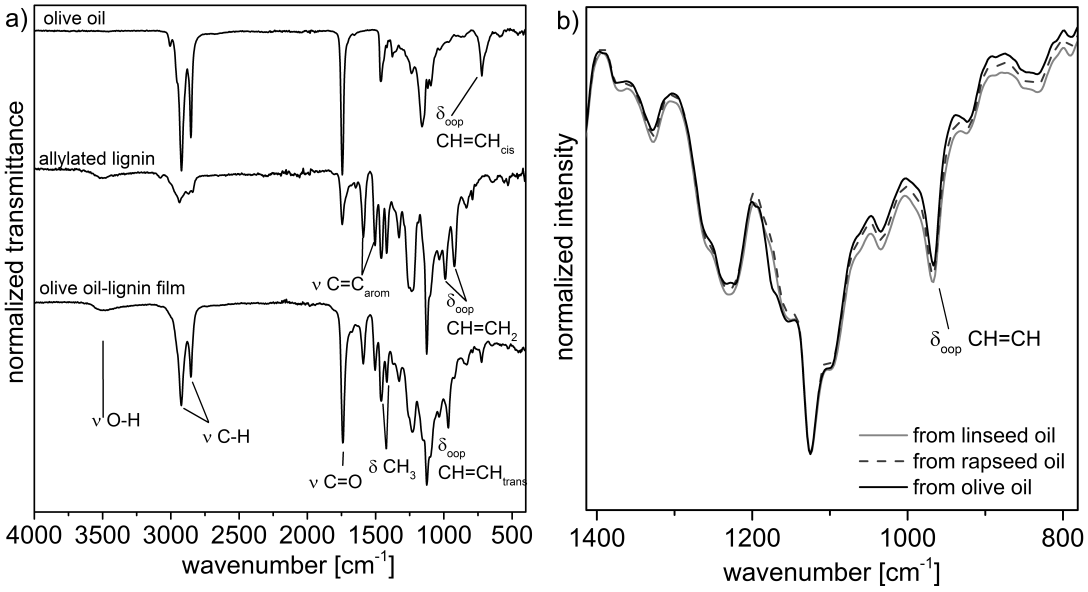

Figure 5.2: Normalized FT-IR spectra of **a)** lignin-olive oil (50:50) film compared to the starting materials olive oil and allylated lignin and **b)** thermosets with different plant oils containing 50 wt% allylated lignin.

formed trans-oriented alkenes and thus indicating the successful metathesis reaction. FT-IR spectra of thermosets from different plant oils show marginal differences in the fingerprint region (Figure 5.2b). Relatively to the strongest peak (C-O ether stretching vibration absorption at 1125 cm^{-1}), the intensity of the H-C=C-H deformation vibration absorption band at 968 cm^{-1} increased from olive oil to rapeseed oil to linseed oil. The effect may be explained by the double bond density in the original plant oil. The number of unsaturated fatty acids increased in the same order (for detailed composition, see Experimental Part). All in all, the FT-IR structural analysis of the films gave proof of an efficient reaction.

5.2.3 Influence of the lignin-to-oil ratio on the film preparation and mechanical properties

Mechanical properties of the films were analyzed *via* stress/strain measurements. Lignin and triglycerides of the oils have different structural characteristics. Indeed, due to its rigid structure, lignin acts as hardener in a film material and usually leads to brittle materials, whereas the long aliphatic side chains of the triglycerides act as soft segments and lead to ductile products. This is expressed by the Young's modulus and ultimate tensile strength values obtained from stress/strain measurements of the products. Representative curves for lignin-olive oil films with lignin contents between 20 and 70 wt% are presented in Figure 5.3. In this range of composition, homogeneous films were obtained. Lower lignin contents led to less efficient cross-linking, higher lignin contents led to brittle materials, which broke prior to sample preparation. Multiple samples from one cured film were measured (see Table 5.1 for detailed results including standard deviation from the measurements). Reproducibility of the results was verified by multiple film formations for selected samples.

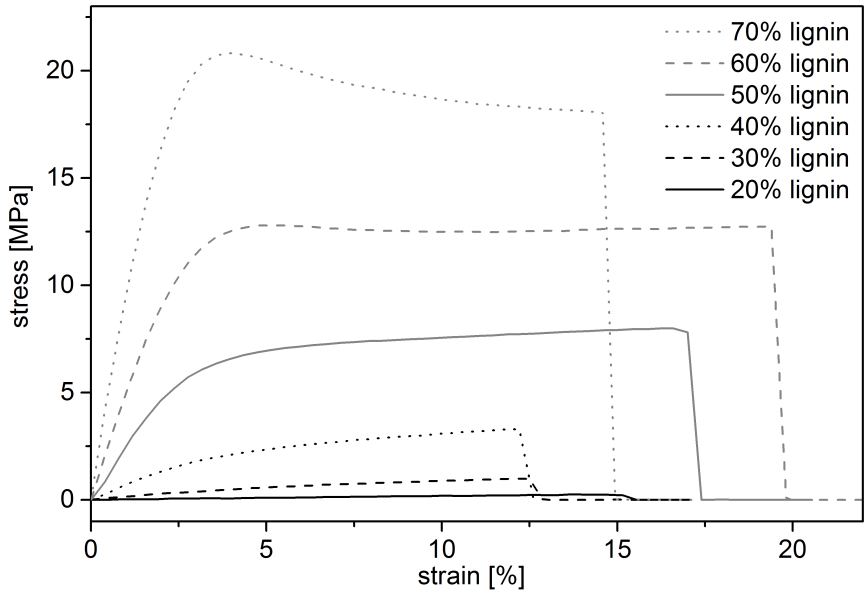

Figure 5.3: Representative stress/strain curves for lignin-olive oil films prepared with DCM and cured at 120 °C, recorded with a 25 N load cell and 0.5 mm min^{-1} as crosshead speed.

For an olive oil film with 70 wt% lignin, the Young's modulus *E* (the slope of the stress/strain curves in Figure 5.3) was 770 MPa. 20 wt% lignin led to a material with a significantly lower Young's modulus of 1.7 MPa. However, all samples show ductile behavior. With increasing lignin content, *E* increased exponentially. This behavior is described in literature for other polymeric materials with

increasing lignin content in blends[145,316] and copolymers.[170] Besides Young's modulus, the ultimate tensile strength increased from 0.25 MPa to 21 MPa with increasing lignin content from 20 wt% to 70 wt%, respectively. Both dimensions, Young's modulus and ultimate tensile strength, describe the hardness of the material. As expected, the increase of oil content leads to poor tensile strength and Young's modulus due to the increasing free volume of the triglyceride chains. The dimensions of the Young's modulus and tensile strength and the tendency to increased values with shorter aliphatic chain or more rigid structures are in agreement with published plant oil-based epoxy thermosetting networks.[317–319] No tendency is observed for the elongation at break. Its variation of < 8% is within the error of the measurement due to the low thickness of the films (0.13–0.20 mm).

Table 5.1: Properties of lignin-plant oil film, formed in DCM, cured at 120 °C with standard deviations of multiple measurements.

Lignin content [wt%]	Elongation at break[a)] [%]	Young modulus[a)] [MPa]	Ultimate tensile strength[a)] [MPa]	Yield [wt%]
Lignin-olive oil film, formed in DCM, cured at 120 °C				
20	16 ± 4	1.7 ± 0.2	0.25 ± 0.07	83
30	12 ± 1	10 ± 0	0.93 ± 0.07	84
40	16 ± 6	66 ± 3	3.6 ± 0.7	85
50	16 ± 3	210 ± 7	7.9 ± 0.2	88
60	21 ± 1	410 ± 7	13 ± 0.3	88
70	14[b)]	770[b)]	21[b)]	92
80	-[c)]	-[c)]	-[c)]	89
Lignin-rapeseed oil films, formed in DCM, cured at 120 °C				
20	26 ± 4	2.1 ± 0.1	0.5 ± 0.1	81
30	33 ± 2	7.9 ± 0.3	2.1 ± 0	83
40	38 ± 0.9	62 ± 0.6	5.7 ± 0.1	84
50	19 ± 7	230 ± 6	8.1 ± 0.7	87
60	21 ± 10	610 ± 30	16 ± 0.7	88
70	-[c)]	-[c)]	-[c)]	87
80	-[c)]	-[c)]	-[c)]	89
Lignin-linseed oil films, formed in DCM, cured at 120 °C				
20	24 ± 2	5.4 ± 0.2	1.1 ± 0.1	76
30	23 ± 3	25 ± 2	2.8 ± 0.3	78
40	16 ± 3	120 ± 4	5.6 ± 0.4	81
50	20 ± 10	400 ± 20	13 ± 1	84
60	26 ± 1	730 ± 20	18 ± 0.3	86
70	-[c)]	-[c)]	-[c)]	88
80	-[c)]	-[c)]	-[c)]	89

[a)] from stress/strain measurements recorded with a 25 N load cell and a crosshead speed of 0.5 mm min^{-1}; [b)] single measurment; [c)] products were too brittle to form dogbone-shaped specimen.

5.2.4 Influence of the plant oil fatty acid composition on the mechanical properties

Besides olive oil, rapeseed oil and linseed oil were tested for the synthesis of lignin-oil films. The tendency of Young's moduli and tensile strength for the variation of the lignin-to-plant oil ratio is comparable for all oils as described in Section 3.4. However, the absolute values differ depending on the nature of the plant oil (Table 5.1). A trend can be observed were the Young's modulus and the ultimate tensile strength increase from olive oil to rapeseed oil to linseed oil (Figure 5.4a and b). For instance, for 60 wt% lignin, *E* increased from 410 to 610 to 730 MPa and the ultimate tensile strength from 13 to 16 to 18 MPa for olive oil, rapeseed oil and linseed oil, respectively. In the same order, the content of polyunsaturated fatty acids increased from 0.09 over 0.28 to 0.66 g mL^{-1} (for detailed composition of the oils, see Experimental Part). For 70 wt% lignin in the films with rapeseed or linseed oil, no specimen for tensile test could be prepared as the samples were too brittle and broke during preparation.

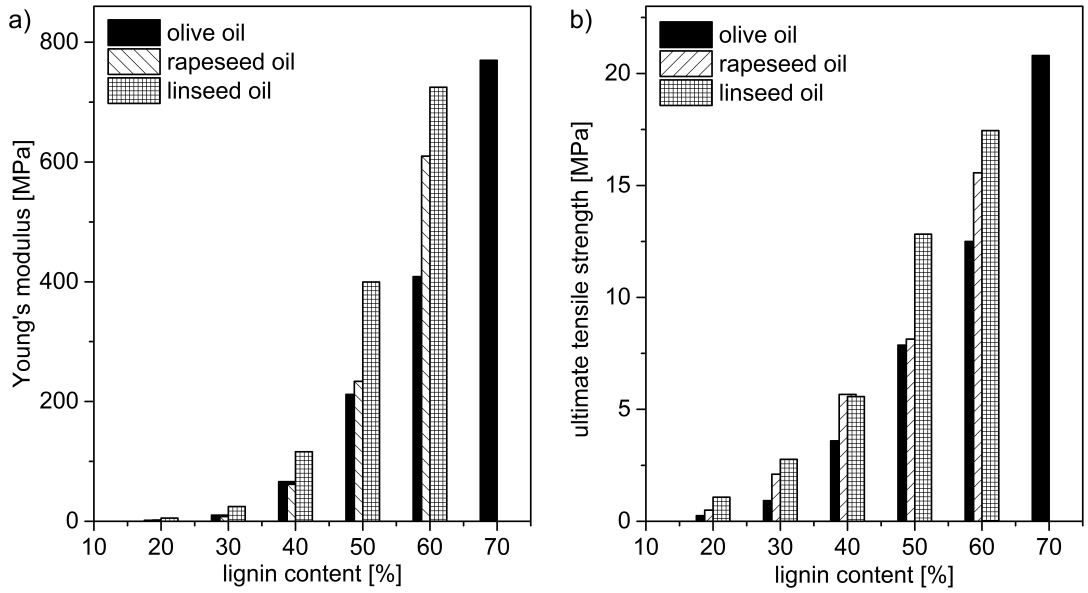

Figure 5.4: Dependency of **a)** the Young modulus (*E*) and **b)** the ultimate tensile strength on the lignin content and the nature of the plant oil for films prepared with DCM and cured at 120 °C. Values were obtained from stress/strain measurements recorded with a 25 N load cell and a crosshead speed of 0.5 mm min^{-1}.

This change in content of polyunsaturated fatty acids influences the properties of the products. Polyunsaturated fatty acid chains, like linoleic and α-linolenic acid, dominate in linseed oil, whereas olive oil consist mainly of monounsaturated oleic acid. Thus, the products and side products of the cross-metathesis differ in their chain length. Linoleic acid and α-linoleic acid, the main building block of linseed oil's triglyceride (**104**), can lead to the formation of a triglyceride dimer (**105**) and hex-3-ene (**106**) in a side reaction (Scheme 5.4). Other side reactions that form short chain products are possible. Those short aliphatic chains are volatile and evaporate faster under the applied conditions at 120 °C in vacuum. In addition, the higher double bond density in the starting material may have led to a more efficient metathesis and thus improved cross-linking. Another evidence for the evaporation of short chain molecules is the isolated yield of the cured films. For all films, the yields tend to decrease going from high to low lignin content (Table 5.1). This effect supports the theory of evaporating olefins produced by triglyceride self-metathesis. The lowest yields were obtained using linseed oil as soft

component. With 20 wt%, the isolated yield was 76 wt% of the starting materials, whereas with olive oil and rapeseed oil 83 and 81 wt% were obtained, respectively. This result is in agreement with the strengthening observed in stress/strain measurements.

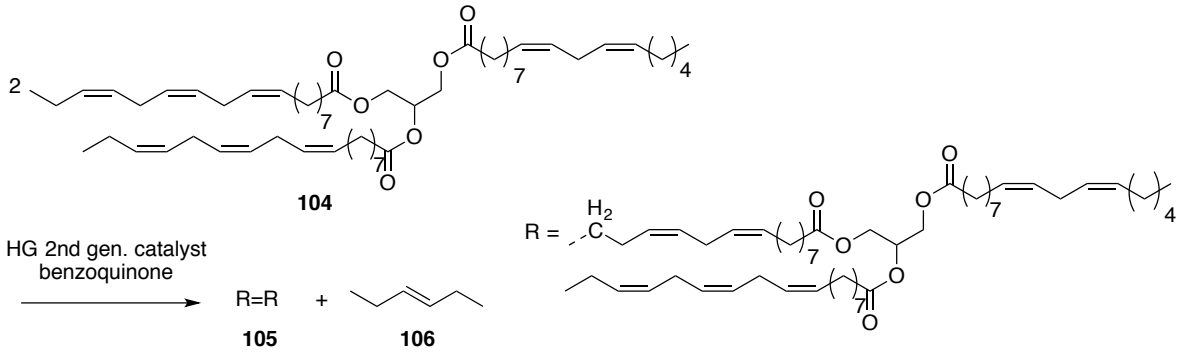

Scheme 5.4: Self-metathesis of linseed oil (representative triglyceride from linoleic and alpha-linolenic acid, **104**) as possible side reaction to form the dimer (**105**) and hex-3-ene (**106**).

5.2.5 Influence of the reaction temperature on the mechanical properties

The curing was performed at an oven temperature of 80 and 120 °C for the samples with 30 and 50 wt% of lignin as hard component together with olive oil as soft component. In stress/strain measurements, the products were compared to analyze the temperature influence on the mechanic properties (Figure 5.5). It was observed that the samples cured at 80 °C for 24 hours show a significantly lower Young's modulus of 160 MPa for 50 wt% lignin compared to 210 MPa for the sample cured at 120 °C for 24 h. Likewise, the ultimate tensile strength is decreased to 6.8 MPa compared to 7.9 MPa for higher temperature. For 30 wt% lignin, a similar trend is observed. The strengthening of the material due to higher curing temperature indicates a higher cross-linking density either due to better evaporation of the solvent as well as side products and/or higher activity of the catalyst.

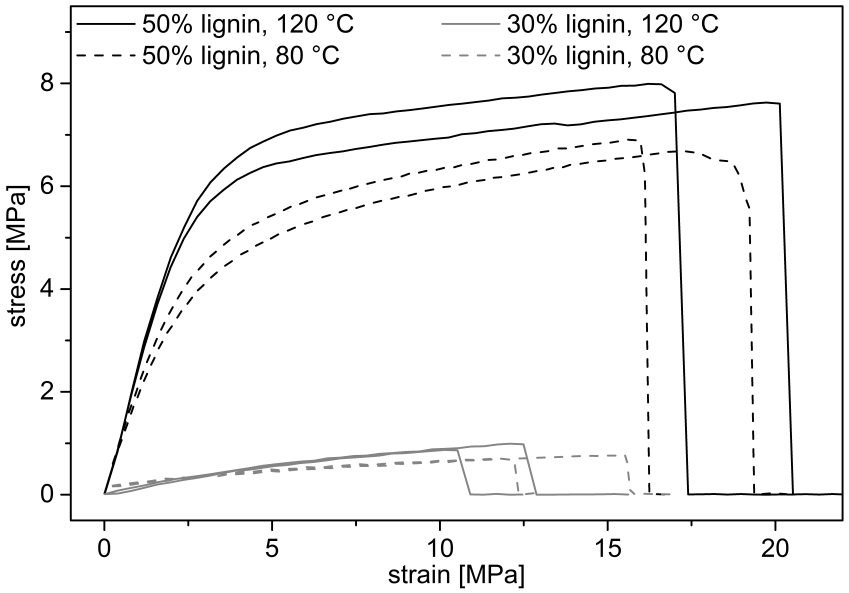

Figure 5.5: Influence in the stress/strain behavior of the reaction temperature of lignin-olive oil film curing obtained from preparation in DCM, recorded with a 25 N load cell and a crosshead speed of 0.5 mm min^{-1}, multiple measurements from one product.

5.2.6 THF uptake and soluble part of the bio-based films

Swelling tests in THF were performed to gain insight into the cross-linking of the cured films and the efficiency of the curing. Swelling percentage and soluble part were calculated from Equations 9.3 and 9.4 in the Experimental Part, Section 9.7.15. For all plant oils, the swelling percentage decreased with increasing lignin content (Table 5.2). For instance, lignin-olive oil films showed a swelling percentage of 300% with a lignin content of 20 wt%, whereas 80 wt% of lignin led to a significantly lower swelling percentage of 110%. Likewise, the swelling percentage depends on the nature of the incorporated plant oil. The use of 80 wt% rapeseed oil or linseed oil (20 wt% lignin) decreased the swelling to 280% and 160%, respectively. A high swelling percentage indicates a low cross-linking density. Linseed oil contains the highest percentage of polyunsaturated fatty acids. The increased double bond density in the starting material could explain the highest cross-linking density in linseed oil films due to a higher reactivity. Additionally, the faster evaporation of possibly formed volatile side products in linseed oil compared to long-chain side products in olive oil can push the equilibrium towards cross-linking reactions, thus increasing the cross-linking density. The evaluation of the soluble part showed an even clearer trend. Linseed oil led to soluble parts under 10% for all lignin-to-oil ratios. Rapeseed oil showed good results for films with 30 to 80 wt% lignin (4–10% soluble part). For olive oil, relatively high soluble parts were obtained (*e.g.*, 35% for 20 wt% lignin). A high soluble part is characteristic for the presence of starting material in the material or products with low cross-linking density. In the present study, the soluble part should mainly consist of low molecular weight side products that did not evaporate during the reaction (confirm Scheme 5.3). In conclusion, the earlier described tendencies of mechanical properties are in agreement with the THF swelling experiments. Indeed, films with lower *E* values and tensile strength exhibit a lower cross-linking density indicated by a higher THF uptake and lower efficiency of the curing, as shown by the soluble part in THF.

Table 5.2: Swelling behavior in THF of lignin-plant oil films formed in DCM and cured at 120 °C.

Lignin content	Olive oil		Rapeseed oil		Linseed oil	
	Swelling	Soluble part	Swelling	Soluble part	Swelling	Soluble part
[wt%]	[%]	[%]	[%]	[%]	[%]	[%]
20	300	35	280	21	160	9
30	180	25	160	10	140	7
40	140	20	140	5	100	4
50	140	16	130	2	110	5
60	140	18	160	5	130	5
70	150	20	140	3	120	5
80	110	18	120	4	120	5

Swelling was performed by immersion a sample for 24 h in THF to obtain the swelling percentage as well as the soluble part in THF from the dry mass after swelling (see Equations 1 and 2 in the Experimental Part).

5.2.7 Replacement of dichloromethane by a "greener" solvent: dimethyl carbonate

Dimethyl carbonate (DMC) was chosen as a "greener" solvent to increase the sustainability of the bio-based thermosets. Conventionally, DMC is obtained from phosgene. More sustainable alternatives are discussed in Chapter 3. In DMC, the utilized Hoveyda-Grubbs catalyst 2nd generation catalyst (HG2) showed worse solubility than in DCM. Thus, the reagents were stirred at 50 °C for 2 hours prior to film formation. On the one hand, this facilitated the solubility of all compounds in DMC. On the other hand, the reagents were thus prepolymerized, which facilitated the film formation afterwards. Stress/strain measurements of samples for both preparations were performed and compared for different weight ratios of lignin with olive oil (Figure 5.6a for 40 and 50 wt% lignin). The ultimate tensile strength is comparable for the two solvents. For instance, 50 wt% of lignin led to an ultimate tensile strength of 7.9 and 7.0 MPa if films are prepared in DCM or DMC, respectively. Young's moduli barely vary for lignin contents of 20 to 40 wt% (Table 5.3). However, higher lignin contents led to a more brittle material if DMC is used. Thus, products with a lignin content higher than 50 wt% could not be analyzed *via* stress/strain measurements as the films broke during sample preparation. The small differences of the product properties may result from the lower reactivity of HG2 in DMC compared to DCM.

Table 5.3: Properties of lignin-olive oil films, formed in DMC, cured at 120 °C with standard deviations of multiple measurements.

Lignin content [wt%]	Elongation at break[a] [%]	Young modulus[a] [MPa]	Ultimate tensile strength[a] [MPa]	Yield [wt%]	Swelling[b] [%]	Soluble part[b] [%]
20	38 ± 10	0.65 ± 0.1	0.23 ± 0.1	82	-[c]	53 ± 0.01
30	30 ± 6	16 ± 1	1.1 ± 0	86	320	39 ± 0.1
40	33 ± 2	77 ± 2	2.9 ± 0.1	86	286	34 ± 0.9
50	13 ± 4	290 ± 8	7.0 ± 0.2	86	200	29 ± 0.6
60	-[d]	-[d]	-[d]	-[d]	175	22 ± 0.2

[a] from stress/strain measurements recorded with a 25 N load cell and a crosshead speed of 0.5 mm min^{-1}; [b] in THF, [c] not possible to measure swelling percentage as the product could not be entirely removed from solvent; [d] products were too brittle to form dogbone-shaped specimen.

In a comparative study, a self-metathesis of allylated lignin was performed in DCM and DMC. In both solvents, a similar molecular weight distribution was obtained after 30 minutes. However, in DCM the reaction was significantly faster in the following 4.5 hours, which was observed by a broadening of the molecular weight distribution (Figure 5.6b). This study showed that the difference in the lignin-oil films is rather a result of reactivity difference than a solubility problem of the catalyst or a problem of solvent removal. Yields of the DMC-cured films were similar to those with DCM. Swelling tests in THF revealed that the use of DMC as solvent instead of DCM led to lower cross-linking density. The use of 20 wt% lignin led to a soluble part of 53% instead of 35% for DCM. However, at higher lignin contents, the values are closer to each other. For 60 wt% lignin, DCM led to a soluble part of 18% and the "greener" alternative DMC to 22% (Table 5.3). In conclusion, it is possible to replace DCM by DMC for the curing of lignin-plant oil films, but mechanical properties show deviations and cross-linking is poor. More optimization studies would be necessary to obtain identical products.

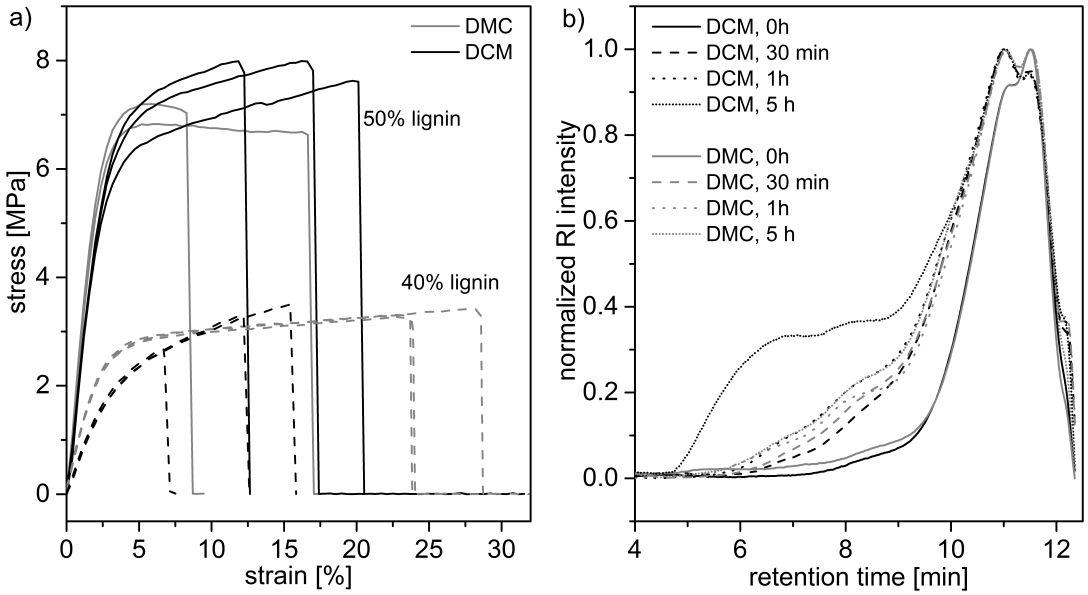

Figure 5.6: a) Stress/strain curves for lignin-olive oil film with 40 and 50 wt% lignin prepared from DCM and DMC, recorded with a 25 N load cell and a crosshead speed of 0.5 mm min^{-1}, multiple measurements from one sample; **b)** SEC (THF) traces of self-metathesis products of allylated lignin of a reactivity test in the two solvents: DCM and DMC. Conditions: allylated lignin (100 mg) was dissolved in DCM or DMC (1000 µL). Hoveyda Grubbs 2nd generation catalyst (0.3 mol%) and benzoquinone (1 mol%) were added. The solution was stirred at 30 °C and SEC samples were measured after 30 minutes, 1 hour and 5 hours.

5.2.8 Differential scanning calorimetric analysis of lignin-plant oil films

Differential scanning calorimetry (DSC) was performed to investigate the thermal properties of the thermoset products. Representative traces for lignin-olive oil films with different weight ratios revealed melting points between 0 and 13 °C (Figure 5.7a). The intensity of the endothermic transitions and thus, of the melting points, decreased with increasing lignin content, thus indicating that it originates from the plant oils. This is pointed out by the absorbed heat (ΔH) during the melting process (Table 5.4). For 20 wt% lignin, the observed enthalpy was -21 J g^{-1}, whereas for 80 wt% lignin, a very weak melting point with only -0.22 J g^{-1} was observed. This supports the above-described incorporation of side products. The presence of a shoulder in the melting point indicates that at least two side products are present (Figure 5.7a). This aligns with the composition of the triglycerides from different fatty acids. DSC analysis of rapeseed oil- and linseed oil-derived films showed melting points with lower intensities (Table 5.4). For instance, with 20 wt% lignin the absorbed heat of the melting point decreased from -21 J g^{-1} for olive oil to -16 J g^{-1} for rapeseed oil to -14 J g^{-1} for linseed oil. A shift to a lower melting point is observed in the same order (Figure 5.7b), indicating that the incorporated products are dependent on the composition of the oil. For rapeseed and linseed oil, films with higher lignin content (60 and 40 wt%, respectively) did not show any melting point. Glass transition temperatures (T_g) of the films are weak, which is typical for inhomogeneous structures like lignin. Compared to the allylated lignin (T_g = 80 °C), the T_g decreased in all films (Figure 5.8). Olive oil films showed a glass transitions around 70 °C (Figure 5.7a), rapeseed oil films around 60 °C and linseed oil films around 55 °C (Table 5.4). This decrease of the glass transition is in agreement with the increasing cross-linking density, verified by swelling tests and also discussed above for IR results. Overall, the DSC study confirmed the presence of side products in the films and the difference in cross-linking efficiency for the different plant oils.

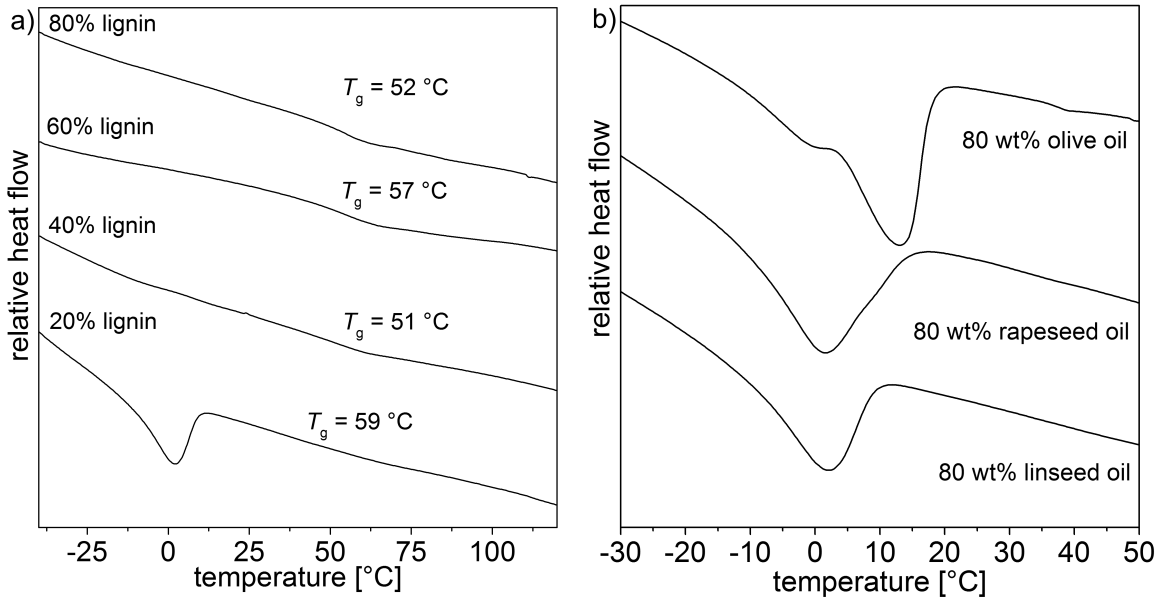

Figure 5.7: DSC traces **a)** of lignin-olive oil films formed in DCM and cured at 120 °C and **b)** for films with different plant oils and 20 wt% lignin (second heating cycle from -70 °C to 140 °C at a heating rate of 20 K min^{-1}).

Table 5.4: Thermal information of DSC analysis of cured lignin-plant oil films formed in DCM: Onset and minimum of the observed melting point and absorbed heat of the transition (ΔH) at a heating rate of 20 K min^{-1}.

Lignin content [wt%]	T_m (onset) [°C]	T_m (minimum) [°C]	ΔH [J g^{-1}]	T_g [°C]
Lignin-olive oil films				
20	-21	13	-21	71
40	-29	2.5	-7.0	68
60	-10	12	-3.3	66
80	-4.3	9.5	-0.22	70
Lignin-rapeseed oil films				
20	-17	1.5	-16 61	
40	-32	-7.9	-2.0	62
60	-[a)]	-	-	59
80	-[a)]	-	-	60
Lignin-linseed oil films				
20	-17	2	-14	59
40	-32	-6	-1.2	51
60	-[a)]	-	-	57
80	-[a)]	-	-	52

[a)] no melting point

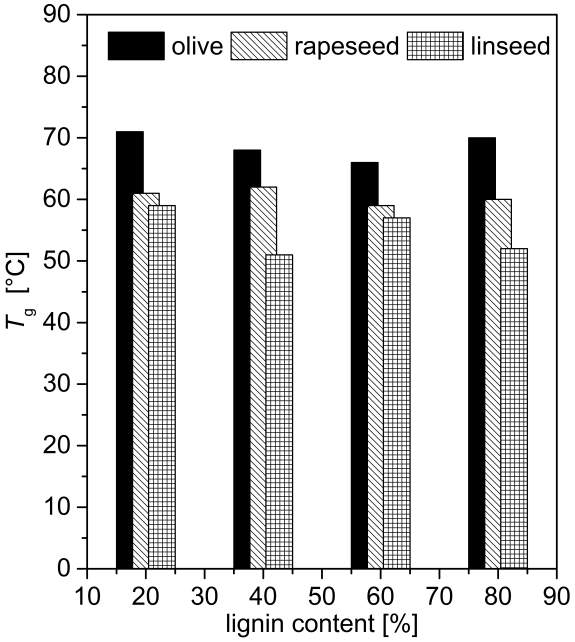

Figure 5.8: Glass transition temperature (T_g) for lignin-plant oil films obtained from DSC studies with a heating rate of 20 K min^{-1}.

5.3 Conclusion and Outlook

In this Chapter, the synthesis of bio-based films prepared by metathesis curing of allylated lignin and different plant oils (olive oil, rapeseed oil and linseed oil) was described. Structural and mechanical analysis was performed with the aid of FT-IR spectroscopy and strain-stress measurements. The lignin-to-plant oil ratio influences the material properties significantly. Lignin's rigid structure leads to brittle materials at high lignin content (70–80 wt%), whereas high plant oil contents lead to ductile and soft films. Comparing different plant oils, the mechanical strength of the material increases with increasing amount of polyunsaturated fatty acids. Under the chosen reaction conditions at 120 °C under vacuum, linseed oil formed materials with the highest Young's moduli (730 MPa for 60 wt% lignin, compared to 610 MPa with rapeseed oil and 410 MPa with olive oil) and lowest soluble part in THF (5–9%). The decrease in T_g is another evidence that a higher density of unsaturated bonds in the starting material leads to a higher cross-linking density. Using linseed oil as soft component for the film, the T_g was decreased to 51 °C. High olive oil content leads to incorporation of side products in the material that act as additional softener. Hence, lower Young moduli and tensile strength as well as high soluble parts are observed. DSC confirmed this incorporation of substrates with melting points around 15 °C.

Film formation was carried out in dichloromethane, but dimethyl carbonate was shown to be a suitable "greener" alternative. The soluble parts were higher and the materials slightly strengthened (higher Young's moduli for same lignin contents) when dimethyl carbonate was used. Optimization needs to be carried out to obtain identical materials with both solvents.

The study in this chapter highlights the possibility of mixing two structurally different renewable materials to prepare cross-linked thermosets with varying and tunable mechanical properties. In addition, allylated lignin was shown to be an reactive cross-linker for thermosets. Its use for other thermoset applications is possible and should be investigated in the future.

6 Epoxy thermosetting polymers from glycidylated lignin

6.1 Introduction

Monomers with two or more terminal epoxide functions are reactive starting materials for epoxy-thermosetting materials. The resulting polymers are characterized by excellent adhesive and tensile strength, toughness, chemical and heat resistance as well as electrical properties. Commonly, epoxy monomers are synthesized from phenolic compounds and epichlorohydrin *via* Williamson ether synthesis. The most commonly used industrial monomer for epoxy resins is bisphenol A (BPA). BPA is one of the most produced chemicals worldwide and broadly used as monomer for epoxy resins, but also for polycarbonates, polyesters or other polymers.[320] It finds applications in consumer products including food containers, bottles, tableware and paper for food packaging and medical equipment.[321] However, BPA exposure to the environment and to humans is followed by health concerns.[321–324] Although its activity as xenoestrogen is already known for decades,[325] the production volume in 2012 was 4.6 million tons, with a rising trend.[326] In addition to health care issues, BPA is obtained from fossil resources. The decreasing fossil feedstock is a growing problem demanding new synthetic routes from renewable resources. As one of the most abundant biopolymers on earth, lignin is a highly available renewable resource.[15] Due to its high aromatic content, it is investigated either for the replacement of aromatic monomers, obtained from lignin degradation (*e.g.*, vanillin, eugenol, other 4-substituted or 2-methoxy phenols[48,67,327]), or used as macromolecular structure for polymeric materials (*i.e.* in blends or composites). The monomer approach towards renewable based epoxy thermosets from lignin-obtained phenols was already intensively investigated. Vanillin-based epoxy thermosets were described in detail by CAILLOL *et al.*[174,328,329] Recently, epoxy thermosets from glycidylated iso-eugenol were presented.[330] In contrast, the macromolecular approach, *i.e.* the use of modified lignin as reactive monomer in epoxy thermosets, is more challenging due to the heterogenic structure of lignin and structural differences emerging through pulping procedures (Kraft, Organosolv, sulfite, pyrolysis, steam explosion,...).

The direct use of lignin as macromolecular structure in polyepoxide networks was limited for a long time to the use in blends and as ring-opening reagents.[115–117,119,331–333] In some cases, modification of lignin becomes necessary. For instance, hydroxy groups in lignin were converted to acidic groups *via* esterification with succinic anhydride, increasing the reactivity towards epoxides.[114] In

the last years, the interest for using glycidylated lignin as epoxide compound increased and various approaches of using lignin-based epoxy thermosetting polymers were presented. MALUTAN *et al.* showed that the glycidylation of Kraft lignin depends on the origin of lignin and on different temperatures and reaction times.[334] For instance, wheat straw lignin led to higher epoxy values than grass straw lignin under the same reaction conditions. Synthesis of cured polyepoxides with lignin are described with a) a conventional coating primer,[335] b) the diglycidylether of BPA (DGEBA) as additional epoxide compound and different hardeners (triethylenetatraamine,[336] 4,4'-diaminodiphenylmethane (DDM)[337,338] or a imidazole-based hardener[45]) or c) without a second epoxide compound, using a tung oil derived hardener[339] or a conventional novolac.[340] The various publications address different aspects of the characteristics of lignin-based epoxy thermosets. Some focus on thermal properties[337,340] and others analyze specific applications, such as epoxy asphalts[339] or coatings.[335] Recent publications examined the DSC curing behavior of lignin-based epoxides, analyzing the activation energy.[338,339]

In this chapter, the influence of macromolecular glycidylated organosolv lignin (GOL) content in a conventional epoxy polymer with DGEBA is described in detail. Isophorone diamine (IPDA) was chosen as cross-linker, since it is a common industrial amine hardener. A full analysis of basic properties is covered by analysis of curing behavior *via* DSC, structural information from IR and SEM, thermal properties from DSC and TGA, mechanical properties obtained by strain/stress measurement and DMA, as well as swelling behavior.

6.2 Results and Discussion

6.2.1 Characterization of the glycidylated organosolv lignin

OL was isolated at Thünen Institute of Wood Research *via* an ethanol—water pulping and used without further fractioning (for details, see Experimental Part). A full characterization of this batch OL can be found in Section 4.2.5. The reaction of OL (**88**) with epichlorohydrin (**15**) to glycidylated OL (GOL, **107**) in the presence of sodium hydroxide and tetrabutylammonium bromide was performed without external heating (Scheme 6.1). The exothermic reaction led to heat evolution, so that ice cooling was necessary in the first hours to avoid temperatures above 50 °C. In literature, the increase of reaction temperatures from 50 to 70 or 90 °C led to lower epoxy contents.[334,341] However, no reaction conditions at room temperature are described.

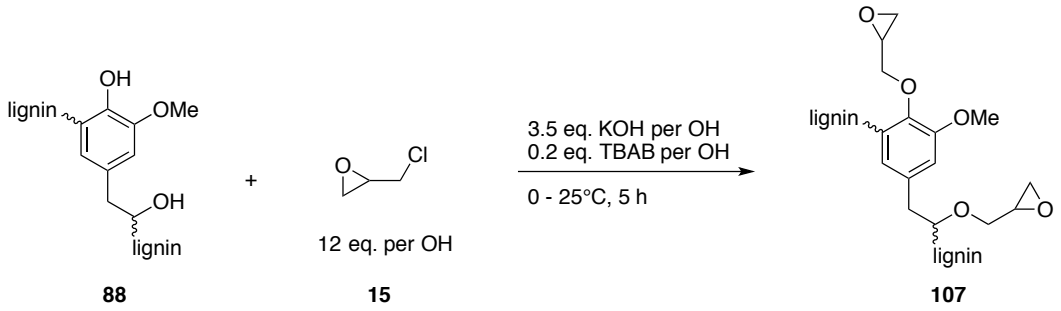

Scheme 6.1: Glycidylation of organosolv lignin (**88**) with epichlorohydrin (**15**).

In the present work, a lignin epoxy material (**107**) with an epoxy content of 3.2 mmol g^{-1} was obtained. The value is in the range of similarly functionalized steam exploded lignin[45,340] or organosolv lignin[337]

and higher than for glycidylated Kraft or acetic acid lignin.[334,336,341] The comparison reveals that organosolv and steam exploded lignin result in higher epoxy contents. A reason for this behavior may be the better solubility and lower molar mass of these lignins. Moreover, a higher aromatic hydroxyl group content in these lignins is present due to the pulping conditions. In addition to the titration result, ^{31}P NMR was performed. The glycidylated compound (**107**) showed a decrease of the aromatic hydroxyl groups from 2.23 mmol g^{-1} to 0 mmol g^{-1}, indicating that all phenolic groups reacted (Table 6.1). The value for the aliphatic hydroxy groups decreased from 3.83 to 2.57 mmol g^{-1} leading to an overall functionalization of around 3.5 mmol g^{-1}. The value is in the range of the one obtained from titration. A ring opening with water as nucleophile would result in two new aliphatic hydroxy groups, explaining a change in signal shape of the aliphatic region (Figure 6.1).

Table 6.1: Analytical results for unmodified and glycidylated lignin.

	Epoxy content[a)] [mmol g^{-1}]	Aliphatic OH content[b)] [mmol g^{-1}]	Aromatic OH content[b)] [mmol g^{-1}]	Total OH content[b)] [mmol g^{-1}]
Unmodified OL (**88**)	0	3.83	2.23	6.06
Glycidylated OL (**107**)	3.2	2.57	0	2.6

[a)]from titration; [b)] from ^{31}P NMR analysis

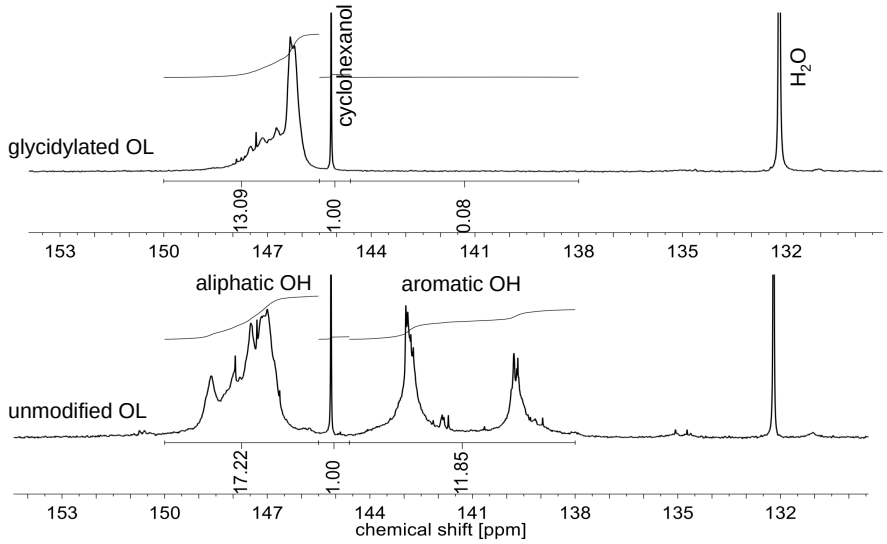

Figure 6.1: ^{31}P NMR spectra of unmodifed (**88**, bottom) and glycidylated OL (**107**, top) with TMDP (**5**) as phosphorylating agent and cyclohexanol as internal standard.

FT-IR analysis of glycidylated lignin revealed a significant decrease of hydroxyl group stretching vibrations at a wavenumber $\tilde{\nu}$ of 3450 cm^{-1} (Figure 6.2a), indicating their functionalization. In addition, a new signal appeared at 909 cm^{-1}, which is typical for the asymmetric stretching vibration band of C-O-C in epoxy functions.[342] Vibrations of ether linkages, such as the newly formed C-O-glycidyl, show typical bands in the region between 1000 and 1200 cm^{-1}. Here, a significant increase was observed. The signals of the functional groups that did not take place in the modification procedure, such as C-H bonds (2600–3000 cm^{-1}) and aromatic C=C bonds (1502 and 1597 cm^{-1}), did not change. The results are in agreement with previous reported FT-IR spectra for glycidylated lignins.[45,334,336,339–341]

Analyzing the degradation temperature for 5% weight loss ($T_{d\,5\%}$), the thermal stability revealed an increase accompanied with glycidylation, from 233 to 269 °C (Figure 6.2b). The main difference occurred during the first 30% weight loss. At the $T_{d\,30\%}$ value, the degradation traces assimilated. Both traces showed two main degradation steps. This first degradation process between 280 and 350 °C can be assigned to inter-unit ether bond cleavage in lignin. This results in evaporation of volatile aromatic compounds.[343,344] A second step occurs between 500 and 600 °C. At this temperature, aromatic rings are expected to decompose.[345] This two-step degradation is characteristic for cross-linked materials with aromatic and ether functional groups as in lignin. This first degradation step is more relevant for glycidylated lignin (**107**) compared to unmodified lignin (**88**) as there are additional ether functions in the product. Increased degradation temperatures for glycidylated lignin compared to unmodified lignin are described in literature for Kraft lignin[341] as well as for organosolv lignin.[346]

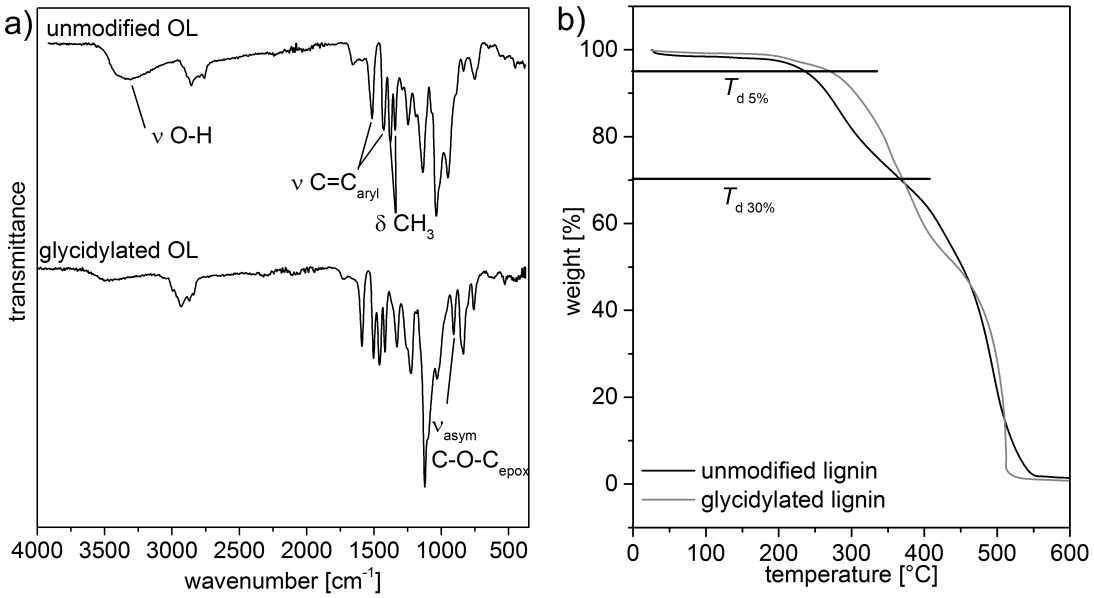

Figure 6.2: a) FT-IR spectra (ATR) of unmodified lignin (**88**, top) and glycidylated lignin (**107**, bottom); **b)** TGA traces of unmodified and glycidylated OL.

6.2.2 Curing behavior of lignin reinforced epoxy thermosetting networks

The curing behavior of lignin reinforced epoxy thermosets was investigated *via* DSC studies. GOL (**107**) and DGEBA (**16**) were mixed with different lignin contents (0 to 50 wt% of the epoxy part, which is 0 to 42 wt% of the final product) and with a stoichiometric amount of IPDA (**108**) to form a cross-linked material (**109**) (Scheme 6.2).

IPDA (**108**) contains two amines – an aliphatic amine and a cycloaliphatic amine. Each amine can react with two epoxides.[347] Thus, the molar ratio *r* is calculated as followed:

$$r = \frac{f_{\mathrm{DGEBA}} \cdot n_{\mathrm{epoxy}}(\mathrm{DGEBA}) + n_{\mathrm{epoxy}}(\mathrm{GOL})}{f_{\mathrm{amine}} \cdot n_{\mathrm{amine}}} \tag{6.1}$$

assuming that the functionality of IPDA (**108**) (f_{amine}) is equal to 4, the functionality of DGEBA (**16**) (f_{DGEBA}) is equal to 2 and the molar quantities of amine (**108**), DGEBA (**16**) and GOL (**107**) are

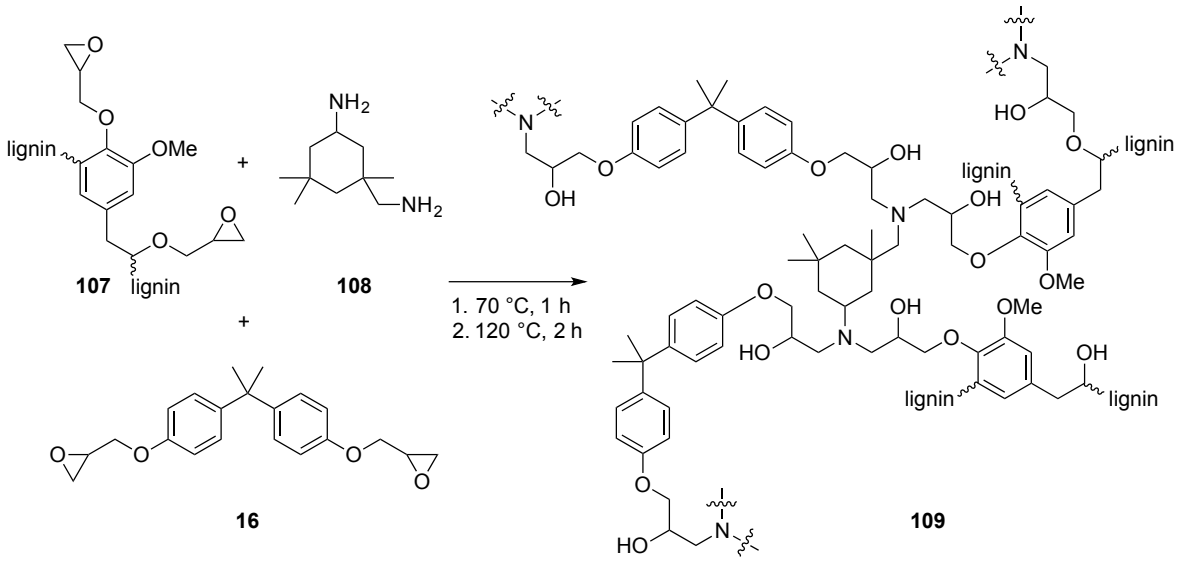

Scheme 6.2: Scheme 2: Cross-linking of GOL (**107**), DGEBA (**16**) with IPDA (**108**) to form a partially bio-based epoxy network (**109**).

assigned to n_{amine}, n_{epoxy}(DGEBA) and n_{epoxy}(GOL), respectively. Hence, a stoichiometric amount is defined by a ratio r = 1 and usually leads to the highest thermomechanical properties.[348] The recorded DSC traces for the curing of epoxy thermosetting networks (**109**) with different lignin contents in the final product are shown in Figure 6.3a. The heating revealed an exothermic peak with a starting point at 50 °C, a maximum around 110 °C and end point at 220 °C. The maximum shifts slightly to lower temperature, from 114 °C to 100 °C, with increased lignin content of 0 wt% to 42 wt%, respectively. A shoulder, observed at 150 °C, decreased in intensity with increasing lignin content. The two peaks result from the difference in reactivity of the aliphatic and cyclo-aliphatic amino groups in IPDA (**108**). Cyclo-aliphatic amines are less reactive than aliphatic amines.[347] A reason for the decrease of the shoulder and the shift of the maximum with increased lignin content may be assigned to the remaining free hydroxyl groups in lignin, that react with epoxides, hindering amines to react. Usually, the reaction of hydroxyl groups with epoxides is only relevant if excess of epoxides are used.[347] Yet, the sterically hindered structure of lignin may favor this reaction.

The residual reaction heat ΔH of the curing process is plotted against the lignin content in the final network (Figure 6.3b). ΔH in J g^{-1} decreased with increasing lignin content from 385 J g^{-1} for 0 wt% to 291 J g^{-1} for 42 wt% (Figure 6.3b, black). The ΔH value for the lignin-free DGEBA-IPDA thermoset is in the order of literature values.[348,349] To the best of my knowledge, no residual heat reaction was analyzed for lignin-based epoxide curing in literature before. Simultaneously with the reaction heat decrease, the epoxy group content in the uncured mixture decreased from 5.88 to 4.54 mmol g^{-1}. Considering this decrease, the reaction heat varies between 56 and 66 J $mmol^{-1}$ epoxide without significant increase or decrease tendency (Figure 6.3b, grey), indicating that the reactivity of the epoxides in GOL (**107**) and DGEBA (**16**) is similar. Small variations of the values (Figure 6.3b, black and grey) may result from the accuracy of the measurement (weighted masses, miscibility problems, accuracy of the instrument). For instance, the highest amount of lignin led to a bad miscibility which may have influenced the curing behavior.

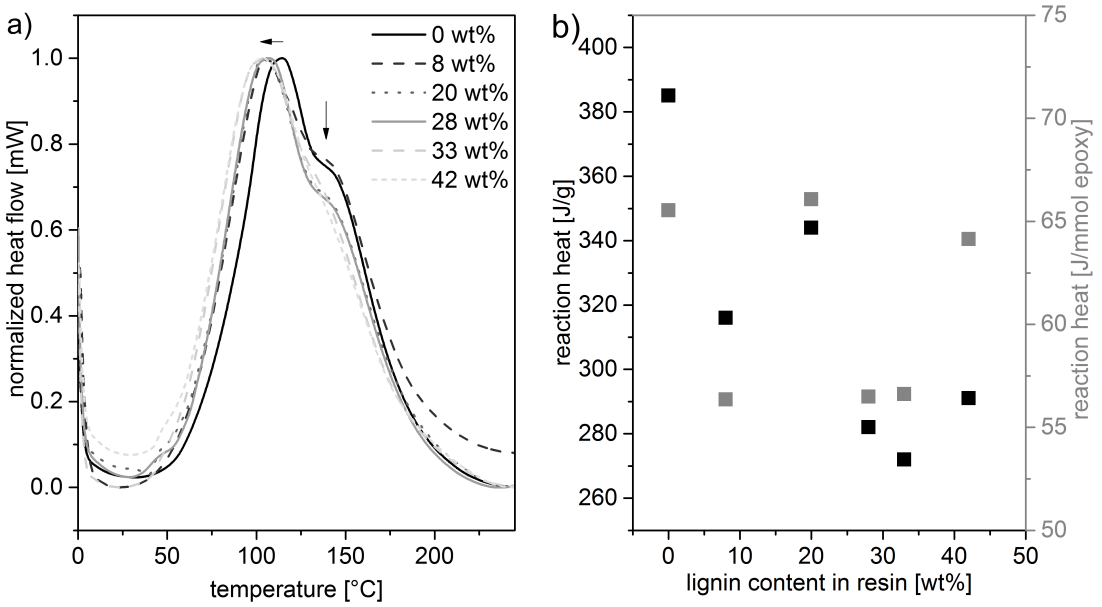

Figure 6.3: a) Normalized DSC traces of the curing of DGEBA-based epoxy networks (lignin content in wt%) at a heating rate of 10 K min^{-1}, black arrows indicate decrease tendencies; **b)** Reaction heat in J g^{-1} (left axis, black) and in J $mmol^{-1}$ epoxy (right axis, grey).

6.2.3 Structure of cured epoxy thermosets

The final networks were cured in an oven at 70 °C for 1 hour and 120 °C for 2 hours in dog bone shape silicon molds to obtain specimens for direct structural and thermomechanical analysis. Comparison of the IR region between 500 and 1800 cm^{-1} for cured epoxy polymers (**109**) with uncured GOL (**107**) shows the decrease of the epoxy C-O deformation vibration band for networks with lignin contents between 0 and 33 wt% (Figure 6.4). Only for the thermoset with 42 wt% GOL, the signal at 909 cm^{-1} is still present, indicating an inefficient curing process. Other changes in signal in Figure 3 can be explained as followed from the lowest wavenumber going to the highest. The broad signal at < 600 cm^{-1} results from skeletal C-C-C and H-C-C deformation vibrations mainly found in BPA and IPDA. The increased signal at 830 cm^{-1} should mainly result from the C-H deformation vibration in the 1-4 substituted BPA.[350] C-N stretching vibrations of tertiary amines contained in the cured epoxy thermosetting networks show a typically band at 1070 cm^{-1}. The signal is overlaying with the symmetric C-O-C stretching vibration of aromatic ether and the C-H deformation vibration of 1,4-substituted BPA. Likewise, the new signal at 1180 cm^{-1} can be assigned to the deformation vibration of benzylic C-H in BPA. Aromatic ether in BPA show a broad band for the asymmetric C-O-C stretching vibration at 1233 cm^{-1}. Due to the different origin of the C=C stretching vibrations in the aromatic rings of BPA compared to GOL, two signals can be found, at 1581 and 1608 cm^{-1}. All in all, the IR analysis showed the expected changes and proved the reaction of the epoxides. Only in the case of the highest applied lignin content, no efficient reaction was observed. The reason for inefficient reaction may be the poor miscibility of glycidylated lignin (**107**), DGEBA (**16**) and IPDA (**108**) due to the high solid-to-liquid ratio. Because of miscibility issues, no higher lignin contents were evaluated.

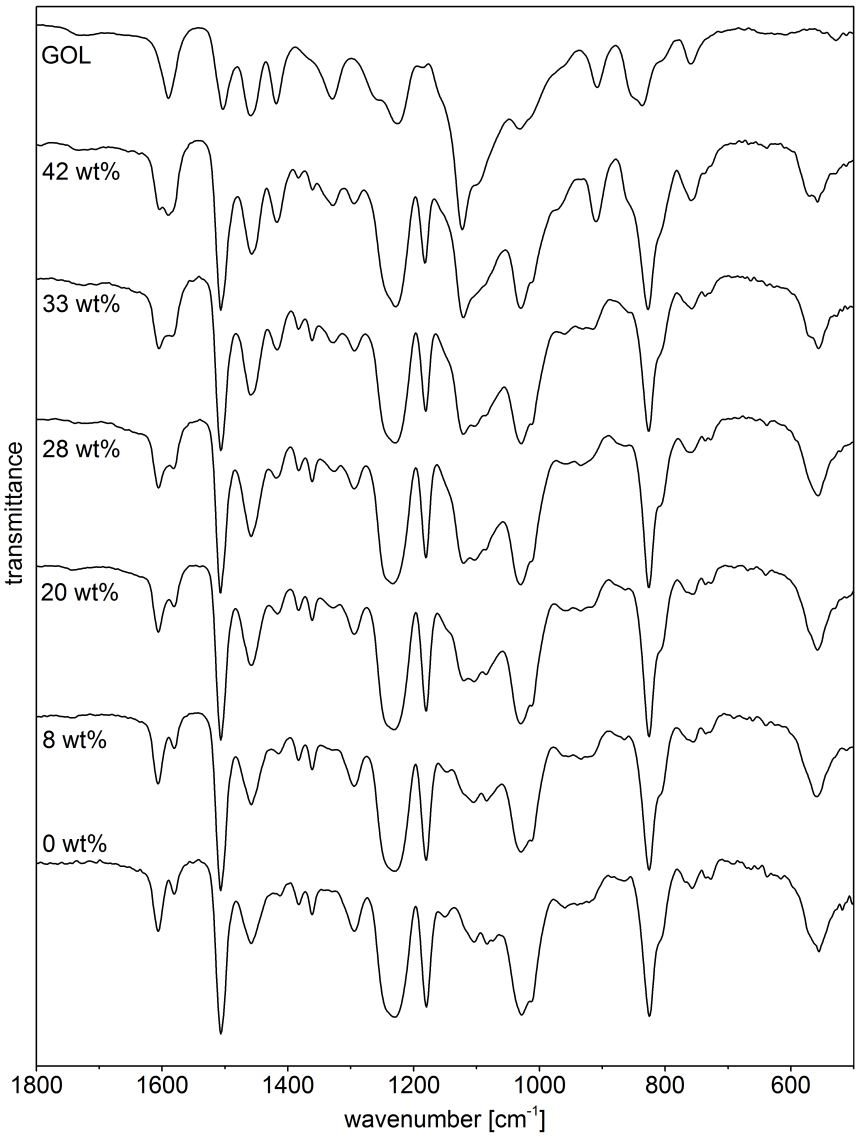

Figure 6.4: IR spectra (ATR) of glycidylated OL (**107**) and cured epoxy thermosets (**109**) between 1800 and 500 cm^{-1}.

SEM images with a magnitude of 5000 of the different epoxy polymers are shown in Figure 6.5a-f. Cured polymers were analyzed at a breaking edge. In all materials, the break caused the visible lamellar structure. Within the structure, homogeneity differences can be observed. The addition of lignin caused the formation of small dots, increasing in number with increasing GOL content. These dots are not observed in lignin-free epoxy thermosetting polymers (Figure 6.5a). With 8, 20 and 28 wt% GOL in the final product, the structure is mostly homogeneous (Figure 6.5b-d). In the thermosets with the highest lignin amounts of 33 and 42 wt% (Figure 6.5e and f), the agglomerations increased compared to lower lignin contents, indicating the partial incompatibility with the epoxy thermoset. This incompatibility can be explained by the inhomogeneous structure of lignin itself. Compared to literature results of SEM images for lignin-based polyepoxides, the herein discussed GOL still shows a better compatibility at higher lignin content: acetic acid lignin-based epoxy network curing with DGEBA and triethylenetetramine led to higher agglomeration and even porosity if 50 wt% of DGEBA were replaced.[336]

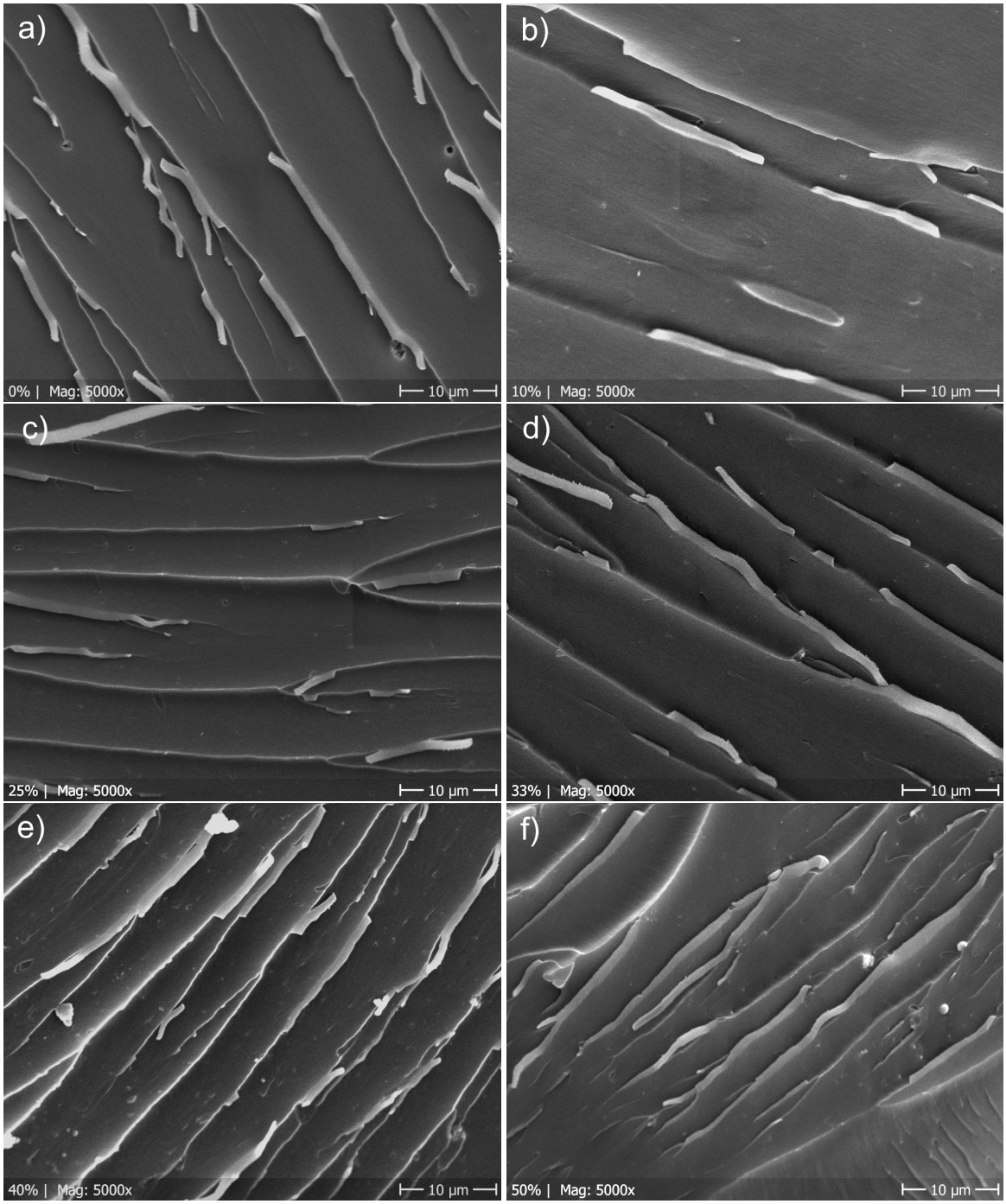

Figure 6.5: SEM images with 5000x magnification at the breaking edge of epoxy thermosets with **a)** 0 wt%, **b)** 8 wt%, **c)** 20 wt%, **d)** 28 wt%, **e)** 33 wt% and **f)** 42 wt% GOL in the final product (the shown percentages indicate the DGEBA replaced by GOL).

6.2.4 Thermomechanical properties of epoxy thermosetting polymers from glycidylated lignin and DGEBA

The influence of the lignin content on thermomechanical properties was studied by TGA, DSC, DMA and stress/strain measurements. The degradation temperature for 5% weight loss ($T_{d\,5\%}$), measured *via* TGA, decreased from 334 °C to 284 °C, with increasing lignin content (Table 6.2). Regarding the weight loss trace (Figure 6.6), the degradation temperature for 30% weight loss ($T_{d\,30\%}$) is in a narrower region between 338 and 350 °C. Likewise, the lignin-free composite is the most stable thermoset. The heat resistant index T_s, calculated from Equation 9.1 (see Experimental Part), varies between 168 and 156 °C and thus, also decreased with increasing lignin content (Table 6.2). Although this initial degradation starts at higher temperatures for lignin-free thermosets, the second degradation step starts later for lignin-containing products. Earlier initial degradation for lignin-containing thermosets coincides with observations for other lignin-DGEBA[336] and lignin epoxy polymers without second epoxy compound.[45,340] The first degradation, as discussed for the unmodified and glycidylated lignin, occurs mainly between 280 and 350 °C and is most significant for all samples. A second degradation step from further cracking processes occurs between 500 and 600 °C. Since this behavior hardly changes with the addition of lignin, the similar characteristics of linkages in lignin-based and lignin-free epoxy material is exhibited.

Table 6.2: Degradation temperatures for modified lignin and epoxy thermosetting polymers.

Lignin content [wt%]	$T_{d\,5\%}$ [°C]	$T_{d\,30\%}$ [°C]	T_s [°C]
Unmodified lignin	233	265	153
Glycidylated lignin	269	371	162
0	334	350	168
8	318	343	163
20	316	341	162
28	308	338	160
33	304	338	159
42	284	342	156

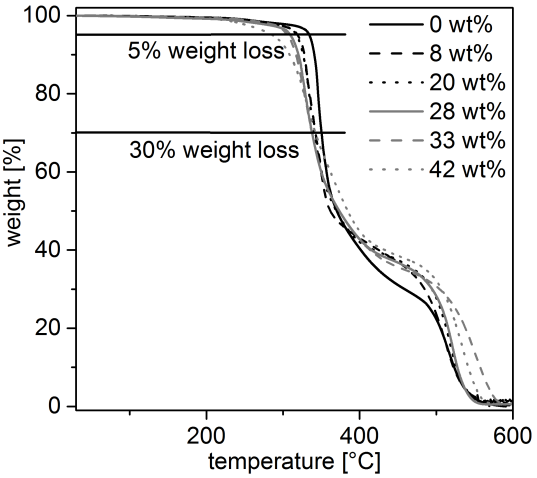

Figure 6.6: Comparison of the weights loss during TGA for the different thermosets at a heating rate of 5 K min^{-1}.

The glass transition temperature (T_g) of the cured materials (**109**) was evaluated from DSC and DMA measurements (Figure 6.7a). T_g increased from 150 °C to 168 °C (DSC), with increasing lignin content from 0 to 33 wt%. DMA results show the same tendency, with T_g values ranging from 123 to 138 °C. Going to 42 wt% lignin, T_g drops to 132 °C (for DMA; no T_g observed in DSC). An increased T_g may indicate a higher cross-linking density in the epoxy thermosetting polymer.[347] Glycidylated lignin contains free hydroxyl groups that could react with epoxides, leading to higher cross-linking. On the other hand, the inhomogeneous structure of lignin may lead to a more rigid structure, also leading to a higher T_g. The drop of T_g going to 42 wt% of lignin should result from the inefficient reaction revealed by IR analysis (see Section 6.2.3). The low reactivity may have its origin in the mentioned miscibility problems that led to partial agglomeration of lignin and inefficient cross-linking

compared to the thermosets with lower lignin content. The relatively large difference between the two T_g obtained from DSC and DMA result from a broad transition that is likewise seen in the change of the storage modulus (Figure 6.7 for a representative curve). The broad transition is also expressed by the difference of T_g obtained from the onset of the change compared to T_α (Table 6.3), the peak of tan delta, that expresses the midpoint of the change. The more narrow the glass transitions, the closer are onset of the change of the storage modulus and T_α. Indeed, the lignin-free thermoset shows the lowest difference between the T_g from the onset and the T_α. The higher inhomogeneity due to the addition of lignin leads to the broadening of T_g region.

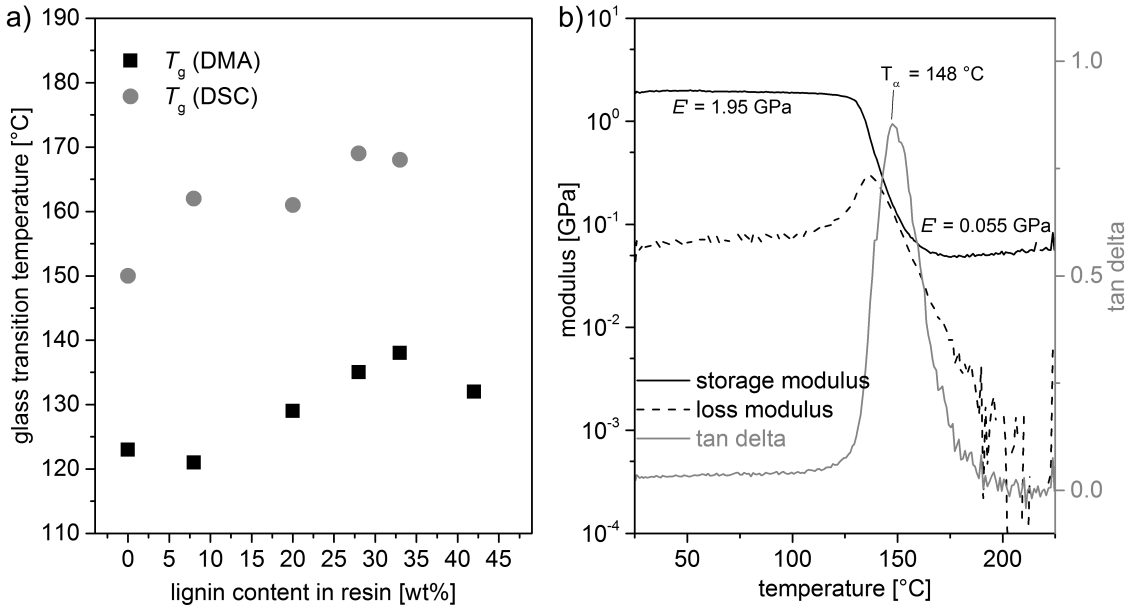

Figure 6.7: a) Glass transition temperature of the thermosetting polymers with different lignin content obtained from the midpoint of the change in heat capacity in DSC (grey) and from the onset of the change of the storage modulus in DMA (black); **b)** Representative DMA trace of a lignin-BPA-IPDA-based thermoset with 20 wt% GOL: Storage (*E'*) and loss modulus (*E"*) and resulting tangente delta (with T_α the maximum of tangente delta) as a function of the temperature.

Mechanical properties of the thermosets from stress/strain and DMA measurements are shown in Table 2. Young's modulus *E* varied between 1.82 and 1.88 GPa. This is within expectations for DGEBA-based epoxy thermosetting polymers. In literature, values around 3 GPa are reported.[351,352] 10% replacement of DGEBA by lignin led to a drop of *E* from 1.88 to 1.82 GPa. A low lignin amount seems to add flexibility to the product, which may be explained by lower epoxy density. Going to a higher lignin content (50 wt% of DGEBA were replaced by GOL), the product became more rigid (*E* increased), leading to a brittle material that could not be fixed to the apparatus without breaking immediately. The increase of *E*, accompanied by higher stiffness, results from the inhomogeneous structure of lignin. This observation coincides with the increasing glass transition with increasing lignin content. The storage modulus *E'* in the glassy state obtained from DMA was in a similar region and showed the same tendency as *E*. Likewise, the observed decrease in the elongation at break for higher GOL content indicates a higher stiffness (Table 6.3, column 3). The cross-linking density, calculated from Equation 9.2 (see Experimental Part) from the storage modulus *E*' in the rubbery phase and T_α, showed an increase with growing lignin content, as already estimated from the glass transition. BPA-IPDA thermosets exhibited a cross-linking density ν of $9.9 \cdot 10^3$ mol m^{-3} and the thermoset with 28 and 33 wt% lignin showed densities of 23 and $22 \cdot 10^3$ mol m^{-3}, respectively.

Only for the product with the highest lignin content of 42 wt%, a decrease was observed. The already discussed for other analytics, GOL (**107**) is poorly miscible with DGEBA (**16**) and IPDA (**108**) if the lignin-content is too high and thus, no satisfying results can be obtained. As described in the discussion of T_g, the optimum can be found for a thermoset with 33 wt% of GOL.

Table 6.3: Values for mechanical properties of cured lignin-BPA-IPDA-based polyepoxides.

Lignin content [wt%]	Young's modulus [GPa]	Elongation at break [%]	E' (36 °C) [GPa]	E' (210 °C) [GPa]	T_g (DMA) [°C]	T_α [°C]	ν [10^3 mol m^{-3}]
0	1.88	3.0	1.37	0.036	123	137	9.8
8	1.82	2.3	2.02	0.048	121	138	13
20	1.84	2.0	1.95	0.055	129	148	15
28	1.92	1.5	1.90	0.087	135	157	23
33	1.90	1.70	1.84	0.083	138	159	22
42	samples broke during traction test preparation		1.07	0.033	132	144	8.8

6.2.5 Swelling properties

The swelling of the cured thermosets (**109**) was performed in THF as described in Section 9.7.15 in the Experimental Part. Swelling and soluble part were calculated from Equation 9.3 and 9.4, respectively, and summarized for all lignin contents (Table 6.4). A lower percentage of swelling usually indicates a higher cross-linking density, as distances within the network are smaller and thus, solvent absorption is lower as well. Swelling decreased from 7 to 1%, in tandem with increased lignin content from 0 to 20 wt%. This implies a higher cross-linking with a lignin content of 20 wt%. Higher lignin contents resulted in increased swelling up to 10% for 42 wt% GOL. The soluble part remained constantly low and then increased with increased lignin content from 0% soluble part for 0, 8 or 20 wt% lignin content to 6% soluble part for 42 wt% lignin content. As estimated from T_g and calculated from DMA, the swelling test revealed the same tendency. The addition of lignin initially stabilized the product due to a higher cross-linking, but led to poor network formation with lignin content of 42 wt%.

Table 6.4: Swelling properties of cured epoxy polymers (**109**) depending on the content of lignin (GOL).

GOL content [%]	0	8	20	28	33	42
Swelling [%]	7	3	1	3	2	10
Soluble part [%]	0	0	0	1	1	6

6.3 Conclusion and Outlook

In this chapter, the synthesis of epoxy thermosetting polymers from glycidylated organosolv lignin and DGEBA in different weight ratios and IPDA as common industrial hardener was described. Under the chosen conditions, lignin could not completely replace BPA. However, in the applied weight ratios, lignin revealed reinforcing properties with weight percentages up to 33% in the final product. DSC curing verified the replacement suitability, indicating a similar reactivity for lignin- and BPA-based

epoxides. The completed reaction in the final products was verified by the disappearance of the epoxy stretching vibration band in IR spectroscopy. In addition, thermal and mechanical analysis revealed that lignin-based thermosets have a higher cross-linking density compared to pure DGEBA-IPDA polyepoxides, if 10 to 40 wt% of DGEBA was replaced. Although, thermal stability decreases with increasing lignin content, degradation temperatures are still in an applicable region for epoxy thermosets. Due to inhomogeneity in lignin itself, inhomogeneity in the product was observed if the renewable content is increased but can still be considered low. All in all, it could be shown that GOL is suitable for partial replacement of DGEBA in an industrial relevant epoxy thermoset.

7 Epoxidation of alkylated compounds

7.1 Introduction

The epoxide function is an interesting functional group for lignin. It can be used as starting point for epoxy thermosetting polymers, can be reacted with CO_2 to form cyclic carbonates or the epoxide can be used to introduce other functional groups *via* a nucleophilic attack, for instance of water to increase the hydroxyl group content. In Chapter 6, it was shown that glycidylated OL (**107**) is a suitable replacement for BPA glycidyl ether (**16**) in epoxy thermosets with an conventional hardener. Although the replacement of the toxic BPA by a renewable, more harmless chemicals is already a good step in the right direction, the whole procedure should be considered following the Principles of Green Chemistry. In the applied procedure, the epoxy function of the utilized lignin was introduced using the toxic compound epichlorohydrin. In addition, the *Williamson Ether Synthesis*, that is necessary in this glycidylation procedure, needs an excess of the reagents sodium hydroxide and epichlorohydrin and produces sodium chloride in equimolar amounts. However, literature on the introduction of the epoxy function to the structure of lignin for epoxy thermoset application, only describes the use of epichlorohydrin (for detailed literature discussion, see Chapter 6). Following the Principles of Green Chemistry, a new pathway to the glycidylated form of lignin starting directly from lignin *via* alkylation with diglycidyl carbonate or starting from the alkylated form using a sustainable epoxidation procedure should be evaluated in this work and is discussed in this chapter.

The search for alternative epoxy monomers starting from renewable resources using sustainable procedures is of high interest. In the field of phenolic and bisphenolic alternatives for bisphenol A (BPA), *e.g.*, from lignin-derived vanillin or eugenol and their derivatives, mainly conventional glycidylation with epichlorohydrin is described.[174,229,328–330,353–355] However, also the epoxidation of allylated compounds is discussed as alternative. For instance, AOUF *et al.* reported the synthesis of epoxy thermosets from gallic acid (**110**), a potentially lignin-derived monomer.[356] In the described work, gallic acid was allylated with allyl bromide (**111**) *via Williamson Ether Synthesis* to the corresponding derivative **110a** (Scheme 7.1). The subsequent epoxidation to polyepoxide **112** was performed with *meta*-chloroperbenzoic acid (*m*CPBA, **113**) as epoxidation reagent or methyl(trifluoromethyl)dioxiran (Scheme 7.1a and b), which was generated *in situ* from 1,1,1-trifluoroacetone (**114**) and oxone^{TM}, both leading to similar yields of over 70% tri- and four-fold epoxidized product. Thus, the use of epichlorohydrin was avoided, but this two-step route still use conventional, toxic allyl bromide (**111**) for the allylation procedure and in addition the epoxidation procedures with *m*CPBA (**113**) or methyl(trifluoromethyl)dioxiran also use non-environmentally benign reagents in excess. In another report, the same group discussed the enzyme-catalyzed epoxidation of allylated vanillic and gallic acid (Scheme 7.1c for gallic acid).[357] This more sustainable approach uses hydrogen peroxide as oxidation agent, which can be considered a "green" reagent as it only produces water as side product.[358] In addition, the use of enzymes is in agreement with the "12 Principles of Green Chemistry" as they usually accelerate reactions under mild conditions, can be reusable and are highly

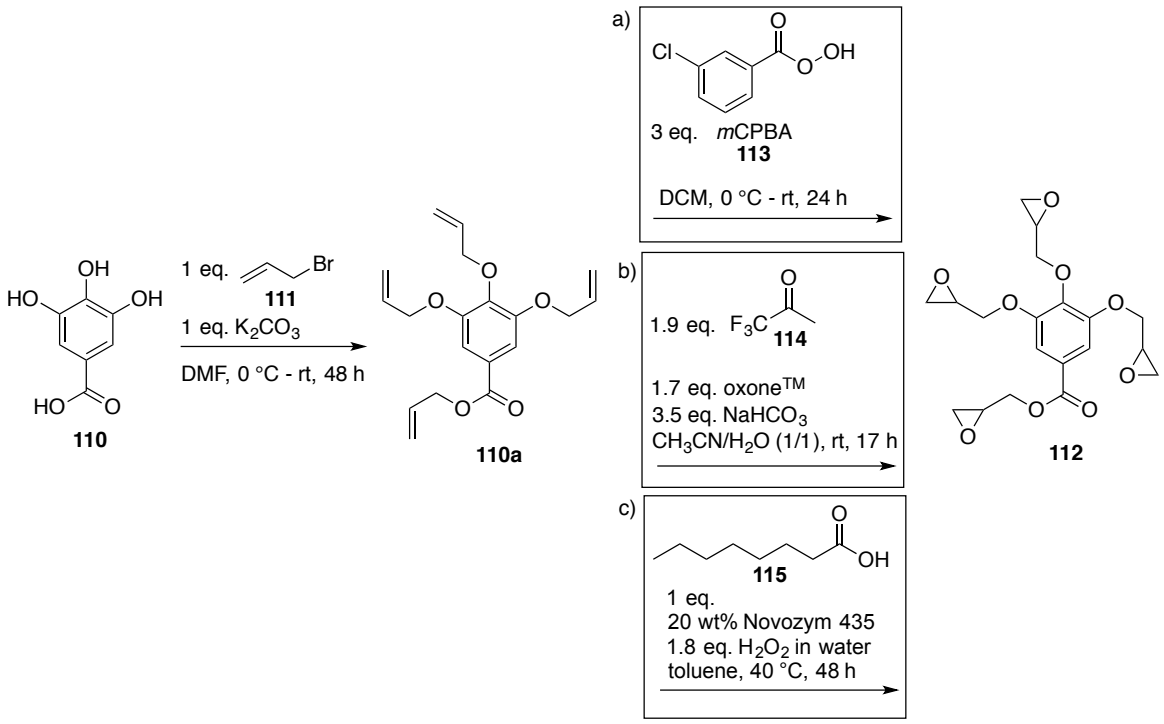

Scheme 7.1: Allylation of gallic acid (**110**) with allyl bromide (**111**) and subsequent epoxidation a) with *m*CPBA (**113**), b) with *in situ* generated methyl(trifluoromethyl)dioxiran or c) *via* an enzyme-catalyzed pathway.[356,357]

selective.[359,360] In the reported study, the enzyme Novozym 435 (immobilized lipase B from *Candida antarctica*) catalyzes the transformation of caprylic acid (**115**) to the peracid derivative, which then acts as oxygen carrier that epoxidized the double bond. Compared to the reaction with *m*CPBA, a lower yield of four-fold epoxidized product was obtained in the enzymatic reaction. However, the overall yield of the three- and four-fold epoxidized product was similar with less equivalents of reagents: 77% with three equivalents *m*CPBA (**113**) and 78% with an equimolar amount caprylic acid (**115**) and 1.8 equivalents hydrogen peroxide. With vanillic acid, the epoxidation with Novozym 435 or *m*CPBA was likewise comparable.

Epoxidation with peracids

The use of peracids, such as *m*CPBA, for the oxidation of unsaturated structures is known since 1909, when PRILESCHAJEW reported the epoxidation of various unsaturated compounds with perbenzoic acid.[361] The general mechanism of this epoxidation procedure is shown in Scheme 7.2.[362] Peracids can be generated *in situ* with hydrogen peroxide (Scheme 7.2a). Additional catalysts may be needed, *e.g.*, Novozym 435 in the case of caprylic acid. This peracid formation is an equilibrium reaction, where the resulting oxygen-oxygen bond in the peracid is weak and thus, intramolecular hydrogen bridges between the carbonyl oxygen and the acid hydrogen stabilize the molecule. Due to the low stability of peracids, *m*CPBA is one of few peracids that are commercially available, but only in purities up to 77%. Stored as powder in the fridge, it is relatively stable. In contrast, peracetic acid is available in a purity of only up to 40% in acetic acid.

The electrophilic oxygen that is present in the peracid molecule is highly reactive. With an

alkene, the electrophilic oxygen reacts in a concerted transition state, where the hydrogen is transferred to the carbonyl oxygen in the same step (Scheme 7.2b). The formed products are the epoxide and the corresponding acid. In additionto epoxidation reactions, peracids can be used for the oxidation of aldehydes and ketones to esters (*Bayer-Villiger Oxidation*), sulfides to sulfoxides or sulfones, amines to nitroalkanes or nitroxides or *N*-oxides.[363–365]

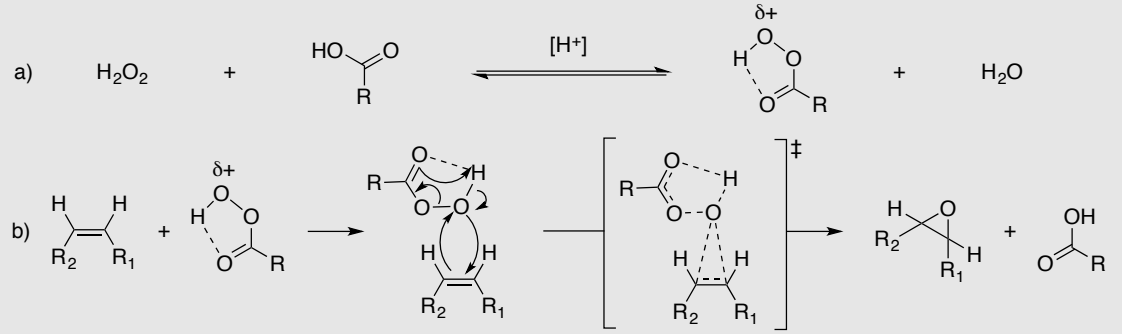

Scheme 7.2: a) Generation of a peracid starting form the corresponding acid and hydrogen peroxide; **b)** mechanism of the epoxidation of an alkene with a peracid.

In recent literature, peracetic acid is described as oxidant in combination with renewable resources. Compared to other peracids, it can be considered more sustainable as acetic acid can be produced from bioethanol *via* catalytic processes and is considered harmless in low concentration, which makes it a relatively "green" reagent.[366,367] CARBONELL-VERDU *et al.* described its use for the epoxidation of cottonseed oil and the subsequent curing with cyclic anhydrides.[368] Properties of the products were tuned by the variation of flexible and rigid anhydrides. In combination with lignin chemistry, the epoxidation of oleic acid modified lignin with peracetic acid was reported (Scheme 7.3).[155] Therefore, an organosolv lignin (**116**) was first esterified with oleoyl chloride (**117**) to introduce an internal double bond into the structure of lignin (**118**). Using two equivalent of peracetic acid, the double bond was completely converted to the corresponding epoxide (**119**) after five hours. This peracid is also reported for the epoxidation for other internal or terminal double bonds. However, no use of peracetic acid for the epoxidation of terminal, allylic double bonds is reported.

Besides peracids and the enzyme-catalyzed epoxidation, many transition metal-catalyzed epoxida-

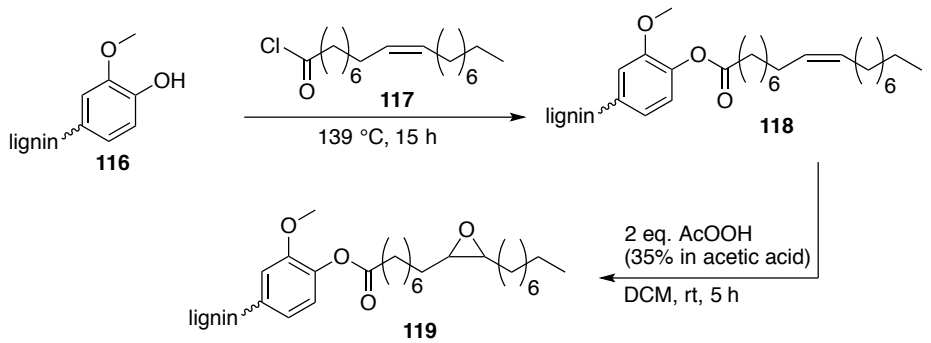

Scheme 7.3: Esterification of an organosolv lignin (**116**) with oleoyl chloride (**117**) and subsequent epoxidation of the internal double bond with peracetic acid.[155]

tion reactions are reported. The most well-known enantioselective epoxidation reaction probable is the titanium-catalyzed *Sharpless Epoxidation* of allylic alcohols.[369] Here, a hydroperoxide, mostly *tert*-butyl hydroperoxide, acts as oxidant and titanium(IV)-isopropoxide as catalyst. The chiral (+)- or (–)-diethyl tartrate (DET) is added to influence the enantioselectivity of the reaction. However, this reaction is only applicable for double bond with an alcohol group in allylic position and thus not suitable for the desired epoxidation of allylated or crotylated functional groups.

Furthermore, manganese-based catalysts are known to catalyze the epoxidation of a broad spectrum of double bonds. For instance, (salen)manganese(III) complexes were discovered by JACOBSEN and KATSUKI in independent research, for the enantioselective, today-named *Jacobsen Epoxidation*.[370–372] In our group, the catalytic oxidation of the renewable α-pinene with mangenese(III) acetate, a manganese-based metal organic framework (MOF) and Al_2O_3-supported manganese oxides to the main products pinene oxide, verbenol and verbenone was investigated.[373]

Another transition metal-based oxidation system is based on sodium tungstate ($Na_2WO_4 \cdot 2H_2O$) with quaternary ammonium salts (*e.g.*, Aliquat 336) as phase-transfer catalyst and hydrogen peroxide as oxidant. This system catalyzes the oxidation of various functional groups, *e.g.*, alcohols, olefins, and sulfides.[374] In 1996, NOYORI *et al.* reported the efficient epoxidation of terminal double bonds using a Na_2WO_4-based system.[375] Excellent yields were achieved after only four hours reaction time at 90 °C. In addition to the high efficiency, the reaction could be performed under organic solvent- and halide-free conditions, which makes it an environmentally-friendly reaction.[374,375] This improvement to a more sustainable procedure was an important break-though compared to the previously reported Na_2WO_4-catalyzed epoxidation reactions that needed chlorinated solvents, such as dichloromethane (DCM).[376] Along with a large variety of unsaturated substrates, also allylic double bonds are reported to be efficiently epoxidized using a Na_2WO_4-system.[377]

In this chapter, various of the discussed epoxidation methods were tested for the epoxidation of diallyl (DAC, **54**), dicrotyl (DCC, **62**) and 10-diundecenyl carbonate (DCC, **63**), as well as the alkylated guaiacol derivatives **71a** and **71c**. These substrates should serve as model substrates for the application of the epoxidation procedures to allylated (**89**) and crotylated organosolv lignin (**99**). For model compounds, reactions were follows *via* GC to gain insight into the reactivity of the substrates. Lignin products that were isolated after epoxidation treatment and characterized with ^{1}H NMR, ^{31}P NMR and IR spectroscopy, as well as SEC measurement.

7.2 Results and Discussion

7.2.1 Epoxidation of model compounds for alkylated organosolv lignin

The first idea was the glycidylation of lignin using diglycidyl carbonate (DGC, **121**), analogous to the allylation with DAC (see Section 4.2.3). However, the synthesis of DGC (**121**) from glycidol (**120**) and dimethyl carbonate (DMC, **45**) with TBD (**67**) at 80 °C, following the general procedure for dialkyl carbonates (Scheme 7.4), failed due to the high reactivity of the epoxide. Instead of the desired product **121**, a viscous, polymeric material with undefined ^{1}H NMR spectrum was obtained (Figure 7.1, bottom). Most probably, the utilized base TBD (**67**) also attacked the epoxide, which led to ring-opening and thus oligomerization. The use of potassium carbonate and DBU as catalyst as well as

a lewis acid approach with tin(II) chloride[378] led to similar products. In a blank reaction without the addition of a catalyst, glycidol was stable within the analyzed time frame of 20 hours in DMC at 80 °C. The ^{1}H NMR of the blank reaction after two hours is shown in Figure 7.1 (top).

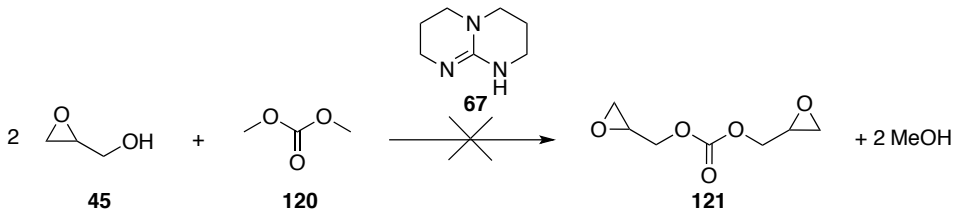

Scheme 7.4: Synthesis attempt of diglycidyl carbonate (**121**) from dimethyl carbonate (**45**) and glycidol (**120**).

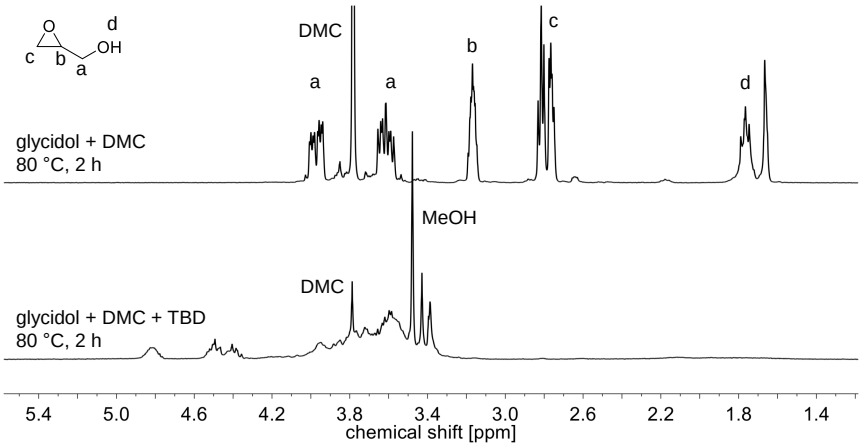

Figure 7.1: ^{1}H NMR in $CDCl_3$ of a blank reaction of glycidol and DMC without catalyst (top) and with TBD as catalyst (bottom) after a reaction time of 2 hours at 80 °C.

For the same reaction time, the use of TBD led to the broad signal between 3.2 and 4.0 ppm in Figure 7.1 (bottom). A decrease of the CH_3 signal from DMC at 3.79 ppm in the reaction with catalyst compared to the blank sample indicates that the indented transesterification proceeded. In addition, the proton signal of evolved methanol could be found at 3.48 ppm.[379] The so formed methanol could also have reacted as nucleophile with the epoxide and induced the oligomerization. Due to the high reactivity of the glycidyl epoxide, it can be assumed that the alkylation of lignin with diglycidyl carbonate under basic condition following the procedure of allylation (Section 9.3.2) would be accompanied by ring-opening as well. Thus, a method must be developed to directly epoxidize the alkylated, respectively allylated or crotylated lignin. For this purpose, the corresponding dialkyl carbonates as well as the alkylated guaiacol were chosen as model substrates and various epoxidation procedure were evaluated.

Epoxidation with *meta*-chloroperbenzoic acid (*m*CPBA) (Method A). *m*CPBA (**113**) is a classical epoxidation reagent that was used for the epoxidation of DAC (**54**) to DGC (**121**) (Scheme 7.5a). Likewise the carbonates DCC (**62**) and DUC (**63**) were epoxidized to **122** and **123**. DMC was chosen as solvent and the reaction was performed at room temperature. For comparability, the same molar (~0.3 mmol mL^{-1}) or mass concentration (~50 mg mL^{-1}) was chosen for all substrates to gain insight into the reactivity of the different compounds. Table 7.1 summarizes the reaction conditions and results from GC analysis. Conversions of the starting materials were obtained from the ratio to

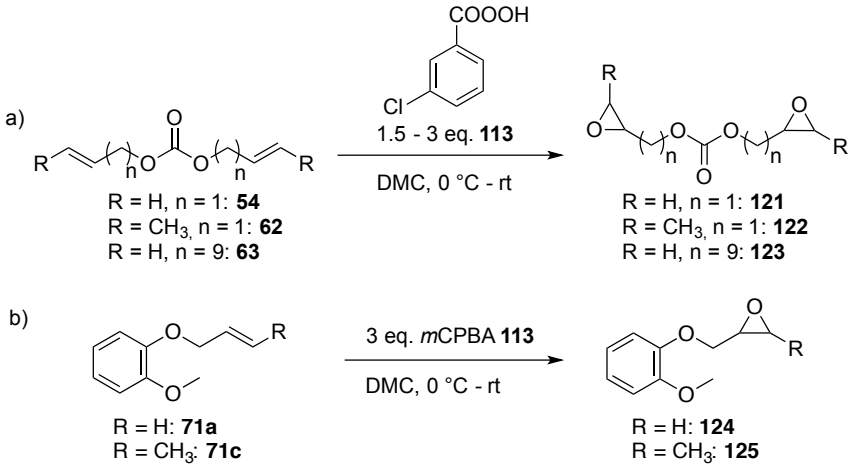

Scheme 7.5: Epoxidation of **a)** diallyl carbonate (**54**) and **b)** allylated (**71a**) or crotylated (**71c**) guaiacol with *m*CPBA (Method A).

tetradecane as internal standard. Full GC conversion of DAC (**54**) was observed after three days reaction time with three equivalents of *m*CPBA per double bond (Table 7.1, entry 1). Kinetic studies *via* GC revealed that besides the desired diepoxy product, 9 or 4% (from GC ratio without calibration) of the monofunctionalized product were still present after three or eight days, respectively (Figure 7.2). The concentration gradients of the three observed substrates show typical behavior of a complex reaction mechanism with a stable intermediate (monoepoxy product) that is first formed and then consumed in two second-order reactions to give the final product DGC (**121**). However, no full conversion of the intermediate was observed. In a 2 g-scale reaction, DGC (**121**) was isolated in a yield of 45% after eight days reaction time with two equivalents *m*CPBA.

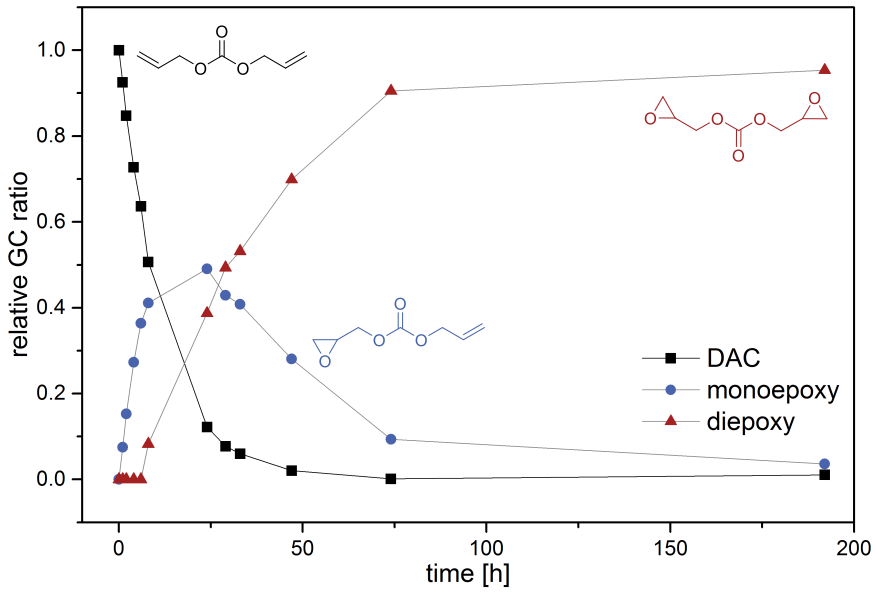

Figure 7.2: Reaction kinetics of the epoxidation of DAC with *m*CPBA (3 eq.) at room temperature to mono- and diepoxy products from relative GC intensities (Method A).

Compared to DAC (**54**), DCC (**62**) and DUC (**63**) reacted significantly faster. Full conversion to the diepoxy compound was obtained after 24 and 4 hours, respectively (Table 7.1, entries 2 and 3).

This behavior can be explained by the epoxidation mechanism, discussed in the introduction of this chapter (Scheme 7.2b). Compared to DAC (**54**), the two carbonates contain additional electron donating groups that increase the electron density at the double bond and thus the reactivity towards the nucleophilic attack at the electrophilic oxygen of the peracid. Especially for DUC (**63**), the reaction was drastically accelerated. Due to the long aliphatic chain, the electron withdrawing effect of the carbonate oxygens have no influence on the reactivity of the double bond compared to the allylic groups of DAC (**54**) and DCC (**62**). In the same order, due to the electron donating groups, the formed epoxide should be more stable against nucleophilic attacks, effecting a lower reactivity in the desired application as epoxy monomer. Decreasing the equivalents of *m*CPBA and the concentration of the substrates led to lower epoxidation reactivity, but still efficient reactions (Table 7.1, entries 4–6).

Allylated (**71a**) and crotylated guaiacol (**71c**) were likewise epoxidized with *m*CPBA to obtain epoxidized guaiacol derivatives **124** and **125** (Scheme 7.5b), respectively. The reactivity of **71a** was lower than the one of DAC (**54**) with a limited conversion of 88% after 3–8 days (Table 7.1, entry 7). Crotylated guaiacol (**71c**) reacted significantly faster. Here, full conversion was observed after eight hours (Table 7.1, entry 8). As described for DCC (**62**), the additional methyl group in crotylated guaiacol (**71c**) compared to the allylated derivative **71a**, increases the electron density of the double bond, thus accelerating the reactivity in epoxidation reactions according to Scheme 7.2b in the introduction of this chapter.

Although *m*CPBA was shown to be an efficient epoxidation agent for the chosen model substances, it is a toxic, unsustainable substrate. Thus, the development of sustainable alternatives were required and are discussed in the following.

Table 7.1: Reaction conditions and GC conversion of the epoxidation of DAC (**54**), DCC (**62**), DUC (**63**), allylated (**71a**) and crotylated guaiacol (**71c**) with *m*CPBA (Method A) followed *via* GC with tetradecane as internal standard.

entry	substrate	*m*CPBA [eq. per C=C]	*c* [mmol mL^{-1}]	*c* [mg mL^{-1}]	t	GC conversion [%]
1	**54**	3	0.29	42	3 d	>99%[a)]
2	**62**	3	0.29	50	24 h	full
3	**63**	3	0.29	108	4 h	full
4	**54**	1.5	0.35	50	6 d	99%[b)]
5	**62**	1.5	0.29	50	23 h	full
6	**63**	1.5	0.14	50	23 h	full
7	**71a**	3	0.30	50	3 d	88%[c)]
8	**71c**	3	0.28	50	8 h	full

Conditions can be found in the Experimental Part. [a)] see Figure 7.2 for gradient; [b)] conversion completed, but still 13% (GC ratio) monoepoxidized product present after 8 days; [c)] no progress after 8 days.

Epoxidation with peracetic acid (Method B). Another peracid that was evaluated is peracetic acid. In literature, it is described to efficiently epoxidize the internal double bonds of fatty acid-modified lignin.[155] Table 7.2 summarizes the results of selected epoxidation reactions with peracetic acid for the chosen model substances. Reactions were performed under argon atmosphere at room temperature or 70 °C. It was found that allylic double bonds in the compounds **54** and **71a** reacted poorly under the chosen conditions (Table 7.2, entries 1 and 4). Only 60% of DAC (**54**) was converted

to mainly monoepoxy product after 30 hours at 70 °C with four peracid additions. For *m*CPBA, a comparable conversion was already obtained after 12 hours at room temperature (Figure 7.2). Allylated guaiacol revealed a conversion of only 13% after three days at room temperature. Due to the low conversion, product **124** was not isolated. To verify the retention time of the glycidylated product **124** in GC, guaiacol (**71**) was glycidylated with epichlorohydrin *via* Williamson ether synthesis to obtain the reference substance (see Experimental Part, Section 9.6.5).

The order of reactivity, influenced by the additional electron donating methyl group in DCC (**62**) and the aliphatic chain in DUC (**63**), was comparable to the reactions performed with *m*CPBA (**113**). DUC (**63**) was fully converted to the desired diepoxy carbonate **123** after four hours and isolated in a yield of 80% after column chromatography (Table 7.2, entry 3). The crotyl-based derivative reacted slower and additional peracetic acid equivalents were needed for a full conversion to the desired product **122** after 29 hours (Table 7.2, entry 2). The isolated yield was 49%. The addition of peracetic acid in several aliquots was necessary due to the evaporation of the epoxidation reagent performing the reaction above the boiling point (40 °C).

Table 7.2: Results for the epoxidation of DAC (**54**), DCC (**62**), DUC (**63**), allylated (**71a**) and crotylated guaiacol (**71c**) with peracetic acid (Method B) followed *via* GC with tetradecane as internal standard.

entry	substrate	peracetic acid [eq. per C=C]	solvent (c in mmol mL^{-1})	T [°C]	t	GC conversion [%]
1	**54**	2.1[a)]	DMC (0.29)	70	30 h	60[b)]
2	**62**	2.1[c)]	DMC (0.29)	70	29 h	full
3	**63**	2.3	DMC (0.68)	70	4 h	full
4	**71a**	2.0	DMC (0.64)	rt	3 d	13
5	**71c**	2.0	DCM (0.28)	rt	14 h	full
6	**71c**	2.0	DMC (0.28)	rt	24 h / 48 h	74 / full
7	**71c**	2.0	THF (0.28)	rt	24 h / 48 h	22 / 42
8	**71c**	2.0	EA (0.56)	rt	17 h / 48 h	54 / 82
9	**71c**	2.8	DMC (0.28)	70	3 h	full

Conditions can be found in the Experimental Part. [a)] additional 0.9 eq. after 9 h and 18 h, 0.4 eq. after 21 h, 2.0 eq. after 24 h; [b)] poor diepoxy formation; [c)] additional 1 eq. after 9 h, 0.5 eq. after 20 h and 0.25 eq. after 22 h.

The influence of different solvents in epoxidation reactions with peracetic acid was investigated using crotylated guaiacol (**71c**) as model substance. At room temperature, full conversion was obtained after 14 hours in DCM as solvent (Table 7.2, entry 5). Besides the conventional solvent DCM, also DMC, ethyl acetate (EA) and tetrahydrofuran (THF) were evaluated as solvent for this epoxidation reaction (Table 7.2, entries 6, 7 and 8). Herein, DMC showed the best efficiency of these alternative solvents, with a full conversion of **71c** after two days. Although, the reaction is significantly slower in DMC than in DCM, the advantage of DMC is its earlier discussed renewability and lower toxicity (see Section 3.1). THF and EA led to conversions of 42 and 82% after two days of reaction time and were thus less suitable solvents than DMC. Furthermore, an increase of the reaction temperature from room temperature to 70 °C led to a decrease of the reaction time to three hours for a full conversion in DMC (Table 7.2, entry 9).

The disadvantage of an increased reaction temperature is the possibility of side reactions observed

in GC analysis during epoxidation of **71c** to yield **125**. It was found that the evolution of the side product was limited to a maximum, if the reaction was performed in a closed system. In contrast, the addition of water to the reaction mixture and simultaneous heating to 100 °C led to a complete conversion to the side product, which was isolated and found to be the ring-opened/hydrolyzed product **126** (Scheme 7.6). Although a complete conversion to the hydrolyzed form was observed in GC, the isolated yield was only 30%. However, this procedure was not further investigated to improve the yield. The ring-opened product **126** is very polar. Solubility tests in water could be performed to verify if the product loss occurred during the washing step.

To avoid the side reaction, the solvent DMC and peracetic acid solution were dried over molecular sieves (3 Å) for two hours prior to the addition of the substrate. In this way, no side product formation was observed *via* GC analysis during the reaction. However, the isolated yield of **125** was only 46%. Further investigation would be necessary to increase the yields. It may be that a degradation/ring-opening took place during the work-up, and thus decreasing the yield.

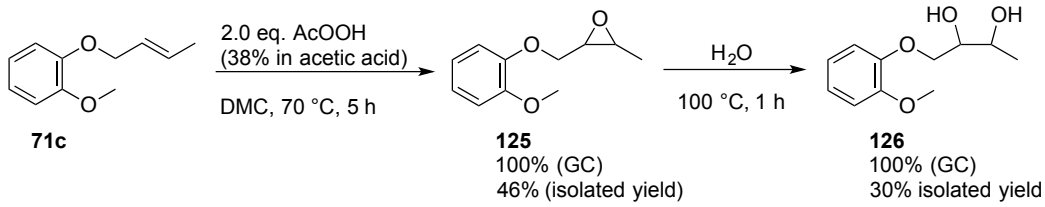

Scheme 7.6: Epoxidation of crotylated Guaiacol (**71c**) to the epoxidized product **125** and subsequent ring-opening with water to form the ring-opened derivative **126** using peracetic acid as oxidant (Method B).

Enzyme-catalyzed epoxidation (Method C). Another sustainable epoxidation method reported in literature is an enzyme-catalyzed procedure.[357] Under literature conditions, DAC **54** was converted in the presence of Novozym 435, caprylic acid (**115**) and hydrogen peroxide in toluene (Scheme 7.7). Here, caprylic acid (**115**) acts as co-catalyst. The acid is converted to the corresponding peracid *in situ* to subsequently transfer an oxygen to the double bond according to the general mechanism in Scheme 7.2b in the introduction of this chapter.

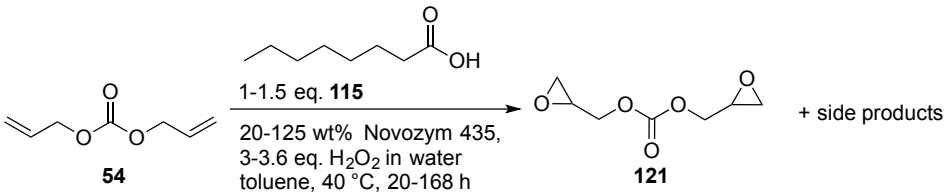

Scheme 7.7: Enzyme-catalyzed epoxidation conditions (Method C) applied to DAC (**54**) to form DGC (**121**).

The performed reactions were followed *via* GC analysis and selected experiments are presented in Table 7.3. Besides caprylic acid, other acids were likewise tested for their suitability as co-catalyst (Table 7.3, entries 1–5). Short chain-acids like glutaric acid and formic acid as well as the aromatic benzoic acid led to a low conversion below 30% (Table 7.3, entries 1–3). A reason for the poor performance may be an incompatibility with lipase. On the one hand, acids with long carbon chains are suitable due to the better solubility in toluene as well as the specialization of lipase to natural, long-chained acids.[380,381] The use of azelaic acid, a diacid, led to a conversion of 28% after 48 hours (Table 7.3, entry 4). In comparison, monofunctionalized acids like stearic acid and caprylic acid,

showed significantly higher reactivities. The conversions after two days were 47% (with 40 wt% lipase) and 37% (with 20 wt% lipase), respectively (Table 7.3, entries 5 and 6). An increase of the amount of lipase and acid or a higher concentration of hydrogen peroxide were further possibilities to accelerate the reaction (Table 7.3, entries 7–9). The reaction time was significantly decreased if the lipase was added in portions (Table 7.3, entry 9). This indicates that Novozym 435 lost its reactivity during the reaction. However, very high amounts were necessary, which can not be considered sustainable anymore. Using 1.5 equivalents of caprylic acid, 225 wt% Novozym 435 and 3.6 equivalents of hydrogen peroxide (50 wt% in water), a conversion of 90% was observed after three days. However, the ^{1}H NMR of the isolated product still showed the allyl function. In analogy to the procedure with peracetic acid, the reaction was not efficient for DAC (**54**). Monoepoxidized DAC was mainly formed and only low concentration of the desired diepoxy compound were detected.

The epoxidation of allylated guaiacol (**71a**) led to equally low conversion under the used conditions (Table 7.3, entries 10 and 11). Although the reaction proceeded up to 57% conversion, only low product formation was detected in the beginning, followed by a complete degradation of the product. In the end of the reactions, no product could be detected in GC or NMR. A mixture of undesired side products was detected that were not further analyzed. In a reactivity control, lipase B was reacted with methyl oleate under reported conditions.[202] The epoxidized product could be successfully isolated proofing the reactivity of the enzyme. Thus, the low efficiency accompanied by product degradation must result from the reactivity of the allylic double bonds. Due to the undefined side reactions and low conversions, this approach was not further investigated.

Table 7.3: Reaction conditions for the enzymatic epoxidation of DAC (**54**) and allylated guaiacol (**71a**) with Novozym 435 (lipase) and GC results followed with tetradecane as internal standard.

entry	substrate	co-catalyst [eq.]	lipase [wt%]	H_2O_2 [eq.]	*t* [h]	GC conversion [%]
1	**54**	glutaric acid (2)	40	3	46	1
2	**54**	formic acid (2)	40	4	20	22
3	**54**	benzoic acid (2)	40	3	20 / 46	7 / 9
4	**54**	azelaic acid (2)	40	3	20 / 46	21 / 28
5	**54**	stearic acid (2)	40	3	20 / 46	40 / 47
6	**54**	caprylic acid (1.1)	20	3	44 / 144	37 / 50
7	**54**	caprylic acid (1.5)	120	3	44 / 120 / 168	48 / 62 / 70
8	**54**	caprylic acid (1.5)	120	3.6[a)]	44 / 120 / 168	63 / 70 / 85
9	**54**	caprylic acid (1.5)	125[b)]	3.6[a)]	48 / 72	80 / 90
10	**71a**	caprylic acid (1)	20	4	112	44[c)]
11	**71a**	caprylic acid (1)	60	7.5	44	57[c)]

Conditions can be found in the Experimental Part. [a)] 50% H_2O_2 in water; [b)]portion-wise addition of lipase, 125 wt% within 7 h, followed by 2 × 25 wt% within 24h (after 48 h: 175 wt%, after 3 days: 225 wt%); [c] no product formation.

Transition metal-catalyzed epoxidation. In addition to peracids and enzyme-catalyzed methods, metal-catalyzed epoxidation procedures were evaluated. For instance, the use of a tungsten-catalyst (Method D) together with hydrogen peroxide as oxidant was successfully applied for the epoxidation. Hydrogen peroxide acts as oxidant in the reaction and phosphorous acid as co-catalyst. DAC (**54**) was fully converted to DGC (**121**) in eight hours using chloroform as solvent (Table 7.4, entry 1).

For allylated guaiacol (**71a**), the reaction was equally efficient and full conversion was achieved after 20 hours (Table 7.4, entry 3). Chloroform is a conventional solvent for this reaction.[377] However, solvent exchange to the more sustainable DMC was possible. In DMC, the reaction was significantly slower, but the epoxidation still efficient (Table 7.4, entries 2 and 4). Crotylated guaiacol (**71c**) was fully converted to the corresponding epoxy derivate after two days in DMC (Scheme 7.8) and was thus more reactive than the allylated compound **71a** (Table 7.4, entries 4 and 5).

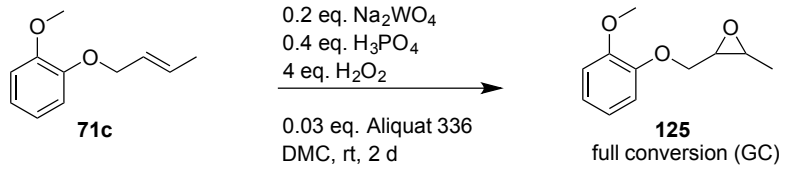

Scheme 7.8: Tungsten-catalyzed epoxidation condition for a full conversion of crotylated guaiacol (**71c**) to **125** (Method D).

Table 7.4: Summary of the results for transition metal-catalyzed epoxidation of DAC (**54**) and allylated guaiacol (**71a**) followed *via* GC analysis with tetradecane as internal standard.

entry	substrate	oxidant (eq.)	catalyst (eq.)	co-catalyst (eq.)	solvent (*c* in mmol mL^{-1})	GC conversion
1	**54**	H_2O_2 (4)	Na_2WO_4 (0.2)	H_3PO_4 (0.4)	$CHCl_3$ (1.0)	full after 8 h
2	**54**	H_2O_2 (4)	Na_2WO_4 (0.3)	H_3PO_4 (0.6)	DMC (1.0)	52% after 66 h
3	**71a**	H_2O_2 (4)	Na_2WO_4 (0.2)	H_3PO_4 (0.4)	$CHCl_3$ (1.7)	full after 20 h
4	**71a**	H_2O_2 (4)	Na_2WO_4 (0.2)	H_3PO_4 (0.4)	DMC (1.7)	full after 4 d
5	**71c**	H_2O_2 (4)	Na_2WO_4 (0.2)	H_3PO_4 (0.4)	DMC (1.5)	full after 2 d
6[a)]	**71c**	synth. air	$Mn(OAc)_3$	pivaldehyde	Toluol/DMF	no conversion
7[b)]	**71c**	O_2	$Mn(OAc)_3$	pivaldehyde	DCM	<50%[c)]

Na_2WO_4-catalyzed procedure can be found in the Experimental Part (Method D); for entry 6 and 7: crotylated guaiacol (**71c**, 100 mg), tetradecane (10 µL) and pivaldehyde (145 mg, 3 eq.) were solved in [a)] toluene/DMF (9 : 1, 1.4 mL), $Mn(OAc)_3 \times 2H_2O$ (6 mg, 4 mol%) was added and a synthetic air flow (60 mL/min) was applied at 130 °C for 5 hours; [b)] in DCM (5 mL) with $Mn(OAc)_3 \times 2H_2O$ (6 mg, 4 mol%) and O_2 was bubbled through the mixture at room temperature for 5 hours; [c)] after 100 minutes no further increase.

Another oxidation procedure that is currently investigated in our group, is the use of $Mn(OAc)_3$ in combination with synthetic air or oxygen.[373] The procedure was applied to crotylated guaiacol (**71c**). With synthetic air as oxidant, no conversion of the starting material and thus no oxidation was observed after a reaction time of five hours at 130 °C (Table 7.4, entry 6). In contrast, the use of oxygen bubbling through the reaction mixture led to a conversion of the starting material, but only in the first 100 minutes of the reaction. In the following time, no further conversion was observed. The reaction was performed at room temperature, but it was observed that the solvent level decreased during the reaction. The oxygen flow may have been too strong and generated the evaporation of the solvent as well as of the co-catalyst pivaldehyde. Here, further optimization of this procedure may increase the conversion but was not performed in the scope of this work.

7.2.2 Epoxy thermosetting polymer from epoxidized DUC

The described epoxidation studies of DAC (**54**), DCC (**62**), DUC (**63**) and alkylated guaiacol (**71a** and **71c**) mainly served as models for later lignin epoxidation. However, especially the difunctionalized epoxy carbonates may be an interesting starting materials for polymer applications. For this purpose,

epoxidized DUC (**123**) was tested as epoxy compound in an epoxy thermosetting polymer with plant oil-based priamine 1075 (**127**), a triglyceride polyamine that was synthesized in our group (**128**)[382] and the conventional hardener IPDA (**108**) (see Figure 7.3).

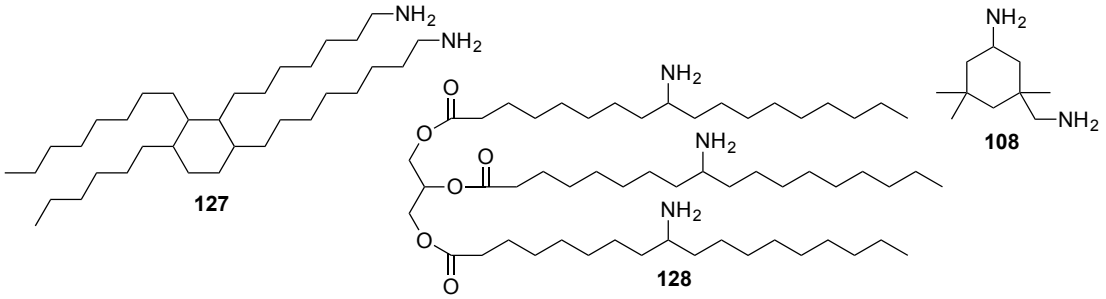

Figure 7.3: Chemical structures of amines used as hardener for epoxy thermosetting polymers with epoxy DUC (**129**): priamine 1075 (**127**), triglyceride-based polyamine (**128**) and IPDA (**108**).

A DSC curing study of the three hardeners with epoxy DUC (**123**) was performed with an amine-to-epoxide ratio of 1 : 2 which gives the molar ratio r = 1 since every amine can react with two epoxides (see Equation 6.1 in Section 6.2.2). The curing is usually characterized by an exothermic transition that can be observed in DSC. For all three amines, this transition shows a maximum peak above 200 °C (Figure 7.4, left). This relatively high reaction temperature may be caused by low reactivity of the terminal epoxide in DUC (**123**). For instance, the maximum of the heat flow during the reaction of epoxy DUC (**123**) with IPDA (**108**) was at 223 °C, whereas IPDA and glycidyl derivatives show maxima around 120 °C (compare Chapter 6). Priamine 1075 (**127**) and epoxy DUC (**123**) led to a maximum in reaction heat of 253 °C, indicating a slightly lower reactivity of priamine 1075 compared to IPDA. Polyamine **128**, which is functionalized with 2.3 amines per triglyceride, showed several heat flow maxima between 140 and 270 °C, which may be induced by differently functionalized polyamines. However, at 170 °C, a sudden drop of the heat flow was observed, accompanied by a decomposition of the material. After the measurement, it was found that the material with compound **128** was foamed, indicating a gas evolution and thus decarboxylation of the ester functions. In contrast, the carbonate function in **123** seemed to be stable at this temperatures as no decarboxylation (no endothermic peak or drop) was observed when other amines, **127** or **108**, were used.

IPDA (**108**) and priamine 1075 (**127**) were further investigated for thermoset curing with epoxy DUC (**123**). The reagents were mixed in a 25 mL teflon form and cured at 100–190 °C for eight hours in an oven. DSC samples were measured to verify the complete reaction. With priamine 1075 (**127**), a rubbery, transparent thermoset product (**130**) was obtained (Figure 7.4, right) with a glass transition temperature of -26 °C, observed in DSC, and a degradation temperature $T_{d\,5\%}$ of 350 °C. IPDA (**108**) did not lead to efficient cross-linking. The product was still liquid, also after heating to higher temperatures (200 °C for 2 hours) and IPDA (**108**) thus not applicable for an epoxy thermoset with **123**. It may be that even higher temperatures are necessary. However, another reason may be the weight ratio for an equimolar ratio that is 4.7 to 1 for **123** to **108** and 1.5 to 1 for **123** to **127**. Thus, the long, flexible chains in both, the DUC derivative **123** and the amine **127** leading to similar molecular weight may be more compatible for an efficient cross-linking. FT-IR analysis of the starting materials and the cured film revealed that the carbonate functions remained stable during the reaction (Figure 7.5). The C=O stretching vibration band at 1738 cm^{-1} as well as the C-O stretching vibration band at 1258 cm^{-1} of the carbonate are still present in the thermoset product. In addition, the appearance

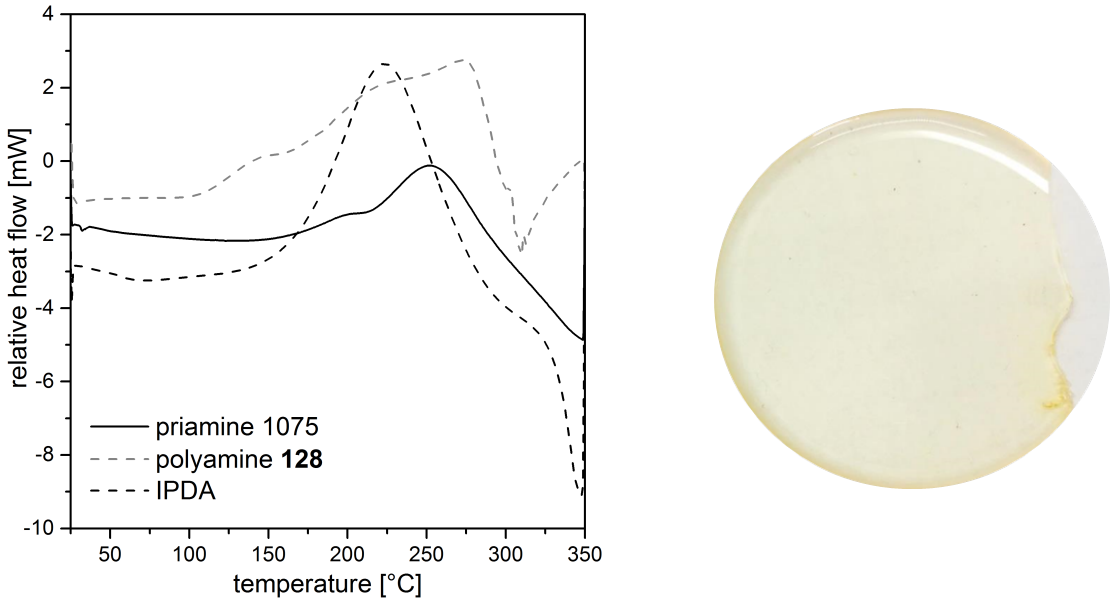

Figure 7.4: DSC traces for the curing of epoxy DUC (**123**) with different amines from 25 to 350 °C at a heating rate of 10K min^{-1} (left) and cured epoxy thermosetting polymer (**130**) from epoxy DUC (**63**) and priamine 1075 (**127**) (right).

of the O-H stretching vibration bands at 3388 cm^{-1} indicated the opening of the epoxides. All in all, this experiment proofed the suitability of epoxy carbonates as reagents in epoxy resin applications with a suitable amine hardener, here priamine 1075 (**127**). Further investigation, *e.g.*, of mechanical properties, are necessary to propose a possible application of this bio-based thermoset.

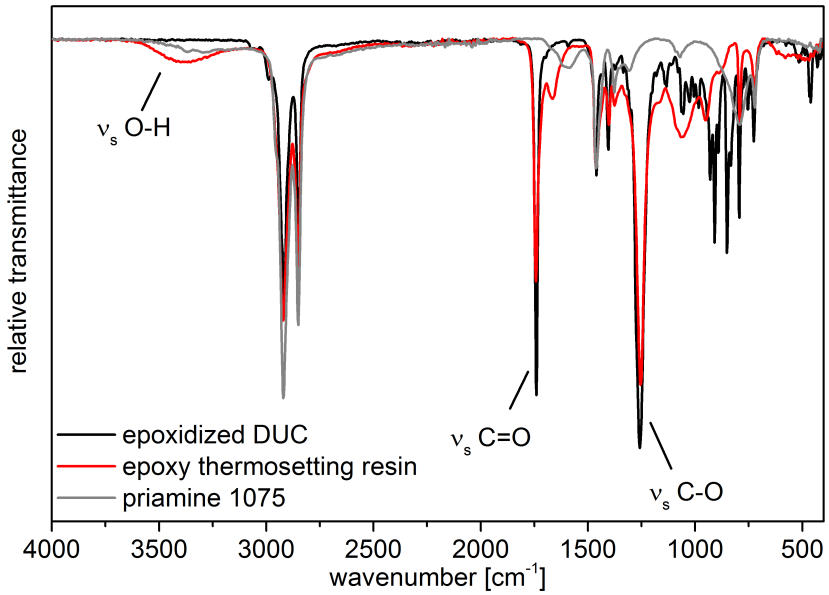

Figure 7.5: FT-IR spectra of epoxy DUC (**123**), priamine 1075 (**127**) and the epoxy thermosetting resin therefrom (**130**).

7.2.3 Epoxidation attempts of allylated organosolv lignin

The reaction conditions previously discussed for the model coumpounds (DAC, DCC, DUC, allylated and crotylated guaiacol) were transferred to the reaction with allylated (**89**) and crotylated lignin (**99**) to obtain epoxidized compounds **131** and **132**, respectively (Scheme 7.9).

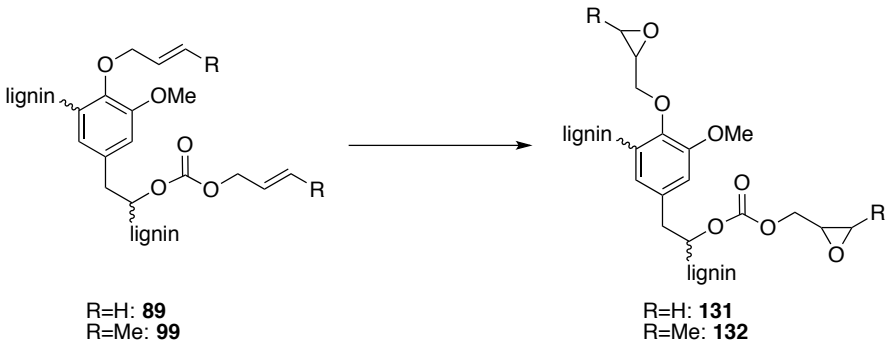

Scheme 7.9: Epoxidation of alkylated lignins **89** and **99** leads to the desired poxidized products **131** and **132**.

For the reaction with *m*CPBA (Method A) and allylated lignin (**89**), the concentration (25–150 mg/mL), reaction time (5 h–3 d) and equivalents of *m*CPBA (1.5–3 eq.) were varied. ^{1}H NMR analysis of the precipitated products revealed that the allyl function could not be converted to the corresponding epoxide. No or low conversion was observed that could not be quantified due to low accuracy of the integrals in the ^{1}H NMR spectra. Tungsten-catalyzed reaction with H_2O_2/H_3PO_4 (Method D) as oxidants led to poor conversion of the allylic groups as well. The double bond region in ^{1}H NMR spectrum remained unchanged. Here, equivalents of Na_2WO_4 (0.2–1 eq.) and concentration of allylated lignin (188–327 mg/mL) with chloroform ($CHCl_3$) or DMC as solvent was varied. In addition to low conversions, evidences for ring opening or other side reactions were found. For the reaction in DMC, it was observed that a precipitate was formed in the first hours of the reaction, assuming that the product is insoluble or worse soluble in DMC. However, after a proceeded reaction time, the solution became clear again (Figure 7.6). Due to the aqueous medium and the long reaction time needed for complete reaction of guaiacol, water may have opened the formed epoxide ring, which could have led to a more soluble product. In $CHCl_3$, the reaction was significantly faster for guaiacol (compare Section 7.2.1): after eight hours, full conversion was observed. The transfer to allylated lignin was not successful. After two days, still low conversion of allylic double bonds was observed in ^{1}H NMR applying the same conditions. However, in all ^{1}H NMR spectra, allyl functions were still present and no calculation of conversion was possible due to bad quality of the baseline correction of the spectra.

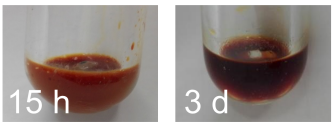

Figure 7.6: Reaction mixture of allylated lignin under tungsten-catalyzed conditions after 15 hours (left) and 3 days (right).

FT-IR spectroscopy of the reacted products was performed to identify the epoxy function and to analyze whether the reaction was partially successful (Figure 7.7). As reference substance, a glycidylated lignin (**107**), obtained from the reaction of OL (**88**) with epichlorohydrin (**15**) to form the corresponding epoxy lignin, was used. Details for the glycidylation procedure and the characterization of the product can be found in Chapter 6. If an epoxy function is formed, the typical asymmetric stretching vibration band of C-O-C is found in the transmittance spectrum around 900 cm^{-1}. Com-

pound **107** showed this band at 909 cm^{-1}. The products after the reaction with *m*CPBA or Na_2WO_4 did not show a significant change in this region compared to allylated or unmodified lignin. A more significant change was observed in the ether/ester region. The broadening of this region indicated significant structural change. In the case of *m*CPBA, an incorporation of *m*CPBA impurities into the material could be possible as the carbonyl vibration was likewise increased. In both products, the O-H stretching vibration increased compared to allylated OL (**89**), another evidence for an occurred ring-opening.

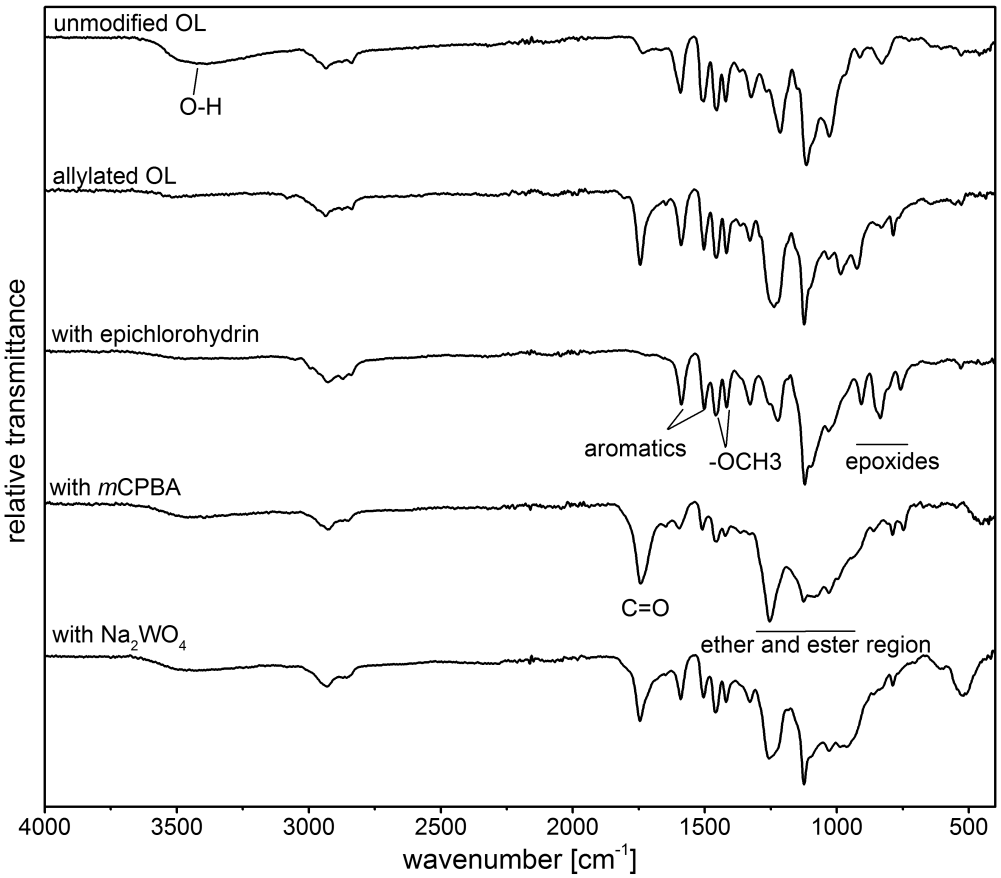

Figure 7.7: FT-IR spectra of epoxidation attempts of allylated organosolv lignin.

7.2.4 Epoxidation attempts of crotylated organosolv lignin

As expected from the model studies, the crotylated double bonds in lignin reacted significantly faster. The proton signals of the double bonds in compound **99** (Figure 7.9, spectrum 1) disappeared after a reaction time of 13 hours with three equivalents *m*CPBA in DCM (Figure 7.9, spectrum 3). It was further found that a shift of the methyl function from 1.65 to 1.06 ppm indicated a proceeded reaction. In a product with incomplete conversion, both peaks could be observed, for instance, if the amount of *m*CPBA is reduced to 1.5 eq. (Figure 7.9, spectrum 2). In addition, the new peak between 2.6 and 3.2 ppm can be attributed to the desired epoxy function. However, additional change of NMR signals was observed in the aromatic region (> 7.00 ppm), indicating a side reaction with *m*CPBA (ring opening) or *m*CPBA impurities enclosed in the material. In IR spectroscopy, no evidence of a successful epoxidation could be found, but an increase in the region of O-H stretching vibration as well as in the carbonyl region suggested ring-opening or enclosed impurities. Additionally, a decreased reaction

time of four hours led to the same result.

In addition, epoxidation of crotylated OL (**99**) was performed with peracetic acid/acetic acid in DMC as solvent (Scheme 7.10). Similar to the epoxidation reaction applying *m*CPBA, the use of peracetic acid led to significant decrease in the double bonds after a reaction time of 24 hours at room temperature (Figure 7.9, spectrum 4). A shift of the terminal CH_3 group was observed, but no peaks of epoxy protons appeared in the spectrum. Under the applied conditions with peracetic acid, a ring-opening of crotylated, epoxidized guaiacol was detected in GC (see Section 7.2.1). Repeating the reaction with peracetic acid and DMC previously dried over molecular sieve, the desired epoxy function appeared in the ^{1}H NMR of the crotyl-based lignin product between 2.6 and 3.2 ppm after a reaction time of 24 hours (Figure 7.9, spectrum 5–7). Elongation of the reaction time to 48 hours led to a significant increase of the desired product's CH_3 group at 1.06 ppm compared to the terminal CH_3 of remaining unreacted crotyl functions at 1.65 ppm. Calculated from the methyl groups ratio, 66% had reacted after 24 hours and 75% after 48 hours. The highest conversion, according to the NMR signal ratio, was achieved when peracetic acid was added in portions (Figure 7.9, spectrum 7). From the methyl group ratio this corresponds to a conversion of 85%. However, no full conversion of all crotyl functions was observed if the reaction was performed at room temperature.

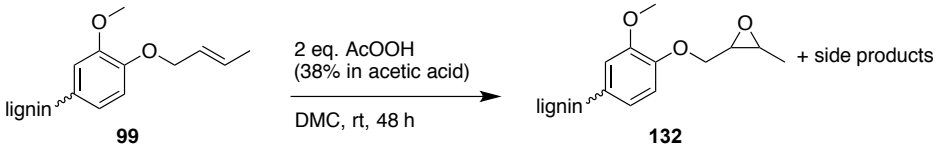

Scheme 7.10: Epoxidation of crotylated OL (**99**) to the desired product **132** with peracetic acid as oxidant (Method B).

Although, increasing the temperature to 70 °C resulted in a shorter reaction time for the guaiacol model substance **71c**, these reaction conditions were not successful for crotylated lignin (**99**). While the signal of crotylic double bonds between 6.0 and 5.0 ppm disappeared completely (Figure 7.9, spectrum 8), no signal appeared in the epoxy region between 2.6 and 3.2 ppm. In addition, no C-O-C stretching vibrations in IR spectroscopy (Figure 7.8a) could be observed around 900 cm^{-1}. However, IR analysis revealed the increase of hydroxyl groups (~3400 cm^{-1}) and a broadening of the ester/ether (1000–1400 cm^{-1}) and carbonyl region (1600 cm^{-1}) in the products. SEC analysis of the OL treated with peracetic acid revealed that the molecular weight distribution of the modified lignin decreased compared to crotylated OL (**99**) (Figure 7.8b). In ^{31}P NMR, the introduction of acid functions in the lignin structure became visible as broad signal between 136.0 and 134.0 ppm (Figure 7.8c, spectrum 3 and 4). Moreover, the analysis showed the reappearance of aromatic hydroxyl groups between 144.6 and 137.0 ppm after the epoxidation procedure. Those hydroxyl groups were previously completely converted during the crotylation of OL (**88**) to the crotylated product **99** (Figure 7.8c, spectrum 1 and 2). Also in the aliphatic region (150.0–145.5 ppm), a clear change in the shape of the peak became visible. The introduction of these new hydroxyl groups could be a result of ring-opening, which would lead to the formation of aliphatic hydroxyl groups. However, especially the appearance of acidic and aromatic hydroxyl groups in ^{31}P NMR in combination with all analytical results, indicated lignin cleavage and oxidation.

In all reactions with peracetic acid, performed at room temperature as well as at 70 °C, a new proton signal at ~2.00 ppm appeared (Figure 7.9, spectrum 5–8). Indicating an acetyl-CH_3 group, the signal

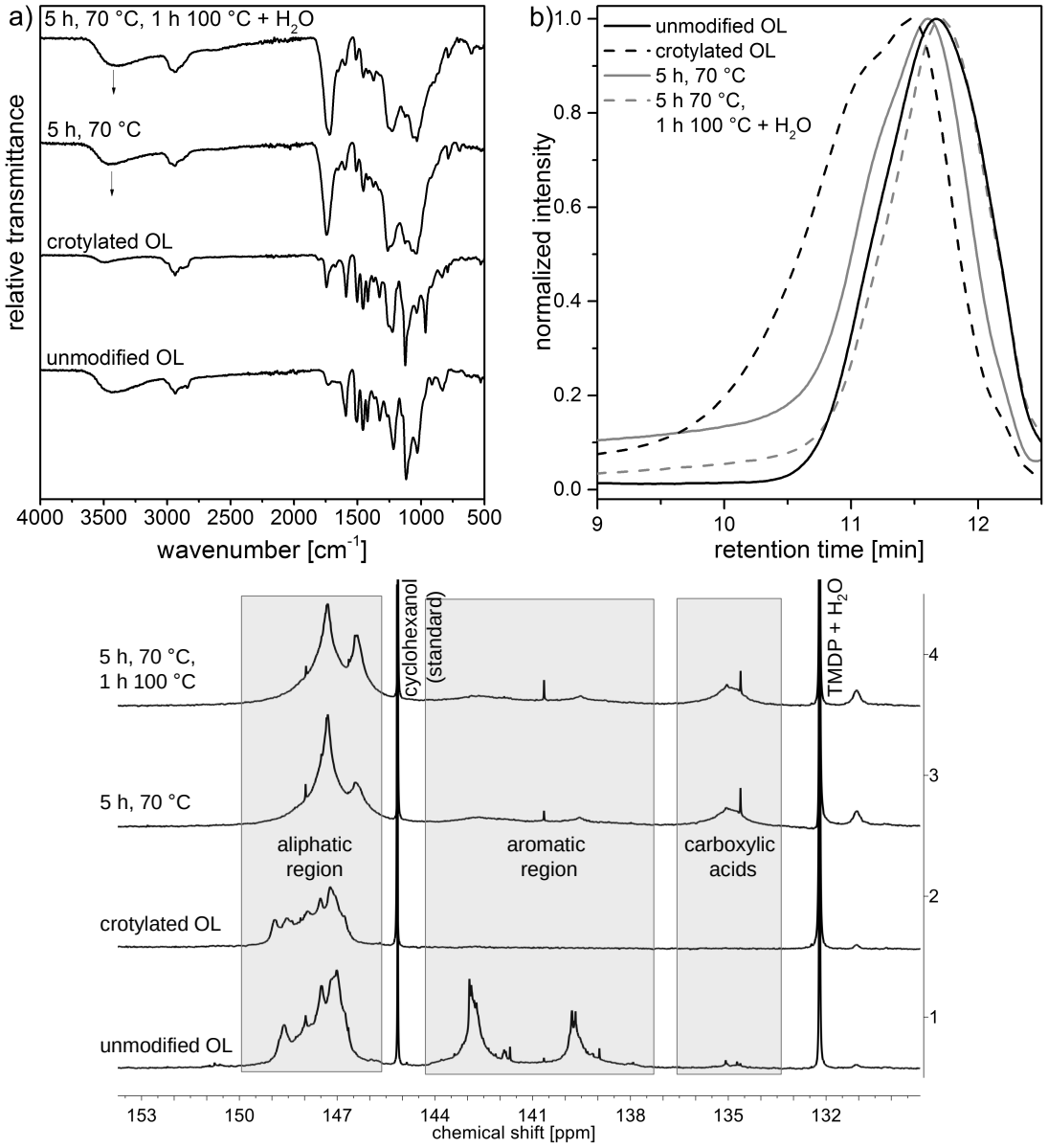

Figure 7.8: a) FT-IR spectra; **b)** SEC traces and **c)** ^{31}P NMR spectra of unmodified (**88**) and crotylated OL (**99**) as well as of the products from the epoxidation attempts with peracetic acid (Method B).

is evidence for undesired ring-opening or degradation by acetic acid. Acetosolv pulping of wood is performed at 120 °C in acetic acid to yield degraded lignin with oxidized groups, such as acid functions.[383] Thus, the degradation of lignin accompanied with acid function insertion at increased temperature in acetic acid is already known. Although the applied conditions for the epoxidation attempts were less concentrated and at lower temperatures, the herein undesired degradation of lignin took already place at room temperature. Further investigations of this reaction would be necessary to analyze whether lower concentrations of peracetic acid/acetic acid could give a better result. In literature, the epoxidation of lignin modified with oleic acid is described with peracetic acid at room temperature within five hours.[155] No degradation of the modified lignin was reported. A higher reactivity of internal double bonds of oleic acid compared to allylic and crotylic double bonds as expected here are supposed to explain the different results.

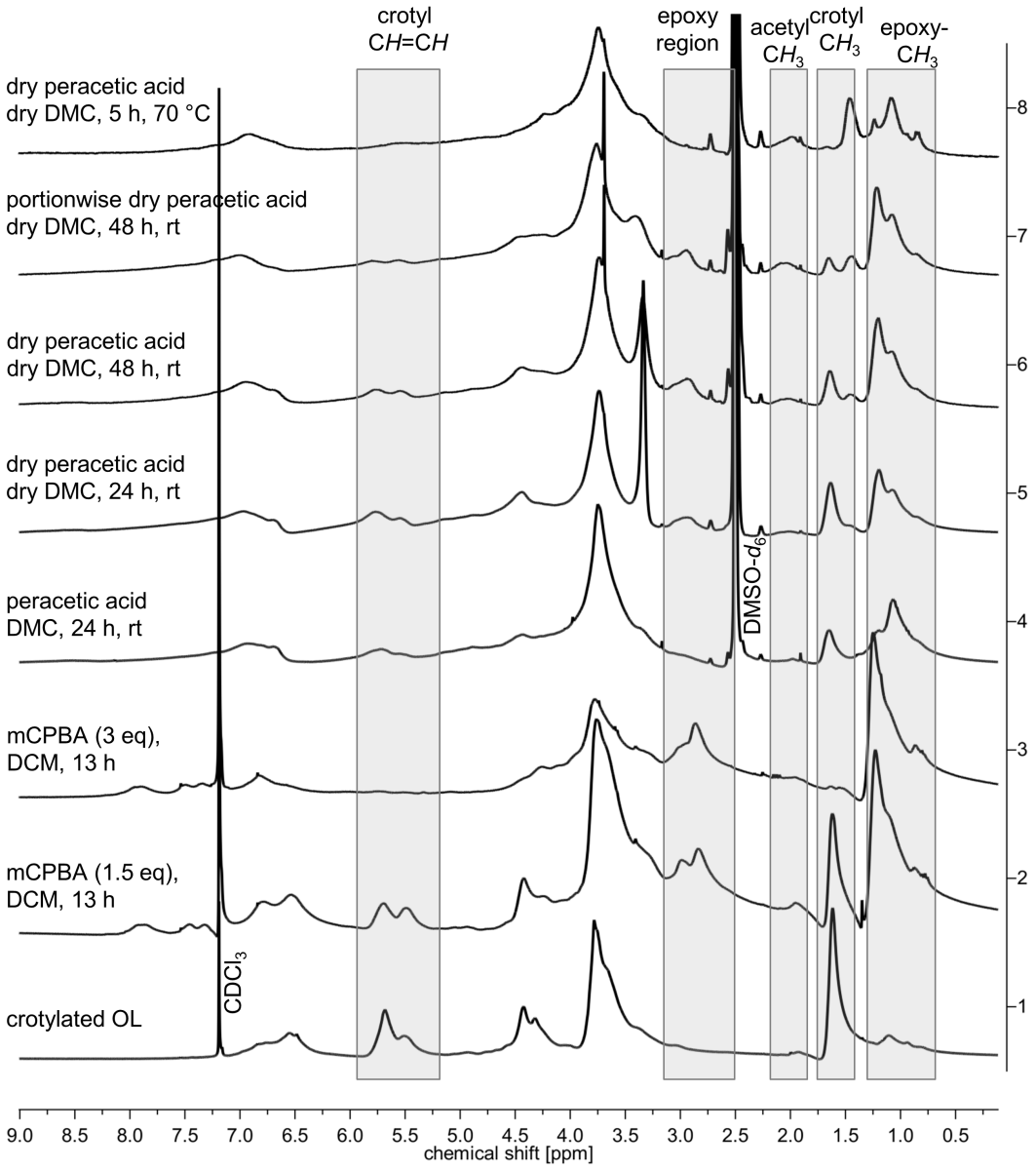

Figure 7.9: ^{1}H NMR of crotylated lignin (**99**, bottom) and epoxidized lignins (**132**) under different conditions (Method A or B) in $CDCl_3$ or DMSO-d_6.

Moreover, other structural motifs in lignin seemed to be sensitive towards reactions in acidic media and led to degradation and oxidation. Catalytic oxidation of lignin to monoaromatic compounds was discussed in the introduction of this thesis (Section 1.2). The described conditions indicate the sensitivity of lignin's structure towards an oxidative medium.

Tungsten-catalyzed epoxidation (Method D), as successfully applied to the epoxidation of model compounds, was also tested for crotylated lignin epoxidation (Scheme 7.11). A significant decrease of double bond signals between 6.0 and 5.0 ppm was observed in ^{1}H NMR, with almost full conversion after 7 days (Figure 7.10). However, at 11.3 ppm a new acid function was detected in ^{1}H NMR indicating an oxidation of lignin as side reaction. Shorter reaction times led to no acid formation but significantly lower conversions were detected by NMR. The appeared acid function in the proton NMR may be an evidence for an oxidation of the lignin structure during the reaction. The applied

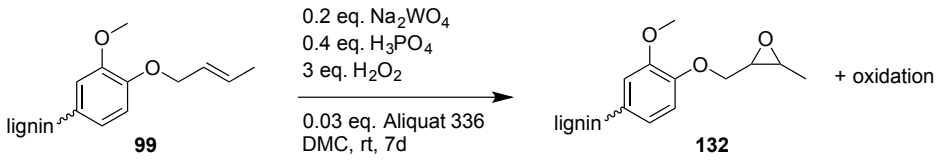

Scheme 7.11: Epoxidation of crotylated OL (**99**) with Na_2WO_4 as catalyst (Method D).

conditions of Method D may be too acidic for the heterogenous structure as already discussed for the epoxidation with peracetic acid.

Although the structure of the epoxidized lignins could not be completely identified, a reactivity test with priamine 1075 was performed in a DSC study. Therefore, the epoxy content of an lignin, epoxidized with peracetic acid, was titrated with NaOH (see Experimental Part for epoxy content titration). The epoxy content was analyzed to be 2.65 mmol/g, which is in an acceptable range. For comparison: the glycidylation of OL led to an epoxy content of 3.2 mmol/g. Epoxidized, crotylated OL (**132**) and glycidylated OL (**107**) were cured with an equimolar amount of priamine 1075 in an aluminum crucible in an DSC oven (Figure 7.11a). Both epoxy lignins reacted with priamine 1075 (**127**), which is proved by the exothermic reaction starting at around 80 °C in the DSC measurement. However, for epoxidized lignin (**132**), the exothermic start is followed by an endothermic transition. Here, evaporation of water remaining in the product could be a reason. In the DSC trace of pure **132**, water evaporates between 50 and 100 °C (Figure 7.11a) and also TGA revealed that 6 wt% of a volatile compound were still incorporated. This test was only a first test to proof the reactivity of epoxidized OL (**132**) and was not further investigated as the structural difficulties were not solved yet.

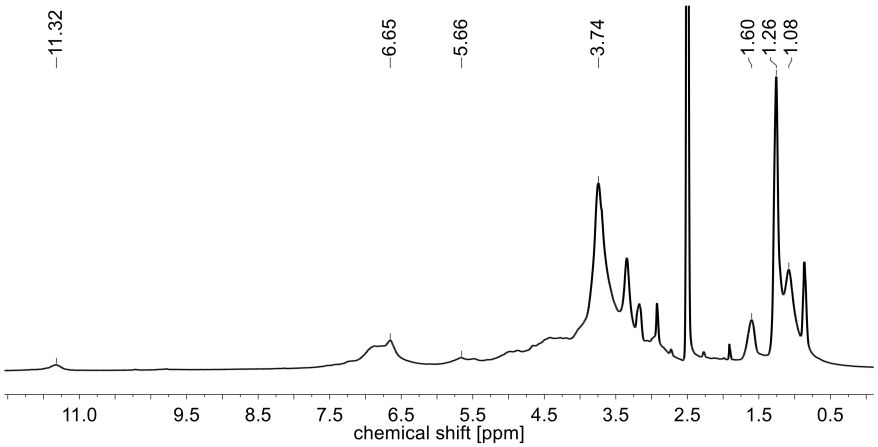

Figure 7.10: .^{1}H NMR (DMSO-d_6) of a epoxidation product obtained from crotylated OL (**99**) *via* epoxidation with Na_2WO_4 as catalyst and a reaction time of seven days (Method D).

7.3 Conclusion and Outlook

In this chapter, different epoxidation procedures were intensively studied for alkylated model compounds: DAC (**54**), DCC (**62**), DUC (**63**), allylated guaiacol (**71a**) and crotylated guaiacol (**71c**). The studies revealed different reactivity of the double bonds. Crotyl functions reacted significantly faster than allylic double bonds. DUC (**63**) showed by far the highest activity towards epoxidation. Applying

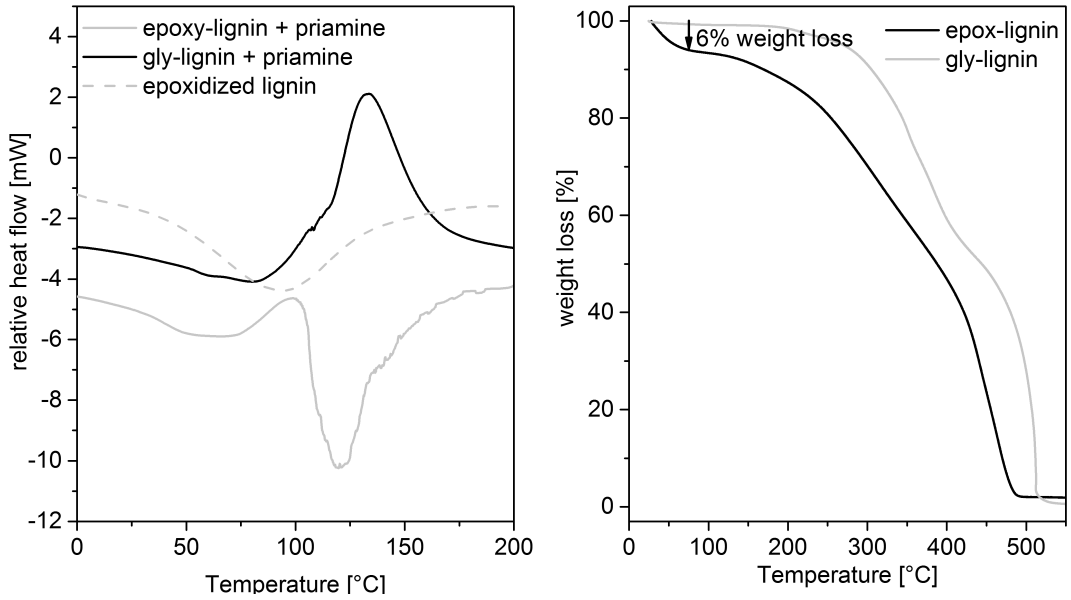

Figure 7.11: a) DSC curing of epoxidized crotylated OL (**132**) with priamine 1075 (**127**), of glycidylated OL (**107**) with priamine 1075 (**127**) and DSC trace of pure epoxidized crotylated OL (**132**); **b)** TGA trace of epoxidized crotylated OL (**132**) and glycidylated OL (**107**, gly-OL).

different epoxidation procedures, peracids, both *m*CPBA and peracetic acid, were the most successful. Another efficient epoxidation was performed using a tungsten catalyst in combination with H_2O_2 as oxidant. In contrast, enzyme-catalysis led to poor conversion, evolution of undefined side products and even product degradation.

A fully bio-based epoxy thermosetting polymer was synthesized from epoxidized DUC (**123**) in combination with a plant-oil based amine hardener (priamine 1075, **127**). The polymer **130** consisted of a low T_g of -26 °C and a thermal stability $T_{d\,5\%}$ of 350 °C. This first study demonstrated an application of diepoxy carbonates. However, further investigations are necessary, *e.g.*, mechanical properties, to propose possible applications. In addition, it would be interesting to analyze the degradability. The carbonate function in the structure may induce biodegradability as additional feature of the product.

Due to the heterogeneous structure of lignin, the transfer of the evaluated epoxidation procedures to alkylated **89** and **99** was only partially successful. For some conditions, ^{1}H NMR analysis indicated a successful epoxide formation. However, side reactions, such as ring-opening of the formed epoxide, degradation and oxidation of lignin, as well as incorporation of impurities that could not be completely clarified, occurred. Double bonds in allylated lignin (**89**) could not be completely converted. Although the crotylated derivate **99** was shown to be more reactive, side products could not be completely prevented and identified. It may be that the double bonds of allylated and crotylated lignin are not reactive enough compared to other undefined motifs in the lignin material, which leads to the observed oxidation and degradation under the applied conditions. However an epoxidized crotylated compound was isolated and, although its structure could not be completely identified, its reactivity towards epoxy thermoset formation with priamine 1075 as hardener was successful in a proof-of-concept.

8 Conclusion

In this thesis, the efficient and sustainable alkylation of phenolic compounds and beech wood organosolv lignin was shown. Furthermore, the modified lignin was used in thermosetting polymers as potential substitute for conventional fossil-based products. In addition to the renewability of the starting material lignin, also the synthesis procedures were designed as sustainable as possible following the "12 Principles of Green Chemistry". For the alkylation procedure, dialkyl carbonates were chosen as reagents as they can be obtained *via* sustainable routes from dimethyl carbonate, which in turn can be synthesized from renewable urea. With this procedure, the conventional, toxic alkylation agents, *i.e.*, alkyl halides and alkyl sulfates, were replaced, and thus a new route for the sustainable introduction of a new functional groups in lignin was described. In addition, lignin was extracted *via* organsolsolv pulping, an environmentally friendly pulping process compared to the conventional kraft process.

The alkylation was first tested for monoaromatic phenols and revealed an increased reactivity of phenols with higher substitution, which predicted a high reactivity of the complex lignin structure (Chapter 3). In a cooperation project, renewable bisphenols were allylated with the same procedure to obtain monomers for thiol-ene polymerization. These bisphenols were also applied in polycarbonate synthesis. All in all, this study revealed a high potential of these renewable polymers as replacement for bisphenol A-based polymers, which were to some extent even less harmful according to an estrogenicity test. Here, further analytical studies, such as mechanical tests of the polymers, are necessary to propose a more distinct substitution field.

Furthermore, especially the allylation of organosolv lignin with diallyl carbonate was discussed in detail. The transfer of the procedure to the crotylation with dicrotyl carbonate proved the reproducibility of the procedure for other dialkyl carbonates with similar reactivity, thus laying the foundation for a new, sustainable modification method for lignin. Under the applied conditions for the allylation of lignin, the aromatic hydroxyl groups were converted to allyl ethers and the aliphatic hydroxyl groups formed allyl carbonates with a total conversion of up to 90% (Chapter 4). The new functional groups were the starting point for a cross-metathesis reaction with plant oils to form thermosetting films with tunable properties, varying the lignin content and the nature of the oil (Chapter 5). The use of plant oils as a second renewable resource aligns with the "principles of green chemistry". However, the conventional solvent dichloromethane was used for the film preparation and its replacement by dimethyl carbonate was only partially successful. The film formation was efficient, but lower crosslinking density was obtained compared to the use of dichloromethane. Here, further investigations are necessary to optimize the procedure with dimethyl carbonate, and thus to increase the sustainability. Nevertheless, the study showed, for the first time, that unmodified plant oils can be combined with a modified lignin in a thermosetting polymer. The ratio between the two feedstocks highly influences the mechanical properties of the material from ductile materials with high oil content to brittle materials with high lignin content. Thus, a large variety of applications in different fields of polymer

chemistry can be proposed.

Epoxy thermosetting polymers were investigated as a second application for modified lignin. In a first attempt, lignin was glycidylated with epichlorohydrin in a conventional *Williamson Ether Synthesis*. The modified lignin replaced up to 50% of bisphenol A in a conventional epoxy polymer with isophorone diamine (Chapter 6). Here, a detailed analytical study of structural, thermal and mechanical properties was performed, revealing no significant change of the product properties. In this way, it was shown that lignin is a suitable replacement for the toxic bisphenol A in thermosets. More applications in thermosets may be possible. However, the replacement of bisphenol A is not enough in terms of sustainability, considering that lignin was modified in a conventional fashion. Thus, a new approach was investigated to introduce the epoxy function *via* epoxidation of allylated or crotylated lignin (Chapter 7). The applied conditions that were previously tested using model compounds were not successful for lignin. The structure of the epoxidized products was not completely clarified, but the analysis indicated degradation and oxidation. However, evidences for formed epoxy functions were found in some products. Moreover, it was found that the double bonds of crotylated lignin were converted significantly faster than those of allylated lignin. In the future, milder conditions could be applied to epoxidize the double bonds selectively and to prevent the undesired side reactions. In addition, other modifications of lignin could be evaluated, such as 10-undecenylation, to introduce an even more reactive double bond and facilitate the epoxidation procedure. Although the structure of the epoxidized, crotylated product is not completely known, it was shown that it was reactive towards thermoset formation with an amine hardener, promising a high potential of this pathway for the future application of lignin in epoxy thermosets.

9 Experimental Part

9.1 Materials

The following chemicals were obtained from commercial sources and used without further purification: allyl alcohol (98%, Sigma-Aldrich), azobisisobutyronitril (AIBN, 98%, Sigma-Aldrich), *p*-benzoquinone (98%, Sigma-Aldrich), benzyl alcohol (>99%, Sigma-Aldrich), bisphenol-A diglycidyl ether (D.E.R.^{TM} 332, Sigma-Aldrich), caprylic acid (>99%, Sigma-Aldrich), cesium carbonate (99%, Sigma-Aldrich), 2-chloro-4,4,5,5-tetramethyl-1,2,3-dioxaphospholane (95%, Sigma-Aldrich), chloroform-d_1 ($CDCl_3$, 99.8 atom-% D, Euriso-top), *meta*-chloroperoxybenzoic acid (*m*CPBA, ≥77%, Sigma-Aldrich), chromium(III) acetylacetonate (99.99% trace metals basis, Sigma-Aldrich), *m*-cresol (99%, Sigma-Aldrich), crotyl alcohol (cis- and trans- mixture, 95%, abcr), cyclohexanol (99%, Sigma-Aldrich), decane dithiol (>98%, TCI), 1,8-diazabicyclo[5.4.0]undec-7-ene (DBU, 98%, Sigma-Aldrich), 2,6-dimethoxyphenol (99%, Sigma-Aldrich), dimethylacetamide (DMAc, 99.8%, Sigma-Aldrich), dimethyl carbonate (anhydrous, >99%, Sigma-Aldrich), dimethyl carbonate (99%, Acros Organics), 1,2-dimethylimidazole (DMI, 98%, Sigma-Aldrich), dimethyl sulfoxide (DMSO, >99.5%, Carl Roth), dimethylsulfoxid-d_6 (DMSO-d_6, 99.8-atom-% D, Euriso-top), dimethylformamide (DMF, 99.9%, VWR), diphenyl carbonate (99%, Sigma-Aldrich), diphosphorous pentoxide (>98%, VWR), epichlorohydrin (99%, Sigma-Aldrich), ethanol (>99.7, VWR), ethyl vinyl ether (99%, contains 0.1% KOH as stabilizer, Sigma-Aldrich), 4-ethylphenol (99%, Sigma-Aldrich), eugenol (99%, Acros Organics), glycidol (96%, Sigma-Aldrich), guaiacol (>98%, Sigma-Aldrich), Hoveyda-Grubbs 1st Generation (HG1, 97%, Sigma-Aldrich), Hoveyda-Grubbs 2nd Generation (HG2, 97%, Sigma-Aldrich), hydrochloric acid (37%, Fluka or Fisher Scientific), hydrogen peroxide (35 wt% in H_2O, Sigma-Aldrich), hydrogen peroxide (50 wt% in H_2O, Sigma-Aldrich), 3-hydroxypyridin (98%, Sigma-Aldrich), isophorone diamine (>99.0%, TCI), lithium hydroxide (98%, Sigma-Aldrich), magnesium sulfate (VWR), 3-methoxyphenol (96%, Sigma-Aldrich), molecular sieve (3 Å, beads, 4-8 mesh, Sigma-Aldrich) Novozym 435 (*Lipase acrylic resin from candida antarctica*, Sigma-Aldrich), 4-phenylphenol (97%, Sigma-Aldrich), peracetic acid (36% in acetic acid, Sigma-Aldrich), peracetic acid (38–40% in acetic acid, Merck), phosphoric acid (ACS reagent, ≥85%, Sigma-Aldrich), potassium carbonate (99%, Sigma-Aldrich), potassium hydroxide (>85%, Carl Roth), priamine 1075 (Croda), pyridine (anhydrous, for analysis, Acros Organics), silica gel 60 (0.040 − 0.063, Sigma-Aldrich), sodium chloride (reagent grade, Fisher Scientific), sodium hydroxide (>99%, Carl Roth), sodium sulfate, anhydrous (pure, Bernd Kraft), sodium sulfite (>98%, Sigma-Aldrich), sodium tungstate dihydrate (ACS reagent, 99%, Sigma-Aldrich) tetrabutylammonium bromid (TBAB, ≥99%, Sigma-Aldrich), tetradecane (>99%, Sigma-Aldrich), tetrahydrofuran (99.7%, VWR), tetrahydrofuran (for SEC, GC-MS, dry, contains 250 ppm BHT as inhibitor, >99.9%, Sigma-Aldrich), tin(II)chloride (MERCK), toluene (99.7%, Bernd Kraft), 1,5,7-triazabicyclo[4.4.0]dec-5-ene (TBD, 98%, Sigma-Aldrich), 10-undecenol (>98%, Sigma-Aldrich) vanillic acid (97%, Sigma-Aldrich), vanillin (99%, Sigma-Aldrich).

Solvents were of technical grade and were distilled in a rotary evaporator prior to use.

Plant oils were purchased in a local supermarket: Olive oil (Brändle, Extra Virgin, 100 mL (ρ = 0.92 g mL^{-1}) contain 13 g saturated, 70 g monounsaturated and 9 g polyunsaturated fatty acids), rapeseed oil (EDEKA, cold-pressed, 100 mL (ρ = 0.91 g mL^{-1}) contain 6.4 g saturated, 57.3 g monounsaturated and 27.7 g polyunsaturated fatty acids), and linseed oil (Brändle, cold-pressed, 100 mL (ρ = 0.92 g mL^{-1}) contain 9 g saturated, 17 g monounsaturated and 66 g polyunsaturated fatty acids)

Stilbene derivatives **82**, **83**, **84** and **85**, as well as allylated BPA (**14a**) were synthesized by the cooperation partners in the group of Prof. Dr. L. J. Gooßen.[236]

9.2 Synthesis procedures for Chapter 3

9.2.1 Synthesis of organic carbonates

Organic carbonates were synthesized from the corresponding alcohol and dimethyl carbonate (DMC) following a previously reported procedure.[185] Reactions were performed, stirring the two substrates in a ratio of 2.2 : 1 with 1–5 mol% of 1,5,7-triazabicyclo[4.4.0]dec-5-ene (TBD, **67**) at 80–120 °C till full conversion was observed in ^{1}H NMR analysis.

9.2.1.1 Diallyl carbonate (DAC, 54)

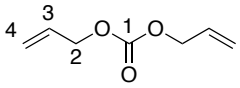

Diallyl carbonate (DAC, **54**) was obtained from DMC (**45**, 81.2 g, 901 mmol, 1.00 eq.) and allyl alcohol (**89**, 115 g, 1.98 mmol, 2.20 eq.) with TBD (**67**, 5.00 g, 35.9 mmol, 4.00 mol%) as catalyst. After distillation (50 °C, 30 mbar), product **54** was isolated as a colorless liquid (102 g, 720 mmol, 80%).

^{1}H NMR ($CDCl_3$, 300 MHz) δ = 5.94 (tdd, J = 16.8 Hz, 10.4 Hz, 6.8 Hz, 2H, CH^3), 5.23–5.42 (m, 4H, C$H_2{}^4$), 4.64 (dd, J = 5.9 Hz, 1.1 Hz, 4H, C$H_2{}^2$) ppm.

^{13}C NMR ($CDCl_3$, 75 MHz) δ = 154.7 (C^1), 131.5 (C^3), 118.7 (C^4), 68.3 (C^2) ppm.

IR (ATR): $\tilde{\nu}$ = 3089, 2988, 2952, 1743, 1659, 1451, 1424, 1375, 1294, 1236, 1164, 1080, 964, 931, 789, 663, 554 cm^{-1}

MS (FAB^+): *m/z* (%) = 142.2 $[M]^+$ (4), 101.1 [M-allyl]$^+$ (100), 85.1 [M-allylO]$^+$ (7).

HRMS (EI^+): $C_7H_{10}O_3$ $[M]^+$ calc. 142.0624; found 142.0620.

NMR data of the synthesized diallyl carbonate (**54**) was identical to literature.[185]

9.2.1.2 Dibenzyl carbonate (DBC, 61)

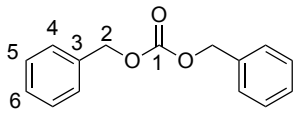

Dibenzyl carbonate (DBC, **61**) was obtained from DMC (**45**, 50.0 g, 555 mmol, 1.00 eq.) and benzyl alcohol (**64**, 126 g, 1.17 mol, 2.11 eq.) with TBD (**67**, 1.93 g, 13.9 mmol, 2.50 mol%). After purification by column chromatography (*n*-hexane/ethyl acetate 9:1–5:1), product **61** was isolated as colorless liquid (105 g, 433 mmol, 78%).

TLC (*n*-hexane/ethyl acetate 5:1): R_f = 0.65.

^{1}H NMR ($CDCl_3$, 300 MHz) δ = 7.39–7.35 (m, 10H, Ar-C$H^{4,5,6}$), 5.18 (s, 4H, 2 C$H_2{}^2$) ppm.

^{13}C NMR ($CDCl_3$, 75 MHz) δ = 155.0 (C^1), 135.1 (C^3), 128.5 (C^5), 128.4 (C^6), 128.2 (C^4), 69.6 (C^2) ppm.

IR (ATR): $\tilde{\nu}$ = 3066, 3034, 2957, 2895, 1754, 1498, 1455,1391, 1370, 1235, 1080, 1029, 942, 909, 788, 736, 693, 611, 594, 576, 554, 482 cm^{-1}.

MS (FAB$^+$): *m/z* (%) = 243.2 [M+H]$^+$ (5), 181.1 (25), 91.1 [Bn]$^+$ (100).

HRMS (EI$^+$): $C_{15}H_{14}O_3$ [M+H]$^+$ calc. 243.1016; found 243.1015.

NMR data of the synthesized dibenzyl carbonate (**61**) was identical to literature.[185]

9.2.1.3 Dicrotyl carbonate (DCC, 62)

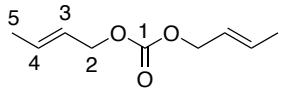

Dicrotyl carbonate (DCC, **62**) was obtained from DMC (**45**, 150 g, 1.66 mol, 1.00 eq.) and crotyl alcohol (**65**, 265 g, 3.66 mol, 2.20 eq.) with TBD (**67**, 2.39 g, 16.6 mmol, 1.00 mol%) as catalyst. After distillation (120 °C, 30 mbar), product **62** was isolated as colorless liquid (146 g, 858 mmol, 52%).

^{1}H NMR (300 MHz, CDCl3): δ = 6.06–5.69 (m, 1H, CH^3), 5.74–5.42 (m, 1H, CH^4), 4.54 (dd, J = 6.5, 0.9 Hz, 2H, C$H_2{}^2$), 2.07–1.38 (m, 3H, C$H_3{}^5$) ppm.

^{13}C NMR (75 MHz, $CDCl_3$): δ = 155.1 (C^1), 132.2 (C^4), 124.7 (C^3), 68.5 (C^2), 17.8 (C^5).

IR (ATR): $\tilde{\nu}$ = 3027, 2946, 2920, 2888, 2859, 1741, 1677, 1585, 1449, 1391, 1299, 1234, 1146, 1082, 1043, 965, 920, 791, 510 cm^{-1}.

MS (FAB$^+$): *m/z* (%) = 116.1 [M+H-crotyl]$^+$ (26), 71.1 [crotylO]$^+$ (26), 55.1 [crotyl]$^+$ (100).

No HRMS analyzed as no $[M]^+$ was detectable with FAB or EI.

NMR data of the synthesized dicrotyl carbonate (**62**) was identical to literature.[384]

9.2.1.4 10-Diundecenyl carbonate (DUC, 63)

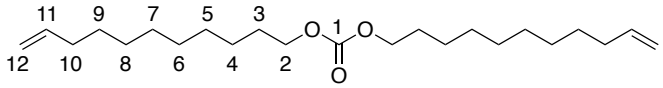

10-Diundecenyl carbonate (DUC, **63**) was obtained from DMC (**45**, 122 g, 1.35 mol, 1.00 eq.) and 10-undecenol (**66**, 442 g, 2.60 mol, 1.93 eq.) with TBD (**67**, 2.40 g, 17.1 mmol, 0.60 mol%) as catalyst. After column chromatography (cyclohexane/ethyl acetate 100:1–10:1), product **63** was isolated as colorless liquid (326 g, 889 mmol, 66%).

TLC (cyclohexane/ethyl acetate 9:1): R_f = 0.72.

^{1}H NMR (300 MHz, $CDCl_3$): δ = 6.04–5.55 (m, 1H, CH^{11}), 5.25–4.59 (m, 2H, C$H_2{}^{12}$), 4.11 (t, J = 6.7 Hz, 2H, C$H_2{}^{2}$), 2.02 (m, 2H, C$H_2{}^{10}$), 1.64 (m, 2H, C$H_2{}^{3}$), 1.52–0.92 (m, 12H, C$H_2{}^{alkyl}$) ppm.

^{13}C NMR (75 MHz, $CDCl_3$): δ = 155.6 (C^1), 139.3 (C^{11}), 114.3 (C^{12}), 68.1 (C^2), 33.9 (1 $C^{3–9}$), 29.5 (1 $C^{3–9}$), 29.5 (1 $C^{3–9}$), 29.3 (1 $C^{3–9}$), 29.2 (1 $C^{3–9}$), 29.0 (1 $C^{3–9}$), 28.8 (1 $C^{3–9}$), 25.8 (1 $C^{3–9}$) ppm.

IR (ATR): $\tilde{\nu}$ = 3077, 2924, 2854, 1744, 1641, 1464, 1402, 1373, 1251, 1047, 992, 952, 908, 793, 722, 636 cm^{-1}.

MS (FAB^+): *m/z* (%) = 367.4 $[M+H]^+$ (10), 137.1 (13), 111.2 (31), 97.1 $[CH_2CH_2CH_2CH_2CH_2Ch{=}CH_2]^+$ (100).

HRMS (FAB^+): $C_{23}H_{42}O_3$ $[M+H]^+$ calc. 367.3207; found 367.3207.

NMR data of the synthesized diundecenyl carbonate (**63**) was identical to literature.[185]

9.2.2 General procedure for the alkylation of phenols

Method A: heating under reflux condition. The phenol, 20.0 mol% of DBU and 1.50 eq. dialkyl carbonate were mixed together in a round bottom flask and heated up to reflux (125 °C) for 17 hours. The crude products were diluted with ethyl acetate and washed with aqueous 2 M hydrochloric acid (2 ×), water and saturated sodium chloride solution. The water layers were extracted with ethyl acetate and the combined organic solutions were dried over sodium sulfate. After filtration, the solutions were evaporated to dryness on a rotary evaporator. The crude products were purified by column chromatography (*n*-hexane/ethyl acetate mixtures) to obtain the pure alkyl phenyl ethers.

Method B: heating under microwave irradiation. The phenol, 20.0 mol% of DBU and 1.50 equivalents dialkyl carbonate per OH were placed in a microwave reaction tube and heated under stirring and microwave irradiation to 120–150 °C for one to six hours in a microwave instrument *Discover* of the company CEM. The work-up was performed as described for Method A.

Method C: heating in a pressure tube. The phenol, 20.0 mol% of a catalyst and 1.50 equivalents dialkyl carbonate per OH were placed in a pressure tube and heated to 120–150 °C for 5 to 15 hours. The work-up was performed as described for Method A.

9.2.2.1 Allyloxy-2-methoxybenzene (71a)

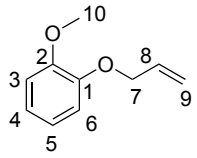

Following method B (microwave irradiation, 130 °C, 5 h), allyloxy-2-methoxybenzene (**71a**) was obtained from guaiacol (**71**, 500 mg, 4.03 mmol, 1.00 eq.) and DAC (**54**, 860 mg, 6.05 mmol, 1.50 eq.) with DBU (**53**, 123 mg, 810 µmol, 20.0 mol%) as catalyst. After column chromatography (*n*-hexane/ethyl acetate 50:1–40:1), product **71a** was isolated as colorless liquid (530 mg, 3.23 mmol, 80%).

TLC (*n*-hexane/ethyl acetate 9:1): R_f = 0.55.

^{1}H NMR ($CDCl_3$, 300 MHz) δ = 7.01–6.82 (m, 4H, 4 C$H^{3\text{-}6}$), 6.09 (ddd, J = 11.7, 10.5, 5.2 Hz, 1H, CH^8), 5.41 (ddd, J = 17.3, 2.9, 1.4 Hz, 1H, C$H_2{}^{9,\text{trans}}$), 5.28 (dd, J = 10.5, 1.3 Hz, 1H, C$H_2{}^{9,\text{cis}}$), 4.62 (dt, J = 5.4, 1.3 Hz, 2H, C$H_2{}^7$), 3.88 (d, J = 3.1 Hz, 3H, C$H_3{}^{10}$) ppm.

^{13}C NMR ($CDCl_3$, 75 MHz) δ = 149.7 (C^2), 148.2 (C^1), 133.6 (C^8), 121.4 (1 $C^{4,5}$), 120.9 ($C^{4,5}$), 118.0 (C^9), 113.8 (C^6), 112.0 (C^3), 70.0 (C^7), 56.0 (C^{10}) ppm.

IR (ATR) $\tilde{\nu}$ = 2933, 1591, 1501, 1454, 1423, 1327, 1248, 1222, 1178, 1122, 1023, 994, 924, 833, 738, 644, 577, 461 cm^{-1}.

MS (FAB$^+$): *m/z* (%) = 164.1 [M]$^+$ (92), 124.1 [M-allyl+H]$^+$ (96), 123.1 [M-allyl]$^+$ (100), 95.0 (60), 77.1 (32).

HRMS (FAB$^+$): $C_{10}H_{12}O_2$ [M]$^+$ calc. 164.0832; found 164.0833.

NMR data of the synthesized allyloxy-2-methoxybenzene (**71a**) was identical to literature.[385]

9.2.2.2 Benzyloxy-2-methoxybenzene (71b)

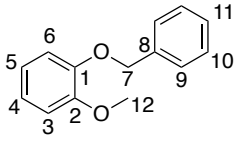

Following method A (reflux, 150 °C, 17 h), Benzyloxy-2-methoxybenzene (**71b**) was obtained from guaiacol (**71**, 500 mg, 4.03 mmol, 1.00 eq.) and DBC (**61**, 1.95 g, 8.06 mmol, 2.00 eq.), with DBU (**53**, 123 mg, 0.81 mmol, 20.0 mol%) as catalyst. After column chromatography (*n*-hexane/ethyl acetate 10:1), product **71b** was obtained as colorless solid (770 mg, 3.59 mmol, 89%).

TLC (*n*-hexane/ethyl acetate 9:1): R_f = 0.50.

DSC: T_m = 58 °C.

^{1}H NMR ($CDCl_3$, 300 MHz) δ = 7.36 (m, 5H, 5 C*H*$^{9\text{-}11}$), 7.05–6.66 (m, 4H, 4 C*H*$^{3\text{-}6}$), 5.17 (s, 2H, CH_2^7), 3.99–3.79 (s, 3H, CH_3^{12}) ppm.

^{13}C NMR ($CDCl_3$, 75 MHz) δ = 148.9 (*C*^{1}), 147.4 (*C*^{2}), 136.4 (*C*^{8}), 127.7 (1 *C*^{9,10}), 126.9 (*C*^{11}), 126.4 (1 *C*^{9,10}), 120.6 (1 *C*$^{3\text{-}6}$), 119.9 (1 *C*$^{3\text{-}6}$), 113.4 (1 *C*$^{3\text{-}6}$), 111.1 (1 *C*$^{3\text{-}6}$), 70.2 (*C*^{7}), 55.1 (*C*^{12}) ppm.

IR (ATR) $\tilde{\nu}$ = 3032, 2836, 1589, 1502, 1453, 1378, 1328, 1289, 1248, 1215, 1181, 1122, 1048, 1006, 917, 857, 770, 737, 695, 620, 581, 552, 518 cm^{-1}.

MS (EI$^+$): *m/z* (%) = 215.1 [M+H]$^+$ (14), 214.1 [M]$^+$ (93), 91.1 [Bn]$^+$ (100).

HRMS (EI$^+$): $C_{14}H_{14}O_2$ [M+H]$^+$ calc. 214.0988; found 214.0986.

NMR data of the synthesized benzyloxy-2-methoxybenzene (**71b**) was identical to literature.[386]

9.2.2.3 Crotyloxy-2-methoxybenzene (71c)

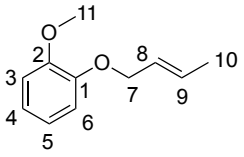

Following method A (120 °C, 20 h, reflux), crotyloxy-2-methoxybenzene (**71c**) was obtained from guaiacol (**71**, 6.00 g, 47.9 mmol, 1.00 eq.) and DCC (**62**, 9.79 g, 57.5 mmol, 1.20 eq.) with TBAB (**50**, 3.09 g, 9.58 mmol, 20.0 mol%) as a base. After column chromatography (cyclohexane/ethyl acetate 40:1), product **71c** was isolated as a colorless liquid (7.26 g, 40.7 mmol, 85%).

TLC (cyclohexane/ethyl acetate 9:1): R_f = 0.55.

^{1}H NMR ($CDCl_3$, 300 MHz) δ = 6.90 (s, 4H, C*H*$^{3–6}$), 6.07–5.44 (m, 2H, C*H*^{8,9}), 4.52 (d, *J* = 5.1 Hz, 2H, CH_2^7), 3.87 (s, 3H, CH_3^{11}), 1.74 (d, *J* = 5.5 Hz, 3H, CH_3^{10}) ppm.

^{13}C NMR ($CDCl_3$, 75 MHz) δ = 149.5 (*C*^{1}), 148.2 (*C*^{2}), 130.8 (*C*^{8}), 126.3 (*C*^{9}), 121.1 (1 *C*^{4,5}), 120.8 (1 *C*^{4,5}), 113.4 (1 *C*^{3,6}), 111.7 (1 *C*^{3,6}), 69.7 (*C*^{7}), 55.9 (*C*^{11}), 18.0 (*C*^{10}) ppm.

IR (ATR) $\tilde{\nu}$ = 3063, 3022, 2939, 2917, 2857, 2835, 1743, 1592, 1501, 1454, 1377, 1329, 1248, 1222, 1178, 1122, 1075, 1051, 1028, 1004, 964, 911, 835, 779, 738, 603, 580, 507 cm^{-1}.

MS (EI$^+$): *m/z* (%) = 178.2 [M]$^+$ (24), 124.1 [M–crotyl]$^+$ (100), 109.1 (55), 55.1 [crotyl]$^+$ (20).

HRMS (EI$^+$): $C_{11}H_{14}O_2$ [M]$^+$ calc. 178.0988; found 178.0989.

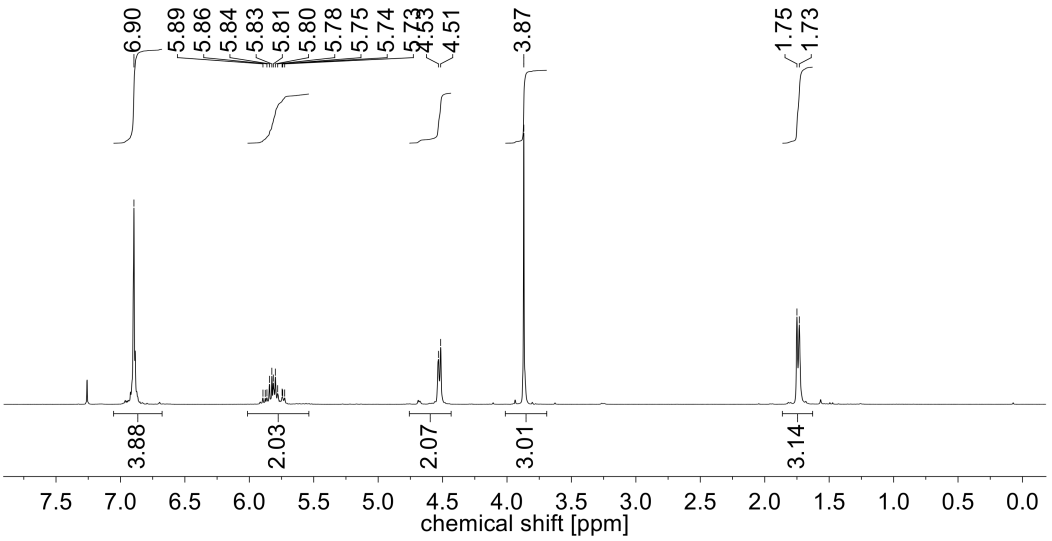

9.2.2.4 1-(Allyloxy)-3-methoxybenzene (72a)

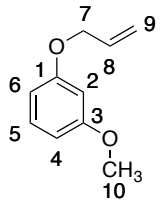

This reaction was performed by Tobias Fischer in the scope of a six-week internship under my co-supervision.

Following Method B (microwave irradiation, 150 °C, 2.5 h), 1-(allyloxy)-3-methoxybenzene **72a**) was synthesized from 3-methoxyphenol (**72**, 250 mg, 2.01 mmol, 1.00 eq.) and DAC (**54**, 428 mg, 3.01 mmol, 1.50 eq.) with DBU (**53**, 61.2 mg, 402 µmol, 20.0 mol%) as catalyst. After column chromatography (*n*-hexane/ethyl acetate 50:1–47:1), product **72a** was obtained as colorless liquid (215 mg, 1.31 mmol, 65%).

TLC (*n*-hexane/ethyl acetate 9:1): R_f = 0.75.

^{1}H NMR (300 MHz, $CDCl_3$): δ = 7.15–7.26 (m, 1H, CH^2), 6.50–6.53 (m, 3H, C$H^{4,5,6}$), 6.01–6.12 (m, 1H, CH^8), 5.41 (d, J = 17.2 Hz, 1H, C$H_2{}^{9,trans}$), 5.29 (d, J = 9.3 Hz, 1H, C$H_2{}^{9,cis}$), 4.52 (s, 2H, C$H_2{}^7$), 3.79 (s, 3H, C$H_3{}^{10}$) ppm.

^{13}C NMR (75 MHz, $CDCl_3$): δ = 161.0 (C^3), 160.0 (C^1), 133.4 (C^8), 130.0 (C^5), 117.8 (C^9), 107.0 (1 C$H^{4,6}$), 106.6 (1 $C^{4,6}$), 101.4 (C^2), 69.0 (C^7), 55.4 (C^{10}) ppm.

IR (ATR): $\tilde{\nu}$ = 2938, 1591, 1490, 1451, 1333, 1283, 1263, 1198, 1147, 1042, 991, 923, 834, 760, 686, 570, 458 cm^{-1}.

MS (EI$^+$): *m/z* (%) = 164.1 [M]$^+$ (100).

HRMS (EI$^+$): $C_{10}H_{12}O_2$ [M]$^+$ calc. 164.0832; found 164.0833.

NMR data of the synthesized 1-(allyloxy)-3-methoxybenzene (**72a**) was identical to literature.[387]

9.2.2.5 1-(Benzyloxy)-3-methoxybenzene (72b)

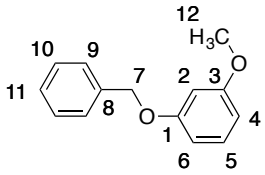

This reaction was performed by Tobias Fischer in the scope of a six-week internship under my co-supervision.

Following Method B (microwave irradiation, 150 °C, 2.5 h), 1-(benzyloxy)-3-methoxybenzene (**72b**) was synthesized from 3-methoxyphenol (**72**, 250 mg, 2.01 mmol, 1.00 eq.) and DBC (**61**, 729 mg, 3.01 mmol, 1.50 eq.), with DBU (**53**, 61.2 mg, 402 µmol, 20.0 mol%) as catalyst. After column chromatography (*n*-hexane/ethyl acetate 50:1–47:1), product **72b** was obtained as colorless liquid (366 mg, 2.23 mmol, 84%).

TLC (*n*-hexane/ethyl acetate 9:1): R_f = 0.63.

^{1}H NMR (300 MHz, $CDCl_3$): δ = 7.26–7.36 (m, 5H, CH^{9-13}), 7.10–7.18 (m, 1H, CH^2), 6.46–6.54 (m, 3H, C$H^{4,6}$), 4.98 (s, 2H, C$H_2{}^7$), 3.72 (s, 3H, C$H_3{}^{14}$) ppm.

^{13}C NMR (75 MHz, $CDCl_3$): δ = 161.0 (C^3), 160.2 (C^1), 137.1 (C^8), 130.0 (C^5), 128.7 (C^{10}), 128.1 (C^{11}), 127.7 (C^9), 107.1 (1 $C^{4,6}$), 106.7 (1 $C^{4,6}$), 101.5 (CH^2), 70.2 (C^7), 55.4 (C^{12}) ppm.

IR (ATR): $\tilde{\nu}$ = 3031, 2938, 2834, 1589, 1490, 1451, 1379, 1334, 1285, 1262, 1195, 1168, 1146, 1081, 1041, 1025, 991, 928, 833, 758, 732, 685, 624, 576, 505, 457 cm^{-1}.

MS (EI$^+$): *m/z* (%) = 214.1 [M]$^+$ (44), 91.1 [Bn]$^+$ (100).

HRMS (EI$^+$): $C_{14}H_{14}O_2$ [M]$^+$) calc. 214.0988; found 214.0986.

NMR data of the synthesized 1-(benzyloxy)-3-methoxybenzene (**72b**) was identical to literature.[388]

9.2.2.6 2-(Allyloxy)-1,3-dimethoxybenzene (73a)

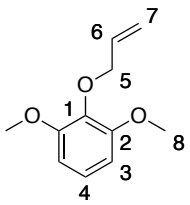

This reaction was performed by Tobias Fischer in the scope of a six-week internship under my co-supervision.

Following Method B (microwave irradiation, 140 °C, 2 h), 2-(allyloxy)-1,3-dimethoxybenzene (**73a**) was obtained from 2,6-dimethoxyphenol (**73**) (250 mg, 1.62 mmol, 1.00 eq.) and DAC (**54**, 346 mg, 2.43 mmol, 1.50 eq.) with DBU (49.3 mg, 324 µmol, 20.0 mol%) as catalyst. After column chromatography (*n*-hexane/ethyl acetate 50:1–30:1), product **73a** was obtained as colorless liquid (97.0 mg, 499 µmol, 31%).

TLC (*n*-hexane/ethyl acetate 9:1): R_f = 0.38.

^{1}H NMR (300 MHz, $CDCl_3$): δ = 6.99 (dd, J = 7.9 Hz, 7.9 Hz, 1H, CH^4), 6.57 (d, J = 7.7 Hz, 2H, CH^3), 6.07–6.16 (m, 1H, CH^6), 5.30 (d, J = 17.2 Hz, 1H, C$H_2{}^{7,trans}$), 5.18 (d, J = 10.0 Hz, 1H, C$H_2{}^{7,cis}$), 4.52 (d, J = 5.1 Hz, 2H, C$H_2{}^5$), 3.85 (s, 6H, C$H_3{}^8$) ppm.

^{13}C NMR (75 MHz, $CDCl_3$): δ = 153.8 (C^2), 136.9 (C^1), 134.7 (C^6), 123.7 (C^4), 117.7 (C^7), 105.4 (C^3), 74.2 (C^5), 56.1 (C^8) ppm.

IR (ATR): $\tilde{\nu}$ = 2937, 2836, 1594, 1492, 1475, 1434, 1294, 1250, 1212, 1184, 1107, 1034, 985, 922, 773, 728, 705, 618, 525 cm^{-1}.

MS (EI$^+$): *m/z* (%) = 194.2 [M]$^+$ (45) , 153.1 [M–Allyl]$^+$ (100).

HRMS (EI$^+$): $C_{11}H_{14}O_3$ [M]$^+$ calc. 194.0938; found 194.0937.

NMR data of the synthesized 2-(allyloxy)-1,3-dimethoxybenzene (**73a**) was identical to literature.[389]

9.2.2.7 2-(Benzyloxy)-1,3-dimethoxybenzene (73b)

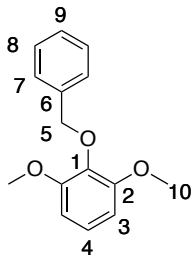

This reaction was performed by Tobias Fischer in the scope of a six-week internship under my co-supervision.

Following method B (microwave irradiation, 150 °C, 2.5 h), 2-(Benzyloxy)-1,3-dimethoxybenzene (**73b**) was obtained from 2,6-dimethoxyphenol (250 mg, 1.62 mmol, 1.00 eq.) and DBC (**61**, 589 mg, 2.43 mmol, 1.50 eq.), with DBU (**53**, 49.2 mg, 324 µmol, 20.0 mol%) as catalyst. After column chromatography (*n*-hexane/ethyl acetate 9:1), product **73b** was isolated as colorless liquid (354 mg, 1.44 mmol, 90%).

TLC (*n*-hexane/ethyl acetate 9:1): R_f = 0.43.

^{1}H NMR (300 MHz, $CDCl_3$): δ = 7.50 (m, 2H, CH^7), 7.33 (m, 3H, CH^8), 7.00 (dd, J = 8.2 Hz,

J = 8.2 Hz, 1H, C*H*^{4}), 6.58 (d, *J* = 8.2 Hz, 2H, C*H*^{3}), 5.01 (s, 2H, CH_2^{5}), 3.83 (s, 6H, CH_3^{10}) ppm.

^{13}C NMR (75 MHz, $CDCl_3$): δ = 154.0 (*C*^{2}), 138.1 (*C*^{6}), 137.2 (*C*^{1}), 128.6 (*C*^{9}), 128.2 (*C*^{8}), 127.9 (*C*^{7}), 123.9 (*C*^{4}), 105.5 (*C*^{3}), 75.1 (*C*^{5}), 56.2 (*C*^{10}) ppm.

IR (ATR): $\tilde{\nu}$ = 2936, 2835, 1594, 1492, 1475, 1373, 1294, 1252, 1217, 1183, 1107, 988, 912, 855, 773, 730, 695, 526 cm^{-1}.

MS (FAB$^+$): *m/z* (%) = 244.1 [M]$^+$ (48), 153.0 [M−Bn]$^+$ (27), 91.0 [Bn]$^+$ (100).

HRMS (FAB$^+$): $C_{15}H_{16}O_3$ [M]$^+$ calc. 244.1094; found 244.1095.

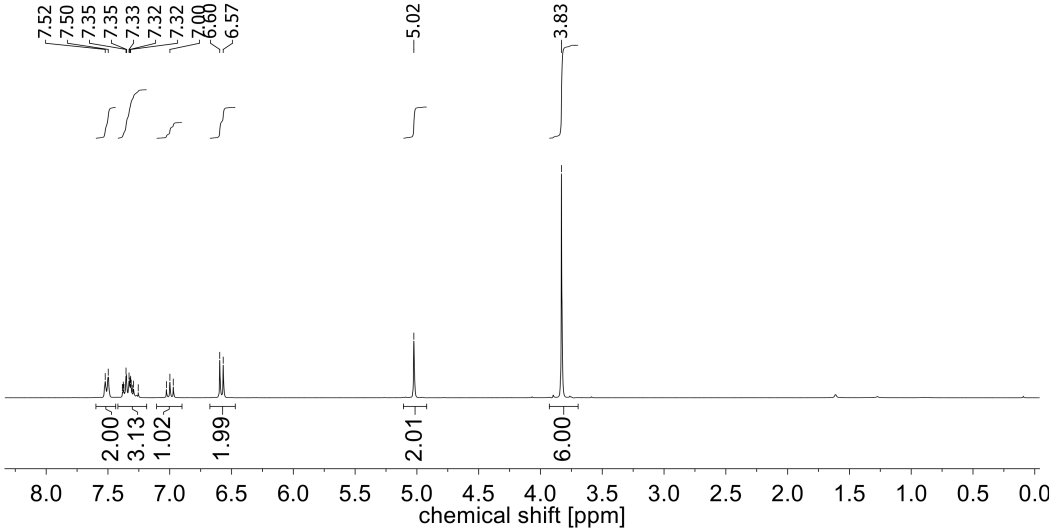

9.2.2.8 1-(allyloxy)-4-methoxybenzene (74a)

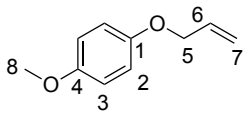

Following method B (microwave irradiation, 150 °C, 2.5 h), 1-(allyloxyoxy)-4-methoxybenzene (**74a**) was obtained from 4-methoxyphenol (**74**, 500 mg, 4.02 mmol, 1.00 eq.) and DAC (**54**, 857 mg, 6.02 mmol, 1.50 eq.), using DBU (**53**, 122 mg, 804 µmol, 20.0 mol%) as catalyst. After column chromatography (*n*-hexane/ethyl acetate 50:1–40:1), product **74a** was isolated as colorless liquid (638 mg, 3.89 mmol, 97%).

TLC (*n*-hexane/ethyl acetate 19:1): R_f = 0.61.

^{1}H NMR (300 MHz, $CDCl_3$): δ = 3.77 (s, 3H, CH_3^{8}), 4.49 (dt, *J* = 5.3 Hz, 1.5Hz, 2H, CH_2^{5}), 5.25–5.45 (m, 2H, CH_2^{7}), 5.99–6.12 (m, 1H, C*H*^{6}), 6.80–6.91 (m, 4H, C*H*^{2,3}) ppm.

^{13}C NMR (75 MHz, $CDCl_3$): δ = 55.6 (*C*^{8}), 69.4 (*C*^{5}), 114.5 (*C*^{2}), 115.6 (*C*^{3}), 117.4 (*C*^{7}), 133.5 (*C*^{6}), 152.6 (*C*^{1}), 153.8 (*C*^{4}) ppm.

IR (ATR): $\tilde{\nu}$ = 2934, 2833, 1647, 1591, 1504, 1462, 1424, 1362, 1289, 1226, 1180, 1106, 1036, 996, 925, 823, 793, 753, 717 cm^{-1}.

HRMS (FAB) of $C_{10}H_{12}O_2$ $[M]^+$ calc. 164.0832; found 164.0830.

NMR data of the synthesized 1-(allyloxy)-4-methoxybenzene (**74a**) was identical to literature.[390]

9.2.2.9 1-(Benzyloxy)-4-methoxybenzene (74b)

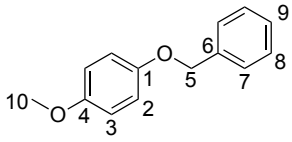

Following method B (microwave irradiation, 150 °C, 2.5 h), 1-(Benzyloxy)-4-methoxybenzene (**74b**) was obtained from 4-methoxyphenol (**74**, 500 mg, 4.02 mmol, 1.00 eq.) and DBC (**61**, 1.46 g, 6.02 mmol, 1.50 eq.), using DBU (**53**, 123 mg, 805 µmol, 20.0 mol%) as catalyst. After column chromatography (*n*-hexane/ethyl acetate 50:1–40:1), product (**74b**) was isolated as colorless solid (775 mg, 3.62 mmol, 90%).

TLC (*n*-hexane/ethyl acetate 19:1): R_f = 0.43.

DSC: T_m = 71 °C.

^{1}H NMR (300 MHz, $CDCl_3$): δ = 3.77 (s, 3H, CH_3^{10}), 5.02 (s, 2H, CH_2^5), 6.81–6.95 (m, 4H, C$H^{2,3}$), 7.29–7.46 (m, 5H, C$H^{7,8,9}$) ppm.

^{13}C NMR (75 MHz, $CDCl_3$): δ = 55.6 (C^{10}), 70.6 (C^5),114.6 (C^2), 115.8 (C^3), 127.4 (C^7), 127.8 (C^9), 128.5 (C^8), 137.2 (C^6), 152.9 (C^4), 153.9 (C^1) ppm.

IR (ATR): $\tilde{\nu}$ = 2995, 2949, 2833,1634,1504,1454, 1439, 1381, 1290, 1267, 1223, 1179, 1111, 1032, 1009, 944, 918, 864, 824, 763, 728, 695 cm^{-1}.

HRMS (FAB) of $C_{14}H_{14}O_2$ $[M]^+$ calc. 214.0988; found 214.0990.

NMR data of the synthesized 1-(benzyloxy)-4-methoxybenzene (**74b**) was identical to literature.[386]

9.2.2.10 Allyloxy-3-methylbenzene (75a)

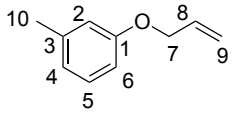

Following method B (microwave irradiation, 150 °C, 1.5 h), allyloxy-3-methylbenzene (**75a**) was obtained from *m*-cresol (**75**, 0.50 g, 4.62 mmol, 1.00 eq.) and DAC (**54**, 0.99 g, 6.94 mmol, 1.50 eq.), with DBU (**53**, 140 mg, 0.92 mmol, 20.0 mol%) as catalyst. After column chromatography (*n*-hexane/ethyl acetate 50:1), product **75a** was obtained as colorless liquid (550 mg, 3.71 mmol, 80%).

TLC (*n*-hexane/ethyl acetate 19:1): R_f = 0.66.

^{1}H NMR ($CDCl_3$, 300 MHz) δ = 7.19–7.14 (m, 1H, CH^5), 6.78–6.72 (m, 3H, 3 C$H^{2.4,6}$), 6.06 (ddd, J = 16.8, 10.3, 5.0 Hz, 1H, CH^8), 5.41 (ddd, J = 17.4, 1.5, 0.6 Hz, 1H, C$H_2{}^{9,trans}$), 5.28 (dd, J = 10.5, 0.8 Hz, 1H, C$H_2{}^{9,cis}$), 4.53 (dd, J = 5.3, 1.2 Hz, 2H, C$H_2{}^7$), 2.33 (s, 3H, C$H_3{}^{10}$) ppm.

^{13}C NMR ($CDCl_3$, 75 MHz) δ = 158.8 (C^1), 139.6 (C^3), 133.6 (C^8), 129.3 (C^5), 121.8 (C^4), 117.6 (C^9), 115.7 (C^2), 111.7 (C^6), 68.8 (C^7), 21.7 (C^{10}) ppm.

IR (ATR) $\tilde{\nu}$ = 3329, 3022, 2916, 2862, 1649, 1600, 1584, 1488, 1454, 1421, 1362, 1288, 1256, 1156, 1029, 989, 922, 873, 855, 768, 689, 567, 443 cm^{-1}.

MS (EI$^+$): *m/z* (%) = 148.1 [M]$^+$ (100), 133.1 [M-CH3]$^+$ (60), 105.1 (55), 91.1 [M-OCH_2CHCH_2]$^+$ (42), 77.1 (67), 69.0 (74), 41.0 (76).

HRMS (EI$^+$): $C_{10}H_{12}O$ [M]$^+$ calc. 148.0883; found 148.0884.

NMR data of the synthesized allyloxy-3-methylbenzene (**75a**) was identical to literature.[387]

9.2.2.11 Benzyloxy-3-methylbenzene (75b)

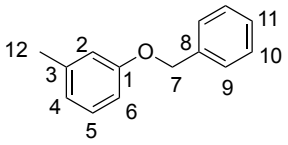

Following method B (microwave irradiation, 150 °C, 2.5 h), benzyloxy-3-methylbenzene (**75b**) was obtained from *m*-cresol (**75**, 500 mg, 4.62 mmol, 1.00 eq.) and DBC (**61**, 2.23 g, 9.24 mmol, 2.00 eq.), with DBU (**53**, 140 mg, 0.92 mmol, 20.0 mol%) as catalyst. After column chromatography (*n*-hexane/ethyl acetate 50:1–40:1), product **75b** was obtained as colorless liquid (850 mg, 4.30 mmol, 93%).

TLC (*n*-hexane/ethyl acetate 19:1): R_f = 0.84.

^{1}H NMR ($CDCl_3$, 300 MHz) δ = 7.39 (m, 5H, C$H^{9\text{-}11}$), 7.17 (t, J = 7.8 Hz, 1H, CH^2), 6.91–6.68 (m, 3H, 3 C$H^{4\text{-}6}$), 5.05 (s, 2H, C$H_2{}^7$), 2.34 (s, 3H, C$H_3{}^{12}$) ppm.

^{13}C NMR ($CDCl_3$, 75 MHz) δ = 159.0 (C^1), 139.7 (C^3), 137.4 (C^8), 129.4 (C^5), 128.7 (2 C^{10}), 128.0 (C^{11}), 127.6 (2 C^9), 121.9 (C^4), 115.9 (C^2), 111.8 (C^6), 70.0 (C^7), 21.7 (C^{12}).

IR (ATR) $\tilde{\nu}$ = 3031, 2917, 1583, 14878, 1453, 1379, 1310, 1289, 1256, 1153, 1081, 1039, 1026, 992, 932, 906, 874, 841, 768, 731, 689, 626, 510, 443 cm^{-1}.

MS (EI$^+$): *m/z* (%) = 199.2 [M+H]$^+$ (8), 198.2 [M]$^+$ (57), 91.1 [M-OBn]$^+$ (100).

HRMS (EI$^+$): $C_{14}H_{14}O$ [M]$^+$ calc. 198.1039; found 198.1037.

NMR data of the synthesized benzyloxy-3-methylbenzene (**75b**) was identical to literature.[391]

9.2.2.12 Allyoxy-4-ethylbenzene (76a)

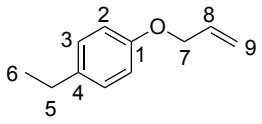

Following method B (microwave irradiation, 140 °C, 30 min), allyoxy-4-ethylbenzene (**76a**) was obtained from 4-ethylphenol (**76**, 500 mg, 4.09 mmol, 1.00 eq.) and DAC (**54**, 870 g, 6.14 mmol, 1.50 eq.), with DBU (**53**, 124 mg, 0.82 mmol, 20.0 mol%) as catalyst. After column chromatography (*n*-hexane/ethyl acetate 100:1), product **76a** was isolated as a colorless liquid (600 mg, 3.70 mmol, 90%).

TLC (*n*-hexane/ethyl acetate 19:1): R_f = 0.90.

^{1}H NMR ($CDCl_3$, 300 MHz) δ = 7.11 (d, J = 8.6 Hz, 2H, 2 CH^3), 6.85 (d, J = 8.6 Hz, 2H, 2 CH^2), 6.07 (ddt, J = 21.1, 10.5, 5.3 Hz, 1H, CH^8), 5.41 (dd, J = 17.3, 1.5 Hz, 1H, C$H^{9,trans}$), 5.28 (dd, J = 10.5, 1.3 Hz, 1H, C$H^{9,cis}$), 4.52 (d, J = 5.3 Hz, 2H, C$H_2{}^7$), 2.60 (q, J = 7.6 Hz, 2H, C$H_2{}^5$), 1.22 (t, J = 7.6 Hz, 3H, C$H_3{}^6$).

^{13}C NMR ($CDCl_3$, 75 MHz) δ = 156.8 (C^1), 136.7 (C^4), 133.7 (C^8), 128.8 (2 C^3), 117.6 (C^9), 114.8 (2 C^2), 69.1 (C^7), 28.1 (C^5), 16.0 (C^6).

IR (ATR) $\tilde{\nu}$ = 2962, 2927, 2870, 1874, 1647, 1609, 1582, 1508, 1455, 1423, 1361, 1295, 1234, 1176, 1115, 1024, 996, 921, 826, 743, 620, 541 cm^{-1}.

MS (EI$^+$): *m/z* (%) = 162.2 [M]$^+$ (80), 133.1 [M-Ethyl]$^+$ (98), 105.1 [M-Allyloxy]$^+$ (100).

NMR data of the synthesized allyoxy-4-ethylbenzene (**76a**) was identical to literature.[392]

9.2.2.13 Benzyloxy-4-ethylbenzene (76b)

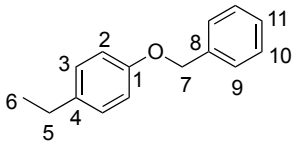

Following method B (microwave irradiation, 150 °C, 2.5 h), benzyloxy-4-ethylbenzene (**76b**) was obtained from 4-ethylphenol (**76**, 500 mg, 4.09 mmol, 1.00 eq.) and DBC (**61**, 1.98 g, 8.20 mmol, 2.00 eq.), with DBU (**53**, 125 mg, 0.82 mmol, 20.0 mol%) as catalyst. After column chromatography (*n*-hexane/ethyl acetate 100:1), product **76b** was obtained as colorless liquid (840 mg, 3.96 mmol, 97%).

TLC (*n*-hexane/ethyl acetate 19:1): R_f = 0.76.

^{1}H NMR ($CDCl_3$, 300 MHz) δ = 7.40 (m, 5H, 5 C$H^{9\text{-}11}$), 7.13 (d, J = 8.6 Hz, 2H, 2 CH^{3}), 6.92 (d, J = 8.6 Hz, 1H, 2 CH^{2}), 5.06 (s, 2H, C$H_2{}^{7}$), 2.61 (q, J = 7.6 Hz, 2H, C$H_2{}^{5}$), 1.22 (t, J = 7.6 Hz, 3H, C$H_3{}^{6}$) ppm.

^{13}C NMR ($CDCl_3$, 75 MHz) δ = 157.0 (C^{1}), 137.5 (C^{8}), 136.9 (C^{4}), 128.9 (C^{3}), 128.7 (C^{10}), 128.0 (C^{11}), 127.6 (C^{9}), 114.9 (2 C^{2}), 70.2 (C^{7}), 28.1 (C^{5}), 16.0 (C^{6}) ppm.

IR (ATR) $\tilde{\nu}$ = 3030, 2961, 2927, 2868, 1609, 1581, 1509, 1378, 1294, 1233, 1174, 1114, 1023, 858, 826, 730, 694, 603, 543 cm^{-1}.

MS (EI$^+$): *m/z* (%) = 212.2 [M]$^+$ (24), 91.1 [Bn]$^+$ (100).

HRMS (EI$^+$): $C_{15}H_{16}O$ [M]$^+$ calc. 212.1196; found 212.1197.

NMR data of the synthesized benzyloxy-4-ethylbenzene (**76b**) was identical to literature.[393]

9.2.2.14 1-Ethyl-4-(undec-10-en-1-yloxy)benzene (76u)

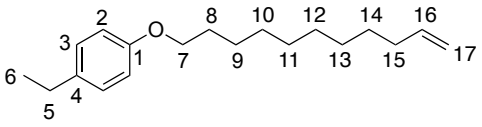

Following method B (microwave irradiation, 220 °C, 4 h), 1-Ethyl-4-(undec-10-en-1-yloxy)benzene (**76u**) was obtained from 4-ethylphenol (**76**, 150 mg, 1.23 mmol, 1.00 eq.) and DUC (**63**, 900 mg, 2.46 mmol, 2.00 eq.), with DBU (**53**, 37.4 mg, 245 µmol, 20.0 mol%) as catalyst. After column chromatography (pure cyclohexane), product **76u** was isolated as colorless liquid (200 mg, 729 µmol, 59%).

TLC (cyclohxane): R_f = 0.21.

^{1}H NMR ($CDCl_3$, 300 MHz): δ = 7.09–7.12 (m, 2H, CH^{3}), 6.80–6.84 (m, 2H, CH^{2}), 5.75–5.89 (m, 1H, CH^{16}), 4.91–5.04 (m, 2H, C$H_2{}^{17}$), 3.93 (t, J = 6.60 Hz, 2H, C$H_2{}^{7}$), 2.59 (q, J = 7.60 Hz, 2H, C$H_2{}^{5}$), 2.04 (dt, J = 7.40 Hz, J = 6.70 Hz, 2H, C$H_2{}^{15}$), 1.72–1.81 (m, 2H, C$H_2{}^{8}$), 1.19 –1.45 (m, 12H, C$H_2{}^{9–13}$), 1.21 (t, J = 7.60 Hz, 3H, C$H_3{}^{6}$) ppm.

^{13}C NMR ($CDCl_3$, 75 MHz): δ = 157.4 (C^{1}), 139.4 (C^{16}), 136.4 (C^{4}), 128.8 (C^{3}), 114.6 (C^{2}), 114.3 (C^{17}), 68.2 (C^{7}), 34.0 (C^{15}), 29.7 ($C^{8–14}$), 29.6 ($C^{8–14}$), 29.6 ($C^{8–14}$), 29.5 ($C^{8–14}$), 29.3 ($C^{8–14}$), 29.1 ($C^{8–14}$), 28.2 (C^{5}), 26.3 ($C^{8–14}$), 16.1 (C^{6}) ppm.

IR (ATR): $\tilde{\nu}$ = 2924, 2853, 1640, 1612, 1582, 1510, 1466, 1389, 1296, 1237, 1175, 1114, 1032, 993, 908, 826, 807, 722, 637, 531 cm^{-1}.

HRMS (FAB$^+$): $C_{19}H_{30}O_1$ [M]$^+$ calc. 271.2291; found 274.2291.

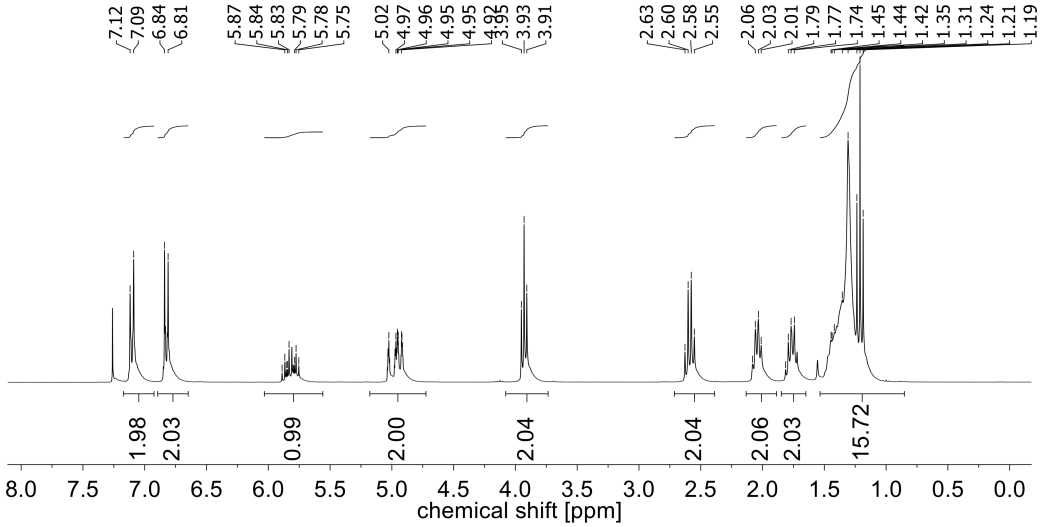

9.2.2.15 4-(Allyloxy)-1,1'-biphenyl (77a)

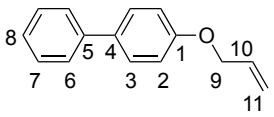

Following method A (microwave irradiation, 150 °C, 2.5 h), 4-(allyloxy)-1,1'-biphenyl (**77a**) was obtained from 4-phenylphenol (**77**, 500 mg, 2.94 mmol, 1.00 eq.) and DAC (**54**, 630 mg, 4.41 mmol, 1.50 eq.), with DBU (**53**, 0.90 g, 0.59 mmol, 20.0 mol%) as catalyst. After crystallization from ethyl acetate, product **77a** was obtained as colorless solid (600 mg, 2.85 mmol, 97%).

TLC (*n*-hexane/ethyl acetate 9:1): R_f = 0.68.

DSC: T_m = 70 °C.

^{1}H NMR ($CDCl_3$, 300 MHz): δ = 7.76–7.21 (m, 7H, 7 C$H^{3,6-8}$), 7.09–6.91 (m, 2H, 2 CH^2), 6.09 (ddt, J = 17.1, 10.5, 5.3 Hz, 1H, CH^{10}), 5.45 (dd, J = 17.3, 1.5 Hz, 1H, C$H^{11,trans}$), 5.31 (dd, J = 10.5, 1.4 Hz, 1H, C$H^{11,cis}$), 4.59 (ddd, J = 5.2, 1.4 Hz, 1.4, 2H, CH_2^9) ppm.

13C NMR (CDCl3, 75 MHz): δ = 158.3 (C^1), 141.0 (C^4), 134.1 (C^5) 133.4 (C^{10}), 128.9 ($C^{3,6,7}$), 128.3 ($C^{3,6,7}$), 126.9 ($C^{3,6,7}$), 126.8 (C^8), 117.9 (C^{11}), 115.2 (2 C^2), 69.1 (C^9) ppm.

IR (ATR): $\tilde{\nu}$ = 3031, 1647, 1604, 1582, 1483, 1451, 1409, 1451, 1409, 1380, 1287, 1269, 1241, 1189, 1120, 1019, 988, 924, 831, 761, 715, 694, 619, 569, 551, 494 cm^{-1}.

MS (EI$^+$): *m/z* (%) = 210.2 [M]$^+$ (76), 169.2 [M-Allyl+H]$^+$ (124), 169.2 [M-Allyl]$^+$ (100).

HRMS (FAB$^+$): $C_{15}H_{14}O$ [M+H]$^+$ calc. 210.1039; found 210.1040.

NMR data of 4-(allyloxy)-1,1'-biphenyl (**77a**) was identical to literature.[394]

9.2.2.16 4-(Benzyloxy)-1,1'-biphenyl (77b)

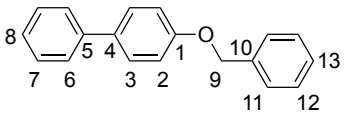

Follwoing Method A (reflux conditions, 150 °C, 17 h), 4-(benzyloxy)-1,1'-biphenyl (**77b**) was obtained from 4-phenyl-phenol (**77**, 500 mg, 2.94 mmol, 1.00 eq.) and DBC (**61**, 1.42 g, 5.88 mmol, 2.00 eq.) with DBU (**53**, 90.0 mg, 0.59 mmol, 20.0 mol%) as catalyst. After crystallization from ethyl acetate, product **77b** was isolated as colorless solid (730 g, 2.80 mmol, 95%).

TLC (*n*-hexane/ethyl acetate 9:1): R_f = 0.68.

^{1}H NMR ($CDCl_3$, 300 MHz): δ = 7.67–7.24 (m, 12H, C$H^{3,6,7,8}$), 7.07 (m, 2H, CH^2), 5.13 (s, 2H, C$H_2{}^9$) ppm.

^{13}C NMR ($CDCl_3$, 75 MHz): δ = 158.5 (C^1), 140.9 (C^4), 137.1 (C^5), 134.2 (C^{10}), 128.9 ($C^{3,6\text{-}8,11–13}$), 128.8 ($C^{3,6–8,11–13}$), 128.3 ($C^{3,6–8,11–13}$), 128.1 ($C^{3,6–8,11–13}$), 127.6 ($C^{3,6–8,11\text{-}13}$), 126.9 ($C^{3,6\text{-}8,11\text{-}13}$), 126.8 ($C^{3,6–8,11–13}$), 115.3 ($C^2$), 70.2 ($C^9$) ppm.

IR (ATR) $\tilde{\nu}$ = 3032, 2906, 1882.7, 1605, 1520, 1484, 1454, 1375, 1283, 1270, 1244, 1195, 1176, 1021, 1005, 915, 858, 824, 748, 715, 686, 623, 511, 486 cm^{-1}.

MS (FAB$^+$): *m/z* (%) = 261.1 $[M+H]^+$ (33), 260.1 $[M]^+$ (100), 107.1 $[Bn\text{-}O]^+$ (61), 91.1 $[Bn]^+$ (98).

HRMS (FAB$^+$): $C_{19}H_{16}O$ $[M+H]^+$ calc. 260.1201; found 260.1197.

NMR data of 4-(benzyloxy)-1,1'-biphenyl (**77b**) was identical to literature.[394]

9.2.2.17 4-Allyl-1-(allyloxy)-2-methoxybenzene (78a)

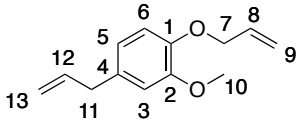

This reaction was performed by Tobias Fischer in the scope of a six-week internship under my co-supervision.

Following method B (microwave irradiation, 150 °C, 3 h), 4-Allyl-1-(allyloxy)-2-methoxybenzene (**78a**) was obtained from eugenol (**78**, 250 mg, 1.52 mmol, 1.00 eq.) and DAC (**54**, 372 mg, 2.62 mmol, 1.50 eq.) with TBAB (**50**, 97.0 mg, 300 µmol, 20.0 mol%) as catalyst. After column chromatography (*n*-hexane/ethyl acetate 20:1), product **78a** was isolated as colorless liquid (232 mg, 1.14 mmol, 75%).

TLC (*n*-hexane/ethyl acetate 9:1): R_f = 0.82.

^{1}H NMR (300 MHz, $CDCl_3$): δ = 6.83–6.80 (m, 1H, CH^3), 6.68–6.72 (m, 2H, C$H^{5,6}$), 5.89–6.15

(m, 2H, C*H*^{8,12}), 5.39 (ddt, *J* = 17.3 Hz, *J* = 1.5 Hz, *J* = 1.5 Hz, 1H, C$H_2{}^{13}$), 5.27 (dd, *J* = 10.5 Hz, *J* = 1.4 Hz, 1H, C$H_2{}^{13}$), 5.05–5.11 (m, 2H, C*H*^{8}, C$H_2{}^{9}$), 4.60 (ddd, *J* = 5.4 Hz, *J* = 1.4 Hz, *J* = 1.4 Hz, 2H, C$H_2{}^{7}$), 3.86 (s, 3H, C$H_3{}^{10}$), 3.33 (d, *J* = 6.6 Hz, 2H, C$H_2{}^{11}$) ppm.

^{13}C NMR (75 MHz, $CDCl_3$): δ = 149.5 (*C*^{2}), 146.4 (*C*^{1}), 137.7 (*C*^{8}), 133.6 (*C*^{12}), 133.1 (*C*^{4}), 120.4 (*C*^{3}), 117.8 (*C*^{9}), 115.7 (*C*^{13}), 113.7 (*C*^{6}), 112.3 (*C*^{5}), 70.1 (*C*^{7}), 55.9 (*C*^{10}), 39.9 (*C*^{11}) ppm.

IR (ATR): $\tilde{\nu}$ = 3076, 2904, 1637, 1588, 1508, 1462, 1418, 1361, 1332, 1257, 1226, 1138, 1022, 992, 913, 849, 801, 746, 656, 599 cm^{-1}.

MS (EI$^+$): *m/z* (%) = 204.2 (63) [M]$^+$, 163.1 (100) [M–Allyl]$^+$, 91.1 (36) [Bn]$^+$.

HRMS (EI$^+$): $C_{13}H_{16}O_2$ [M]$^+$ calc. 204.1144; found 204.1145.

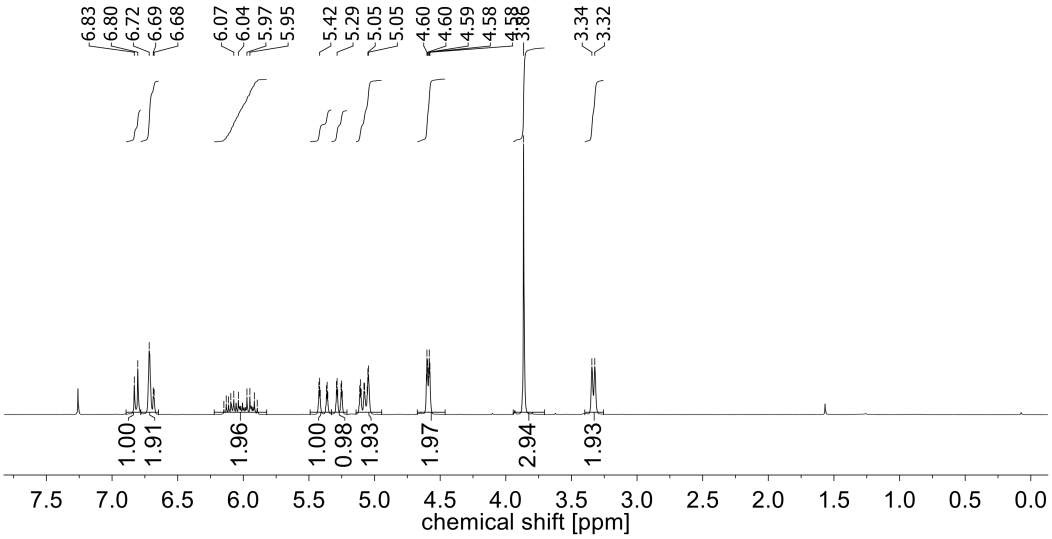

9.2.2.18 4-Allyl-1-(benzyloxy)-2-methoxybenzene (78b)

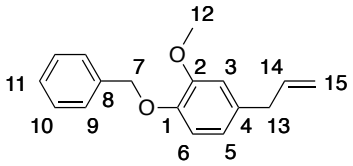

This reaction was performed by Tobias Fischer in the scope of a six-week internship under my co-supervision.

Following method B (microwave irradiation, 150 °C, 2 h), 4-Allyl-1-(benzyloxy)-2-methoxybenzene (**78b**) was obtained from eugenol (**78**, 250 mg, 1.52 mmol, 1.00 eq.) and DBC (**61**, 677 mg, 2.62 mmol, 1.50 eq.) with 1,2-dimethylimidazole (DMI, 20.0 mg, 120 µmol, 14.0 mol%) as catalyst. Remaining DBC was destroyed by stirring with LiOH (110 mg, 4.60 mmol, 3.00 eq.) in THF/water (6 mL/3 mL) for four days. After column chromatography (*n*-hexane/ethyl acetate 46:1), product **78b** was isolated as colorless liquid (336 mg, 1.29 mmol, 87%).

TLC (*n*-hexane/ethyl acetate 9:1): R_f = 0.59.

^{1}H NMR (300 MHz, $CDCl_3$): δ = 7.29–7.45 (m, 5H, C$H^{9,10,11}$), 6.65–6.83 (m, 3H, C$H^{3,5,6}$), 5.91–6.00 (m, 1H, CH^{14}), 5.05–5.13 (m, 4H, C$H_2{}^{7,15}$), 3.88 (s, 3H, CH^{12}), 3.33 (d, J = 6.0 Hz, 2H, C$H_2{}^{13}$) ppm.

^{13}C NMR (75 MHz, $CDCl_3$): δ = 149.8 (C^2), 146.7 (C^1), 137.8 (C^{14}), 137.5 (C^8) 133.5 (C^4), 128.6 (C^{10}), 127.9 (C^{11}), 127.4 (C^9), 120.6 (C^3), 115.8 (C^5), 114.4 (C^{15}), 112.6 (C^6), 71.4 (C^7), 56.1 (C^{12}), 40.0 (C^{13}) ppm.

IR (ATR): $\tilde{\nu}$ = 3000, 2932, 1744, 1636, 1588, 1508, 1452, 1417, 1379, 1333, 1257, 1223, 1154, 1137, 1023, 993, 910, 848, 803, 767, 735, 695, 652, 597, 463 cm^{-1}.

MS (EI$^+$): *m/z* (%) = 254.2 (100) $[M]^+$, 163.1 (18) $[M-Bn]^+$, 91.1 (67) $[Bn]^+$.

HRMS (EI$^+$): $C_{17}H_{18}O_2$ $[M]^+$ calc. 254.1303; found 254.1301.

NMR data of 4-allyl-1-(benzyloxy)-2-methoxybenzene (**78b**) was identical to literature.[395]

9.2.2.19 *O*-Allylvanillin (9a)

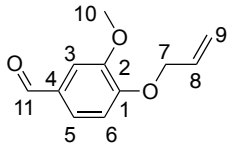

Following Method C (pressure tube, 120 °C, 5 h), *O*-allylvanillin (**9a**) was obtained from vanillin (**9**, 500 mg, 3.29 mmol, 1.00 eq.) and DAC (**54**, 1.06 g, 9.87 mmol, 3.00 eq.) with TBAB (**50**, 1.06 g, 3.29 mmol, 1.00 eq.) as base. After column chromatography (cyclohexane/ethyl acetate 10:1), product **9a** was obtained as colorless liquid (309 mg, 1.61 mmol, 49%).

TLC (cyclohexane/ethyl acetate 10:1): R_f = 0.19.

^{1}H NMR (300 MHz, $CDCl_3$): δ = 9.83 (s, 1H, CH^{11}O), 7.61 – 7.31 (m, 2H, C$H^{3,5}$), 6.96 (d, J = 8.7 Hz, 1H, CH^6), 6.07 (ddt, J = 17.2, 10.6, 5.4 Hz, 1H, CH^8), 5.42 (ddd, J = 17.3, 2.9, 1.4 Hz, 1H, C$H^{9,trans}$), 5.36 (ddd, J = 11.8, 6.7, 1.4 Hz, 2H, C$H^{9,cis}$), 4.69 (ddd, J = 5.4, 1.4, 1.4 Hz, 2H, C$H_2{}^7$), 3.92 (s, 3H, C$H_3{}^{10}$) ppm.

^{13}C NMR (75 MHz, $CDCl_3$): δ = 190.97 (C^{11}), 153.6 (C^1), 150.0 (C^2), 132.3 (C^8), 130.3 (C^4), 126.7 (C^5), 118.9 (C^9), 112.0 (C^6), 109.4 (C^3), 69.9 (C^7), 56.1 (C^{10}) ppm.

IR (ATR): $\tilde{\nu}$ = 3080, 2923, 2835, 2727, 1679, 1649, 1584, 1505, 1463, 1422, 1395, 1337, 1262, 1231, 1194, 1158, 1132, 1030, 992, 929, 865, 806, 781, 729, 660, 631, 589, 567 cm^{-1}.

MS (EI$^+$): *m/z* (%) = 192.1 $[M]^+$ (100), 151.1 $[M–allyl]^+$ (62), 95.1 (31), 77.1 (12).

HRMS (EI$^+$): $C_{11}H_{12}O_3$ $[M]^+$ calc. 192.0781; found 192.0782.

NMR data of *O*-allylvanillin (**9a**) was identical to literature.[396]

9.2.2.20 *O*-Benzylvanillin (9b)

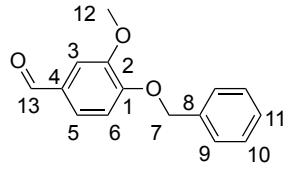

Following method A (reflux conditions, 150 °C, 17 h), *O*-benzylvanillin (**9b**) was obtained from vanillin (**9**, 500 mg, 3.29 mmol, 1.00 eq.) and DBC (**61**, 1.59 g, 6.57 mmol, 1.99 eq.) with DBU (**53**, 100 mg, 660 µmol, 20.0 mol%) as catalyst. The crude product was purified by column chromatography (*n*-hexane/ethyl acetate 60:1–10:1). The obtained mixture of benzyl alcohol and product was was separated by *kugelrohr* distillation at 110 °C and 40 mbar. Pure *O*-Benzyl-vanillin **9b** was obtained as colorless liquid (370 mg, 1.53 mmol, 47%).

TLC (*n*-hexane/ethyl acetate 9:1): R_f = 0.09.

^{1}H NMR ($CDCl_3$, 300 MHz) δ = 9.84 (s, 1H, CH^{13}), 7.40 (m, 7H, C$H^{5,6,9\text{-}11}$), 6.99 (m, 1H, CH^3), 5.25 (s, 2H, C$H_2{}^7$), 3.95 (s, 3H, C$H_3{}^{12}$) ppm.

^{13}C NMR ($CDCl_3$, 75 MHz) δ = 191.0 (C^{13}), 153.8 (C^2), 150.3 (C^1), 136.2 (C^4), 133.0 (C^{11}), 130.5 (C^8), 128.9 (C^9), 128.4 ($C^{3,5,6}$), 127.4 (C^{10}), 126.7 (C^{11}), 112.6 ($C^{3,5,6}$), 109.6 ($C^{3,5,6}$), 71.0 (C^7), 56.2 (C^{12}) ppm.

IR (ATR) $\tilde{\nu}$ = 2832, 1670, 1584, 1498, 1467, 1453, 1123, 1398, 1341, 1262, 1221, 1156, 1130, 1027, 1001, 858, 796, 775, 750, 729, 697, 642, 586, 560, 526, 475, 423 cm^{-1}.

MS (EI$^+$): *m/z* = 243.1 [M+H]$^+$ (13), 242.1 [M]$^+$ (100), 91.1 [Bn]$^+$ (18).

HRMS (EI$^+$): $C_{15}H_{14}O_3$ [M]$^+$ calc. 242.0937; found 242.0936.

NMR data of *O*-benzylvanillin (**9b**) was identical to literature.[397]

9.2.2.21 Allyl 4-(allyloxy)-3-methoxybenzoate (10a)

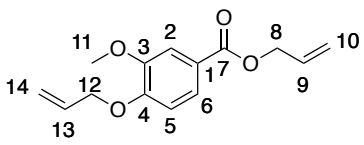

This reaction was performed by Tobias Fischer in the scope of a six-week internship under my co-supervision.

Performing method B (microwave irradiation, 130 °C, 1 h), allyl 4-(allyloxy)-3-methoxybenzoate (**10a**) was obtained from vanillic acid (**10**, 250 mg, 1.49 mmol, 1.00 eq.) and DAC (**54**, 372 mg, 4.46 mmol,

3.00 eq.) with TBAB (**50**, 192 mg, 600 µmol, 40.0 mol%) as catalyst in DMSO (0.1 mL). After column chromatography (*n*-hexane/ethyl acetate 10:1), the product **10a** was isolated as yellowish liquid (228 mg, 918 µmol, 62%).

TLC (*n*-hexane/ethyl acetate 9:1): R_f = 0.36.

^{1}H NMR (300 MHz, $CDCl_3$): δ = 7.67 (dd, J = 8.4, J = 2.0 Hz, 1H, CH^6), 7.57 (d, J = 1.8 Hz, 1H, CH^2), 6.88 (d, J = 8.5 Hz, 1H, CH^5), 5.97–6.14 (m, 2H, C$H^{9,13}$), 5.25–5.45 (m, 4H, C$H_2{}^{10,14}$), 4.80 (d, J = 4.3, 2H, C$H_2{}^8$), 4.67 (d, J = 5.4 Hz, 2H, C$H_2{}^{12}$), 3.92 (s, 3H, C$H_3{}^{11}$) ppm.

^{13}C NMR (75 MHz, $CDCl_3$): δ = 166.1 (C^7), 152.1 (C^4), 149.1 (C^3), 132.7 (C^9), 132.6 (C^{13}), 123.6 (C^6), 122.9 (C^1), 118.7 (C^{10}), 118.2 (C^{14}), 112.5 (C^2), 112.0 (C^5), 69.8 (C^{12}), 65.5 (C^8), 56.1 (C^{11}) ppm.

IR (ATR): $\tilde{\nu}$ = 3082, 2936, 1708, 1647, 1597, 1509, 1454, 1416, 1360, 1341, 1266, 1213, 1178, 1132, 1104, 981, 925, 875, 818, 782, 761, 727, 623 cm^{-1}.

MS (FAB$^+$): *m/z* (%) = 248.1 (100) [M]$^+$, 207.0 (18) [M–Allyl]$^+$, 191.0 (37) [M–Allyloxy]$^+$.

HRMS (FAB$^+$): $C_{14}H_{16}O_4$ [M]$^+$ calc. 248.1044; found 248.1043.

NMR data of allyl 4-(allyloxy)-3-methoxybenzoate (**10a**) was identical to literature.[229]

9.2.2.22 Benzyl 4-(benzyloxy)-3-methoxybenzoate (10b)

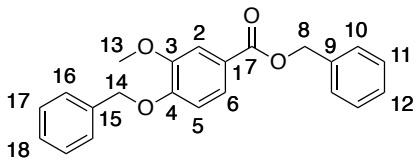

This reaction was performed by Tobias Fischer in the scope of a six-week internship under my co-supervision.

Performing mehod B (microwave irradiation, 130 °C, 1 h), benzyl 4-(benzyloxy)-3-methoxybenzoate (**10b**) was obtained from vanillic acid (**10**, 250 mg, 1.49 mmol, 1.00 eq.) and DBC (**61**, 1.08 g, 4.46 mmol, 3.00 eq.) in DMSO (1 mL), with TBAB (**50**, 192 mg, 600 µmol, 40.0 mol%) as catalyst. After column chromatography (*n*-hexane/ethyl acetate 50:1–10:1), product **10b** was isolated as yellowish solid (227 mg, 1.47 mmol, 44%).

TLC (*n*-hexan/ethyl acetate 9:1): R_f = 0.35.

DSC: T_m = 86 °C.

^{1}H NMR (300 MHz, $CDCl_3$): δ = 7.67–7.60 (m, 2H, C$H^{6,2}$), 7.45–7.31 (m, 10H, C$H^{10,11,12,16,17,18}$), 6.89 (d, J = 8.4 Hz, 1H, CH^5), 5.34 (s, 2H, C$H_2{}^8$), 5.22 (s, 2H, C$H_2{}^{14}$), 3.93 (s, 3H, C$H_3{}^{13}$) ppm.

^{13}C NMR (75 MHz, $CDCl_3$): δ = 166.3 (C^7), 152.3 (C^4), 149.3 (C^3), 136.5 (C^{15}), 136.4 (C^9), 128.8 (C^{17}), 128.7 (C^{11}), 128.3 (C^{18}), 128.2 (C^{16}), 128.2 (C^{12}), 127.3 (C^{10}), 123.9 (C^6), 123.4 (C^1), 112.7 (C^5), 112.6 (C^2), 70.9 (C^{14}), 66.7 (C^8), 56.2 (C^{13}) ppm.

IR (ATR): $\tilde{\nu}$ = 2933, 1702, 1594, 1510, 1456, 1413, 1380, 1345, 1292, 1270, 1208, 1179, 1127, 1101, 1022, 980 , 921, 872, 846, 828, 761, 743, 695, 644, 584, 533, 508, 486, 288 cm^{-1}.

MS (EI$^+$): *m/z* (%) = 348.3 $[M]^+$ (38), 91.1 (100) $[Bn]^+$.

HRMS (EI$^+$): $C_{22}H_{20}O_4$ $[M]^+$ calc. 348.1354; found 348.1356.

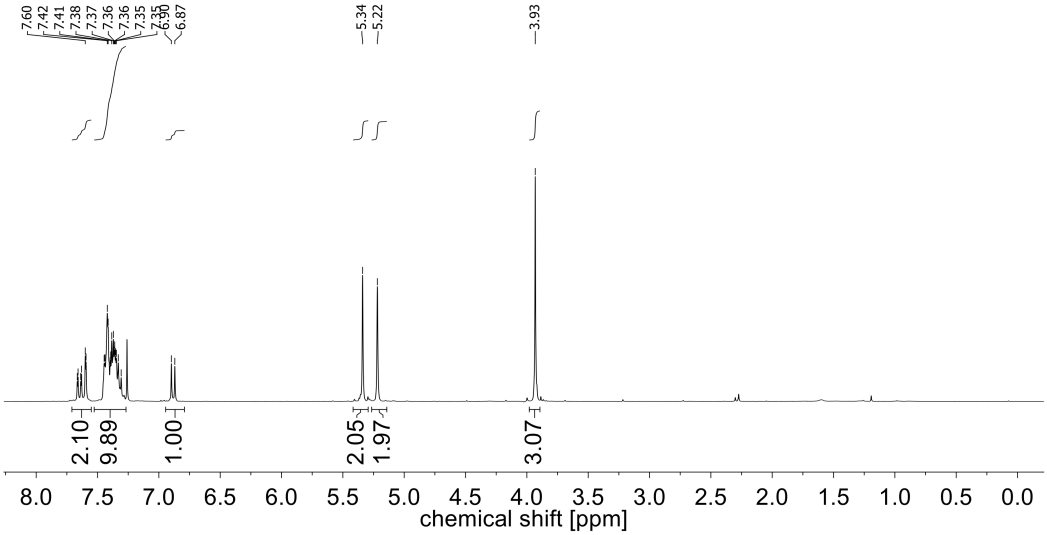

9.2.2.23 Allyl (4-(allyloxy)-3-methoxybenzyl) carbonate (79a)

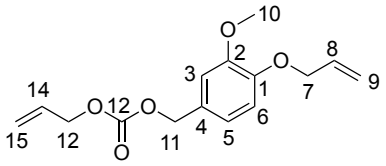

Following method A (reflux, 100 °C, 29 h), **79a** was obtained from vanillic alcohol (**79**, 500 mg, 3.2 mmol, 1.00 eq.) and DAC (**54**, 9.09 g, 64 mmol, 20.0 eq.). After column chromatography (cyclohexane/ethyl acetate 100:1), compound **79a** was obtained as colorless liquid (286 mg, 1.03 mmol, 32%).

TLC (cyclohexane/ethyl acetate 9:1): R_f = 0.37.

^{1}H NMR ($CDCl_3$, 300 MHz) δ = 7.06 – 6.72 (m, 3H, C$H^{3,5,6}$), 6.28 – 5.69 (m, 2H, C$H^{8,14}$), 5.62 – 5.14 (m, 1H, C$H^{9,15}$), 5.10 (s, 2H, CH^{11}), 4.81 – 4.41 (m, 4H, C$H^{7,12}$), 3.88 (s, 3H, CH^{10}) ppm.

^{13}C NMR ($CDCl_3$, 75 MHz) δ = 155.1 (C^{12}), 149.6 ($C^{1,2}$), 148.4 ($C^{1,2}$), 133.3 ($C^{8,14}$), 131.7 ($C^{8,14}$), 128.1 (C^4), 121.5 (C^5), 119.0 ($C^{9,15}$), 118.2 ($C^{9,15}$), 113.2 (C^6), 112.3 (C^3), 70.0 (C^{11}) 69.9 ($C^{7,12}$), 68.7 ($C^{7,12}$), 56.1 (C^{10}) ppm.

IR (ATR) $\tilde{\nu}$ = 3085, 2940, 1740, 1649, 1607, 1592, 1514, 1454, 1422, 1384, 1360, 1335, 1227, 1164, 1140, 1019, 994, 928, 853, 805, 790, 765, 630, 553 cm^{-1}.

MS (FAB$^+$): *m/z* = 279.1 $[M+H]^+$ (15), 278.1 $[M]^+$ (74), 178.1 (15), 177.1 $[M–CH_2CHCH_2OCOO]^+$ (100), 137.1 (16).

HRMS (EI$^+$): $C_{15}H_{18}O_5$ $[M]^+$ calc. 278.1149; found 278.1150.

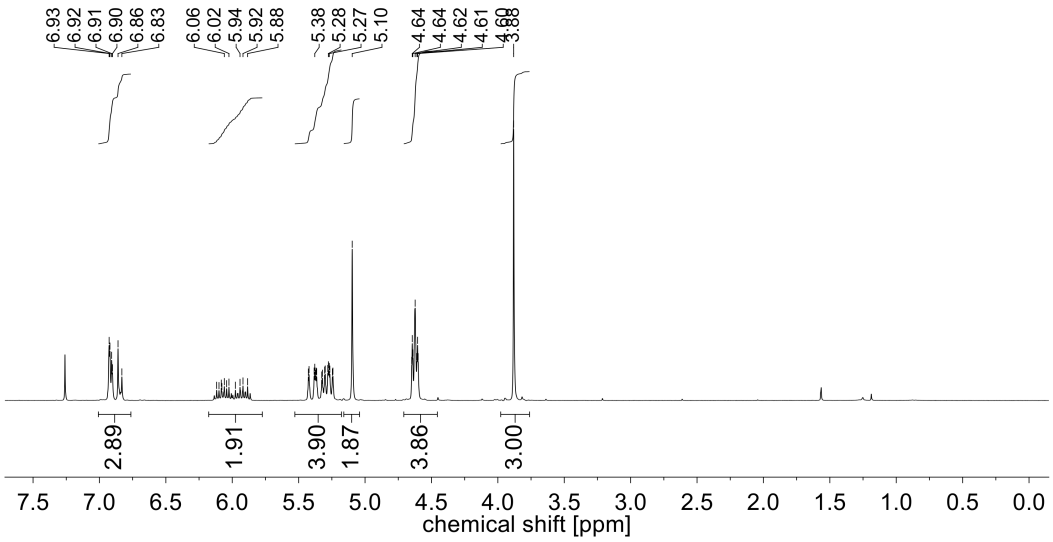

9.2.3 General procedure for the allylation of diols

A pressure tube heated to 120 °C was charged with the bisphenol (4.00 mmol, 1.00 eq.) and DAC (**54**, 3.41 g, 24.0 mmol, 6.00 eq.). If the bisphenol was not completely soluble, up to 18.0 eq. DAC were used. TBAB (**50**, 1.29 g, 4.00 mmol, 1.00 eq.) was added at 120 °C and the solution was stirred at this temperature for 20 h. After cooling to room temperature, the compound was extracted with ethyl acetate (30 mL) and washed with water (2×20 mL). TBAB (**50**, 1.21 g, 3.76 mmol, 94%) was recovered from the aqueous phase by evaporation of the water. The organic layer was further washed with aqueous 1 M hydrochloric (20 mL) and saturated sodium chloride solution (20 mL), then dried over magnesium sulfate, filtered and concentrated under reduced pressure. The crude product was purified by column chromatography using a *n*-hexane/ethyl acetate gradient.

9.2.3.1 Synthesis of (*E*)-1,2-bis(4-(allyloxy)-3-methoxyphenyl)ethene (82a)

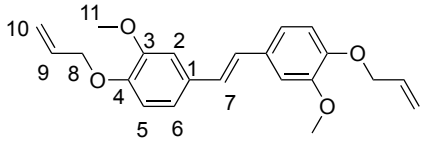

This reaction was performed by Sven Riegsinger in the scope of his bachelor thesis under my co-supervision.

Following the general procedure, (*E*)-1,2-bis(4-(allyloxy)-3-methoxyphenyl)ethene (**82a**) was synthesized starting from (*E*)-4,4'-dihydroxy-3,3'-dimethoxystilbene (**82**, 1.09 g, 4.00 mmol, 1.00 eq.) and isolated as colorless solid (1.18 g, 3.35 mmol, 84%).

TLC (*n*-hexane/ethyl acetate 3:1): R_f = 0.42.

DSC: T_m = 141–142 °C.

^{1}H NMR ($CDCl_3$, 300 MHz, 25 °C): δ = 7.06 (d, *J* = 1.8 Hz, 2H, C*H*^{2}), 7.00 (dd, *J* = 8.3, *J* = 1.9 Hz, 2H, C*H*^{6}), 6.92 (s, 2H, C*H*^{7}), 6.86 (d, *J* = 8.3 Hz, 2H, C*H*^{5}), 6.10 (ddt, *J* = 17.2 Hz, *J* = 10.5 Hz, *J* = 5.4 Hz, 2H, =C*H*^{9}-R), 5.41 (dd, *J* = 17.3 Hz, *J* = 1.5 Hz, 2H, =C*H*^{10,trans}), 5.29 (dd, *J* = 10.5 Hz, *J* = 1.3 Hz, 2H, =C*H*^{10,cis}), 4.63 (ddd, *J* = 5.4 Hz, *J* = 1.3 Hz, *J* = 1.3 Hz, 4H, =CH_2^8), 3.93 (s, 6H, CH_3^{11}) ppm.

^{13}C NMR ($CDCl_3$, 75 MHz, 25 °C): δ = 149.6 (*C*^{3}), 147.7 (*C*^{4}), 133.3 (*C*^{9}), 131.0 (*C*^{1}), 126.7 (*C*^{7}), 119.4 (*C*^{6}), 118.1 (*C*^{10}), 113.41 (*C*^{5}), 109.0 (*C*^{2}), 69. 9 (*C*^{8}), 55.9 (*C*^{11}) ppm.

IR (ATR): $\tilde{\nu}$ = 2838, 1836, 1646, 1582, 1468, 1455, 1421, 1410, 1383, 1336, 1290, 1226, 1180, 1135, 1033, 989, 959, 915, 852, 801, 727, 634, 614, 574, 551, 463, 441 cm^{-1}.

MS (EI$^+$): *m/z* (%) = 353.1 [M+H]$^+$ (45), 352.1 [M]$^+$ (100), 311.0 [M-allyl]$^+$ (50).

HRMS (EI$^+$): $C_{22}H_{24}O_4$ [M]$^+$ calc. 352.1669; found: 352.1671.

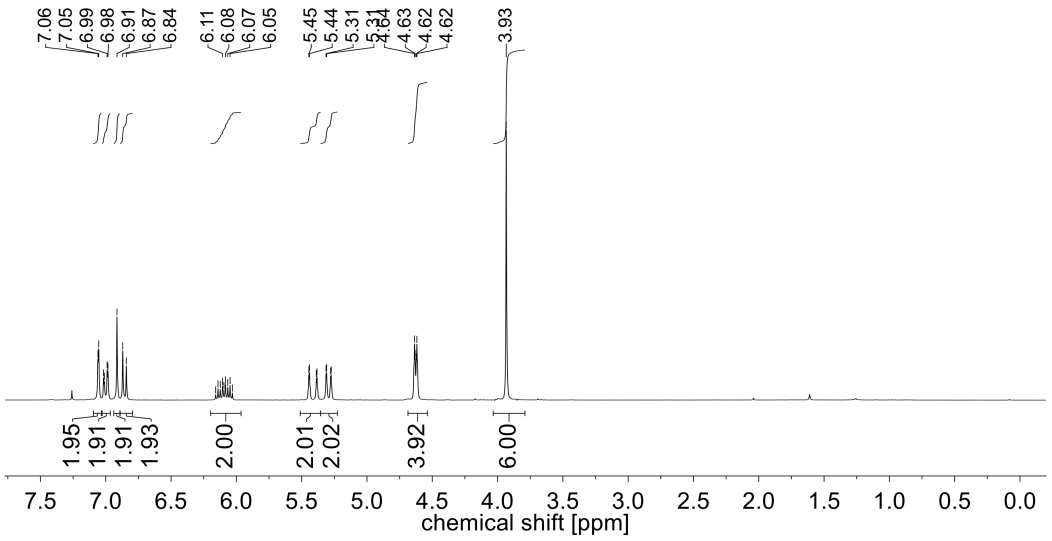

9.2.3.2 Synthesis of (*E*)-1,2-bis(3-(allyloxy)phenyl)ethene (83a)

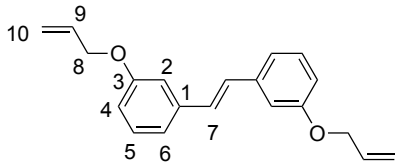

This reaction was performed by Sven Riegsinger in the scope of his bachelor thesis under my co-supervision.

Following the general procedure, (*E*)-1,2-bis(3-(allyloxy)phenyl)ethene (**83a**) was synthesized starting from (*E*)-3,3'-hydroxystilbene (**83**, 800 mg, 3.77 mmol, 1.00 eq.) and isolated as yellowish liquid (1.02 g, 3.49 mmol, 93%).

TLC (*n*-hexane/ethyl acetate 8:1): R_f = 0.56.

^{1}H NMR ($CDCl_3$, 300 MHz, 25 °C): δ = 7.30–7.25 (m, 2H, CH^5), 7.13–7.06 (m, 6H, C$H^{2,6,7}$), 6.84 (d, $J_{H4\text{-}H5}$= 8.1 Hz, 2H, CH^4), 6.10 (ddt, J = 17.2 Hz, J = 10.5 Hz, J = 5.3 Hz, 2H, =CH^9), 5.45 (d, J = 17.3 Hz, 2H, =C$H^{10,trans}$), 5.32 (d, J = 10.5 Hz, 2H, =C$H^{10,cis}$), 4.59 (d, $J_{H8\text{-}H9}$ = 5.2 Hz, 4H, C$H_2{}^8$) ppm.

^{13}C NMR ($CDCl_3$, 75 MHz, 25 °C): δ = 159.1 (C^3), 138.8 (C^1) 133.4 (C^9), 129.8 (C^5) 129.0 (C^7), 119.6 (C^{10}), 117.9 (C^2) 114.3 (C^6), 112.8 (C^4) 69.0 (C^8) ppm.

IR (ATR): $\tilde{\nu}$ = 3024, 2860, 1648, 1596, 1576, 1487, 1443, 1421, 1314, 1263, 1156, 1027, 992, 957, 923, 858, 776, 691, 569, 538, 460 cm^{-1}.

MS (EI$^+$): *m/z* (%) = 293.1 [M+H]$^+$ (100), 292.1 [M]$^+$ (95), 252.1 [M-allyl]$^+$ (15).

HRMS (EI$^+$): $C_{20}H_{20}O_2$ [M]$^+$ calc. 292.1536; found: 292.1537.

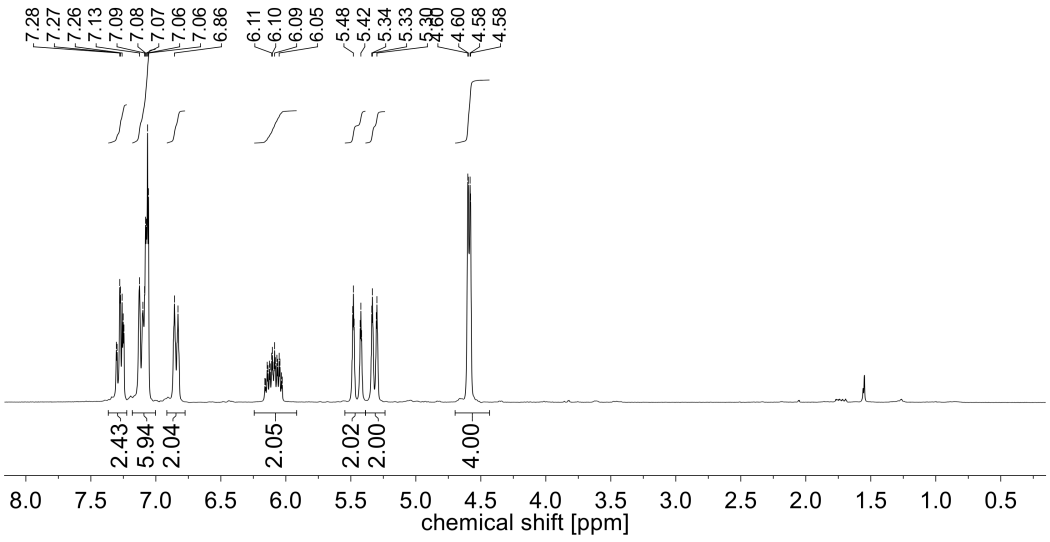

9.2.3.3 Synthesis of 1,2-bis(4-(allyloxy)-3-methoxyphenyl)ethane (84a)

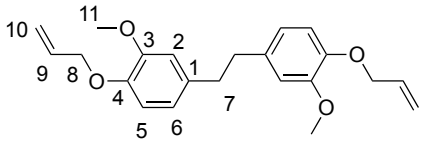

This reaction was performed by Sven Riegsinger in the scope of his bachelor thesis under my co-supervision.

Following the general procedure, 1,2-bis(4-(allyloxy)-3-methoxyphenyl)ethane (**84a**) was synthesized starting from 4,4'-dihydroxy-3,3'-dimethoxy-diphenylethane (**84**, 1.10 g, 4.00 mmol, 1.00 eq.) and isolated as colorless solid (1.25 g, 3.53 mmol, 89%).

TLC (*n*-hexane/ethyl acetate 3:1): R_f = 0.51.

DSC: T_m = 92 °C.

^{1}H NMR ($CDCl_3$, 300 MHz, 25 °C): δ = 6.80 (d, J = 8.3 Hz, 2H, CH^6), 6.68 (d, J = 7.3 Hz, 2H, CH^5), 6.66 (s, 2H, CH^2), 6.09 (ddt, J = 17.1 Hz, J = 10.6 Hz, J = 5.4 Hz, 2H, CH^9), 5.40 (dd, J = 17.3, 1.2 Hz, 2H, =C$H^{10,trans}$), 5.27 (dd, J = 10.5, 0.9 Hz, 2H, =C$H^{10,cis}$), 4.59 (d, J = 5.4 Hz, 4H, C$H_2{}^8$), 3.83 (s, 6H, C$H_3{}^{11}$), 2.84 (s, 4H, C$H_2{}^7$) ppm.

^{13}C NMR ($CDCl_3$, 75 MHz, 25 °C): δ = 149.4 (C^3), 146.3 (C^4) 135.0 (C^1), 133.7 (C^9), 120.4 (C^5), 117.9 (C^{10}), 113.7 (C^6), 112.47 (C_2), 70.2 (C^8), 56.0 (C^{11}), 37.8 (C^7) ppm.

IR (ATR): = 2996, 2932, 2859, 1589, 1509, 1466, 1414, 1362, 1330, 1260, 1223, 1162, 1133, 1010, 993, 935, 844, 803, 755, 653, 628, 590, 545, 457, 417 cm^{-1}.

MS (EI$^+$): *m/z* (%) = 354.2 [M]$^+$ (100), 355.2 [M+H]$^+$ (40), 177.1 [M]$^{2+}$ (90).

HRMS (EI$^+$): $C_{22}H_{26}O_4$ [M]$^+$ calc. 354.1826; found: 354.1827.

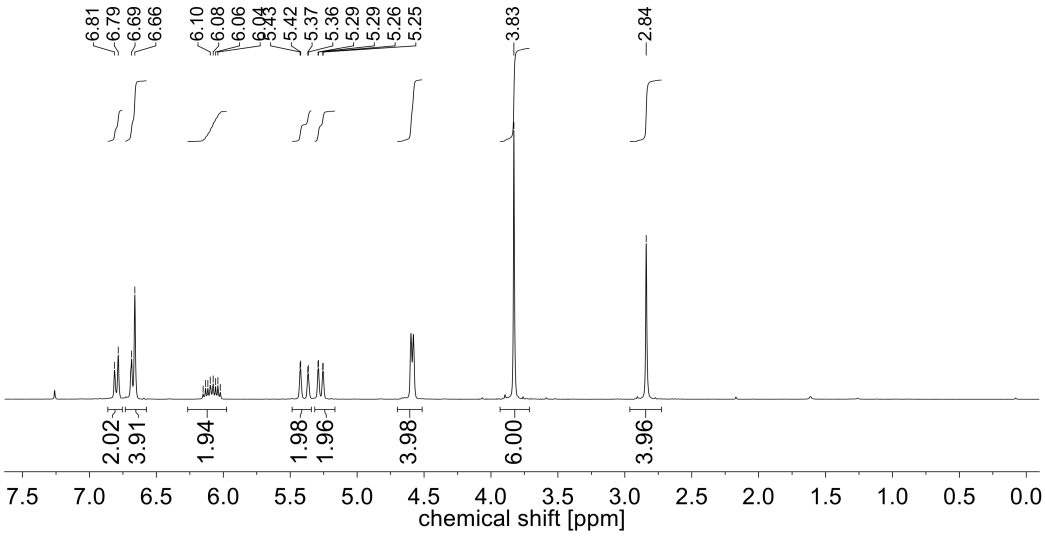

9.2.3.4 Synthesis of 1,2-bis(3-(allyloxy)phenyl)ethane (85a)

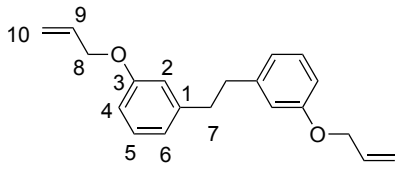

This reaction was performed by Sven Riegsinger in the scope of his bachelor thesis under my co-supervision.

Following the general procedure, 1,2-bis(3-(allyloxy)phenyl)ethane (**85a**) was synthesized starting from 3,3'-dihydroxy-diphenylethane (**85**, 1.00 g, 4.67 mmol, 1.00 eq.) and isolated as colorless liquid (1.29 g, 4.39 mmol, 94%).

TLC (*n*-hexane/ethyl acetate 8:1): R_f = 0.61.

^{1}H NMR ($CDCl_3$, 300 MHz, 25°C): δ = 7.27 (dd, J = 8.8, 7.6 Hz, 2H, CH^5), 6.94–6.76 (m, 6H, CH6, CH4, CH^2), 6.13 (ddt, J = 17.0, 10.5, 5.3 Hz, 2H, =CH^9-R), 5.49 (dd, J = 17.3, 1.5 Hz, 2H, =C$H^{10,trans}$), 5.36 (dd, J = 10.5, 1.4 Hz, 2H, =C$H^{10,cis}$), 4.58 (d, J = 5.3 Hz, 4H, C$H_2{}^8$), 2.97 (s, 4H, C$H_2{}^7$) ppm.

^{13}C NMR ($CDCl_3$, 75 MHz, 25°C): δ = 158.7 (C^3), 143.4 (C^1), 133.5 (C^9), 129.4 (C^5), 121.1 (C^6), 117.6 (C^{10}), 115.1 (C^2), 112.2 (C^4), 68.8 (C^8), 37.9 (C^7) ppm.

IR (ATR): $\tilde{\nu}$ = 3018, 2915, 2858, 1649, 1581, 1485, 1444, 1421, 1255, 1253, 1024, 991, 921, 870, 775, 692, 670, 666, 573, 461 cm^{-1}.

MS (EI$^+$): *m/z* (%)= 294.2 [M]$^+$ (100), 293.1, 147.1 [M]$^{2+}$ (55).

HRMS (EI$^+$): $C_{20}H_{22}O_2$ [M]$^+$ calc. 294.1614; found: 294.1613.

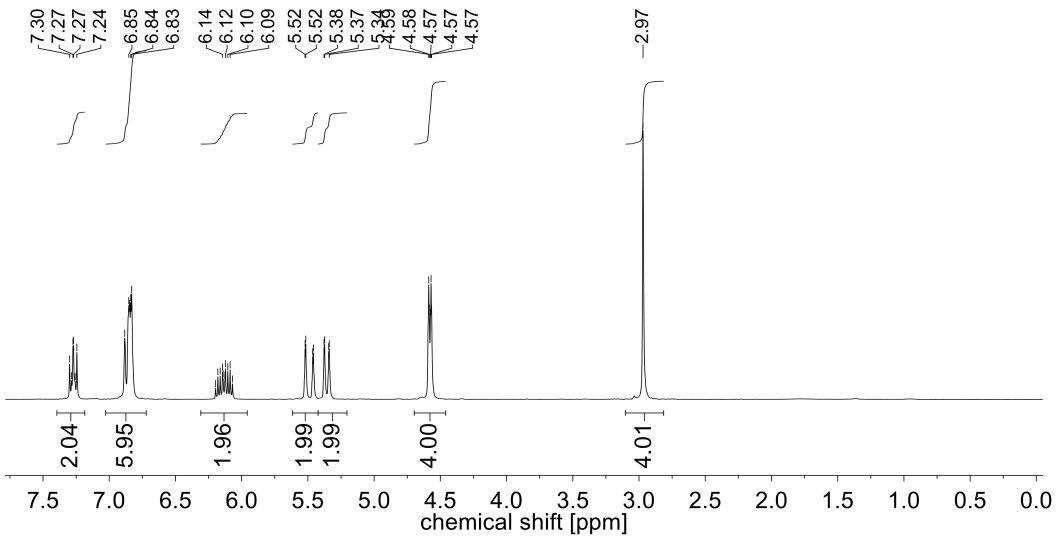

9.2.4 General procedure for the polycarbonate synthesis

A 30 mL radleys carousel tube was charged with the bisphenol (900 µmol, 1.00 eq.), diphenyl carbonate (193 mg, 900 µmol, 1.00 eq.) and lithium hydroxide (1.10 mg, 46.0 µmol, 5.00 mol%) under argon atmosphere. The mixture was reacted at 180 °C for 24 hours and quenched by cooling to rt and addition of THF (3 mL). The polymer was precipitated in cold methanol (30 mL), filtered and dried over diphosphorous pentoxide at 10^{-3} mbar for 24 h.

9.2.4.1 Polycarbonate of (*E*)-1,2-bis(4-(allyloxy)-3-methoxyphenyl)ethene (PC82)

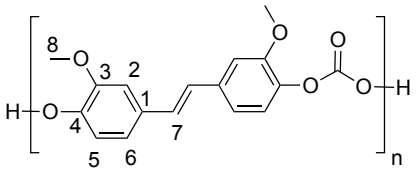

Following the general procedure for the polycarbonates, **PC82** was obtained from (*E*)-1,2-bis(4-(allyloxy)-3-methoxyphenyl)ethane (**82**, 245 mg, 900 µmol) and isolated as colorless solid (181 mg, 74 wt% based on the diol).

SEC (THF): M_n = 2800 g mol^{-1} ($Đ$ = 2.0).

DSC: T_m = 146–148 °C; T_g = 127 °C.

TGA : $T_{d\,5\%}$ = 305 °C.

^{1}H NMR (300 MHz, DMSO-d_6): δ = 7.46–6.77 (m, 8H, C$H^{2,5,6,7}$), 3.95–3.84 (m, 6H, CH^8) ppm.

IR (ATR): $\tilde{\nu}$ = 1778, 1600, 1507, 1416, 1301, 1264, 1222, 1185, 1148, 1106, 1033, 954, 875, 845, 808, 766, 730, 687, 633, 548, 463 cm^{-1}.

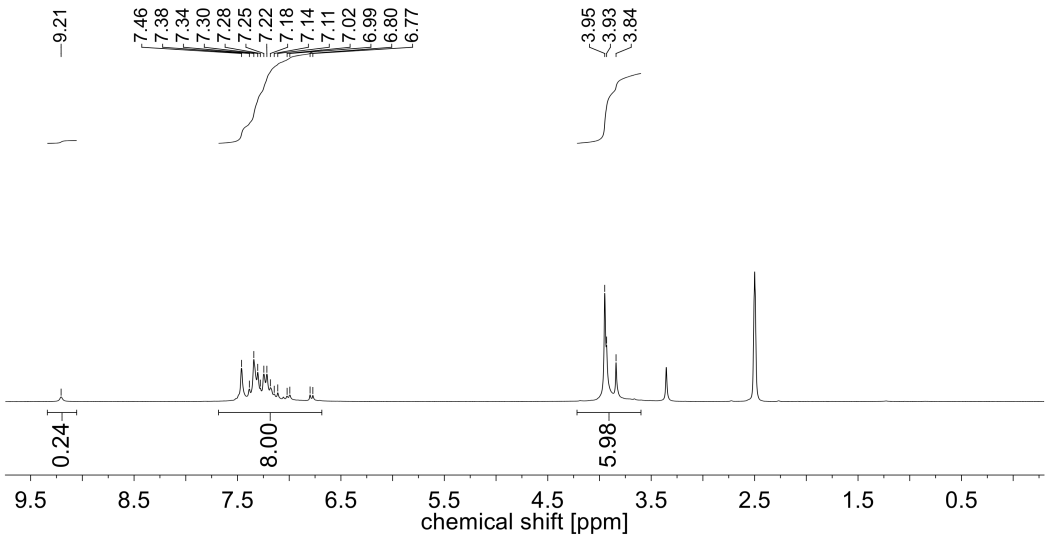

9.2.4.2 Polycarbonate of (*E*)-1,2-bis(3-(allyloxy)phenyl)ethene and diphenyl carbonate (PC83)

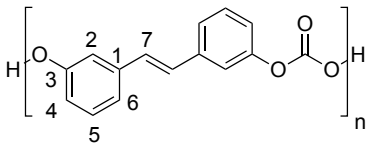

Following the general procedure for the polycarbonates, **PC83** was obtained from (*E*)-1,2-bis(3-(allyloxy)phenyl)ethane (**83**, 191 mg, 901 µmol) and isolated as grey solid (154 mg, 81 wt% based on the diol). The product was not soluble for SEC or NMR analysis.

DSC: T_m = 258–262 °C; T_g = 160 °C.

TGA : $T_{d\,5\%}$ = 313 °C.

IR (ATR): $\tilde{\nu}$ = 3019, 1763, 1573, 1487, 1438, 1244, 1205, 1137, 997, 962, 929, 880, 783, 759, 730, 686, 590, 546, 516, 458 cm^{-1}.

9.2.4.3 Polycarbonate of 1,2-bis(4-(allyloxy)-3-methoxyphenyl)ethane and diphenyl carbonate (PC84)

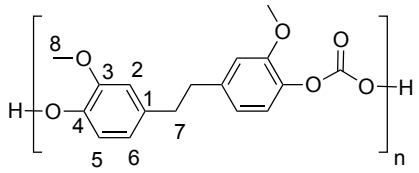

Following the general procedure for the polycarbonates, **PC84** was obtained from 1,2-bis(4-(allyloxy)-3-methoxyphenyl)ethane (**84**, 247 mg, 901 µmol) and isolated as colorless solid (204 mg, 83 wt% based on the diol).

SEC (THF): M_n = 3500 g mol^{-1} ($Đ$ = 1.5).

DSC: T_m = 106–108 °C; T_g = 81 °C.

TGA : $T_{d\,5\%}$ = 319 °C.

^{1}H NMR (300 MHz, DMSO-d_6): δ = 7.50–6.60 (m, 6H, C$H^{2,5,6}$), 3.81 (s, 6H, CH^8), 2.91 (s, 4H, CH^7) ppm.

IR (ATR): $\tilde{\nu}$ = 2940, 1774, 1598, 1507, 1458, 1416, 1282, 1233, 1185, 1143, 1112, 1033, 997, 851, 814, 766, 633, 547, 463 cm^{-1}.

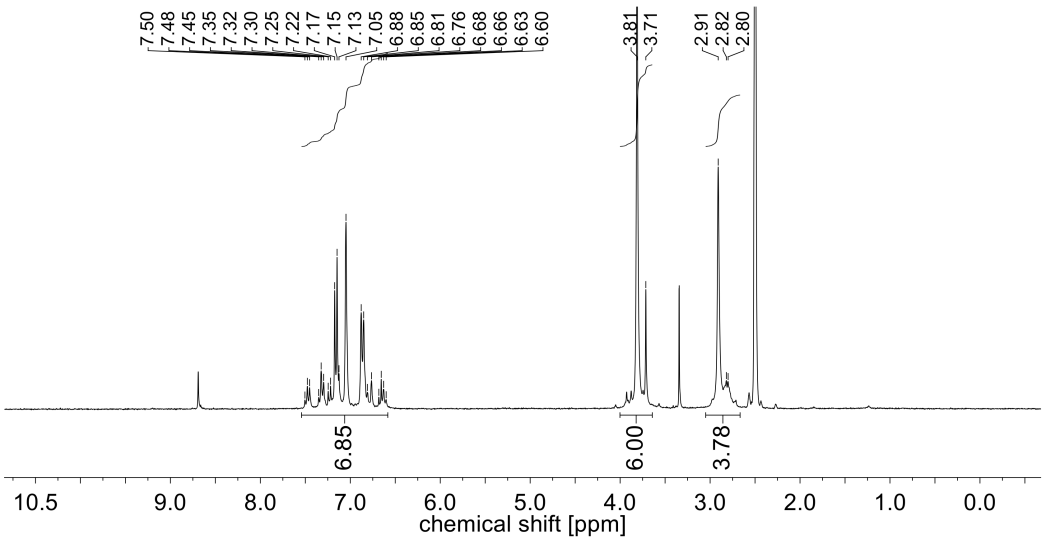

9.2.4.4 Polycarbonate of 1,2-bis(3-(allyloxy)phenyl)ethane and diphenyl carbonate (PC85)

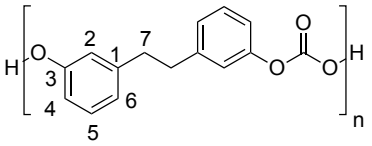

Following the general procedure for the polycarbonates, **PC85** was obtained from 1,2-bis(3-(allyloxy)-phenyl)ethane (**85**, 193 mg, 901 µmol) and isolated as colorless solid (58 mg, 35 wt% based on the diol).

SEC (THF): M_n = 2200 g mol^{-1} ($Đ$ = 1.6).

DSC: T_m = 143–146 °C; T_g = 25 °C.

TGA: $T_{d\,5\%}$ = 292 °C.

^{1}H NMR (300 MHz, DMSO-d_6): δ = 7.36–6.56 (m, 8H, C$H^{2,4,5,6}$), 2.94–2.82 (m, 4H, CH^7) ppm.

IR (ATR): $\tilde{\nu}$ = 2933, 1762, 1617, 1585, 1483, 1444, 1208, 1129, 1078, 1000, 921, 878, 768, 681, 551, 445 cm^{-1}.

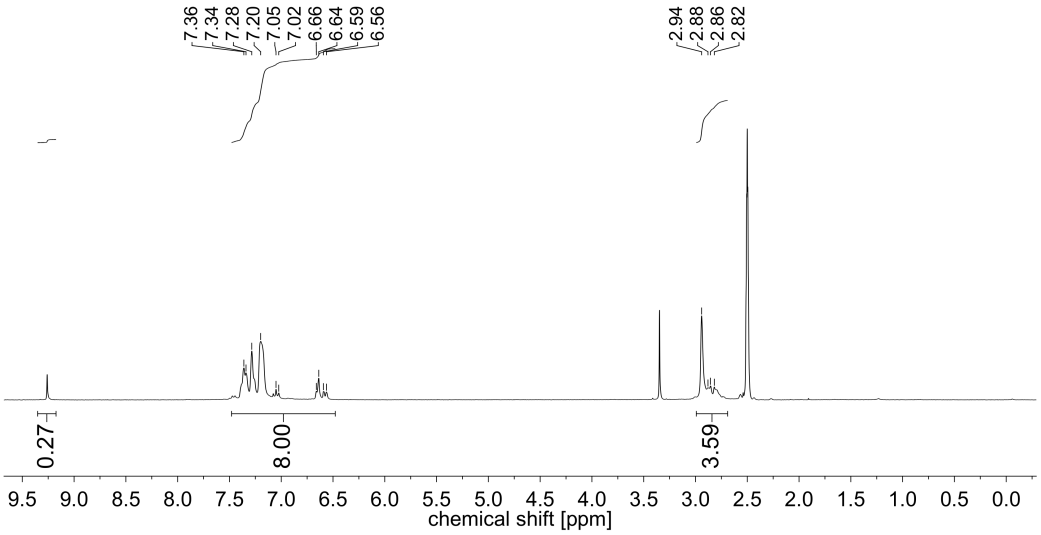

9.2.4.5 Polycarbonate of 4,4'-(propane-2,2-diyl)bis((allyloxy)benzene) and diphenyl carboante (PC14)

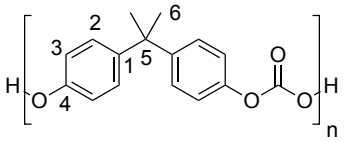

Following the general procedure for the polycarbonates, **PC14** was obtained from 4,4'-(propane-2,2-diyl)bis((allyloxy)benzene) (BPA, **14**, 206 mg, 902 µmol) and isolated as colorless solid (154 mg, 76 wt%). The product was not soluble for SEC or NMR analysis.

DSC: T_m = 280–290 °C; T_g = 115 °C.

TGA: $T_{d\,5\%}$ = 332 °C.

SEC (THF): M_n (after 3.5 hours) = 3000 g mol^{-1} ($Đ$ = 2.9).

IR (ATR): $\tilde{\nu}$ = 2967, 1767, 1594, 1503, 1406, 1361, 1229, 1192, 1157, 1105, 1078, 1012, 883, 825, 766, 711, 555 cm^{-1}.

9.2.5 General procedure for the thiol-ene polymerization

A 10 mL pressure tube was charged with the diallyl compound and an equimolar amount of decane dithiol under argon atmosphere. After stirring at 50 °C for 10 min, AIBN (2.8 mg, 17.0 µmol, 2.50 mol%) was added and the resulting mixture was heated at 75 °C for five hours. The mixture was then dissolved in THF (2 mL) and the polymer was precipitated in cold methanol (30 mL), filtered and dried over diphosphorous pentoxide at 10^{-3} mbar for 24 hours.

9.2.5.1 Thiol-ene polymer of (*E*)-1,2-bis(4-(allyloxy)-3-methoxyphenyl)ethene (PTE82)

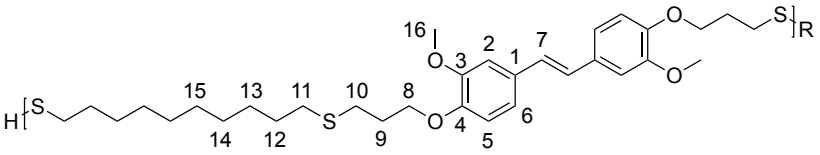

Following the general procedure for the thiol-ene polymerization, **PTE82** was obtained from (*E*)-1,2-bis(4-(allyloxy)-3-methoxyphenyl)ethane (**82a**, 247 mg, 701 µmol, 1.00 eq.) and decane dithiol (**87**, 146 mg, 707 µmol, 1.01 eq.) and isolated as yellow solid (260 mg, 66 wt% compared to used diene + dithiol). Additional THF (400 µL) was necessary as solvent as the monomer **82a** melts at 141 °C.

SEC (THF): M_n = 2700 g mol^{-1} ($Đ$ = 1.7).

DSC: T_m = 25–50 °C.

TGA : $T_{d\ 5\%}$ = 301 °C.

^{1}H NMR (300 MHz, $CDCl_3$): δ = 7.05 (d, J = 1.3 Hz, 2H, CH^7), 7.04–7.00 (m, 2H, C$H^{5,6}$), 6.92 (s, 2H), 6.90–6.85 (m, 2H, CH^2), 6.15–6.04 (m, 0.6H, C$H_{\text{allyl end group}}$), 5.45–5.29 (m, 1.2H, C$H_{\text{allyl end group}}$), 4.64 (d, J = 5.4 Hz, 1.1H, C$H_{\text{allyl end group}}$), 4.14 (t, J = 6.2 Hz, 3H, C$H_2{}^8$), 3.92 (s, 6H, C$H_3{}^{16}$), 2.72 (t, J = 7.0 Hz, 3H, C$H_2{}^{10}$), 2.53 (t, J = 7.2 Hz, 4H, C$H_2{}^{11}$), 2.17–2.08 (m, 3H, C$H_2{}^9$), 1.63–1.54 (m, 5H, CH^{alkyl}), 1.42-1.27 (m, 15H, CH^{alkyl}) ppm.

IR (ATR): $\tilde{\nu}$ = 2923, 2847, 1588, 1508, 1464, 1421, 1329, 1261, 1245, 1213, 1126, 1026, 950, 923, 839, 799, 723, 632, 544, 453 cm^{-1}.

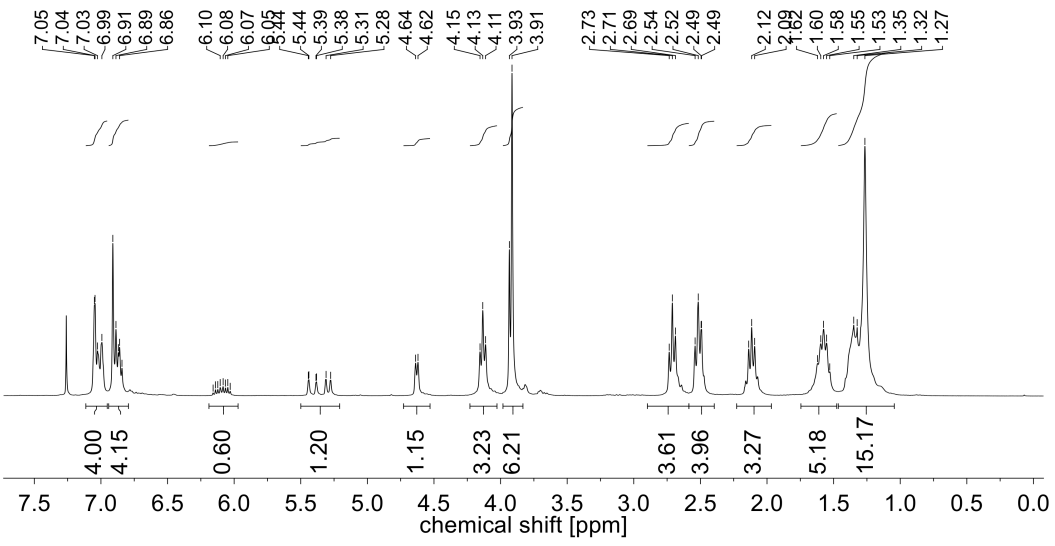

9.2.5.2 Thiol-ene polymer of (*E*)-1,2-bis(3-(allyloxy)phenyl)ethene (PTE83)

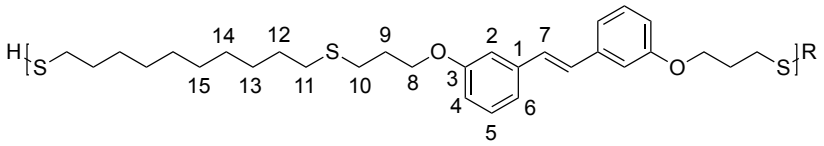

Following the general procedure for the thiol-ene polymerization, **PTE83** was obtained from (*E*)-1,2-bis(3-(allyloxy)phenyl)ethane (**83a**, 208 mg, 712 µmol, 1.00 eq.) and and decane dithiol (**87**, 148 mg, 718 µmol, 1.01 eq.) and isolated as colorless solid (220 mg, 62 wt% based on the diene and dithiol).

SEC (THF): M_n = 3100 g mol^{-1} ($Đ$ = 7.1).

DSC: T_m = 25–50 °C.

TGA : $T_{d\,5\%}$ = 316 °C.

^{1}H NMR (300 MHz, $CDCl_3$): δ = 7.27 (t, J = 7.8 Hz, 2H, CH^4), 7.11–7.06 (m, 6H, C$H^{2,5,6}$), 6.83–6.81 (m, 2H, CH^7), 4.11 (t, J = 5.9 Hz, 4H. C$H_2{}^8$), 2.73 (t, J = 7.1 Hz, 4H, C$H_2{}^{10}$), 2.54 (t, J = 7.4 Hz, 4H, C$H_2{}^{11}$), 2.13–2.04 (m, 4H, C$H_2{}^9$), 1.64–1.55 (m, 4H, C$H_2{}^{12}$), 1.42–1.28 (m, 12H, CH^{alkyl}) ppm.

IR (ATR): $\tilde{\nu}$ = 2918, 2843, 1603, 1576, 1484, 1440, 1389, 1321, 1273, 1245, 1158, 1066, 1030, 950, 859, 771, 716, 687, 616, 536, 465 cm^{-1}.

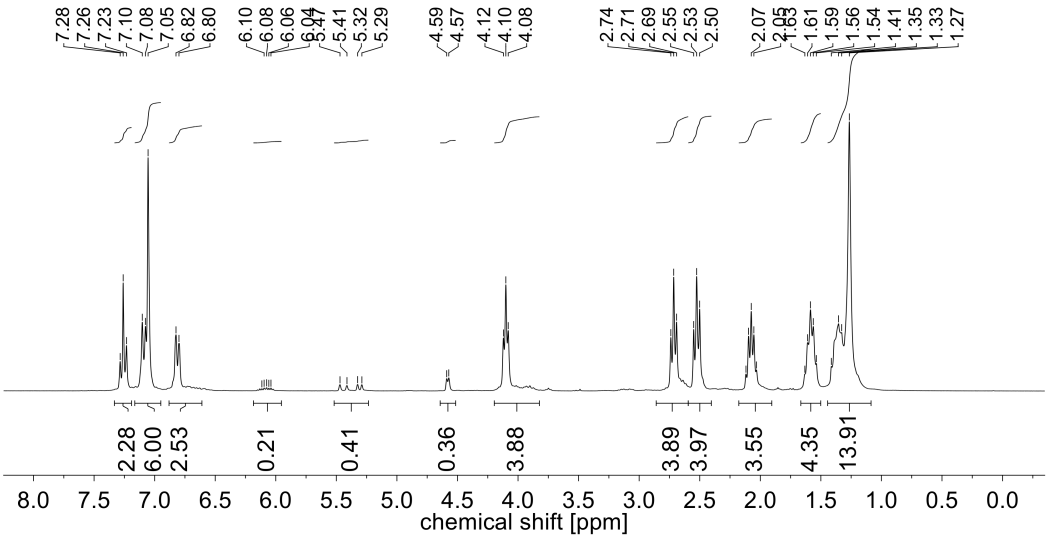

9.2.5.3 Thiol-ene polymer of 1,2-bis(4-(allyloxy)-3-methoxyphenyl)ethane (PTE84)

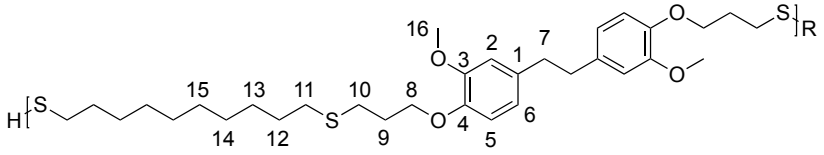

Following the general procedure for the thiol-ene polymerization, **PTE84** was obtained from 1,2-bis(4-(allyloxy)-3-methoxyphenyl)ethane (**84a**, 248 mg, 701 µmol) and decane dithiol (**87**, 146 mg,

707 µmol, 1.01 eq.) and isolated as colorless solid (320 mg, 81 wt% based on the diene and dithiol).

SEC (THF): M_n = 4300 g mol^{-1} ($Đ$ = 3.0).

DSC: T_m = 25–50 °C.

TGA : $T_{d\,5\%}$ = 336 °C.

^{1}H NMR (300 MHz, $CDCl_3$): δ = 6.82 (d, J = 8.0 Hz, 2H, CH^5), 6.70–6.67 (m, 4H, C$H^{2,6}$), 4.10 (t, J = 6.3 Hz, 4H, C$H_2{}^8$), 3.82 (s, 6H, C$H_3{}^{16}$), 2.84 (s, 4H, C$H_2{}^7$), 2.71 (t, J = 6.9 Hz, 4H, C$H_2{}^{10}$), 2.52 (t, J = 7.2 Hz, 4H, C$H_2{}^{11}$), 2.15–2.08 (m, 4H, C$H_2{}^9$), 1.63–1.54 (m, 4H, C$H_2{}^{12}$), 1.41–1.28 (m, 12H, CH^{alkyl}) ppm.

IR (ATR): $\tilde{\nu}$ = 2923, 2847, 1584, 1513, 1457, 1416, 1329, 1261, 1237, 1225, 1129, 1026, 923, 851, 795, 767, 752, 728, 636, 592, 540, 457 cm^{-1}.

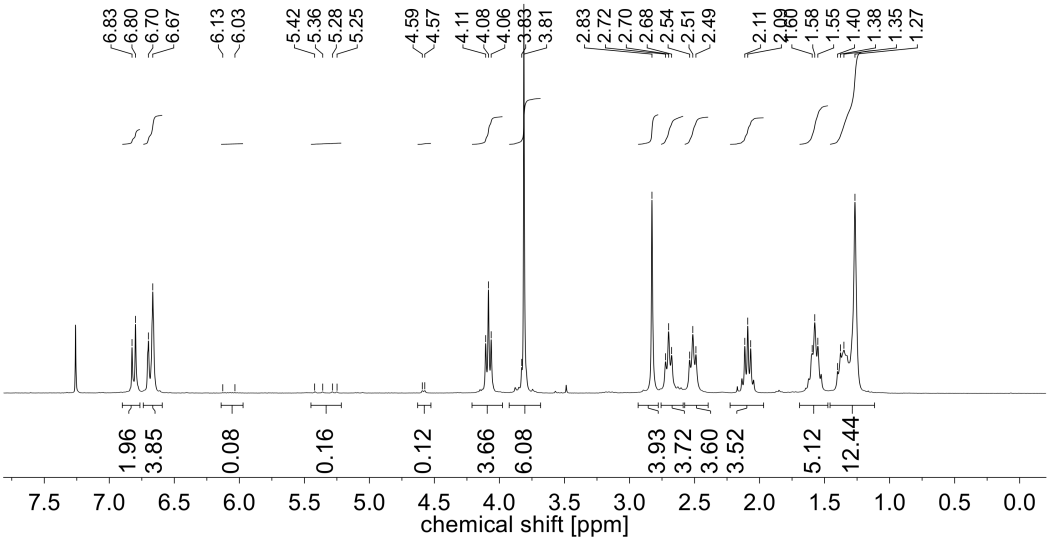

9.2.5.4 Thiol-ene polymer of 1,2-bis(3-(allyloxy)phenyl)ethane (PTE85)

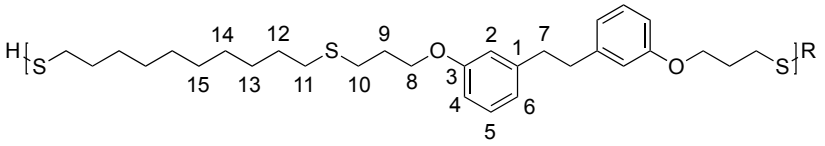

Following the general procedure for the thiol-ene polymerization, **PTE85** was obtained from 1,2-bis(3-(allyloxy)phenyl)ethane (**85a**, 206 mg, 701 µmol) and decane dithiol (**87**, 145 mg, 701 µmol, 1.00 eq.) and isolated as colorless solid (290 mg, 83 wt% based on the diene and dithiol).

SEC (THF): M_n = 16600 g mol^{-1} ($Đ$ = 5.3).

DSC: T_m = 25–50 °C.

TGA : $T_{d\,5\%}$ = 311 °C.

^{1}H NMR (300 MHz, $CDCl_3$): δ = 7.22–7.17 (m, 2H,CH^5), 6.80–6.74 (m, 6H, C$H^{2,4,6}$), 4.04 (t, J = 6.1 Hz, 4H, C$H_2{}^8$), 2.88 (s, 4H, C$H_2{}^7$), 2.70 (t, J = 7.1 Hz, 4H, C$H_2{}^{10}$), 2.53 (t, J = 7.3 Hz, 4H, C$H_2{}^{11}$), 2.10–2.01 (m, 4H, C$H_2{}^9$), 1.64–1.54 (m, 4H, C$H_2{}^{12}$), 1.40–1.28 (m, 12H, CH^{alkyl}) ppm.

IR (ATR): $\tilde{\nu}$ = 2923, 2843, 1608, 1580, 1488, 1445, 1385, 1273, 1249, 1154, 1090, 1062, 1034, 954, 875, 775, 716, 687, 612, 448 cm^{-1}.

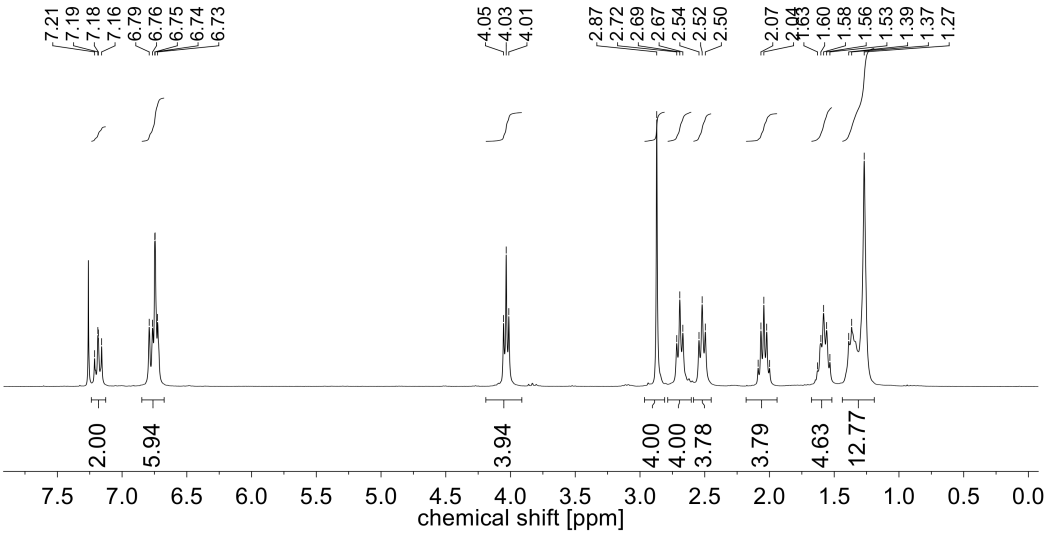

9.2.5.5 Thiol-ene polymer of 4,4'-(propane-2,2-diyl)bis((allyloxy)benzene) (PTE14)

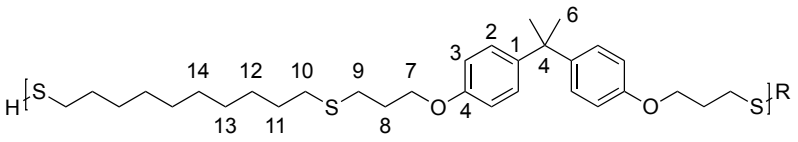

Following the general procedure for the thiol-ene polymerization, **PTE14** was obtained from 4,4'-(propane-2,2-diyl)bis((allyloxy)benzene) (**14a**, 200 mg, 648 µmol) and decane dithiol (**87**, 138 mg, 657 µmol, 1.01 eq.) and isolated as colorless solid (290 mg, 87 wt% based on the diene and dithiol).

T_m = rt.

SEC (THF): M_n = 5200 g mol^{-1} ($Đ$ = 3.6).

TGA: $T_{d\,5\%}$ = 270 °C.

^{1}H NMR (300 MHz, $CDCl_3$): δ = 7.12 (d, J = 8.7 Hz, 4H, CH^3), 6.80 (d, J = 8.7 Hz, 4H, CH^2), 4.03 (t, J = 6.0 Hz, 4H, C$H_2{}^7$), 2.69 (t, J = 7.2 Hz, 4H, C$H_2{}^9$), 2.52 (t, J = 7.4 Hz, 4H, C$H_2{}^{10}$), 2.08–2.00 (m, 4H, C$H_2{}^8$), 1.63–1.54 (m, 10H, C$H_2{}^{6,11}$), 1.36–1.28 (m, 12H, C$H_2{}^{12,13,14}$) ppm.

IR (ATR): $\tilde{\nu}$ = 2921, 2850, 1607, 1581, 1508, 1466, 1382, 1296, 1240, 1180, 1028, 1011, 927, 826, 807, 724, 572, 554 cm^{-1}.

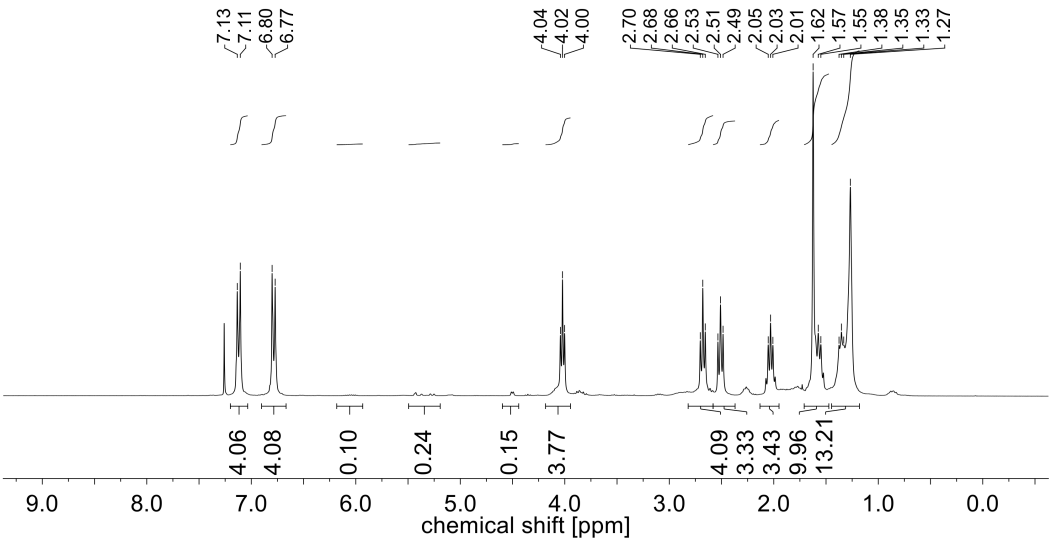

9.3 Synthesis procedures for Chapter 4

9.3.1 Organosolv lignin (88)

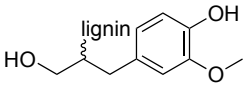

The organosolv pulping was performed at the Thünen Institute of Wood Research (Hamburg, Germany). European beech wood (*F. sylvatica L.*) chips (10.8 kg) were treated with ethanol/ water (50 vol%) at 170 °C for 90 minutes with a catalytic amount sulfuric acid (0.5 wt% based on dry wood). The solid to liquid ratio was 1 : 4. The lignin fraction in solution was separated from the solid fraction by filtration. OL (**88**) was precipitated in water at a pH value of around 2.0. The suspension was centrifuged and OL (**88**) separated. OL (**88**) was dried at 40 °C in a vacuum drying oven and isolated as a brown solid (785 g, 7.8 wt%). The total hydroxy content of this unmodified lignin (**88**) was calculated to be 6.1 mmol g^{-1} (from ^{31}P NMR analysis).

SEC (THF): M_n = 1200 g mol^{-1} ($Đ$ = 3.1).

DSC: T_g = 121 °C.

TGA: $T_{d\,5\%}$ = 235 °C (5 K min^{-1}, synthetic air); 243 °C (10 K min^{-1}, N_2).

^{1}H NMR (300 MHz, DMSO-d_6) δ = 7.30–6.30 (m, CH^{aryl}), 4.40–3.40 (m, -OCH_3), 1.40–0.60 (m, CH^{alkyl}) ppm.

IR (ATR): $\tilde{\nu}$ = 3412, 2936, 1722, 1586, 1507, 1459, 1321, 1211, 1112, 1031, 908, 828 cm^{-1}.

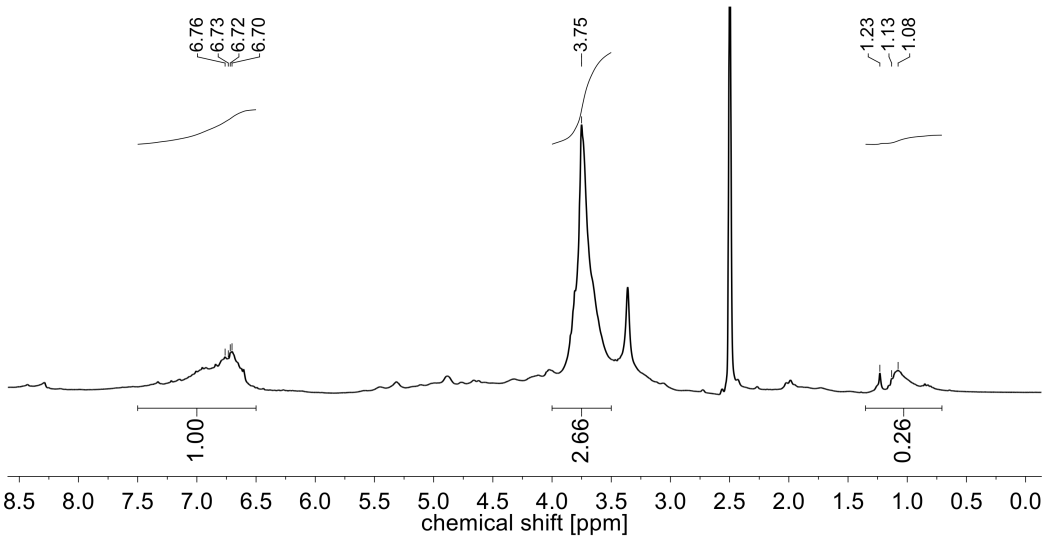

9.3.2 Allylated organosolv lignin (89)

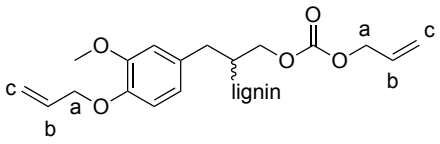

OL (**88**, 150 mg, 0.915 mmol, 1.00 eq. OH) was placed in a 15 mL pressure tube, suspended in DAC (**54**, 1.30 g, 9.15 mmol, 10.0 eq. per OH) and heated to 120 °C. TBAB (**50**, 295 mg, 0.915 mmol, 1.00 eq. per OH) was added and the solution was stirred at 120 °C for 5 hours.

Work-up method A (recovery of TBAB). After the reaction mixture was cooled to room temperature, water (12 mL) was added dropwise to the solution and forming two phases. The mixture was stirred at room temperature until a brown solid precipitated and one single colorless liquid phase was formed. After filtration and washing with water (2 × 5 mL), the solid product was dried at $5{\cdot}10^{-3}$ mbar over diphosphorous pentoxide for 24 h. Allylated OL (**89**, 140 mg, 93 wt%, 86% allylated) was obtained as a brown solid. TBAB (**50**, 285 mg, 97 wt%) was recovered as a yellowish solid from the filtrate by removing the solvents under reduced pressure (60 °C, 80 mbar). The NMR data of the recovered TBAB (**50**) was identical with the data of the commercial product and the isolated TBAB (**50**) can be directly reused for allylation.

Work-up method B (extraction method for DAC recovery). The reaction solution was cooled to room temperature and dissolved in ethyl acetate (10 mL). The organic phase was extracted with water (2 × 20 mL). The aqueous phase was washed with ethyl acetate (5 mL) and evaporated under reduced pressure. TBAB (**50**) was obtained as yellowish solid (268 mg, 91%). The combined organic phases were dried over magnesium sulfate and concentrated under reduced pressure to 5 mL. The solution was precipitated in cold *n*-hexane (100 mL), the solid was filtered, washed with *n*-hexane (2 × 5 mL) and dried at 10^{-3} mbar. Allylated OL (**89**) was obtained as brown solid (146 mg, 97 wt%). The filtrate solvent was removed under reduced pressure and DAC was recovered as yellow liquid (770 mg, 59%).

Work-up method C (distillation method for DAC recovery). The hot reaction mixture is transferred into a round bottom flask for subsequent *kugelrohr* distillation. DAC (**54**, 807 mg, 62%) was collected at 100 °C and 35 mbar. The distillation residue was treated as described for the reaction mixture in method A.

Analytical data for allylated OL (89):

SEC (THF): M_n = 2700 g mol^{-1}; $Đ$ = 3.5.

DSC: T_g = 70 °C.

TGA: $T_{d\,5\%}$ = 218 °C (5 K min^{-1}, air).

^{1}H NMR (300 MHz, DMSO-d_6) δ = 7.50–6.50 (m, CH^{aryl}), 6.20–5.63 (m, CH^{b}), 5.23 (m, CH^{c}), 4.71–4.18 (m, CH^{a}), 3.72 (s, -OCH_3, -OH), 1.30–0.65 (m, CH^{alkyl}) ppm.

IR (ATR): $\tilde{\nu}$ = 2936, 2843, 1748, 1580, 1501, 1459, 1418, 1326, 1240, 1123, 1035, 988, 922 cm^{-1}.

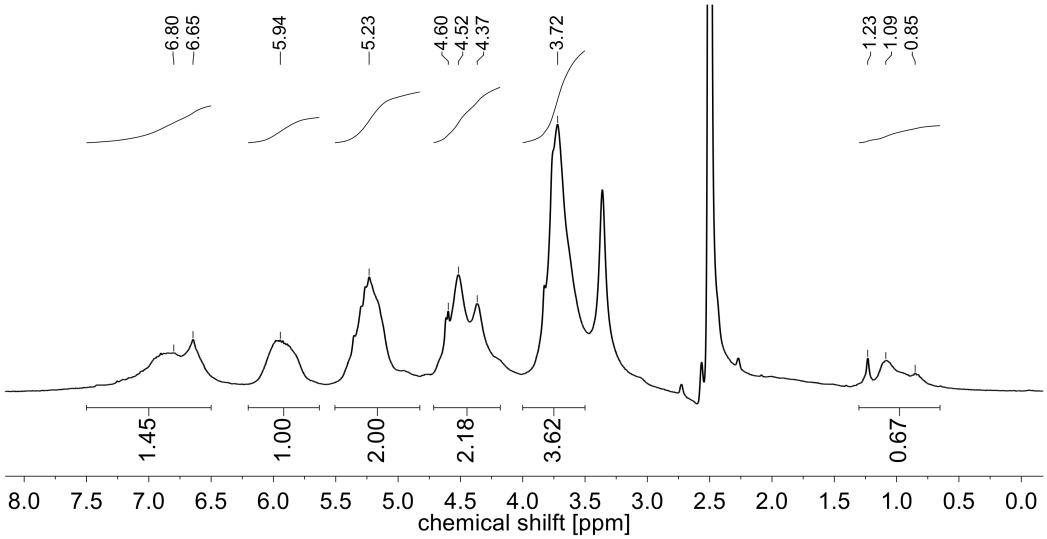

9.3.3 Decarboxylation of allylated organosolv lignin (94)

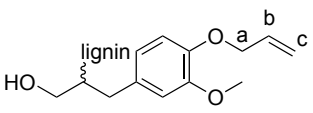

Allylated OL (**89**, 99.7 mg, 608 mmol, 1.00 eq.) was dissolved in THF (1 mL) and water (1 mL). Lithium hydroxide (43.0 mg, 1.80 mmol, 2.96 eq.) was added and the mixture was stirred at room temperature for five days. Aqueous 1 M hydrochloric acid (100 mL) was added to precipitate the product. The product was filtered, washed with aqueous 1 M hydrochloric acid (50 mL) and water (2 × 50 mL) and dried at 5·10^{-3} mbar over diphosphorous pentoxide for 24 hours. The modified OL **94** (65 mg, 67 wt%) was obtained as a brown solid.

SEC (THF): M_n = 2400 g mol^{-1} ($Đ$ = 3.3).

^{1}H NMR (300 MHz, DMSO-d_6) δ = 7.50–6.50 (m, CH^{aryl}), 6.20–5.63 (m, CH^{b}), 5.23 (m, CH^{c}), 4.71–4.18 (m, CH^{a}), 3.72 (s, 15H), 1.30–0.65 (m, CH^{alkyl}) ppm.

IR (ATR): $\tilde{\nu}$ = 3497 (O-H), 2936, 2870, 1586, 1503, 1455, 1417, 1325, 1222, 1124, 1028, 987, 925, 835 cm^{-1}.

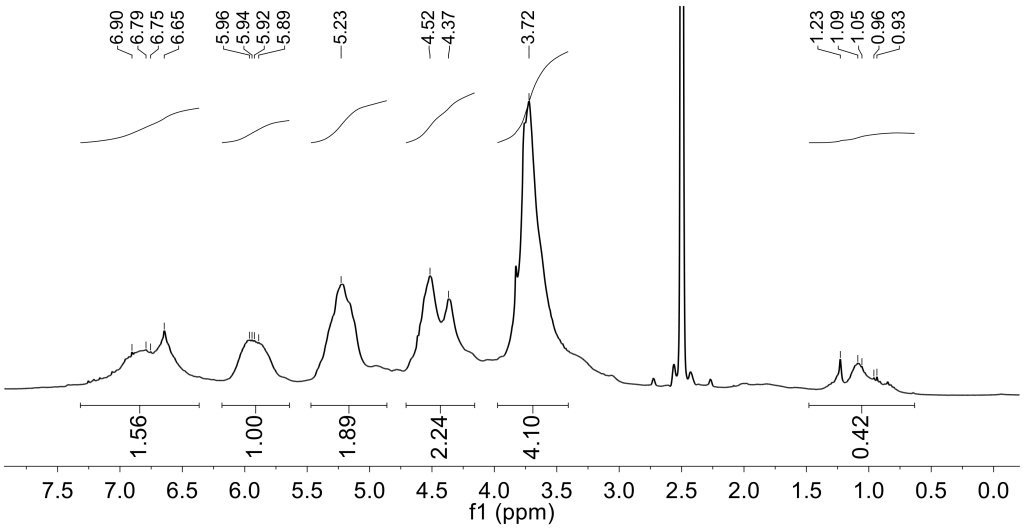

9.3.4 Self-metathesis of allylated OL (95)

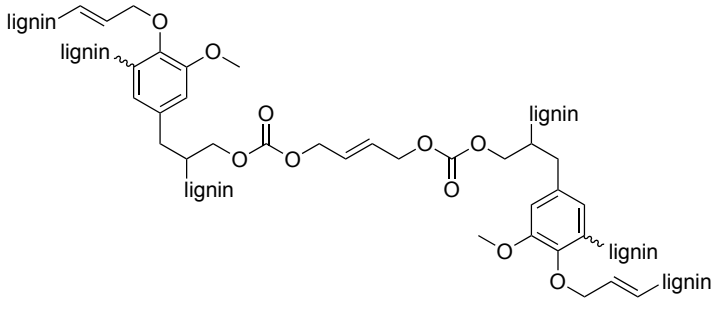

Allylated OL (**89**, 100 mg, 80% allylated, 0.401 mmol C=C) was dissolved in dry DCM (1.00 mL), benzoquinone (2.6 mg, 6 mol%) and Hoveyda-Grubbs 1st Generation catalyst (4.9 mg, 2.0 mol%) or Hoveyda-Grubbs 2nd Generation catalyst (5.2 mg, 2.0 mol%) were added. After 15 h, ethyl vinyl ether (500 µL) was added. The solid was precipitated in methanol (30 mL), filtered and washed with methanol (2 × 5 mL). After drying over phsphorous pentoxide at 10^{-3} mbar, the cross-linked product **95** was isolated as brown solid (99.0 mg, 99 wt%).

SEC (THF): M_n = 9600 g mol^{-1} ($Đ$ = 1.8) (Hoveyda-Grubbs 1st generation catalyst).

SEC (THF): M_n = 7700 g mol^{-1} ($Đ$ = 84) (Hoveyda-Grubbs 2nd generation catalyst).

9.3.5 Claisen rearangement study

9.3.5.1 First allylation of OL, without Claisen rearrangement (96)

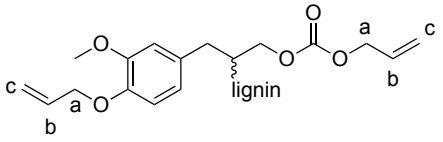

This reaction was performed by Marcel Hergert in the scope of a six-week internship under my co-supervision.

Procedure in analogy by section 9.3.2, but in a 1 g-scale. OL (**88**, 1.00 g, 6.10 mmol, 1.00 eq. OH) was suspended in DAC (**54**, 2.60 g, 18.3 mmol, 3.00 eq. per OH), heated to 120 °C and then TBAB (**50**, 1.96 g, 6.10 mmol, 1 eq. per OH) was added. The solution was stirred for 15 hours at 120 °C. Work-up Method B in section 9.3.2 led to recovery of TBAB (1.91 g, 97%) and DAC (780 mg, 30%). The desired compound **96** was isolated as brown solid (930 mg, 93 wt%).

SEC (THF): M_n = 2200 g mol^{-1} ($Đ$ = 3.7).

^{1}H NMR (DMSO-d_6, 300 MHz): δ = 7.30–6.30 (m, CH^{aryl}), 6.13–5.55 (m, CH^{b}), 5.45–4.80 (m, CH^{c}), 4.70–4.15 ppm (m, CH^{a}), 3.95–3.20 (m, -OCH_3), 1.40–0.80 (m, CH^{alkyl}) ppm.

Analytical data are identical to Section 9.3.2.

9.3.5.2 Claisen rearranged, allylated Lignin (97)

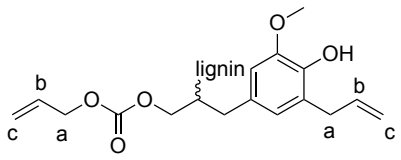

This reaction was performed by Marcel Hergert in the scope of a six-week internship under my co-supervision.

Allylated Lignin (**96**, 830 mg) was dissolved in DMSO (2.5 mL) and stirred at 150 °C for 24 hours. The solution was added drop-wise to water (400 mL) and the precipitate was collected and washed with water (50 mL). Afterwards it was dried in vacuo over diphosphorous pentoxide for 24 hours to afford compound **97** as brown solid (675 mg, 81 wt%).

SEC (THF): M_n = 1400 g mol^{-1} ($Đ$ = 2.6).

^{1}H NMR (DMSO-d_6, 300 MHz): δ = 7.30–6.30 (m, CH^{aryl}), 6.13–5.55 (m, CH^{b}), 5.45–4.80 (m, CH^{c}), 4.70–4.15 ppm (m, CH^{a}), 3.95–3.20 (m, -OCH_3), 1.40–0.80 (m, CH^{alkyl}) ppm.

NMR spectrum was comparable to Section 9.3.2.

9.3.5.3 Second allylation of claisen rearranged, allylated Lignin (98-1)

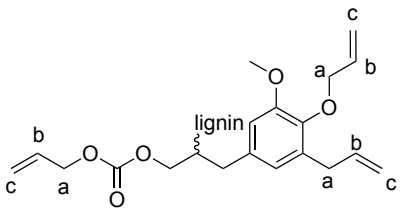

This reaction was performed by Marcel Hergert in the scope of a six-week internship under my co-supervision.

Claisen rearranged, allylated lignin (**97**, 575 mg, 3.51 mmol original OH) was suspended in DAC (**54**, 1.50 g, 10.5 mmol, 3.00 eq. per original OH), heated to 120 °C and then TBAB (**50**, 567 mg, 1.76 mol, 1.00 eq. per original OH) was added. The solution was stirred for 15 hours at 120 °C. Work-up Method B in section 9.3.2 led to recovery of TBAB (**50**, 548 mg, 97%) and DAC (600 mg, 40 %). The desired compound **98-1** was isolated as brown solid (517 mg, 90 wt%).

SEC (THF): M_n = 2300 g mol^{-1} ($Đ$ = 2.7).

^{1}H NMR (DMSO-d_6, 300 MHz): δ = 7.30–6.30 (m, CH^{aryl}), 6.13–5.55 (m, CH^{b}), 5.45–4.80 (m, CH^{c}), 4.70–4.15 ppm (m, CH^{a}), 3.95–3.20 (m, -OCH_3), 1.40–0.80 (m, CH^{alkyl}) ppm.

NMR spectrum was comparable to Section 9.3.2.

9.3.5.4 Allylation and simultaneous Claisen rearrangement of OL (98-2)

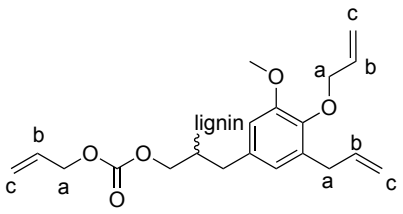

This reaction was performed by Marcel Hergert in the scope of a six-week internship under my co-supervision.

OL (**88**, 30.0 g, 183 mmol, 1.00 eq.) was suspended in DAC (**54**, 76.0 g, 534 mmol, 2.92 eq.). After the addition of TBAB (**50**, 11.9 g, 37.0 mmol, 20.0 mol%) at 120 °C, the solution was heated to 150 °C and stirred at constant temperature for 72 hours. Work-up of the reaction was performed following the work-up Method B in section 9.3.2. TBAB (**50**, 10.9 g, 92%) and DAC (**54**, 18.1 g, 24%) were recovered. The desired product **98-2** was isolated as brown solid (28.5 g, 95 wt%).

SEC (THF): M_n = 2500 g mol^{-1} ($Đ$ = 5.1).

DSC: T_g = 80 °C.

^{1}H NMR (DMSO-d_6, 300 MHz): δ = 7.30–6.30 (m, CH^{aryl}), 6.13–5.55 (m, CH^{b}), 5.45–4.80 (m, CH^{c}),

4.70–4.15 ppm (m, C*H*^{a}), 3.95–3.20 (m, -OCH_3), 1.40–0.80 (m, C*H*^{alkyl}) ppm.

NMR spectrum was comparable to Section 9.3.2.

9.3.6 Crotylated organosolv lignin (99)

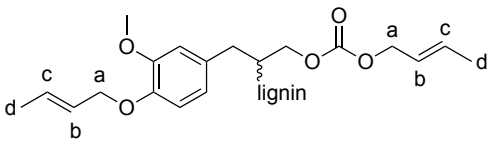

OL (**88**, 1.00 g, 6.10 mmol OH, 1.00 eq.) was suspended in DCC (**62**, 3.10 g, 18.3 mmol, 3.00 eq.) and heated to 120 °C in a pressure tube. TBAB (**50**, 1.93 g, 6.00 mmol, 1.00 eq.) was added to solve OL completely. The reaction mixture was stirred at 120 °C for 12 hours. Ethyl acetate (50 mL) were added to the cooled mixture and the organic phase washed with aqueous 1 M hydrochloric acid (3 × 50 mL), water (50 mL) and saturated aqueous sodium chloride solution. The desired product **99** was dropwise precipitated from ethyl acetate in *n*-hexane (500 mL), filtered, dried over diphosphorous pentoxide and isolated as brown powder (795 mg, 80 wt%).

SEC (THF): M_n = 2600 g mol^{-1} ($Đ$ = 3.5).

DSC: T_g = 83 °C.

TGA: $T_{d\,5\%}$ = 234 °C (10 K min^{-1}, N_2).

^{1}H NMR (300 MHz, DMSO-d_6) δ = 6.91–6.55 (m, C*H*^{aryl}), 5.75–5.59 (m, C*H*^{b,c}), 4.50–4.39 (m, CH_2^{a}), 3.91–3.50 (m, -OCH_3), 1.80–1.32 (m, C*H*^{d}), 1.32–0.67 (m, C*H*^{alkyl}) ppm.

IR (ATR): $\tilde{\nu}$ = 3492. 2937, 1744, 1590, 1504, 1456, 1418, 1374, 1327, 1224, 1124, 1035, 965, 834, 790 cm^{-1}.

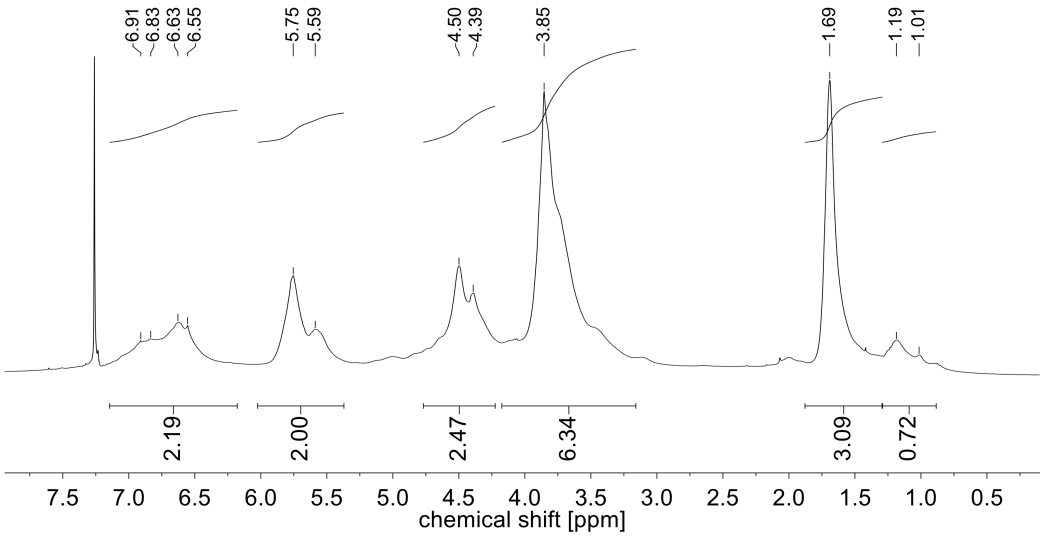

9.4 Synthesis procedures for Chapter 5

9.4.1 Lignin-plant oil film curing

A total amount of 750 mg (4.90 mmol C=C, based on 100 wt%, 80% converted allylated lignin) plant oil and allylated lignin (**98-2**) (in ratio 2:8–8:2), 8.3 mg *p*-benzoquinone (8.3 mg, 77 μmol, 1.5 mol%) and Grubbs-Hoveyda 2nd generation catalyst (13.8 mg, 22.0 µmol, 0.45 mol%) were dissolved in 7.5 mL dimethyl carbonate (DMC) or dichloromethane (DCM). For DMC, the reaction mixture was stirred in a glass tube at 50 °C for two hours prior to film formation to completely dissolve all reagents and then poured in a 50 mL Teflon form. For DCM, the components were directly mixed in a Teflon form. In both cases, the solvent was removed at 50–80 °C reducing the pressure in a vacuum oven over two hours (1000–600 mbar). Films were cured for 24 hours at 80 or 120 °C under reduced pressure (~0 mbar). Analytical evaluation of the films was performed after the films were stored in a desiccator over diphosphorous pentoxide at 10^{-3} mbar for two weeks.

9.5 Synthesis procedures for Chapter 6

9.5.1 Glycidylation of organosolv lignin (107)

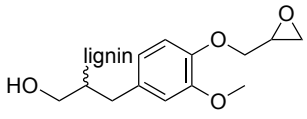

OL (**88**, 25.0 g, 152 mmol OH, 1.00 eq.) was suspended in epichlorohydrin (**15**, 100 mL, 1.28 mol, 8.42 eq.). Under ice cooling, TBAB (**50**, 9.5 g, 29.6 mmol, 19.4 mol%) was slowly added and the mixture stirred for 30 min. Portion-wise, potassium hydroxide (29.9 g, 534 mmol, 3.51 eq.) was added over 2.5 hours. After stirring for another five hours at room temperature, the mixture was diluted with dichloromethane (300 mL) and extracted with water (3 × 200 mL). The aqueous phase was extracted with dichloromethane (2 × 50 mL) and the combined organic layers were washed with saturated sodium chloride solution (100 mL). After separation, the organic layer was dried over magnesium sulfate, filtrated and concentrated in a rotary evaporator to 200 mL. The product was precipitated in *n*-hexane, filtrated and dried at 10^{-3} mbar over diphosphorous pentoxide. GOL (**107**) was obtained as brown powder (24.9 g, 99 wt%).

Epoxy content titration (NaOH): n_{epoxy} per gramm = 3.2 mmol g^{-1}

^{1}H NMR (300 MHz, DMSO-d_6, δ): 7.30 – 6.30 (m, CH^{aryl}), 4.40 – 3.40 (m, -OCH_3, -OH), 2.86 – 2.55 (m, epoxy-CH), 1.40 – 0.60 (m, CH^{alkyl}) ppm.

IR (ATR): $\tilde{\nu}$ = 3450, 2994, 2943, 2873, 1725, 1597, 1502, 1457, 1413, 1330, 1228, 1125, 1030, 909, 845, 758 cm^{-1}.

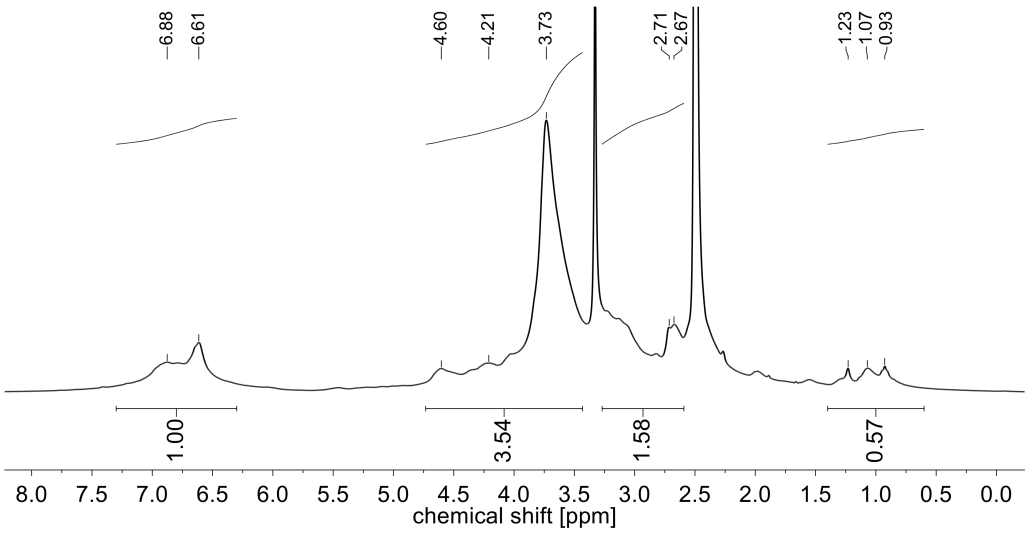

9.5.2 Preparation of epoxy thermosetting polymers from glycidylated lignin (109)

Glycidylated lignin (**107**) and BPA diglycidyl ether (**16**) were mixed in different ratios to a total amount of 1.50 g. IPDA (**108**) was added in the ratio $n_{epoxide} : n_{amine} = 2 : 1$, giving a molar ratio of one, as one amine can react with two epoxides. The materials were mixed homogeneously, poured into dog bone shaped molds and cured in the oven for one hour at 70 °C, then heated to 120 °C for two more hours to obtain **109**.

9.6 Synthesis procedures for Chapter 7

9.6.1 Gereral epoxidation procedure

The following procedures were tested for epoxidation of model compounds DAC (**54**), DCC (**62**), DUC (**63**), allylated (**71a**) and crotylated guaiacol (**71c**) as well as of allylated (**89**) and crotylated organosolv lignin (**99**). If the reaction was followed by GC analysis, 10 wt% of tetradecane were added as internal standard. Equivalents of reagents are given in eq. per C=C.

Method A: Epoxidation with *m*CPBA. The alkylated compound (150 mg) was diluted in dichloromethane (3 mL). Under argon atmosphere and ice cooling, *meta*-chloroperbenzoic acid (1.5–3 eq.) was added and the reaction mixture stirred at room temperature for 5–13 hours. Dichloromethane (10 mL) was added and the organic layer was washed with aqueous sodium sulfite solution (10 wt% in water, 2 × 20 mL), saturated aqueous sodium bicarbonate solution (2 × 20 mL), water (10 mL) and saturated sodium chloride solution (10 mL). The organic layer was dried over sodium sulfate and filtered before model compounds were purified *via* column chromatography and the lignin products were precipitated in *n*-hexane. Analysis of the obtained lignin products was performed after drying at 10^{-3} mbar over diphosphorous pentoxide.

Method B: Epoxidation with peracetic acid. Anhydrous dimethyl carbonate (2 mL) and peracetic acid (36–40% in acetic acid, 2 eq.) were dried over molecular sieve (3 Å, 400 mg) under argon atmosphere for 2 hours. After removal of the molecular sieve, the alkylated compound (100 mg) was

added to the mixture and the solution was stirred at room temperature or heated to 70 °C untill full convertion was observed (NMR or GC analysis). **For model compounds:** the product was collected in ethyl acetate (20 mL), extracted with sodium sulfite solution (10 wt% in water, 2 × 10 mL), saturated sodium chloride solution (2 × 100 mL), dried over sodium sulfate and filtered. The solvent was removed under reduced pressure to obtain the crude product which was purified *via* column chromatography. **For alkylated lignin:** the product was directly precipitated in aqueous 1 M hydrochloric acid. Products were filtered, washed with 1 M hydrochloric acid (2 × 10 mL) and water (2 × 10 mL) and dried at 10^{-3} mbar over diphosphorous pentoxide.

Method C: Enzyme-catalyzed epoxidation (only tested for model compounds). In a 5 mL-screw cap vial, the alkylated compound (150 mg) and caprylic acid (1.5 eq.) were solved in toluene (2 mL). Lipase B from *c. antarctica* (Novozyme 435, 200 mg) was added and the solution stirred at 40 °C. Hydrogen peroxide (50% in H_2O, 3.6 eq.) was added portionwise over 5 hours, the solution was stirred at 40 °C and followed *via* GC analysis till full conversion was obtained. Ethyl acetate (20 mL) was added, remaining enzyme acrylic resin filtered off and the organic phase washed with water (3 × 30 mL), dried over sodium sulfate, filtered. The solvent was evaporated under reduced pressure and the products analyzed without further purification.

Method D: Tungsten-catalyzed epoxidation. The alkylated substrate (100 mg) and Aliquat 336 (0.03 eq.) were solved in 500 µL chloroform or DMC and added to a catalyst solution that contained Na_2WO_4 (0.2 eq.), H_3PO_4 (40% in H_2O, 0.4 eq.) and H_2O_2 (35% or 50% in H_2O, 4 eq.). The reaction mixture was stirred at room temperature untill full conversion was observed (GC analysis). **For model compounds:** ethyl acetate (10 mL) was added and the organic layer was washed with saturated aqueous sodium bicarbonate (2 × 20 mL), water (10 mL) and saturated sodium chloride solution (10 mL). The organic layer was dried over sodium sulfate and filtered before model compounds were purified *via* column chromatography. **For alkylated lignin compounds:** all reactions were performed in DMC and the products were directly precipitated in aqueous 1 M hydrochloric acid. Products were filtered, washed with 1 M hydrochloric acid (2 × 10 mL) and water (2 × 10 mL) and dried at 10^{-3} mbar over diphosphorous pentoxide.

9.6.2 Diglycidyl carbonate (121)

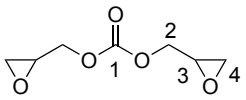

DAC (**54**, 2.00 g, 14.1 mmol, 1.00 eq.) was diluted in DMC (20 mL). Under argon atmosphere, *meta*-chloroperbenzoic acid (**113**,12.6 g, 56.3 mmol, 2.00 eq.) was added and the reaction mixture stirred at room temperature for eight days. Ethyl acetate (50 mL) was added and the organic layer was washed with sodium sulfite solution (10 wt% in water, 2 × 50 mL), saturated aqueous sodium bicarbonate solution (2 × 50 mL), water (50 mL) and saturated sodium chloride solution (50 mL). The organic layer was dried over sodium sulfate and filtered before the organic solvents were removed under reduced pressure. After column chromatography (cyclohexane/ethyl acetate 9:1), product **121** (1.11 g, 6.38 mmol, 45%) was isolated as colorless liquid.

TLC (cyclohexane/ethyl acetate 9:1): R_f = 0.05.

^{1}H NMR (300 MHz, $CDCl_3$): δ = 4.42 (dd, *J* = 12.1, 3.1 Hz, 2H, C*H*^{2}), 4.06 (dd, *J* = 12.1, 6.1 Hz, 2H, C*H*^{2}), 3.25 (m, 2H, C*H*^{3}), 2.86 (dd, *J* = 4.5 Hz, 4.5 2H, C*H*^{4}), 2.68 (dd, *J* = 4.7, 2.6 Hz, 2H, C*H*^{4}) ppm.

^{13}C NMR (75 MHz, $CDCl_3$): δ = 154.9 (*C*^{1}), 68.69 (*C*^{2}), 49.1 (*C*^{3}), 44.7 (*C*^{4}) ppm.

IR (ATR): $\tilde{\nu}$ = 3006, 2919, 2850, 1744, 1444, 1391, 1358, 1239, 1166, 1137, 1076, 964, 904, 859, 787, 768, 601, 522, 471, 446 cm^{-1}.

MS (FAB^{+}): *m/z* (%) = 175.1 [M+H]$^{+}$ (87), 137.1 (100), 136.1 (73), 120.1 (15), 107.1 (23), 89.0 (18).

HRMS (EI^{+}): $C_7H_{10}O_5$ [M+H]$^{+}$ calc. 175.0601; found 175.0600.

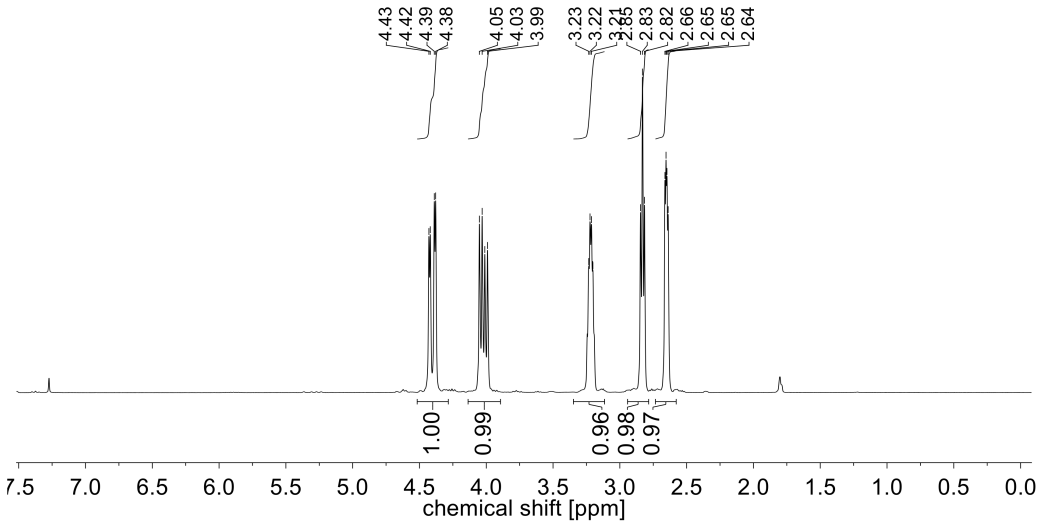

9.6.3 Bis((3-methyloxiran-2-yl)methyl) carbonate (122)

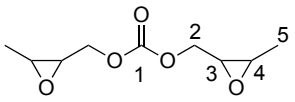

Anhydrous DMC (200 mL) and peracetic acid (36% in acetic acid, 26.0 g, 123 mmol, 2.10 eq.) was dried over molecular sieve (3 Å, 40.0 g) under argon atmosphere for two hours. DCC (**62**, 10.0 g, 58.8 mmol, 1.00 eq.) was added to the mixture and the solution heated to 70 °C for 20 hours. After four and after eight hours, additional peracetic acid (36% in acetic acid, 11.6 g, 54.9 mmol, 0.90 eq. and 5.00 g, 25.0 mmol, 0.40 eq.) was added to obtain full conversion (GC). The reaction mixture was cooled to room temperature, molecular sieve was filtered off and the product collected in ethyl acetate. The organic phase was extracted with sodium sulfite solution (10 wt% in water, 2 × 50 mL), saturated sodium chloride solution (2 × 100 mL), dried over sodium sulfate and filtered. The solvent was removed under reduced pressure to obtain the crude product. After column chromatography (cyclohexane/ethyl acetate 5:1), product **122** was obtained as colorless liquid (5.83 g, 28.9 mmol, 49%).

TLC (cyclohexane/ethyl acetate 5:1): R_f = 0.17.

^{1}H NMR (300 MHz, $CDCl_3$): δ = 4.33 (dd, J = 12.0, 3.2 Hz, 1H, CH^3), 4.05 (dd, J = 12.0, 5.7 Hz, 1H, CH^4), 2.96–2.93 (m, 2H, C$H_2{}^2$), 1.32 (d, J = 5.0 Hz, 3H, C$H_3{}^5$) ppm.

^{13}C NMR (75 MHz, $CDCl_3$): δ = 154.9 (C^1), 68.2 (2 $C^{2,4}$), 55.8 (1 C^2), 52.6 (1 C^2), 17.2 (C^5) ppm;

IR (ATR): $\tilde{\nu}$ = 3010, 2982, 2934, 1739, 1489, 1451, 1398, 1372, 1333, 1273, 1238, 1157, 1127, 1093, 1000, 933, 903, 857 (epoxide), 789, 731, 716, 705, 587, 526, 510 cm^{-1}.

MS (FAB$^+$): *m/z* (%) = 203.1 [M+H]$^+$ (100), 137.0 (15), 133.0 (18).

HRMS (EI$^+$): $C_9H_{15}O_5$ [M+H]$^+$ calc. 203.0914; found 203.0914.

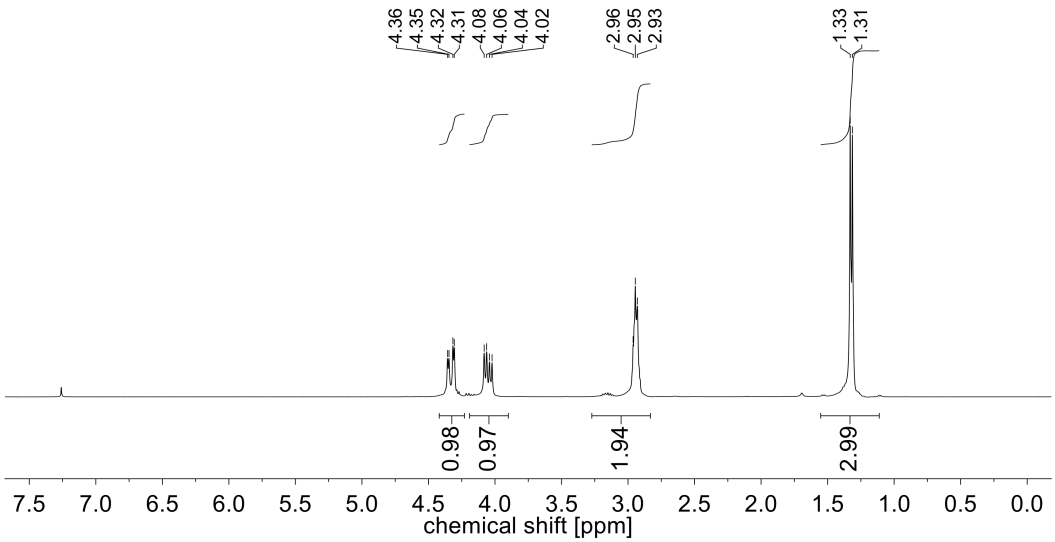

9.6.4 Bis(9-(oxiran-2-yl)nonyl) carbonate (123)

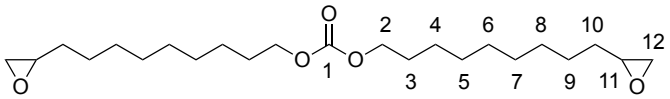

Anhydrous DMC (200 mL) and peracetic acid (38–40% in acetic acid, 62.4 g, 312 mmol, 2.30 eq.) were dried over molecular sieve (3 Å, 50.0 g) under argon atmosphere for two hours. DUC (**63**, 50.0 g, 136 mmol, 1.00 eq.) was added and the solution heated to 70 °C for 4.5 hours. After cooling to room temperate, the reaction mixture was filted and ethyl acetate (200 mL) was added. The organic phase was washed with sodium sulfite solution (10 wt% in water, 200 mL), water (100 mL), saturated sodium chloride solution (200 mL) and 1 M sodium hydroxide solution (200 mL). The product solution was dried over sodium sulfate and filtered before the organic solvents were removed under reduced pressure. After column chromatography (cyclohexane/ethyl acetate 9:1), product **123** was obtained as colorless liquid (43.4 g, 109 mmol, 80%).

TLC (cyclohexane/ethyl acetate 9:1): R_f = 0.19.

^{1}H NMR (300 MHz, $CDCl_3$): δ = 4.11 (t, J = 6.7 Hz, 4H, CH_2^2), 2.89 (m, 2H, CH^{11}), 2.74 (dd, J = 4.9, 4.5 Hz, 2H, CH_2^{12cis}), 2.45 (dd, J = 4.9, 2.7 Hz, 2H, C$H_2^{12trans}$), 1.73 – 1.58 (m, 4H, CH_2^{10}), 1.59 – 0.84 (m, 28H, C$H_2^{3–9}$) ppm.

^{13}C NMR (75 MHz, $CDCl_3$): δ = 155.6 (C^1), 68.1 (C^2), 52.5 (C^{11}), 47.2 (C^{12}), 32.6 ($C^{3–9}$), 29.6 ($C^{3–9}$), 29.5 ($C^{3–9}$), 29.5 ($C^{3–9}$), 29.3 ($C^{3–9}$), 28.8 (C^{10}), 26.1 ($C^{3–9}$), 25.8 ($C^{3–9}$) ppm.

IR (ATR): $\tilde{\nu}$ = 2916, 2847, 1741, 1460, 1405, 1258, 1134, 1026, 1005, 983, 930, 909, 892, 851 (epoxide), 795, 754, 726, 461 cm^{-1}.

MS (FAB$^+$): *m/z* (%) = 399.4 (53), 154.1 (67), 137.1 (100), 136.1 (55), 109.1 (42), 95.1 (87).

HRMS (EI$^+$): $C_{23}H_{42}O_5$ [M+H]$^+$ calc. 399.3105; found 399.3107.

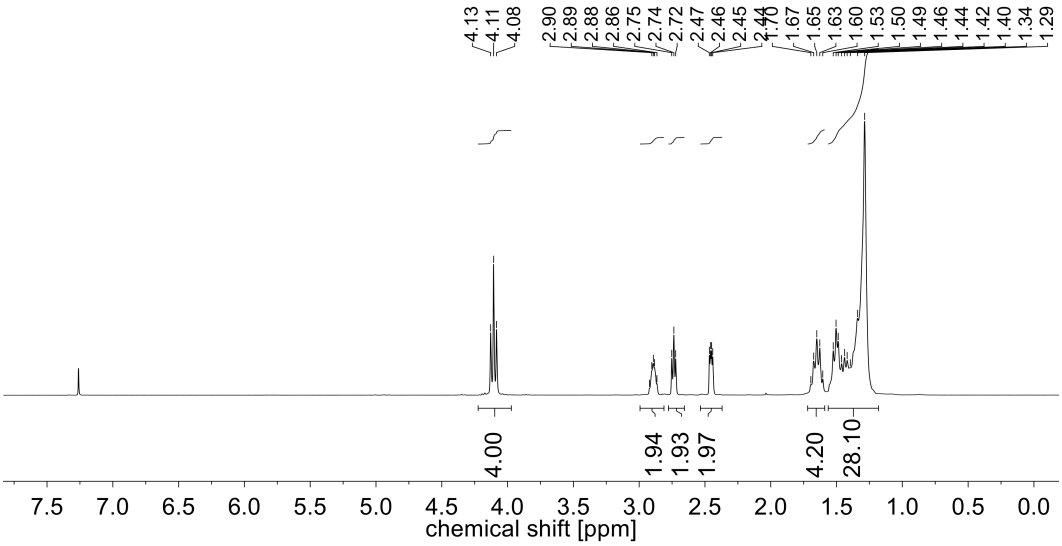

9.6.5 2-(2-Methoxyphenoxymethyl)oxirane (124)

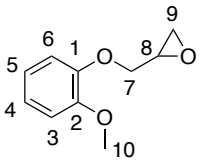

Guaiacol (**71**, 500 mg, 4.00 mmol, 1.00 eq.) and epichlorohydrin (4.72 g, 50 mmol, 12.5 eq.) were mixed with potassium hydroxide (800 mg, 14.3 mmol, 3.50 eq.) and TBAB (125 mg, 0.388 mmol, 10.0 mol%) and stirred at room temperature for four hours. Dichloromethane (20 mL) and water (10 mL) was added. The organic layer was washed with water (2 × 10 mL), dried over sodium sulfate, filtered and evaporated under reduced pressure. After column chromatography (cyclohexane/ethyl acetate 9:1), product **124** (575 mg, 3.38 mmol, 84%) was obtained as colorless liquid.

TLC (cyclohexane/ethyl acetate 9:1): R_f = 0.19.

^{1}H NMR (300 MHz, $CDCl_3$): δ = 6.97 – 6.90 (m, 4H, C$H^{3–6}$), 4.25 (dd, J = 11.4, 3.4 Hz, 1H, C$H^{7,trans}$),

4.06 (dd, J = 11.4, 5.5 Hz, 1H, C$H^{7,cis}$), 3.88 (s, 3H, CH^{10}), 3.43 – 3.38 (m, 1H, CH^{8}), 2.91 (dd, J = 4.5, 4.5 Hz 1H, C$H^{9,cis}$), 2.75 (dd, J = 4.8, 2.6 Hz, 1H, C$H^{9,trans}$) ppm.

^{13}C NMR (75 MHz, $CDCl_3$): δ = 149.8 (C^2), 148.1 (C^1), 122.1 ($C^{3–6}$), 121.0 ($C^{3–6}$), 114.5 ($C^{3–6}$), 112.1 ($C^{3–6}$), 70.4 (C^7), 56.0 (C^{10}), 50.3 (C^8), 45.1 (C^9) ppm.

IR (ATR): $\tilde{\nu}$ = 3000, 2928, 2836, 1592, 1502, 1454, 1327, 1290, 1250, 1222, 1178, 1122, 1024, 971, 913, 835, 800, 778, 740, 594, 580, 533, 446 cm^{-1}.

MS (FAB$^+$): *m/z* (%) = 181.1 [M+H]$^+$ (31), 180.1 [M]$^+$ (100), 137.0 (13), 123.0 [M-glycidyl]$^+$ (8).

HRMS (EI$^+$): $C_{10}H_{12}O_3$ [M]$^+$ calc. 180.0781; found 180.0782.

NMR data of 2-(2-Methoxyphenoxymethyl)oxirane (**124**) was identical to literature.[398]

9.6.6 2-((2-methoxyphenoxy)methyl)-3-methyloxirane (125)

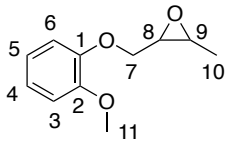

Crotyliertes guaiacol (**71c**, 500 mg, 2.81 mmol, 1.00 eq.) was solved in DMC (10 mL) and peracetic acid (36–40% in acetic acid, 1.19 g, 5.63 mmol, 2.00 eq.) was added under ice cooling. The reaction mixture was stirred at room temperature for 48 h. Ethyl acetate was added and the organic layer washed with sodium sulfite solution (10 wt% in water, 20 mL), water (20 mL) and saturated sodium chloride solution (20 mL). The product layer was dried over sodium sulfate and filtered before the organic solvents were removed under reduced pressure. After column chromatography (cyclohexane/ethyl acetate 19:1–9:1), product **125** (252 mg, 1.30 mmol, 46%) was isolated as colorless liquid.

TLC (cyclohexane/ethyl acetate 9:1): R_f = 0.17.

^{1}H NMR (300 MHz, $CDCl_3$): δ = 6.95 – 6.89 (m, 4H, C$H^{3–6}$), 4.19 (dd, J = 11.4, 4.0 Hz, 1H, C$H^{7,trans}$), 4.07 (dd, J = 11.4, 5.2 Hz, 1H, C$H^{7,cis}$), 3.87 (s, 1H, 3H, C$H_3{}^{11}$), 3.10 (d, J = 5.0 Hz, 1H, CH^{8}), 3.02 (dd, J = 5.2, 2.0 Hz, 1H, CH^{9}), 1.36 (d, J = 5.3 Hz, 3H, C$H_3{}^{10}$) ppm.

^{13}C NMR (75 MHz, $CDCl_3$): δ = 149.8 (C^2), 148.2 (C^1), 122.0 ($C^{3–6}$), 121.0 ($C^{3–6}$), 114.5 ($C^{3–6}$), 112.1 ($C^{3–6}$), 69.9 (C^7), 57.2 (C^8), 56.0 (C^{11}), 53.0 (C^9), 17.4 (C^{10}) ppm.

IR (ATR): $\tilde{\nu}$ = 3481, 3326, 2927, 2837, 1592, 1503, 1453, 1375, 1329, 1288, 1250, 1220, 1178, 1124, 1069, 1024, 905, 870, 817, 741, 581, 536 cm^{-1}.

MS (FAB$^+$): *m/z* (%) = 195.1 [M+H]$^+$ (36), 194.1 [M]$^+$ (100), 177.1 (13), 154.0 (12), 137.0 (17), 124.0 (26).

HRMS (EI$^+$): $C_{11}H_{14}O_3$ [M]$^+$ calc. 194.0937 found 194.0937.

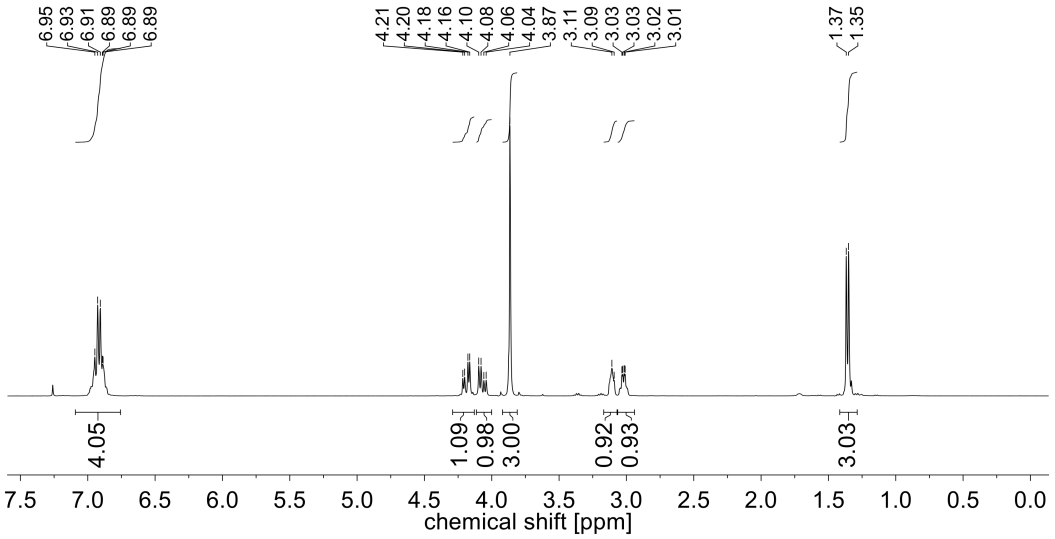

9.6.7 1-(2-Methoxyphenoxy)butane-2,3-diol (126)

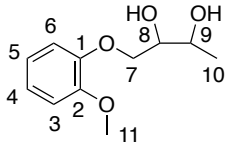

Crotylated guaiacol (**71c**, 500 mg, 2.81 mmol, 1.00 eq.) was solved in dimethyl carbonate (10 mL). Peracetic acid (36% in acetic acid, 1.19 g, 15.6 mmol, 5.50 eq.) was slowly added and the reaction mixture heated to 70 °C. After 15 hours, water (10 mL) was added and the mixture heated to 100 °C for one hour. After cooling to room temperature, ethyl acetate (20 mL) was added and the organic phase was washed with sodium sulfite solution (10 wt% in water, 20 mL), water (20 mL) and saturated sodium chloride solution (20 mL). The product solution was dried over sodium sulfate and filtered before the organic solvents were removed under reduced pressure. After column chromatography (cyclohexane/ethyl acetate 1:1–1:5), product **126** (180 mg, 849 µmol, 30%) was isolated as colorless solid.

TLC (cyclohexane/ethyl acetate 1:1): R_f = 0.11.

DSC: T_m = 72 °C.

^{1}H NMR (300 MHz, $CDCl_3$): δ = 6.93 – 6.80 (m, 4H, C$H^{3–6}$), 4.15 – 3.89 (m, 3H, CH_2^7,CH^8), 3.89 – 3.62 (m, 4H, CH^9, CH_3^{11}), 3.12 (s, 2H, OH), 1.19 (d, J = 6.5 Hz, 3H, CH_3^{10} ppm.

^{13}C NMR (75 MHz, $CDCl_3$): δ = 149.8 (C^2), 148.1 (C^1), 122.4 ($C^{3–6}$), 121.2 ($C^{3–6}$), 115.0 ($C^{3–6}$), 111.9 ($C^{3–6}$), 73.1 (C^9), 71.5 (C^7), 69.0 (C^8), 55.9 (C^{11}), 18.8 (C^{10}) ppm.

IR (ATR): $\tilde{\nu}$ = 3479, 3321, 2969, 2922, 2839, 2040, 1590, 1504, 1467, 1451, 1378, 1330, 1287, 1250, 1217, 1175, 1145, 1125, 1106, 1069, 1042, 1017, 983, 942, 903, 865, 814, 778, 753, 671, 581, 510 cm^{-1}.

MS (FAB$^+$): *m/z* (%) = 213.1 $[M+H]^+$ (43), 212.1 $[M]^+$ (100), 124.0 (95), 109.1 (42), 95.1 (73).

HRMS (EI$^+$): $C_{11}H_{16}O_4$ $[M+H]^+$ calc. 212.1043 found 212.1043.

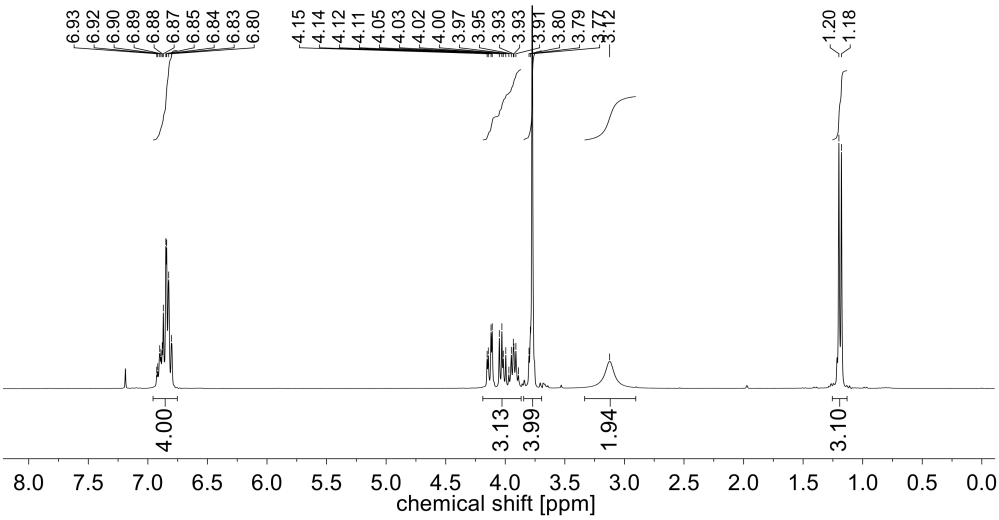

9.6.8 Epoxy thermosetting resin from epoxy DUC and priamine 1075 (130)

Epoxidized DUC (**123**, 750 mg, 3.76 mmol epoxide, 1.00 eq.) and priamine 1075 (517 mg, 1.88 mmol amine, 0.5 eq.) were mixed in a 25 mL Teflon form and heated from 60 °C to 150 °C within 90 minutes. The reaction mixtures was cured at 150 °C for 4 hours, then at 170 °C for 2.5 hours to yield **130**.

DSC: T_g = -26 °C.

TGA: $T_{d\,5\%}$ = 350 °C.

IR (ATR): $\tilde{\nu}$ = 3353, 2922, 2852, 1243, 1665, 1463, 1402, 1376, 1254, 1066, 951, 792, 722, 468 cm^{-1}.

9.7 Analytical procedures and instruments

9.7.1 Nuclear magnetic resonance (NMR) spectroscopy

^{1}H NMR spectroscopy. ^{1}H NMR spectra were measured with a Bruker AC 300 at 25 °C. For lignin derivatives 256 scans and a time delay *d1* of 10 seconds was applied. The sample concentration was 20 mg mL^{-1}. All ^{1}H NMR data are reported in ppm relative to the solvent signal for chloroform-d_1 at 7.26 ppm or DMSO-d_6 at 2.50 ppm.

^{13}C NMR spectroscopy. ^{13}C NMR spectra were measured with a Bruker AC 300 at 25 °C. All ^{13}C NMR data are reported in ppm relative to the solvent signal for Chloroform-d_1 at 77.16 ppm or DMSO-d_6 at 39.52 ppm.

For the quantitative ^{13}C analysis of lignin, a sample (95.0 mg) was dissolved in 450 µL DMSO-d_6. 100 µL of a solution of the internal standard 1,3,5-trioxane (62.4 mg mL^{-1}) and the relaxation agent

chromium(III) acetylacetonate (24.9 mg mL^{-1}) in DMSO-d_6 were added. ^{13}C NMR spectra were measured with a Bruker Avance DRX 500 with delay time *d1* of 4 seconds and 60 416 scans. Data are reported in ppm relative to DMSO-d_6 at 39.5 ppm.

^{31}P NMR studies. For ^{31}P NMR studies, an exact amount of 28–32 mg of the lignin sample was diluted in 400 µL $CDCl_3$/pyridine (1:1.6). 150 µL of a solution of chromium(III) acetylacetonate (3.6 mg mL^{-1}) as relaxation agent and cyclohexanol (4.0 mg mL^{-1}) as internal standard in $CDCl_3$/pyridine (1:1.6) were added and the solution was stirred for five minutes. 2-Chloro-4,4,5,5-tetramethyl-1,2,3-dioxaphospholane (70 µL) was added and the solution was transferred into a NMR tube for subsequent measurement in a Bruker Ascend™ 400 MHz spectrometer with 512 scans, a delay time *d1* of 3 seconds and a spectral width of 50 ppm (165–115 ppm). The chemical shifts are reported relative to the reaction product of 2-chloro-4,4,5,5tetramethyl-1,2,3-dioxaphospholane with water at 132.2 ppm. Integrals are assigned to the functional groups as followed: δ = 150.0–145.5 (aliphatic hydroxyl groups), 145.5–144.7 (cyclohexanol), 144.7–136.6 (phenolic hydroxyl groups), 136.6–133.6 (carboxylic acids) ppm.[53] In the region of the phenolic hydroxyl groups, syringyl (144.7–141.0 ppm) and guiacyl units (141.0–136.6 ppm) can be distinguished.

9.7.2 Infrared (IR) spectroscopy

Infrared spectra (IR) were recorded on a Bruker alpha-p instrument applying ATR technology.

9.7.3 Mass spectrometry (MS)

Fast atom bombardment (FAB) mass spectra and electron ionization (EI) mass spectra and high resolution mass spectra (HRMS) were measured with MAT95 of the company Finnigan.

9.7.4 Gas chromatography (GC)

GC-MS (EI). GC-MS (EI) chromatograms were recorded with a Varian 431 GC instrument with a capillary column FactorFour™ VF-5ms (30m × 0.25mm × 0.25 mm) and a Varian 210 ion trap mass detector.

GC (FID). GC chromatograms were recorded with a Bruker 430 GC instrument with a capillary column FactorFour™ VF-5ms (30m × 0.25mm × 0.25 mm) and a flame ionization detector (FID).

9.7.5 Size exclusion chromatography (SEC)

Molecular weight distributions M_n and M_w and their dispersities $Đ = M_n/M_w$ were determined using a SEC system LC-20A from Shimadzu equipped with a SIL-20A autosampler, a PSS SDV analytical main-column (5 µm, 300 mm × 8.0 mm, 10,000 Å), a PSS SDV analytical pre-column (5 µm, 50 mm × 8.0 mm), and a RID-10A refractive index detector in THF (flow rate 1 mL min^{-1}) at 50 °C. All determinations of molar mass were performed relative to PMMA standards (PSS, M_p 1,100–981,000 Da).

9.7.6 Size exclusion chromatography–electrospray ionization–mass spectrometry (SEC–ESI–MS)

Spectra were recorded on a Q Exactive (Orbitrap) mass spectrometer (Thermo Fisher Scientific) equipped with an HESI II probe. The instrument was calibrated in the *m/z* range 74–1822 using premixed calibration solutions (Thermo Scientific). A constant spray voltage of 4.6 kV, a dimensionless sheath gas of 8, and a dimensionless auxiliary gas flow rate of 2 were applied. The capillary temperature and the S-lens RF level were set to 320 °C and 62.0, respectively. The Q Exactive was coupled to a UltiMate 3000 UHPLC System (Dionex, Sunnyvale, CA, USA) consisting of a pump (LPG 3400SD), autosampler (WPS 3000TSL), and a thermostated column department (TCC 3000SD). Separation was performed on two mixed bed size exclusion chromatography columns (Polymer Laboratories, Mesopore 250 × 4.6 mm, particle diameter 3 µm) with pre-column (Mesopore 50 × 4.6 mm) operating at 30 °C. THF at a flow rate of 0.30 mL min^{-1} was used as eluent. The mass spectrometer was coupled to the column in parallel to a RI-detector (RefractoMax520, ERC, Japan) in a setup described earlier.[258] 0.27 mL min^{-1} of the eluent were directed through the RI-detector and 30 µL min^{-1} infused into the electrospray source after postcolumn addition of a 100 µM solution of sodium iodide in methanol at 20 µL min^{-1} by a micro-flow HPLC syringe pump (Teledyne ISCO, Model 100DM). A 20 µL aliquot of a polymer solution with a concentration of 2 mg mL^{-1} was injected onto the HPLC system.

9.7.7 Differential scanning calorimetry (DSC)

DSC experiments were carried out under nitrogen atmosphere with a DSC821e (Mettler Toledo) calorimeter using 40 µL aluminum crucibles and a sample mass of 6–8 mg. The glass transition temperature (T_g) was defined as the midpoint of the change in heat capacity occurring over the transition. The baseline was measured with an empty 40 µL aluminum crucible.

9.7.8 Differential Scanning Calorimetry (DSC) of epoxy thermosetting polymers

Differential Scanning Calorimetry (DSC) of epoxy thermosetting polymers was used to evaluate the residual reaction heat of the curing process as well as glass transition of the final product. Measurements were performed on a DSC Q100 system from TA instruments. For reaction heat studies, 6–8 mg of the reaction mixture was heated in aluminum crucibles from 0 °C to 250 °C with a heating rate of 10 K min^{-1} . The cured polymer networks were analyzed with the following heating program with two cycles: first heating cycle: -50 °C to 200 °C in 10 K min^{-1}; Cooling: 200 °C to -50 °C in -20 K min^{-1}; second heating cycle: -50 °C to 250 °C in 10 K min^{-1}. The glass transition temperature (T_g) was defined as the midpoint of the change in heat capacity occurring over the transition in the second heating cycle.

9.7.9 Differential thermal analysis (DTA)/thermal gravimetric analysis (TGA)

DTA/TGA measurements were performed with a Netzsch STA 409C instrument applying α-Al_2O_3 as a crucible material and reference sample. The samples were heated under synthetic air flow to 500 °C with a heating rate of 5 K min^{-1} if not stated otherwise, employing a sample mass of approximately 15 mg.

9.7.10 Thermogravimetric analysis (TGA) of epoxy thermosetting polymers

Thermogravimetric analyses (TGA) of epoxy thermosetting polymers were performed on a TGA-Q500 system from TA instruments at a heating rate of 5 K min^{-1} under synthetic air flow employing a sample mass of approximately 15 mg. From the two degradation temperatures of 5% ($T_{d\,5\%}$) and 30% ($T_{d\,30\%}$) weight loss, the statistic heat-resistant index (T_s) is calculated as follows:[399]

$$T_s = 0.49 \cdot (T_{d\,5\%} + 0.6 \cdot (T_{d\,30\%} - T_{d\,5\%}) \tag{9.1}$$

9.7.11 Dynamic Mechanical Analysis (DMA)

A DMA RSA 3 system from TA instruments was used to modulate from 25 °C to 240 °C at a heating rate of 5 K min^{-1}. The measurements were performed in 3-point bending mode at a frequency of 1 Hz, an initial force of 0.5 N and a strain sweep of 0.01%. The storage modulus *E'* is defined as the constant value below and over the glass transition. The glass transition temperature (T_g) is defined as the onset of the change in the storage modulus. The cross-linking density can be calculated from the following equation according to rubber elastic theory:[400]

$$\nu = \frac{E'}{\Phi \cdot R \cdot (T_\alpha + 30\ \mathrm{K})} \tag{9.2}$$

where *E*' is the storage modulus of the cured thermoset in the rubbery state, Φ is the front factor (approximately 1 in Flory theory[401]), R = 8.314 J mol^{-1} K^{-1} the gas constant and T_α is the maximum of tan delta (tan delta = *E*"/*E*', with *E*" defined as loss modulus).

9.7.12 Stress/strain measurements of lignin-plant oil film

Stress/strain measurements of lignin-plant oil film were recorded with an Eplexor 150N from Gabor with a 25 N load cell and a crosshead speed of 0.5 mm min^{-1}. Dog bone-shaped specimens were cut from the cured films to perform the measurement (width = 2 mm, thickness = 0.13–0.20 mm, length of the fixed section = 16.0 mm) Young's modulus (*E*) was determined from the linear part of the stress/strain curves for all samples. Reproducibility of the results was guaranteed by evaluating the average of three samples from the same film. Selected films were cured several times to verify the results.

9.7.13 Stress/strain measurements of epoxy thermosetting polymers

Stress/strain measurements of epoxy thermosetting polymers were performed on a MTS Elite 25 system using a elongation at break method with dog bone shaped specimens (width = 2 mm; thickness = 2 mm and length of fixed section = 17.5 mm) using a 500 N load cell and a crosshead speed of 1 mm min^{-1}. Young's modulus (*E*) was determined from the linear part of the stress/strain curves for all samples.

9.7.14 Scanning electron microscopy (SEM)

SEM was performed on a HITACHI-S570 with an accelerating voltage of 12 kV. The surface was coated with gold by sputtering for 14 s prior to the measurements using a Balzers UNION SCD 040. Digital Image Scanning System and Processing System (DISS and DIPS) from point electronic were used to generate the images.

9.7.15 Swelling properties

Swelling properties of weighed bar samples (m_0) of the cured epoxy thermosets were analyzed. After immersion in THF for 24 hours, the swollen samples were dried between paper and weighed again (m_{SW}). The samples were dried at 60 °C for 24 hours and weighed (m_D) to obtain the swelling percentage

$$\textit{Swelling}\ (\%) = \frac{m_{SW} - m_D}{m_D} \cdot 100 \tag{9.3}$$

and the soluble part of the networks

$$\textit{Soluble part}\ (\%) = 1 - \frac{m_D}{m_0} \cdot 100 \tag{9.4}$$

9.7.16 Epoxy content titration

An exact amount (m_S) of approximately 200 mg glycidylated lignin was solved in 25.0 mL pyridine/HCl solution (Stock solution: 500 mL pyridine and 8.30 mL concentrated hydrochloric acid (37%)) and refluxed for 20 min at 115 °C. The sample solution was titrated with 2 M NaOH solution to neutral pH with a required volume V_s. A blank was measured using unmodified OL resulting in a required volume V_{blank}. The epoxy content (n_{epoxy} per g) was calculated as followed:

$$n_{epoxy}\ \text{per g} = \frac{(V_{blank} - V_S) \cdot 2\ \text{mol/L}}{m_S} \tag{9.5}$$

References

[1] M. Eissen, J. O. Metzger, E. Schmidt, U. Schneidewind, *Angew. Chem. Int. Ed.* **2002**, *41*, 414–436.

[2] M. A. R. Meier, J. O. Metzger, U. S. Schubert, *Chem. Soc. Rev.* **2007**, *36*, 1788–1802.

[3] PlasticsEurope (PEMRG), *Plastics - the Facts 2016*.

[4] R. Mülhaupt, *Macromol. Chem. Phys.* **2013**, *214*, 159–174.

[5] A. Llevot, M. A. R. Meier, *Green Chem.* **2016**, *18*, 4800–4803.

[6] A. Llevot, P.-K. Dannecker, M. von Czapiewski, L. C. Over, Z. Söyler, M. A. R. Meier, *Chem. Eur. J.* **2016**, *22*, 11510–11521.

[7] P. M. Subramanian, *Resour. Conserv. Recy.* **2000**, *28*, 253–263.

[8] *Abfälle im Meer - Ein gravierendes ökologisches, ökonomisches und ästhetisches Problem*, Umweltbundesamt (eds.), **2010**.

[9] T. Yamamoto, A. Yasuhara, H. Shiraishi, O. Nakasugi, *Chemosphere* **2001**, *42*, 415–418.

[10] I. A. Lang, T. S. Galloway, A. Scarlett, et al., *JAMA* **2008**, *300*, 1303–1310.

[11] P. T. Anastas, J. C. Warner, *Green Chemistry: Theory and Practice*, Oxford University Press: New York, **1998**, p. 30.

[12] J. Elkington, *Calif. Manage. Rev.* **1994**, *36*, 90–100.

[13] E. S. Beach, Z. Cui, P. T. Anastas, *Energy Environ. Sci.* **2009**, *2*, 1038–1049.

[14] S. Li, X. Yang, K. Huang, M. Li, J. Xia, *Prog. Org. Coat.* **2014**, *77*, 388–394.

[15] R. Whetten, R. Sederoff, *The Plant Cell* **1995**, *7*, 1001–1013.

[16] D. S. Argyropouls, S. B. Menachem, *Adv. Biochem. Engin./Biotechnol.* **1997**, 127–158.

[17] J. de la Torre, A. Moral, D. Hernández, E. Cabeza, A. Tijero, *Ind. Crops Prod.* **2013**, *45*, 58–63.

[18] W. O. S. Doherty, P. Mousavioun, C. M. Fellows, *Ind. Crops Prod.* **2011**, *33*, 259–276.

[19] P. Azadi, O. R. Inderwildi, R. Farnood, D. A. King, *Renew. Sust. Energ. Rev.* **2013**, *21*, 506–523.

[20] C. Wang, S. S. Kelley, R. A. Venditti, *ChemSusChem* **2016**, *9*, 770–783.

[21] H. H. M. Kaltschmitt, *Energie aus Biomasse, Grundlagen, Techniken und Verfahren*, Springer Verlag, Berlin, Heidelberg, 1st ed., **2001**, p. 249.

[22] F. S. Chakar, A. J. Ragauskas, *Ind. Crops Prod.* **2004**, *20*, 131–141.

[23] H. Nägele, J. Pfitzer, *Thermoplaste auf Ligninbasis in: Die Kunststoffe und ihre Eigenschaften*, Springer, **2005**, pp. 1477–1488.

[24] J. Cho, S. Chu, P. J. Dauenhauer, G. W. Huber, *Green Chem.* **2012**, *14*, 428–439.

[25] H. G. Schlegel, *Allgemeine Mikrobiologie*, Georg Thieme Verlag, Stuttgart, 6th ed., **1985**, p. 249.

[26] W. Boerjan, J. Ralph, M. Baucher, *Annu. Rev. Plant Biol.* **2003**, *54*, 519–546.

[27] J. Ralph, K. Lundquist, G. Brunow, F. Lu, H. Kim, P. F. Schatz, J. M. Marita, R. D. Hatfield, S. A. Ralph, J. H. Christensen, W. Boerjan, *Phytochem. Rev.* **2004**, *3*, 29–60.

[28] X. Li, C. Chapple, *Plant Physiology* **2010**, *154*, 449–452.

[29] J. E. Holladay, J. J. Bozell, J. F. White, D. Johnson, *Top Value-Added Chemicals from Biomass - Volume II - Results of Screening for Potential Candidates from Biorefinery Lignin*, Pacific Northwest National Laboratory, Richland, USA, **2007**.

[30] A. Tejado, C. Pena, J. Labidi, J. M. Echeverria, I. Mondragon, *Bioresour. Technol.* **2007**, *98*, 1655–1663.

[31] E. K. Pye, *Pulping Conference* **1990**, 991–996.

[32] T. J. McDonough, *TAPPI Solvent Pulping Symposium* **1992**, 1–7.

[33] L. Hu, Y. Luo, B. Cai, J. Li, D. Tong, C. Hu, *Green Chem.* **2014**, *16*, 3107–3116.

[34] J. J. Bozell, A. Astner, D. Baker, B. Biannic, D. Cedeno, T. Elder, O. Hosseinaei, L. Delbeck, J. W. Kim, C. J. O'Lenick, T. Young, *Bioenergy Res.* **2014**, *7*, 856–866.

[35] W. Schutyser, S. Van den Bosch, T. Renders, T. De Boe, S.-F. Koelewijn, A. Dewaele, T. Ennaert, O. Verkinderen, B. Goderis, C. M. Courtin, B. F. Sels, *Green Chem.* **2015**, *17*, 5035–5045.

[36] Y.-C. Sun, M. Wang, R.-C. Sun, *ACS Sustain. Chem. Eng.* **2015**, *3*, 2443–2451.

[37] X. Erdocia, R. Prado, J. Fernandez-Rodriguez, J. Labidi, *ACS Sustain. Chem. Eng.* **2016**, *4*, 1373–1380.

[38] L. Shuai, J. Luterbacher, *ChemSusChem* **2016**, *9*, 133–155.

[39] L. Shuai, M. T. Amiri, Y. M. Questell-Santiago, F. Héroguel, Y. Li, H. Kim, R. Meilan, C. Chapple, J. Ralph, J. S. Luterbacher, *Science* **2016**, *354*, 329–333.

[40] R. Pucciariello, C. Bonini, M. D'Auria, V. Villani, G. Giammarino, G. Gorrasi, *J. Appl. Polym. Sci.* **2008**, *109*, 309–313.

[41] K. Wang, J.-X. Jiang, F. Xu, R.-C. Sun, *J. Appl. Polym. Sci.* **2010**, *116*, 1617–1625.

[42] C. Bonini, M. D'Auria, L. Emanuele, R. Ferri, R. Pucciariello, A. R. S., *J. Appl. Polym. Sci.* **2005**, *98*, 1451–1456.

[43] H. Chung, N. R. Washburn, *Green Mater.* **2012**, *1*, 137–160.

[44] M. Wayman, J. H. Lora, *TAPPI* **1978**, *61*, 55–57.

[45] C. Sasaki, M. Wanaka, H. Takagi, S. Tamura, C. Asada, Y. Nakamura, *Ind. Crops Prod.* **2013**, *43*, 757–761.

[46] S. Fernando, S. Adhikari, C. Chandrapal, N. Murali, *Energy Fuels* **2006**, *20*, 1727–1737.

[47] B. Kamm, M. Kamm, *Appl. Microbiol. Biotechnol.* **2004**, *64*, 137–145.

[48] M. Kleinert, T. Barth, *Energy Fuels* **2008**, *22*, 1371–1379.

[49] A. Aden, T. D. Foust, *Cellulose* **2009**, *16*, 535–545.

[50] T. Leskinen, S. S. Kelley, D. S. Argyropoulos, *ACS Sustain. Chem. Eng.* **2015**, *3*, 1632–1641.

[51] D. Salvachúa, R. Katahira, N. S. Cleveland, P. Khanna, M. G. Resch, B. A. Black, S. O. Purvine, E. M. Zink, A. Prieto, M. J. Martínez, A. T. Martínez, B. A. Simmons, J. M. Gladden, G. T. Beckham, *Green Chem.* **2016**, *18*, 6046–6062.

[52] M. V. Galkin, J. S. M. Samec, *ChemSusChem* **2016**, *9*, 1544–1558.

[53] A. Granata, D. S. Argyropoulos, *J. Agric. Food Chem.* **1995**, *43*, 1538–1544.

[54] A. E. Wroblewski, C. Lensink, R. Markuszewski, J. G. Verkade, *Energy Fuels* **1988**, *2*, 765–774.

[55] P. Korntner, I. Sumerskii, M. Bacher, T. Rosenau, A. Potthast, *Holzforschung* **2015**, *69*, 807–814.

[56] Y. Pu, S. Cao, A. J. Ragauskas, *Energy Environ. Sci.* **2011**, *4*, 3154–3166.

[57] Z. Xia, L. G. Akim, D. S. Argyropoulos, *J. Agric. Food Chem.* **2001**, *49*, 3573–3578.

[58] N.-E. El Mansouri, J. Salvadó, *Ind. Crops Prod.* **2007**, *26*, 116–124.

[59] R. Vanholme, B. Demedts, K. Morreel, J. Ralph, W. Boerjan, *Plant physiology* **2010**, *153*, 895–905.

[60] A. A. S. C. D. T. Balogh, R. A. M. C. de Groote, *Holzforschung* **1992**, *46*, 343–348.

[61] E. Adler, *Wood Sci. Technol.* **1977**, *11*, 169–218.

[62] I. Sulaeva, G. Zinovyev, J.-M. Plankeele, I. Sumerskii, T. Rosenau, A. Potthast, *ChemSusChem* **2017**, *10*, 629–635.

[63] M. B. Hocking, *J. Chem. Educ.* **1997**, *74*, 1055–1059.

[64] G. C. H. L. R. Sandborn, J. R. Salvesen, *Process of making vanillin*, **1936**, U.S. Patent 2057117.

[65] H. Evju, *Process for preparation of 3-methoxy-4-hydroxybenzaldehyde*, **1979**, U.S. Patent 4151207.

[66] J. Jae, G. A. Tompsett, Y.-C. Lin, T. R. Carlson, J. Shen, T. Zhang, B. Yang, C. E. Wyman, C. Connera, G. W. Huber, *Energy Environ. Sci.* **2010**, *3*, 358–365.

[67] J. Zakzeski, P. C. A. Bruijnincx, A. L. Jongerius, B. M. Weckhuysen, *Chem. Rev.* **2010**, *110*, 3552–3599.

[68] S.-H. Li, S. Liu, J. C. Colmenares, Y.-J. Xu, *Green Chem.* **2015**, *18*, 594–607.

[69] M. Kärkäs, B. Matsuura, T. Monos, G. Magallanes, C. Stephenson, *Org. Biomol. Chem.* **2016**, *14*, 1853–1914.

[70] W.-J. Liu, H. Jiang, H.-Q. Yu, *Green Chem.* **2015**, *17*, 4888–4907.

[71] S. Zhou, Y. Xue, A. M. Sharma, X. Bai, *ACS Sustain. Chem. Eng.* **2016**, *4*, 6608–6617.

[72] J. Barbier, N. Charon, N. Dupassieux, A. Loppinet-Serani, L. Mahé, J. Ponthus, M. Courtiade, A. Ducrozet, A. A. Quoineaud, F. Cansell, *Biomass and Bioenergy* **2012**, *46*, 479–491.

[73] S. Kang, X. Li, J. Fan, J. Chang, *Renew. Sust. Energ. Rev.* **2013**, *27*, 546–558.

[74] A. Kruse, A. Funke, M. M. Titirici, *Curr. Opin. Chem. Biol.* **2013**, *17*, 515–521.

[75] K. H. Kim, B. Simmons, S. Singh, *Green Chem.* **2017**, *19*, 215–224.

[76] R. Chaudharya, P. L. Dhepe, *Green Chem.* **2017**, *19*, 778–788.

[77] L. Wiermans, H. Schumacher, C.-M. Klaaßen, P. Domínguez de María, *RSC Adv.* **2015**, *5*, 4009–4018.

[78] R. Prado, A. Brandt, X. Erdocia, J. Hallet, T. Welton, J. Labidi, *Green Chem.* **2016**, *18*, 834–841.

[79] E. Feghali, G. Carrot, P. Thuéry, C. Genre, T. Cantat, *Energy Environ. Sci.* **2015**, *8*, 2734–2743.

[80] E. Feghali, T. Cantat, *ChemSusChem* **2015**, *8*, 980–984.

[81] R. Rinaldi, R. Jastrzebski, M. T. Clough, J. Ralph, M. Kennema, P. C. A. Bruijnincx, B. M. Weckhuysen, *Angew. Chem. Int. Ed.* **2016**, *55*, 8164–8215.

[82] S. Van den Bosch, W. Schutyser, R. Vanholme, T. Driessen, S.-F. Koelewijn, T. Renders, B. De Meester, W. J. J. Huijgen, W. Dehaen, C. M. Courtin, B. Lagrain, W. Boerjan, B. F. Sels, *Energy Environ. Sci.* **2015**, *8*, 1748–1763.

[83] P. Ferrini, R. Rinaldi, *Angew. Chem. Int. Ed.* **2014**, *53*, 8634–8639.

[84] O. Morales Gonzalez, J. Zhu, X. Huang, T. I. Korányi, M. Boot, E. J. Hensen, *Green Chem.* **2017**, *19*, 175–187.

[85] D. Kai, M. J. Tan, P. L. Chee, Y. K. Chua, Y. L. Yap, X. J. Loh, *Green Chem.* **2016**, *18*, 1175–1200.

[86] S. Laurichesse, L. Avérous, *Prog. Polym. Sci.* **2014**, *39*, 1266–1290.

[87] L. Hu, H. Pan, Y. Zhou, M. Zhang, *BioResources* **2011**, *6*, 1–11.

[88] T. Okamoto, H. Takeda, T. Funabiki, M. Takatani, R. Hamada, *React. Kinet. Catal. L.* **1996**, *58*, 237–242.

[89] F. G. Calvo-Flores, J. A. Dobado, J. Isac-García, F. J. Martín-Martínez, *Lignin and Lignans as Renewable Raw Materials: Chemistry, Technology and Applications*, John Wiley & Sons, Chichester, United Kingdom, **2015**, p. 306.

[90] K. Hwang, S. Park, *Synth. Commun.* **1993**, *23*, 2845–2849.

[91] H. Chung, N. R. Washburn, *ACS Appl. Mater. Interfaces* **2012**, *4*, 2840–2846.

[92] S. Zhao, M. M. Abu-Omar, *ACS Sustain. Chem. Eng.* **2017**, DOI: 10.1021/acssuschemeng.7b00440.

[93] L.-W. Zhao, B. Griggs, C.-L. Chen, J. Gratzl, C.-Y. Hse, *J. Wood Chem. Technol.* **1994**, *14*, 127–145.

[94] Y. Matsushita, S. Yasuda, *J. Wood Sci.* **2003**, *49*, 166–171.

[95] X. Yue, F. Chen, X. Zhou, *BioResources* **2011**, *6*, 2022–2034.

[96] S.-P. Huo, M.-C. Nie, Z.-W. Kong, G.-M. Wu, J. Chen, *J. Appl. Polym. Sci.* **2012**, *125*, 152–157.

[97] L. Zhang, J. Huang, *J. Appl. Polym. Sci* **2001**, *80*, 1213–1219.

[98] J. Huang, L. Zhang, *Polymer* **2002**, *43*, 2287–2294.

[99] S. Thiebaud, M. E. Borredon, *Bioresour. Technol.* **1995**, *52*, 169–173.

[100] O. Gordobil, I. Egüés, J. Labidi, *Reactive and Functional Polymers* **2016**, *104*, 45–52.

[101] Y. Chen, N. M. Stark, Z. Cai, C. R. Frihart, L. F. Lorenz, R. E. Ibach, *Bioresources* **2014**, *9*, 5488–5500.

[102] W. Thielemans, R. P. Wool, *Biomacromolecules* **2005**, *6*, 1895–1905.

[103] A. Effendi, H. Gerhauser, A. V. Bridgwater, *Renew. Sust. Energ. Rev.* **2008**, *12*, 2092–2116.

[104] L. C.-F. Wu, W. G. Glasser, *J. Appl. Polym. Sci.* **1984**, *29*, 1111–1123.

[105] H. Sadeghifar, C. Cui, D. S. Argyropoulos, *Ind. Eng. Chem. Res* **2012**, *51*, 16713–16720.

[106] C. Cui, H. Sadeghifar, S. Sen, D. S. Argyropoulos, *BioResources* **2013**, *8*, 864–886.

[107] H. Sadeghifar, D. S. Argyropoulos, *ACS Sustain. Chem. Eng.* **2015**, *3*, 349–356.

[108] V. E. Madzhidova, G. N. Dalimova, K. A. Abduazimov, *Chem. Nat. Compd.* **1998**, *34*, 179–181.

[109] M. K. R. Konduri, P. Fatehi, *ACS Sustain. Chem. Eng.* **2015**, *3*, 1172–1182.

[110] T. Aro, P. Fatehi, *ChemSusChem* **2017**, *10*, 1861–1877.

[111] E. Heuser, R. Sieber, *Angew. Chem.* **1913**, *26*, 801–806.

[112] E. Johansson, C. Krantz-Rülcker, B. X. Zhang, G. Öberg, *Soil Biol. Biochem.* **2000**, *32*, 1029–1032.

[113] P. Buono, A. Duval, P. Verge, L. Averous, Y. Habibi, *ACS Sustain. Chem. Eng.* **2016**, *4*, 5212–5222.

[114] S. Hirose, T. Hatakeyama, H. Hatakeyama, *Macromol. Symp.* **2003**, *197*, 157–169.

[115] D. Feldman, M. Khoury, *J. Adhes. Sci. Technol.* **1988**, *2*, 107–116.

[116] D. Feldman, D. Banu, A. Natansohn, J. Wang, *J. Appl. Polym. Sci.* **1991**, *42*, 1537–1550.

[117] D. Feldman, D. Banu, C. Luchian, J. Wang, *J. Appl. Polym. Sci.* **1991**, *42*, 1307–1318.

[118] J. Wang, D. Banu, D. Feldman, *J. Adhes. Sci. Technol.* **1992**, *6*, 587–598.

[119] G.-H. Delmas, B. Benjelloun-Mlayah, Y. L. Bigot, M. Delmas, *J. Appl. Polym. Sci.* **2013**, *127*, 1863–1872.

[120] H. Cheradame, M. Detoisien, A. Gandini, F. Pla, G. Roux, *British Polymer Journal* **1989**, *21*, 269–275.

[121] V. P. Saraf, W. G. Glasser, G. L. Wilkes, J. E. McGrath, *J. Appl. Polym. Sci.* **1985**, *30*, 2207–2224.

[122] H. Pohjanlehto, H. M. Setälä, D. E. Kiely, A. G. McDonald, *J. Appl. Polym. Sci.* **2014**, *131*, 39714.

[123] L. B. Tavares, C. V. Boas, G. R. Schleder, A. M. Nacas, D. S. Rosa, D. J. Santos, *Express Polymer Letters* **2016**, *10*, 927–940.

[124] H. Nadji, C. Bruzzèse, M. N. Belgacem, A. Benaboura, A. Gandini, *Macromol. Mater. Eng.* **2005**, *290*, 1009–1016.

[125] G. Griffini, V. Passoni, R. Suriano, M. Levi, S. Turri, *ACS Sustain. Chem. Eng.* **2015**, *3*, 1145–1154.

[126] Z. Jia, C. Lu, P. Zhou, L. Wang, *RSC Adv.* **2015**, *5*, 53949–53955.

[127] H. Yoshida, R. Mörck, K. P. Kringstad, H. Hatakeyama, *J. Appl. Polym. Sci.* **1990**, *40*, 1819–1832.

[128] M. N. Vanderlaan, R. W. Thring, *Biomass Bioenergy* **1998**, *14*, 525–531.

[129] D. V. Evtuguin, J. P. Andreolety, A. Gandini, *Eur. Polym. J.* **1998**, *34*, 1163–1169.

[130] T. Hatakeyama, Y. Asano, H. Hatakeyama, *Macromol. Symp.* **2003**, *197*, 171–180.

[131] H. Hatakeyama, N. Kato, T. Nanbo, T. Hatakeyama, *J. Mater. Sci.* **2012**, *47*, 7254–7261.

[132] V. P. Saraf, W. G. Glasser, G. L. Wilkes, J. E. McGrath, *Polymer Bulletin* **1984**, *12*, 1–5.

[133] O. Faruk, M. Sain, R. Farnood, Y. Pan, H. Xiao, *J. Polym. Environ.* **2013**, *22*, 279–288.

[134] K. Weissermel, H.-J. Arpe, *Ind. Org. Chem.*, WILEY-VCH, 4th ed., **2003**.

[135] P. C. Muller, S. S. Kelley, W. G. Glasser, *J. Adhes.* **1984**, *17*, 185–206.

[136] P. C. Muller, W. G. Glasser, *J. Adhes.* **1984**, *17*, 157–173.

[137] L. Kouisni, Y. Fang, M. Paleologou, B. Ahvazi, J. Hawari, Y. Zhang, X.-M. Wang, *Cell. Chem. Technol.* **2011**, *45*, 515–520.

[138] P. Benar, A. R. Gonçalves, D. Mandelli, U. Schuchardt, *Bioresour. Technol.* **1999**, *68*, 11–16.

[139] A. Tejado, G. Kortaberria, C. Pena, J. Labidi, J. M. Echeverría, *J. Appl. Polym. Sci.* **2007**, *106*, 2313–2319.

[140] A. Donmez Cavdar, H. Kalaycioglu, S. Hiziroglu, *J. Mater. Process. Technol.* **2008**, *202*, 559–563.

[141] M. Kuroe, T. Tsunoda, Y. Kawano, A. Takahashi, *J. Appl. Polym. Sci.* **2013**, *129*, 310–315.

[142] M. Kunaver, E. Jasiukaityte, N. Cuk, J. T. Guthrie, *J. Appl. Polym. Sci.* **2010**, *115*, 1265–1271.

[143] G. Sivasankarapillai, A. G. McDonald, *Biomass Bioenergy* **2011**, *35*, 919–931.

[144] G. E. Agafitei, M. C. Pascu, G. Cazacu, A. Stoleriu, N. Popa, R. Hogea, C. Vasile, *Angew. Makromol. Chem.* **1999**, *267*, 44–51.

[145] H. Nitz, H. Semke, R. Mülhaupt, *Macromol. Mater. Eng.* **2001**, *286*, 737–743.

[146] Y. Li, S. Sarkanen, *Macromolecules* **2002**, *35*, 9707–9715.

[147] Y. Li, S. Sarkanen, *Macromolecules* **2002**, *35*, 9707–9715.

[148] A. V. Maldhure, J. D. Ekhe, E. Deenadayalan, *J. Appl. Polym. Sci.* **2012**, *125*, 1701–1712.

[149] M. Mikulasova, B. Kosikova, P. Alexy, F. Kacik, *World J. Microbiol. Biotechnol.* **2001**, *17*, 601–607.

[150] P. Alexy, B. Košíková, G. Podstránska, *Polymer* **2000**, *41*, 4901–4908.

[151] D. Feldman, D. Banu, *J. Appl. Polym. Sci.* **1997**, *66*, 1731–1744.

[152] S. Kubo, J. F. Kadla, *Macromolecules* **2004**, *37*, 6904–6911.

[153] J. F. Kadla, S. Kubo, *Macromolecules* **2003**, *36*, 7803–7811.

[154] F. Monteil-Rivera, L. Paquet, *Ind. Crops Prod.* **2015**, *65*, 446–453.

[155] S. Laurichesse, C. Huillet, L. Avérous, *Green Chem.* **2014**, *16*, 3958–3970.

[156] S. Sen, S. Patil, D. S. Argyropoulos, *Green Chem.* **2015**, *17*, 1077–1087.

[157] A. Llevot, B. Monney, A. Sehlinger, S. Behrens, M. A. R. Meier, *Chem. Commun.* **2017**, *53*, 5175–5178.

[158] I. Kühnel, J. Podschun, B. Saake, R. Lehnen, *Holzforschung* **2015**, *69*, 531–538.

[159] M. A. Rahman, D. De Santis, G. Spagnoli, G. Ramorino, M. Penco, V. T. Phuong, A. Lazzeri, *J. Appl. Polym. Sci.* **2013**, *129*, 202–214.

[160] C. Mu, L. Xue, J. Zhu, M. Jiang, Z. Zhou, *BioResources* **2014**, *9*, 5557–5566.

[161] I. Spiridon, K. Leluk, A. M. Resmerita, R. N. Darie, *Compos. Part B Eng.* **2015**, *69*, 342–349.

[162] S. Livi, V. Bugatti, M. Marechal, B. G. Soares, G. M. O. Barra, J. Duchet-Rumeau, J.-F. Gérard, *RSC Adv.* **2015**, *5*, 1989–1998.

[163] S. Wang, Y. Li, H. Xiang, Z. Zhou, T. Chang, M. Zhu, *Compos. Sci. Technol.* **2015**, *119*, 20–25.

[164] Y. L. Chung, J. V. Olsson, R. J. Li, C. W. Frank, R. M. Waymouth, S. L. Billington, E. S. Sattely, *ACS Sustain. Chem. Eng.* **2013**, *1*, 1231–1238.

[165] Y. Sun, L. Yang, X. Lu, C. He, *J. Mat. Chem. A* **2015**, *3*, 3699–3709.

[166] S. Laurichesse, L. Avérous, *Polymer* **2013**, *54*, 3882–3890.

[167] X. Liu, E. Zong, J. Jiang, S. Fu, J. Wang, B. Xu, W. Li, X. Lin, Y. Xu, C. Wang, F. Chu, *Int. J. Biol. Macromolec.* **2015**, *81*, 521–529.

[168] R. A. Pérez-Camargo, G. Saenz, S. Laurichesse, M. T. Casas, J. Puiggalí, L. Avérous, A. J. Müller, *J. Polym. Sci. Pol. Phys.* **2015**, *53*, 1736–1750.

[169] Y. Matsushita, T. Inomata, Y. Takagi, T. Hasegawa, K. Fukushima, *J. Wood Sci.* **2011**, *57*, 214–218.

[170] A. Lee, Y. Deng, *Eur. Polym. J.* **2015**, *63*, 67–73.

[171] C. G. da Silva, S. Grelier, F. Pichavant, E. Frollini, A. Castellan, *Ind. Crops Prod.* **2013**, *42*, 87–95.

[172] A. Llevot, E. Grau, S. Carlotti, S. Grelier, H. Cramail, *Macromol. Rapid Commun.* **2016**, *37*, 9–28.

[173] A. Llevot, E. Grau, S. Carlotti, S. Grelier, H. Cramail, *J. Mol. Catal. B: Enzym.* **2016**, *125*, 34–41.

[174] M. Fache, B. Boutevin, S. Caillol, *Green Chem.* **2016**, *18*, 712–725.

[175] L. Mialon, A. G. Pemba, S. A. Miller, *Green Chem.* **2010**, *12*, 1704–1706.

[176] L. Mialon, R. Vanderhenst, A. G. Pemba, S. A. Miller, *Macromol. Rapid Commun.* **2011**, *32*, 1386–1392.

[177] A.-A. G. Shaikh, S. Sivaram, *Chem. Rev.* **1996**, *96*, 951–976.

[178] Y. P. Patil, P. J. Tambade, S. R. Jagtap, B. M. Bhanage, *Frontiers of Chemical Engineering in China* **2010**, *4*, 213–235.

[179] O. Kreye, H. Mutlu, M. A. R. Meier, *Green Chem.* **2013**, *15*, 1431–1455.

[180] F. Aricò, P. Tundo, *Russ. Chem. Rev.* **2010**, *79*, 479–489.

[181] X. Miao, C. Fischmeister, C. Bruneau, P. H. Dixneuf, *ChemSusChem* **2008**, *1*, 813–816.

[182] M. Unverferth, O. Kreye, A. Prohammer, M. A. R. Meier, *Macromol. Rapid Commun.* **2013**, *34*, 1569–1574.

[183] O. Kreye, S. Wald, M. A. R. Meier, *Adv. Synth. Catal.* **2013**, *355*, 81–86.

[184] P. Tundo, *Pure Appl. Chem.* **2012**, *84*, 411–423.

[185] H. Mutlu, J. Ruiz, S. C. Solleder, M. A. R. Meier, *Green Chem.* **2012**, *14*, 1728–1735.

[186] Y. Ono, *Appl. Catal. A* **1997**, *155*, 133–166.

[187] P. Tundo, M. Selva, *Acc. Chem. Res.* **2002**, *35*, 706–716.

[188] S. Ouk, S. Thiébaud, E. Borredon, P. Le Gars, *Green Chem.* **2002**, *4*, 431–435.

[189] S. Ouk, S. Thiébaud, E. Borredon, P. Le Gars, *Appl. Catal. A* **2003**, *241*, 227–233.

[190] J. N. G. Stanley, M. Selva, A. F. Masters, T. Maschmeyer, A. Perosa, *Green Chem.* **2013**, *15*, 3195–3204.

[191] W.-C. Shieh, S. Dell, O. Repic, *Org. Lett.* **2001**, *3*, 4279–4281.

[192] L. Guerrero R., I. A. Rivero, *ARKIVOC* **2008**, *11*, 295–306.

[193] Z. L. Shen, X. Z. Jiang, W. M. Mo, B. X. Hua, N. Suna, *Green Chem.* **2005**, *7*, 97–99.

[194] M. Selva, P. Tundo, T. Foccardi, *J. Org. Chem.* **2005**, *70*, 2476–2485.

[195] M. Selva, P. Tundo, *J. Org. Chem.* **2006**, *71*, 1464–1470.

[196] M. Selva, E. Militello, M. Fabris, *Green Chem.* **2008**, *10*, 73–79.

[197] W.-C. Shieh, S. Dell, O. Repic, *J. Org. Chem.* **2002**, *67*, 2188–2191.

[198] A. Dhakshinamoorthy, A. Sharmila, K. Pitchumani, *Chem. Eur. J.* **2010**, *16*, 1128–1132.

[199] T. Weidlich, M. Pokorny, Z. Padelkova, A. Ruzicka, *Green Chem. Lett. Rev.* **2007**, *1*, 53–59.

[200] M. Selva, C. A. Marques, P. Tundo, *J. Chem. Soc. Perkin Trans. 1* **1995**, 1889–1893.

[201] A. Procopio, P. Costanzo, M. Curini, M. Nardi, M. Oliverio, R. Paonessaa, *Synthesis* **2011**, 73–78.

[202] O. Kreye, T. Tóth, M. A. R. Meier, *Eur. Polym. J.* **2011**, *47*, 1804–1816.

[203] T. Posner, *Chem. Ber.* **1905**, *38*, 646–657.

[204] L. V. Natarajan, C. K. Shepherd, D. M. Brandelik, R. L. Sutherland, S. Chandra, V. P. Tondiglia, D. Tomlin, T. J. Bunning, *Chem. Mat.* **2003**, *15*, 2477–2484.

[205] C. Walling, W. Helmreich, *J. Am. Chem. Soc.* **1959**, *81*, 1144–1148.

[206] O. Türünç, M. A. R. Meier, *Eur. J. Lipid Sci. Tech.* **2013**, *115*, 41–54.

[207] U. Biermann, W. Butte, R. Koch, P. a. Fokou, O. Türünç, M. A. R. Meier, J. O. Metzger, *Chem. Eur. J.* **2012**, *18*, 8201–8207.

[208] M. Black, J. W. Rawlins, *Eur. Polym. J.* **2009**, *45*, 1433–1441.

[209] M. Desroches, S. Caillol, V. Lapinte, R. Auvergne, B. Boutevin, *Macromolecules* **2011**, *44*, 2489–2500.

[210] R. J. González-Paz, C. Lluch, G. Lligadas, J. C. Ronda, M. Galià, V. Cádiz, *J. Polym. Sci. A Polym. Chem.* **2011**, *49*, 2407–2416.

[211] O. Türünç, M. A. R. Meier, *Green Chem.* **2011**, *13*, 314–320.

[212] O. van den Berg, T. Dispinar, B. Hommez, F. E. Du Prez, *Eur. Polym. J.* **2013**, *49*, 804–812.

[213] N. Kolb, M. A. R. Meier, *Eur. Polym. J.* **2013**, *49*, 843–852.

[214] M. Unverferth, M. A. R. Meier, *Polymer* **2014**, *55*, 5571–5575.

[215] K. L. Killops, L. M. Campos, C. J. Hawker, *J. Am. Chem. Soc.* **2008**, *130*, 5062–5064.

[216] A. Dondoni, *Angew. Chem. Int. Ed.* **2008**, *47*, 8995–8997.

[217] P. Antoni, M. J. Robb, L. Campos, M. Montanez, A. Hult, E. Malmström, M. Malkoch, C. J. Hawker, *Macromolecules* **2010**, *43*, 6625–6631.

[218] A. Sehlinger, R. Schneider, M. A. R. Meier, *Eur. Polym. J.* **2014**, *50*, 150–157.

[219] S. C. Solleder, M. A. R. Meier, *Angew. Chem. Int. Ed.* **2014**, *53*, 711–714.

[220] L. M. Campos, K. L. Killops, R. Sakai, J. M. J. Paulusse, D. Damiron, E. Drockenmuller, B. W. Messmore, C. J. Hawker, *Macromolecules* **2008**, *41*, 7063–7070.

[221] I. M. Gabbasova, L. A. Baeva, Z. F. Rakhimova, E. A. Kantor, N. K. Lyapina, *Petroleum Chemistry* **2015**, *55*, 235–237.

[222] S. Reinelt, D. Steinke, H. Ritter, *Beilstein J. Org. Chem.* **2014**, *10*, 680–691.

[223] T. Tamai, K. Fujiwara, S. Higashimae, A. Nomoto, A. Ogawa, *Org. Lett.* **2016**, *18*, 2114–2117.

[224] G. Yang, S. L. Kristufek, L. A. Link, K. L. Wooley, M. L. Robertson, *Macromolecules* **2015**, *48*, 8418–8427.

[225] M. Firdaus, M. A. R. Meier, *Eur. Polym. J.* **2013**, *49*, 156–166.

[226] M. E. Jawerth, M. Lawoko, S. Lundmark, C. Perez-Berumen, M. Johansson, *RSC Adv.* **2016**, *6*, 96281–96288.

[227] P. Buono, A. Duval, L. Averous, Y. Habibi, *ChemSusChem* **2017**, *10*, 984–992.

[228] L. Zoia, A. Salati, P. Frigerio, M. Orlandi, *BioResources* **2014**, *9*, 6540–6561.

[229] M. Fache, E. Darroman, V. Besse, R. Auvergne, S. Caillol, B. Boutevin, *Green Chem.* **2014**, *16*, 1987–1998.

[230] R. Brückner, *Reaktionsmechanismen*, Spektrum Akademischer Verlag, Springer Verlag, Berlin und Heidelberg, 3rd ed., **2004**, p. 626.

[231] L. Claisen, *Chemische Berichte* **1912**, *45*, 3157–3166.

[232] H. Mutlu, M. A. R. Meier, *Eur. J. Lipid Sci. Tech.* **2010**, *112*, 10–30.

[233] A. S. Trita, *PhD thesis*, Ruhr-Universität Bochum, *current work*.

[234] S. Baader, P. E. Podsiadly, D. J. Cole-Hamilton, L. J. Gooßen, *Green Chem.* **2014**, *16*, 4885–4890.

[235] S. Riegsinger, *bachelor thesis*, Karlsruhe Institute of Technology (KIT), November **2015**.

[236] A. S. Trita, L. C. Over, J. Pollini, S. Baader, S. Riegsinger, M. A. R. Meier, L. J. Gooßen, *Green Chem.* **2017**, *19*, 3051–3060.

[237] C. K. Lyon, E. O. Hill, E. B. Berda, *Macromol. Chem. Phys.* **2016**, *217*, 501–508.

[238] C. Cao, A. S. Hay, *J. Polym. Sci. A Polym. Chem.* **1995**, *33*, 2731–2739.

[239] B. G. Harvey, A. J. Guenthner, H. a. Meylemans, S. R. L. Haines, K. R. Lamison, T. J. Groshens, L. R. Cambrea, M. C. Davis, W. W. Lai, *Green Chem.* **2015**, *17*, 1249–1258.

[240] K. Kunal, C. G. Robertson, S. Pawlus, S. F. Hahn, A. P. Sokolov, *Macromolecules* **2008**, *41*, 7232–7238.

[241] Q. Qin, G. B. McKenna, *J. Non-Cryst. Solids* **2006**, *352*, 2977–2985.

[242] J. Font, J. Muntasell, *Mater. Res. Bull.* **2000**, *35*, 681–687.

[243] G. Adam, J. Hay, I. Parsons, R. Haward, *Polymer* **1976**, *17*, 51–57.

[244] C. E. Hoyle, T. Y. Lee, T. Roper, *J. Polym. Sci. Pol. Chem.* **2004**, *42*, 5301–5338.

[245] C. E. Hoyle, C. N. Bowman, *Angew. Chem. Int. Ed.* **2010**, *49*, 1540–1573.

[246] P. J. Deuss, K. Barta, *Coord. Chem. Rev.* **2016**, *306*, 510–532.

[247] V. P. Saraf, W. G. Glasser, *J. Appl. Polym. Sci.* **1984**, *29*, 1831–1841.

[248] C. A. Cateto, M. F. Barreiro, C. Ottati, M. Lopretti, A. E. Rodrigues, M. N. Belgacem, *J. Cell. Plast.* **2013**, *50*, 81–95.

[249] H. Zhu, Z. Peng, Y. Chen, G. Li, L. Wang, Y. Tang, R. Pang, Z. U. H. Khan, P. Wan, *RSC Adv.* **2014**, *4*, 55271–55279.

[250] A. Tejado, G. Kortaberria, C. Pena, M. Blanco, J. Labidi, J. M. Echeverría, I. Mondragon, *J. Appl. Polym. Sci.* **2008**, *107*, 159–165.

[251] E. Jakab, O. Faix, F. Till, T. Székely, *Holzforschung* **1991**, *45*, 355–360.

[252] A. W. Williamson, *Liebigs Ann. Chem.* **1851**, *77*, 37–49.

[253] P. Tundo, F. Trotta, G. Moraglio, F. Logorati, *Ind. Eng. Chem. Res* **1988**, *27*, 1565–1571.

[254] P. Tundo, G. Moraglio, F. Trotta, *Ind. Eng. Chem. Res.* **1989**, *28*, 881–890.

[255] Y. Lee, I. Shimizu, *Synlett* **1998**, *10*, 1063–1064.

[256] D. S. Argyropoulos, H. I. Bolker, C. Heitner, Y. Archipov, *Holzforschung* **1993**, *47*, 50–56.

[257] A. Bomben, M. Selva, T. Pietro, L. Valli, *Ind. Eng. Chem. Res* **1999**, *38*, 2075–2079.

[258] T. Gruendling, M. Guilhaus, C. Barner-Kowollik, *Anal. Chem.* **2008**, *80*, 6915–6927.

[259] L. Montero De Espinosa, M. A. R. Meier, *Eur. Polym. J.* **2011**, *47*, 837–852.

[260] M. R. Islam, M. D. H. Beg, S. S. Jamari, *J. Appl. Polym. Sci.* **2014**, *131*, 9016–9028.

[261] A. Llevot, *J. Am. Oil Chem. Soc.* **2017**, *94*, 169–186.

[262] M. A. R. Meier, *Macromol. Chem. Phys.* **2009**, *210*, 1073–1079.

[263] N. Calderon, *Acc. Chem. Res.* **1972**, *5*, 127–132.

[264] M. G. M. A. W. Anderson, *M. G. M. A. W. Anderson*, **1955**, US-A 2721 189, [*Chem. Abstr.* **1955**, *50*, 3008i].

[265] R. L. Banks, G. C. Bailey, *Ind. Eng. Chem. Prod. Res. Dev.* **1964**, *3*, 170–173.

[266] G. Dall'Asta, G. Mazzanti, G. Natta, L. Porri, *Makromol. Chem.* **1962**, *56*, 224–227.

[267] G. Natta, *Experientia* **1963**, *19*, 609–618.

[268] G. Natta, G. Dall'Asta, G. Mazzanti, *Angew. Chem. Int. Ed.* **1964**, *3*, 723–729.

[269] G. Natta, G. Dall'Asta, L. Porri, *Makromol. Chem.* **1965**, *81*, 253–257.

[270] R. H. Grubbs, T. K. Brunk, *J. Am. Chem. Soc.* **1972**, *94*, 2538–2540.

[271] R. H. Grubbs, A. Miyashita, *J. Am. Chem. Soc.* **1978**, *100*, 7416–7418.

[272] J.-L. Herisson, Y. Chauvin, *Makromol. Chem.* **1971**, *141*, 161–176.

[273] C. P. Casey, T. J. Burkhardt, *J. Am. Chem. Soc.* **1974**, *96*, 7808–7809.

[274] T. J. Katz, J. McGinnis, *J. Am. Chem. Soc.* **1975**, *97*, 1592–1594.

[275] R. H. Grubbs, P. L. Burk, D. D. Carr, *J. Am. Chem. Soc.* **1975**, *97*, 3265–3267.

[276] R. H. Grubbs, D. D. Carr, C. Hoppin, P. L. Burk, *J. Am. Chem. Soc.* **1976**, *98*, 3478–3483.

[277] T. M. Trnka, R. H. Grubbs, *Acc. Chem. Res.* **2001**, *34*, 18–29.

[278] R. R. Schrock, J. Feldman, L. F. Cannizzo, R. H. Grubbs, *Macromolecules* **1987**, *20*, 1169–1172.

[279] R. R. Schrock, J. S. Murdzek, G. C. Bazan, J. Robbins, M. DiMare, M. O'Regan, *J. Am. Chem. Soc.* **1990**, *112*, 3875–3886.

[280] G. C. Bazan, E. Khosravi, R. R. Schrock, W. J. Feast, V. C. Gibson, M. B. O'Regan, J. K. Thomas, W. M. Davis, *J. Am. Chem. Soc.* **1990**, *112*, 8378–8387.

[281] G. C. Bazan, J. H. Oskam, H. N. Cho, L. Y. Park, R. R. Schrock, *J. Am. Chem. Soc.* **1991**, *113*, 6899–6907.

[282] S. T. Nguyen, R. H. Grubbs, J. W. Ziller, *J. Am. Chem. Soc.* **1993**, *115*, 9858–9859.

[283] M. Scholl, S. Ding, C. W. Lee, R. H. Grubbs, *Org. Lett.* **1999**, *1*, 953–956.

[284] S. B. Garber, J. S. Kingsbury, B. L. Gray, A. H. Hoveyda, *J. Am. Chem. Soc.* **2000**, *122*, 8168–8179.

[285] T. Vorfalt, K. J. Wannowius, V. Thiel, H. Plenio, *Chem. Eur. J.* **2010**, *16*, 12312–12315.

[286] S. H. Hong, D. P. Sanders, C. W. Lee, R. H. Grubbs, *J. Am. Chem. Soc.* **2005**, *127*, 17160–17161.

[287] N. Gimeno, P. Formentín, J. H. G. Steinke, R. Vilar, *Eur. J. Org. Chem.* **2007**, 918–924.

[288] K. C. Hultzsch, J. A. Jernelius, A. H. Hoveyda, R. R. Schrock, *Angew. Chem. Int. Ed.* **2002**, *41*, 589–593.

[289] J. Hartung, P. K. Dornan, R. H. Grubbs, *J. Am. Chem. Soc.* **2014**, *136*, 13029–13037.

[290] K. Endo, R. H. Grubbs, *J. Am. Chem. Soc.* **2011**, *133*, 8525–8527.

[291] S. Warwel, F. Brüse, C. Demes, M. Kunz, *Ind. Crops Prod.* **2004**, *20*, 301–309.

[292] X. Miao, C. Fischmeister, C. Bruneau, P. H. Dixneuf, *ChemSusChem* **2009**, *2*, 542–545.

[293] A. Rybak, M. A. R. Meier, *Green Chem.* **2007**, *9*, 1356–1361.

[294] S. Warwel, F. Brüse, C. Demes, M. Kunz, M. Rüsch gen. Klaas, *Chemosphere* **2001**, *43*, 39–48.

[295] Q. Tian, R. C. Larock, *J. Am. Oil Chem. Soc.* **2002**, *79*, 479–488.

[296] H. Mutlu, L. Montero de Espinosa, M. A. R. Meier, *Chemical Society reviews* **2011**, *40*, 1404–1445.

[297] M. Sacristán, J. C. Ronda, M. Galià, V. Càdiz, *J. Appl. Polym. Sci.* **2011**, *122*, 1649–1658.

[298] L. Montero de Espinosa, M. A. R. Meier, J. C. Ronda, M. Galià, V. Càdiz, *J. Polym. Sci. A Polym. Chem.* **2010**, *48*, 1649–1660.

[299] T. Lebarbé, A. S. More, P. S. Sane, E. Grau, C. Alfos, H. Cramail, *Macromol. Rapid Commun.* **2014**, *35*, 479–483.

[300] T. Lebarbé, M. Neqal, E. Grau, C. Alfos, H. Cramail, *Green Chem.* **2014**, *16*, 1755–1758.

[301] M. Winkler, J. O. Mueller, K. K. Oehlenschlaeger, L. Montero De Espinosa, M. A. R. Meier, C. Barner-Kowollik, *Macromolecules* **2012**, *45*, 5012–5019.

[302] L. Montero de Espinosa, M. A. R. Meier, *Chem. Commun.* **2011**, *47*, 1908–1910.

[303] O. Kreye, T. Tóth, M. A. R. Meier, *Eur. J. Lipid Sci. Tech.* **2011**, *113*, 31–38.

[304] P. A. Fokou, M. A. R. Meier, *J. Am. Chem. Soc.* **2009**, *131*, 1664–1665.

[305] P. A. Fokou, M. A. R. Meier, *Macromol. Rapid Commun.* **2010**, *31*, 368–373.

[306] S. J. Park, F. L. Jin, J. R. Lee, J. S. Shin, *Eur. Polym. J.* **2005**, *41*, 231–237.

[307] M. A. Tehfe, J. Lalevée, D. Gigmes, J. P. Fouassier, *Macromolecules* **2010**, *43*, 1364–1370.

[308] A. Zlatanić, Z. S. Petrović, K. Dušek, *Biomacromolecules* **2002**, *3*, 1048–1056.

[309] A. Campanella, J. J. La Scala, R. P. Wool, *Polym. Eng. Sci.* **2009**, *49*, 2384–2392.

[310] P. H. Henna, R. C. Larock, *Macromol. Mater. Eng.* **2007**, *292*, 1201–1209.

[311] Y. Xia, Y. Lu, R. C. Larock, *Polymer* **2010**, *51*, 53–61.

[312] Y. Xia, R. C. Larock, *Polymer* **2010**, *51*, 2508–2514.

[313] Y. Lu, R. C. Larock, *ChemSusChem* **2009**, *2*, 136–147.

[314] S. Sen, S. Patil, D. S. Argyropoulos, *Green Chem.* **2015**, *17*, 4862–4887.

[315] M. Bandini, P. G. Cozzi, S. Licciulli, A. Umani-Ronchi, *Synthesis* **2004**, *3*, 409–414.

[316] Y. Teramoto, S.-H. Lee, T. Endo, *Polymer Journal* **2009**, *41*, 219–227.

[317] S. F. Thames, H. Yu, *Surf Coat Technol.* **1999**, *115*, 208–214.

[318] T. Tsujimoto, H. Uyama, *ACS Sustain. Chem. Eng.* **2014**, *2*, 2057–2062.

[319] C. Ding, P. S. Shuttleworth, S. Makin, J. Clark, A. S. Matharu, *Green Chem.* **2015**, *17*, 4000–4008.

[320] T. Geens, L. Goeyens, A. Covaci, *Int. J. Hyg. Environ. Health* **2011**, *214*, 339–347.

[321] M. Bondesson, J. Jönsson, I. Pongratz, N. Olea, J.-P. Cravedi, D. Zalko, H. Håkansson, K. Halldin, D. Di Lorenzo, C. Behl, D. Manthey, P. Balaguer, B. Demeneix, J.-B. Fini, V. Laudet, J.-A. Gustafsson, *Reprod. Toxicol.* **2009**, *28*, 563–567.

[322] H. H. Le, E. M. Carlson, J. P. Chua, S. M. Belcher, *Toxicol. Lett.* **2008**, *176*, 149–156.

[323] L. N. Vandenberg, R. Hauser, M. Marcus, N. Olea, W. V. Welshons, *Reprod. Toxicol.* **2007**, *24*, 139–177.

[324] J. H. Kang, F. Kondo, Y. Katayama, *Toxicology* **2006**, *226*, 79–89.

[325] E. C. Dodds, W. Lawson, *Nature* **1936**, *137*, 996.

[326] Merchant Research & Consulting, *World BPA Production*, `https://mcgroup.co.uk/`, online; accessed June 2017.

[327] M. P. Pandey, C. S. Kim, *Chem. Eng. Technol.* **2011**, *34*, 29–41.

[328] M. Fache, R. Auvergne, B. Boutevin, S. Caillol, *Eur. Polym. J.* **2015**, *67*, 527–538.

[329] M. Fache, A. Viola, R. Auvergne, B. Boutevin, S. Caillol, *Eur. Polym. J.* **2015**, *68*, 526–535.

[330] C. François, S. Pourchet, G. Boni, S. Fontaine, Y. Gaillard, V. Placet, M. V. Galkin, A. Orebom, J. Samec, L. Plasseraud, *RSC Adv.* **2016**, *6*, 68732–68738.

[331] C. I. Simionescu, V. Rusan, M. M. Macoveanu, G. Cazacu, R. Lipsa, C. Vasile, A. Stoleriu, A. Ioanid, *Compos. Sci. Technol.* **1993**, *48*, 317–323.

[332] Y. Nonaka, B. Tomita, Y. Hatano, *Holzforschung* **1997**, *51*, 183–187.

[333] Q. F. Yin, M. W. Di, *Adv. Compos. Mater.* **2012**, *482-484*, 1959–1962.

[334] T. Malutan, R. Nicu, V. I. Popa, *BioResources* **2008**, *3*, 1371–1376.

[335] A. Singh, K. Yadav, A. Kumar Sen, *American Journal of Polymer Science* **2012**, *2*, 14–18.

[336] P. Feng, F. Chen, *BioResources* **2012**, *7*, 2860–2870.

[337] F. Ferdosian, Z. Yuan, M. Anderson, C. C. Xu, *J. Anal. Appl. Pyrolysis* **2016**, *119*, 124–132.

[338] F. Ferdosian, Y. Zhang, Z. Yuan, M. Anderson, C. C. Xu, *Eur. Polym. J.* **2016**, *82*, 153–165.

[339] J. Xin, M. Li, R. Li, M. P. Wolcott, J. Zhang, *ACS Sustain. Chem. Eng.* **2016**, *4*, 2754–2761.

[340] C. Asada, S. Basnet, M. Otsuka, C. Sasaki, Y. Nakamura, *Int. J. Biol. Macromolec.* **2015**, *74*, 413–419.

[341] N. E. El Mansouri, Q. Yuan, F. Huang, *BioResources* **2011**, *6*, 2647–2662.

[342] M. G. González, J. C. Cabanelas, J. Baselga, *Infrared Spectroscopy - Materials Science, Engineering and Technology*, InTech, Rijeka, Chapter 13, 2nd ed., **2012**, pp. 261–284.

[343] H. El-Saied, A. A. M. A. Nada, *Polymer Degrad. Stabil.* **1993**, *40*, 417–421.

[344] R. Sun, J. Tomkinson, G. Lloyd Jones, *Polymer Degrad. Stabil.* **2000**, *68*, 111–119.

[345] H. Yoshida, R. Mörck, K. P. Kringstad, *Holzforschung* **1987**, *41*, 171–176.

[346] F. Ferdosian, Z. Yuan, M. Anderson, C. C. Xu, *J-FOR* **2012**, *2*, 11–15.

[347] R. Auvergne, S. Caillol, G. David, B. Boutevin, J. P. Pascault, *Chem. Rev.* **2014**, *114*, 1082–1115.

[348] J. Galy, A. Sabra, J.-p. Pascault, *Polym. Eng. Sci.* **1986**, *26*, 1514–1523.

[349] M. Chrysanthos, J. Galy, J.-P. Pascault, *Polymer* **2011**, *52*, 3611–3620.

[350] A. Cherdoud-Chihani, M. Mouzali, M. J. M. Abadie, *J. Appl. Polym. Sci.* **2003**, *87*, 2033–2051.

[351] A. A. Roche, J. Bouchet, *Application of Fracture Mechanics to Polymers, Adhesives and Composites*, Elsevier Ltd and ESIS, 1st ed., **2004**, pp. 249–257.

[352] T. Okabe, Y. Oya, K. Tanabe, G. Kikugawa, K. Yoshioka, *Eur. Polym. J.* **2016**, *80*, 78–88.

[353] T. Koike, *Polym. Eng. Sci.* **2012**, *52*, 701–717.

[354] I. Kaya, F. Doĝan, M. Gül, *Polymers and Polymer Composites* **2011**, *121*, 3211–3222.

[355] J. Qin, H. Liu, P. Zhang, M. Wolcott, J. Zhang, *Polymer International* **2014**, *63*, 760–765.

[356] C. Aouf, H. Nouailhas, M. Fache, S. Caillol, B. Boutevin, H. Fulcrand, *Eur. Polym. J.* **2013**, *49*, 1185–1195.

[357] C. Aouf, J. Lecomte, P. Villeneuve, E. Dubreucq, H. Fulcrand, *Green Chem.* **2012**, *14*, 2328–2336.

[358] A. Goti, F. Cardona, *Hydrogen Peroxide in Green Oxidation Reactions: Recent Catalytic Processes*, in *Green Chemical Reactions* (Eds.: P. Tundo, V. Esposito), Springer Netherlands, Dordrecht, **2008**.

[359] P. Kumar, S. M. Sharma, *Int. J. Appl. Res.* **2016**, *2*, 337–341.

[360] T. Itoh, U. Hanefeld, *Green Chem.* **2017**, *19*, 331–332.

[361] N. Prileschajew, *Ber. Dtsch. Chem. Ges.* **1909**, *42*, 4811–4815.

[362] S. C. Chua, X. Xu, Z. Guo, *Process Biochem.* **2012**, *47*, 1439–1451.

[363] S. L. Friess, *J. Am. Chem. Soc.* **1949**, *71*, 2571–2575.

[364] D. Swern, *Chem. Rev.* **1949**, *45*, 1–68.

[365] H. Hagiwara, K. Kobayashi, S. Miya, T. Hoshi, T. Suzuki, M. Ando, T. Okamoto, M. Kobayashi, I. Yamamoto, S. Ohtsubo, M. Kato, H. Uda, *J. Org. Chem.* **2002**, *67*, 5969–5976.

[366] J. J. Bozell, G. R. Petersen, *Green Chem.* **2010**, *12*, 525–728.

[367] O. Akdim, U. B. Demirci, P. Miele, *Int. J. Hydrogen Energy* **2009**, *34*, 7231–7238.

[368] A. Carbonell-Verdu, L. Bernardi, D. Garcia-Garcia, L. Sanchez-Nacher, R. Balart, *Eur. Polym. J.* **2015**, *63*, 1–10.

[369] Y. Gao, J. M. Klunder, R. M. Hanson, H. Masamune, S. Y. Ko, K. B. Sharpless, *J. Am. Chem. Soc.* **1987**, *109*, 5765–5780.

[370] W. Zhang, J. L. Loebach, S. R. Wilson, E. N. Jacobsen, *J. Am. Chem. Soc.* **1990**, *112*, 2801–2803.

[371] E. N. Jacobsen, W. Zhang, A. R. Muci, J. R. Ecker, L. Deng, *J. Am. Chem. Soc.* **1991**, *113*, 7063–7064.

[372] R. Irie, K. Noda, Y. Ito, N. Matsumoto, T. Katsuki, *Tetrahedron: Asymmetry* **1991**, *2*, 481–494.

[373] Y. Raupp, *master thesis*, Karlsruhe Institute of Technology (KIT), April **2016**.

[374] R. Noyori, M. Aoki, K. Sato, *Chem. Commun.* **2003**, *24*, 1977–1986.

[375] K. Sato, M. Aoki, M. Ogawa, T. Hashimoto, R. Noyori, *J. Org. Chem.* **1996**, *61*, 8310–8311.

[376] C. Venturello, E. Alneri, M. Ricci, *J. Org. Chem.* **1983**, *48*, 3831–3833.

[377] E. Kaczmarczyk, E. Milchert, E. Janus, *Chem. Eng. Technol.* **2009**, *32*, 881–886.

[378] A. Casas, M. J. Ramos, J. F. Rodríguez, A. Pérez, *Fuel Processing Technology* **2013**, *106*, 321–325.

[379] H. E. Gottlieb, V. Kotylar, A. Nudelman, *J. Org. Chem.* **1997**, *62*, 7512–7515.

[380] A. Houde, A. Kademi, D. Leblanc, *Appl. Biochem. Biotechnol.* **2004**, *118*, 155–170.

[381] C. Aouf, E. Durand, J. Lecomte, M.-C. Figueroa-Espinoza, E. Dubreucq, H. Fulcrand, P. Villeneuve, *Green Chem.* **2014**, *16*, 1740–1754.

[382] M. von Czapiewski, *PhD thesis*, Karlsruhe Institute of Technology (KIT), *current work*.

[383] H. H. Nimz, R. Casten, *Holz als Roh- und Werkstoff* **1986**, *44*, 207–212.

[384] M. Aresta, A. Dibenedetto, E. Fracchiolla, P. Giannoccaro, C. Pastore, I. Pápai, G. Schubert, *J. Org. Chem.* **2005**, *70*, 6177–6186.

[385] S. T. A. Shah, K. M. Khan, H. Hussain, M. U. Anwar, M. Fecker, W. Voelter, *Tetrahedron* **2005**, *61*, 6652–6656.

[386] T. Shintou, T. Mukaiyama, *J. Am. Chem. Soc.* **2004**, *126*, 7359–7367.

[387] F. C. Gozzo, S. A. Fernandes, D. C. Rodrigues, M. N. Eberlin, A. J. Marsaioli, *J. Org. Chem.* **2003**, *68*, 5493–5499.

[388] R. Kuwano, H. Kusano, *Org. Lett.* **2008**, *10*, 1979–1982.

[389] X. Jing, W. Gu, P. Bie, X. Ren, X. Pan, *Synth. Commun.* **2001**, *31*, 861–867.

[390] J. Barluenga, F. J. Fananas, R. Sanz, C. Marcos, J. M. Ignacio, *Chem. Commun.* **2005**, 933–935.

[391] X. Huang, L. Zhang, *Org. Lett.* **2007**, *9*, 4627–4630.

[392] A. A. Bredikhin, D. V. Zakharychev, R. R. Fayzullin, O. A. Antonovich, A. V. Pashagin, Z. A. Bredikhina, *Tetrahedron: Asymmetry* **2013**, *24*, 807–816.

[393] C. Zhu, N. Yukimura, M. Yamane, *Organometallics* **2010**, *29*, 2098–2103.

[394] J. P. Parrish, B. Sudaresan, K. W. Jung, *Synth. Commun.* **1999**, *29*, 4423–4431.

[395] B. F. Sun, R. Hong, Y. B. Kang, L. Deng, *J. Am. Chem. Soc.* **2009**, *131*, 10384–10385.

[396] P. K. Pradhan, P. Jaisankar, B. Pal, S. Dey, V. S. Giri, *Synth. Commun.* **2004**, *34*, 2863–2872.

[397] M. Del Carmen Cruz, J. Tamariz, *Tetrahedron* **2005**, *61*, 10061–10072.

[398] A. V. Shindikar, C. L. Viswanathan, *Synth. Commun.* **2011**, *41*, 1141–1145.

[399] Y. C. Chiu, I. C. Chou, W. C. Tseng, C. C. M. Ma, *Polymer Degrad. Stabil.* **2008**, *93*, 668–676.

[400] T. Iijima, N. Yoshioka, M. Tomoi, *Eur. Polym. J.* **1992**, *28*, 573–581.

[401] P. J. Flory, *Polymer* **1979**, *20*, 1317–1320.

List of Figures

List of Schemes

List of Tables

List of Abbreviations

ADMET	acyclic diene metathesis
AIBN	azobis(isobutyronitrile)
APC	advanced polymer chromatography
ATR	attenuated total reflection
BPA	bisphenol A
^{13}C NMR	carbon nuclear magnetic resonance
CNSL	cashew nut shell liquid
c	concentration
Đ	dispersity
d	day(s)
DAC	diallyl carbonate
DBC	dibenzyl carbonate
DBU	1,8-diazabicyclo[5.4.0]undec-7-ene
DCC	dicrotyl carbonate
DCM	dichloromethane
DEC	diethyl carbonate
DET	diethyl tartrate
DGC	diglycidyl carbonate
DGEBA	diglycidyl ether bispheonol A
DMC	dimethyl carbonate
DMA	dynamic mechanical analysis
DMAc	dimethylacetamide
DMF	dimethylformamide
DMI	1,2-dimethylimidazole
DMPA	2,2-dimethoxy-2-phenylacetophenone
DMSO	dimethyl sulfoxide
DSC	differential scanning calorimetry
DTA	differential thermal analysis
DUC	di-10-undecenyl carbonate
E	Young's modulus
ECCL	Early-stage Catalytic Conversion of Lignins
E'	storage modulus
E"	loss modulus
EA	ethyl acetate
EI	electron ionization
eq.	equivalents
FAB	fast atom bombardment
FID	flame ionization detector

GC	gas chromatography
GOL	glycidylated organosolv lignin
h	hours
ΔH	residual reaction heat
HG1	Hoveyda-Grubbs 1st generation
HG2	Hoveyda-Grubbs 2nd generation
^{1}H NMR	proton nuclear magnetic resonance
HRMS	high resolution mass spectrometry
HW	hardwood
IPDA	isophorone diamine
IR	infrared
***m*CPBA**	*meta*-chloroperbenzoic acid
min	minutes
M_n	number average molecular weight
MOF	metal organic framework
MS	mass spectrometry
Δm	mass difference
m_0	weighted dry mass before swelling text
m_D	weighted dry mass after swelling and drying
m_{SW}	weighted mass of swollen sample
m_S	sample mass
M_w	weight average molecular weight
m/z	mass-to-charge ratio
$\Delta m/z$	mass-to-charge ratio difference
NIPU	non-isocyanate polyurethane
n	amount in mol
OL	organosolv lignin
PE	polyethylene
PEG	polyethylene glycol
PET	polyethylene terephthalate
PLA	polylactic acid
PP	polypropylene
PTE	poly thiol-ene
PTFE	polytetrafluorethylen
PU	polyurethane
PVC	polyvinyl chloride
RCM	ring closing metathesis
RDB	ring double bond
R_f	retention factor for TLC
RI	refractive index
ROM	ring opening metathesis
ROMP	ring opening metathesis polymerization
ROP	ring opening polymerization
rt	room temperature
SEC	size-exclusion-chromatography

SW	softwood
synth.	synthetic
t	time
T	temperature
T_{α}	the maximum of tan delta (tan delta = E”/E’)
TBAB	tetrabutylammonium bromide
TBD	1,5,7-triazabicyclo[4.4.0]dec-5-ene
$T_{d\ 5\%}$	decomposition temperature for 5% mass loss in TGA measurement
$T_{d\ 30\%}$	decomposition temperature for 30% mass loss in TGA measurement
T_g	glas transition temperature
TGA	thermogravimetric analysis
THF	tetrahydrofuran
TLC	thin layer chromotography
T_m	melting point
TMDP	2-chloro-4,4,5,5-tetramethyl-1,2,3-dioxaphospholan
T_s	heat resistant index
UV	ultra violett
V_{blank}	titration volume of blank sample
wt%	weight percent
w/v	weight per volume
$X_{OH}^{aliph.}$	converted aliphatic hydroxyl groups
$X_{OH}^{arom.}$	converted aromatic hydroxyl groups
X_{OH}^{total}	total converted hydroxyl groups
YES	yeast estrogen screen

Publications

Publications arising from the present thesis

6) L. Charlotte Over, Marcel Hergert, Michael A. R. Meier, *Macromol. Chem. Phys.* **2017**, *accepted manuscript*: *"Metathesis curing of allylated lignin and different plant oils for the preparation of thermosetting polymer films with tunable mechanical properties"*.

5) A. Stefania Trita, L. Charlotte Over, Jacqueline Pollini, Sabrina Baader, Sven Riegsinger, Michael A. R. Meier, Lukas J. Gooßen, *Green Chem.* **2017**, *accepted manuscript*, DOI: 10.1039/C7GC00553A: *"Synthesis of potential bisphenol A substitutes by isomerising metathesis of renewable raw materials"*.

4) L. Charlotte Over, Etienne Grau, Stéphane Grelier, Michael A. R. Meier, Henri Cramail, *Macromol. Chem. Phys.* **2017**, *218*, 1600411: *"Synthesis and characterization of epoxy thermosetting polymers from glycidylated organosolv lignin and bisphenol A"*.

3) Audrey Llevot, Patrick-Kurt Dannecker, Marc von Czapiewski, L. Charlotte Over, Zafer Söyler, Michael A. R. Meier, *Chem. A Eur. J.* **2016**, *22*, 11510–11521: *"Renewability is not enough: Recent advances in the sustainable synthesis of biomass-derived monomers and polymers"*.

2) L. Charlotte Over, Michael A. R. Meier, *Green Chem.* **2016**, *18*, 197–207: *"Sustainable allylation of organosolv lignin with diallyl carbonate and detailed structural characterization of modified lignin"*.

1) Oliver Kreye, L. Charlotte Over, Tobias Nitsche, Ralph Z. Lange, Michael A. R. Meier, *Tetrahedron* **2015**, *71*, 293–300: *"Organic Carbonates: Sustainable and environmentally-friendly ethylation, allylation, and benzylation reagents"*.

Additional publications

2) Bernd Kohl, L. Charlotte Over, Thorsten Lohr, Mariya Vasylyeva, Frank Rominger, Michael Mastalerz, *Org. Lett.* **2014**, *16*, 5596–5599: *"Selective even-numbered bromination of triptycene tris(thiadiazoles)"*.

1) Timo Söhner, Felix Braun, L. Charlotte Over, Sven Mehlhose, Frank Rominger, Bernd F. Straub, *Green Chem.* **2014**, *16*, 4696–4707: *"Halogen-free water-stable aluminates as replacement for persistent fluorinated weakly-coordinating anions"*.